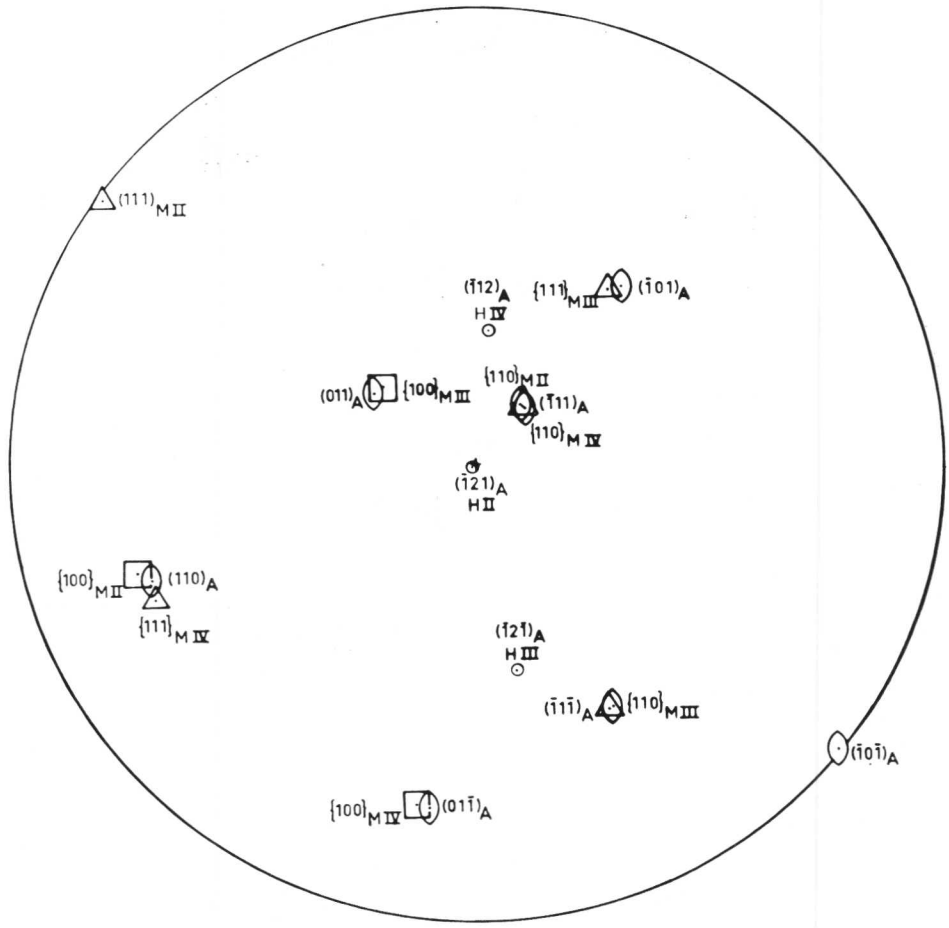

Fig. 7 Orientation relationships of the weak variants II, III, and IV.

lationship deduced from the maximum of the intensity distribution, which is indicated by the contour lines in Fig. 9, the rotated final Bain cone is B. The intersection of B_i with B is P. However, the experimental invariant line P does not lie in the experimental habit plane h (indicated in Fig. 9 with the great circle). This difference is so large that it cannot be a consequence of inaccuracy of the measurements.

It is possible to choose an orientation relationship so that a triple intersection of $\mathbf{B}_i$, B_{fr}, and the habit plane is obtained, but then we must choose a martensite orientation rather far away from the maximum of the measured distribution. It might be assumed that such a martensite orientation existed in the initial stages of growth. The martensite orientation observed experimentally could then be gradually produced by rotation resulting from accommodation deformations. However, this assumption is not attractive, since if this were the case one would expect a large influence of the orientation of the habit plane relative to the specimen surface. Furthermore the orientation relationship should then be less well defined.

Thus, it can be concluded that for surface martensite the lattice invariant deformation is not an invariant plane strain, and the I.P.S. theory is not applicable.

The formation of a straight boundary at the end of a needle (Type-III boundary) indicates that the boundary energy will be important. Fig. 11 is a micrograph of a martensite needle with three straight boundaries. In Fig. 10 the austenite orientation of this specimen is shown. It appears that the normals of the three boundaries α_1, α_2, and α_{11} all pass, or nearly pass, through a $\{112\}_A$ pole. From Fig. 10 it can be observed that boundary α_{11} (Type II) seems to meet the conditions of continuity and of orientation simultaneously.

To obtain a low boundary energy, the fit on an atomic scale will be important, as suggested by Frank.[10] If one supposes that the martensite and austenite lattices fit together in such a way that close-packed atom rows in both lattices are parallel and spaced equally, it can be seen from Table I that the $\{112\}_A$ austenite plane is the only lattice plane with low indices that fits with a martensite plane, in fact the $\{123\}_M$ plane. Naturally the condition must be fulfilled that the correspondence matrix for planes transforms the austenite plane into the martensite plane that fits with it. The boundary obtained in this way is closely related to that proposed by Frank.[10] However, we think that the boundary will be somewhat more complicated and the compression in the close-packed direction will probably be compensated by dislocations.

One of the most surprising phenomena is the observation that surface martensite grows slowly. This could be interpreted on the basis of the evolution of the heat of transformation or of Zener disordering. Perhaps these two effects exert some influence but they cannot account for the very great differences in growth velocity. Probably the most

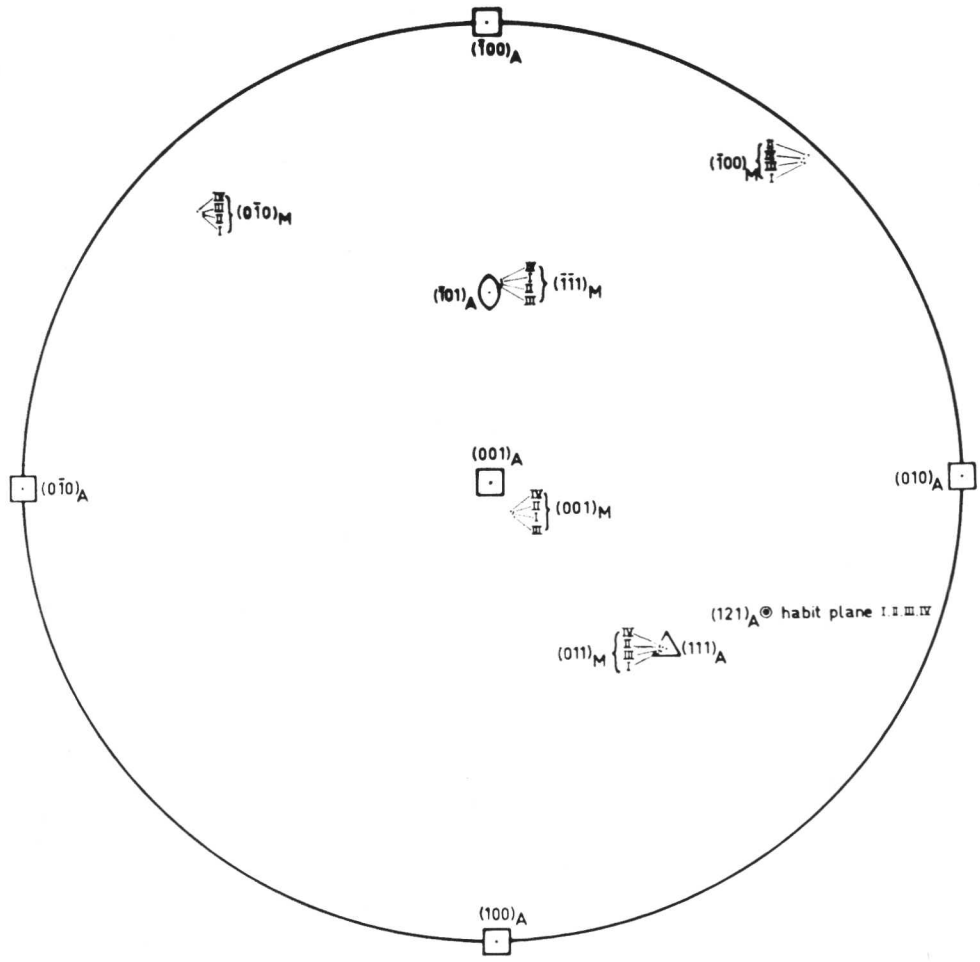

Fig. 8 Orientation relationships of the variants I, II, III, and IV all rotated to " standard orientation ".

important reason for the slow growth is thermally activated creep. It is difficult to visualize how diffusion in iron–nickel alloys can occur at room temperature. However, very large internal stresses may change the activation energy for self-diffusion. The great differences in growth velocity are probably a consequence of dislocation tangles blocking the passage of the phase boundary until thermally activated creep makes movement possible again. This can be illustrated by Figs. 12(*a*) and (*b*). These micrographs were taken from a specimen in which angle-profile martensite[7] had formed after cooling. The angle profiles were austenitized by heating to 600° C but a deformed austenite structure was left. The deformed region in the austenite was made visible by etch-pits as shown in Figs. 12(*a*) and (*b*); the midrib of the austenitized angle profile is clearly shown (it appears to be highly deformed). Surface martensite needles which grew in this specimen were greatly retarded in their growth in the deformed region. Fig. 12(*a*) shows several surface martensitic needles that have been slowed down in the deformed region. Fig. 12(*b*) shows a needle that has grown through this region but the needle remains narrow in the deformed austenite. It is probable that the sideways growth of surface martensite needles stops as a consequence of loss of coherency of the phase boundary. Such an effect may be caused by dislocations which are absorbed in the interface. As a consequence it can be expected that in a deformed austenite, surface martensite needles will remain narrow. Fig. 13 shows surface martensite that grew on a deformed specimen. The interpretation of this curved growth is that only a few dislocations in the austenite are absorbed in the phase boundary. Most of them are transformed in the boundary to their corresponding dislocations in the b.c.c. lattice so that the martensite is deformed by the dislocations in the same way as the austenite was previously.

TABLE I

Plane Containing the [$\bar{1}$01] Direction in Austenite	Separation of Closest-Packed [$\bar{1}$01] Rows in Austenite, Å	Plane Containing the [$\bar{1}\bar{1}$1] Direction in Martensite	Separation of Closest-Packed [$\bar{1}\bar{1}$1] Rows in Martensite, Å
(101)	3·58	(0$\bar{1}\bar{1}$)	2·33
(111)	2·19	(2$\bar{1}$1)	4·04
(121)	6·20	($\bar{1}$32)	6·16
(212)	8·39*	($\bar{1}$43)	8·38

*(212)A and ($\bar{1}$43)M are not corresponding planes for the Bain correspondence.

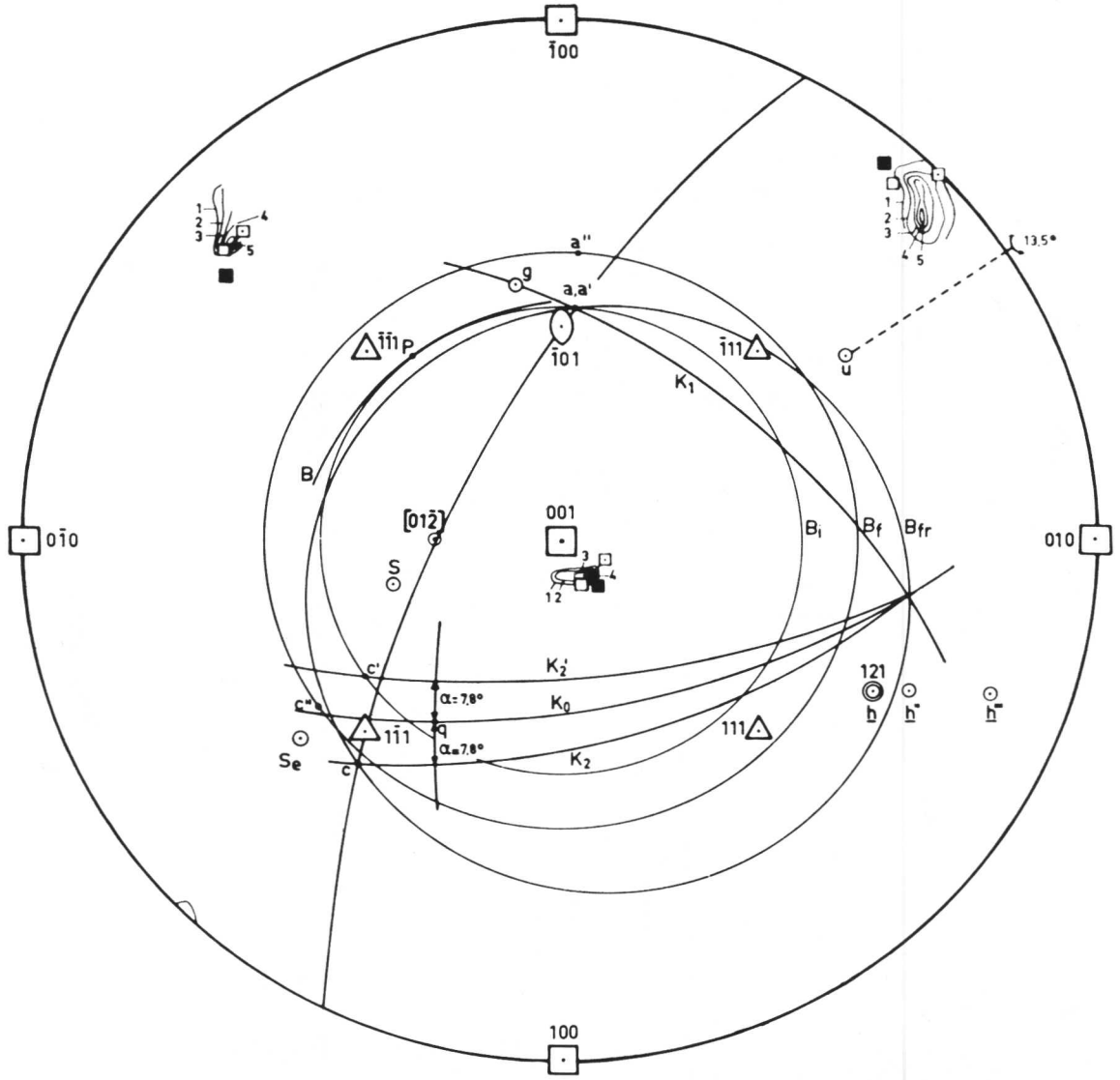

Fig. 9 Analysis of surface martensite by the graphical method. P is the experimental invariant line which does not lie in the habit plane.

Conclusion

(1) Growth of surface martensite in Fe–30% Ni has unidirectional (polar) characteristics. Three types of boundaries (I, II, and III) form on a needle in its fully grown stage. The direction of growth is opposite to the movement of the atoms caused by the total deformation. Consequently, new martensite is formed in a region where a " hydrostatic " tensile stress is promoted.

(2) In spite of a nearly complete compensation of the lattice deformation by the lattice invariant deformation, a very sharp and well-defined orientation of the martensite relative to the austenite exists. The invariant plane strain theory is not applicable for this type of martensite because the lattice invariant deformation is not an invariant plane strain, and the invariant line of the lattice deformation does not lie in the habit plane.

(3) The orientation relationship of surface martensite is independent of the orientation of the habit plane relative to the specimen surface.

(4) Experimental observations indicated that the boundary energy is an important factor. The {112} habit plane of surface martensite can be interpreted as an austenite plane fitting with a corresponding {123} martensite plane on an atomic scale.

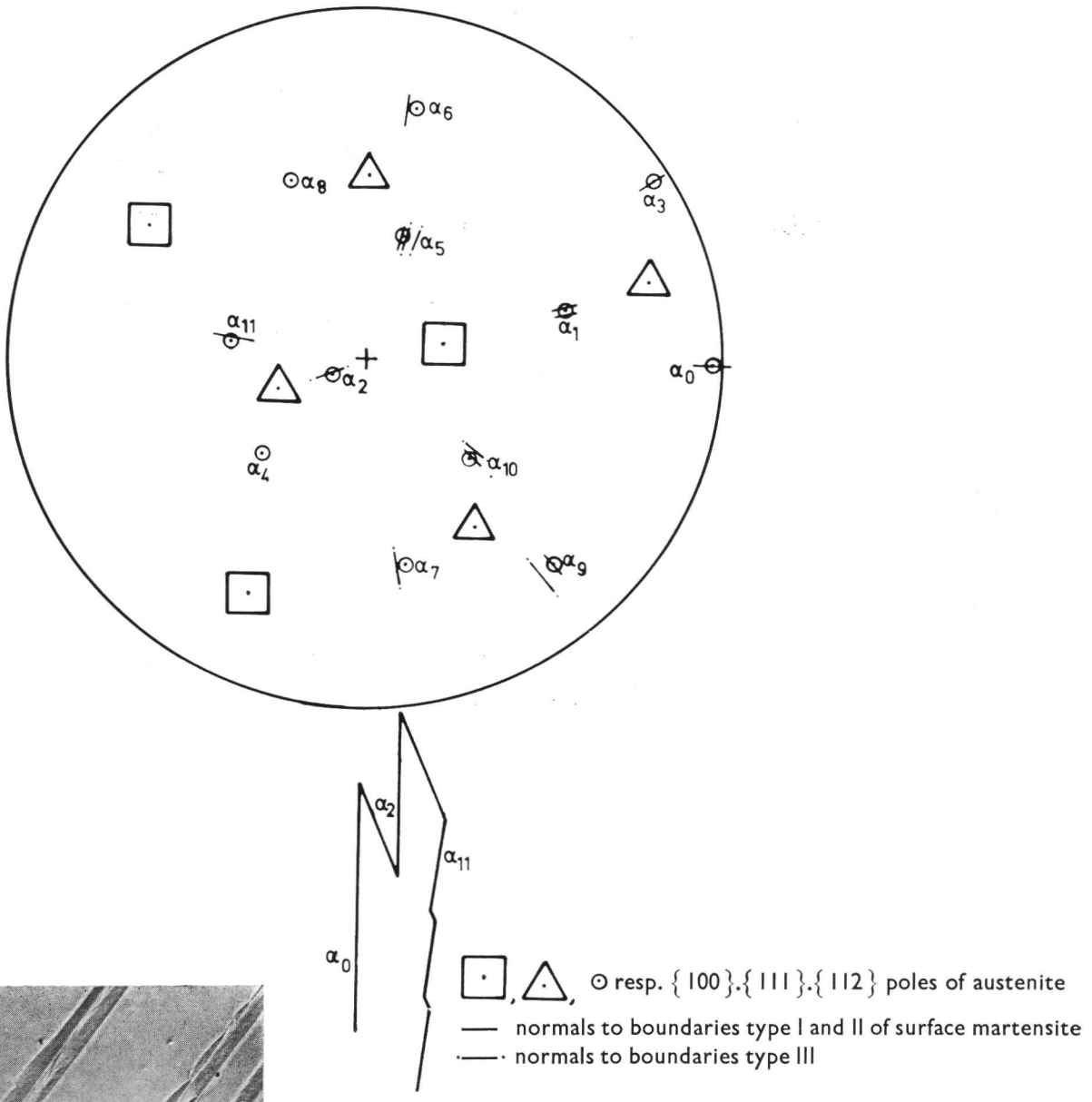

Fig. 10 *Orientations of the boundaries relative to the austenite of the broad surface martensite needle of Fig.* 11.

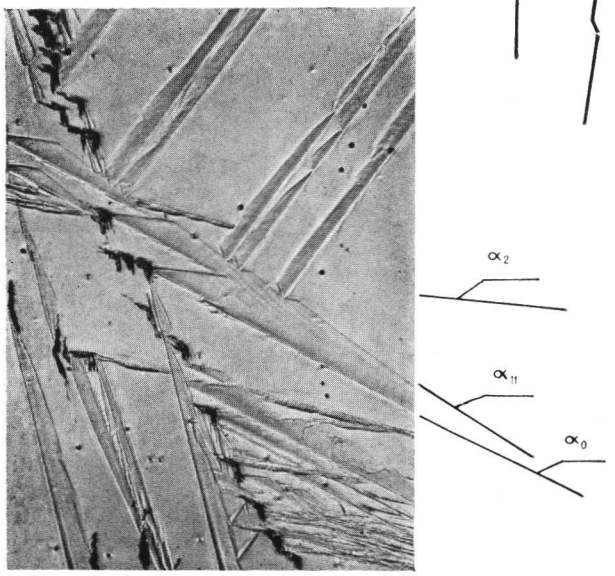

Fig. 11 *Broad surface martensite needle with straight boundaries in three different orientations.* × 100.

(5) Systematic nucleation of new martensite needles was observed on Type-II boundaries.

(6) Large differences in growth velocity and the impediment of growth in deformed material indicate that thermally activated creep will be an important process for the slow growth characteristics of surface martensite.

(7) Curved austenite causes the martensite needles to curve in the same way.

Acknowledgements

The author is much indebted to Professor Dr. W. G. Burgers for his constant interest in this work, and for many ideas and enlightening discussions. Thanks are also due to Ir. R. Bosma for reading the manuscript. This work is a part of the research programme of the Metals Research Group " FOMTNO " sponsored by Z.W.O.

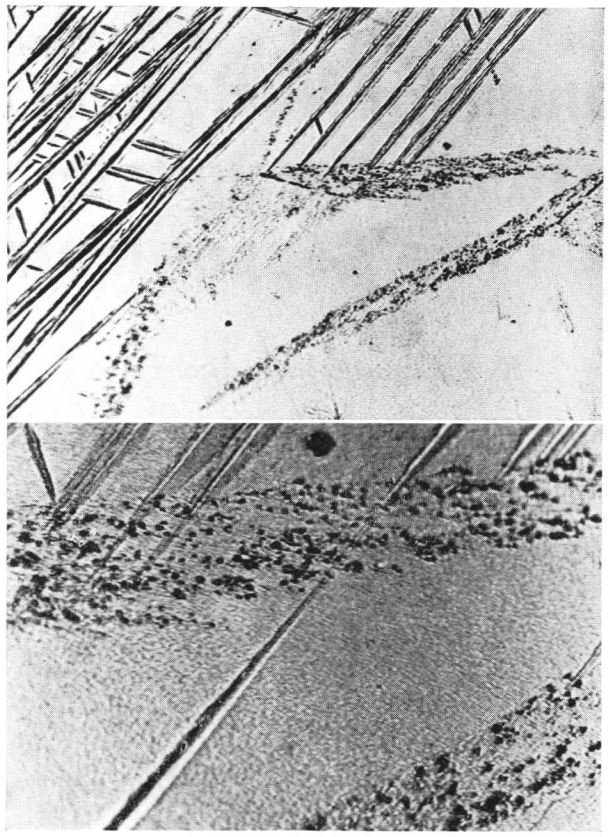

Fig. 12(a) *Deformation in re-austenitized angle profile demonstrated by etch-pits.* × 120. (b) *Surface martensite remains narrow in deformed region.* × 500.

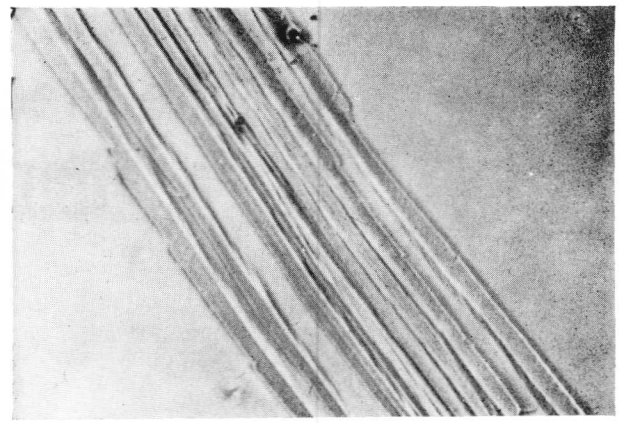

Fig. 13 *Curved growth of surface martensite in deformed austenite.* × 250.

References

1. J. S. Bowles and J. K. Mackenzie, *Acta Met.*, 1954, **2,** 129.
2. M. S. Wechsler, D. S. Lieberman, and T. A. Read, *Trans. Amer. Inst. Min. Met. Eng.*, 1953, **197,** 1503.
3. D. S. Lieberman and R. Bullough, *Physica Status Solidi*, 1965, **12,** 657.
4. R. F. Bunshah and R. F. Mehl, *Trans. Amer. Inst. Min. Met. Eng.*, 1953, **197,** 1251.
5. T. Honma, *J. Japan Inst. Metals*, 1957, **21,** 122.
6. J. A. Klostermann and W. E. Burgers, *Acta Met.*, 1964, **12,** 355.
7. J. A. Klostermann, " Physical Properties of Martensite and Bainite " (Iron Steel Inst. Special Rep. No. 93) pp. 20, 43. **1965:** London (Iron Steel Inst.).
8. A. J. Bogers, Thesis, Univ. Delft, **1962**.
9. D. S. Lieberman, *Acta Met.*, 1958, **6,** 680.
10. F. C. Frank, *ibid.*, 1953, **1,** 15.

The Mechanism of Nucleation of Martensite in Precipitates of Iron in a Copper Matrix

K. E. Easterling and P. R. Swann

The mechanism of nucleation of martensite in small defect-free precipitates of γ-iron in a matrix of copper has been studied in single crystals of an aged Cu–1·12 wt.-% Fe alloy deformed in uniaxial tension. Magnetic measurements show that the transformation to martensite is closely related to the slip behaviour of the crystal. Electron micrographs reveal that martensite is nucleated by matrix dislocations as they pass through the precipitate during deformation. Growth proceeds by the formation of thin martensite discs, apparently by the motion of screw dislocations in the $(110)_\gamma$ habit plane of the discs. Thickening of the discs does not occur immediately and it is deduced that this is because a suitable dislocation source is not present to develop the appropriate interface. To complete the transformation, further interaction with matrix dislocations is thus required.

Copper-rich copper–iron alloys can be suitably heat-treated to bring about the homogeneous precipitation of iron-rich spheres which, up to some 500–600 Å in dia., are fully coherent with the copper lattice. The complete coherency between the copper and iron lattices, as seen from electron micrographs of this alloy,[1] implies that the precipitates are of the γ-iron structure, which confirms earlier magnetic[2] and X-ray[3] measurements.

Experiments have shown that athermal treatment alone does not bring about the $Fe^{\gamma\rightarrow\alpha}$ transformation in these precipitates but that plastic deformation is necessary before it will occur. This was confirmed by Easterling and Miekk-oja[4] on the basis of magnetic measurements and electron microscopy. The fact that the transformation can be made to occur instantly at room temperature implies that it must be martensitic. Before cold working, however, no defects can be observed in these slightly elastically strained precipitates, which makes them particularly suitable for the study of martensite nucleation.

In the paper of Easterling and Miekk-oja[4] it was shown that cold rolling caused thin plates or discs of martensite with a $(110)_\gamma$ habit plane to form across previously fully austenitic precipitates. An example of these discs in a partially transformed precipitate is shown in Fig. 1. It was deduced that the discs of martensite were nucleated by matrix dislocations as they passed through the precipitates during plastic deformation.

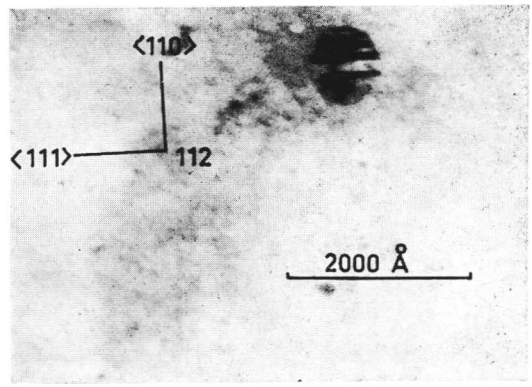

Fig. 1 A partially transformed precipitate in a single crystal deformed by cold rolling 15% in the [110] direction shown.

In the present work the dislocation role in martensite nucleation was studied in single-crystal test-specimens of the alloy deformed in uniaxial tension. Besides the electron-microscope observations, the transformation was followed by continuously recording the magnetic permeability of samples during deformation and also by measuring the magnetic moment of sections of the specimen after deformation.

Experimental Procedure

An alloy of Cu–1·12 wt.-% Fe was prepared from 99·998% copper and Armco iron in a high-vacuum induction furnace. The ingots were machined, hot extruded, and cold drawn to a final size of 8-mm rod. The relatively low iron content was chosen to avoid the drastic quenching needed to retain higher amounts of iron in solution in this alloy.

The single crystals were grown directly in the shape of tensile-test specimens using a method described by Lindroos and Miekk-oja.[5] Crystal orientations were found by Laue X-ray measurement. The crystals were solution-treated at 900° C for 100 min in a salt bath, quenched into water, aged at 700° C for 12 h and then air-cooled. The resulting structure was a homogeneous dispersion of fully coherent iron-rich precipitates of 550 Å mean dia. in a copper-rich matrix, and the structure was only weakly paramagnetic.

Manuscript received 27 February 1968. K. E. Easterling, D.Sc., and P. R. Swann, Ph.D., B.Sc., are in the Department of Metallurgy, Imperial College of Science and Technology, London.

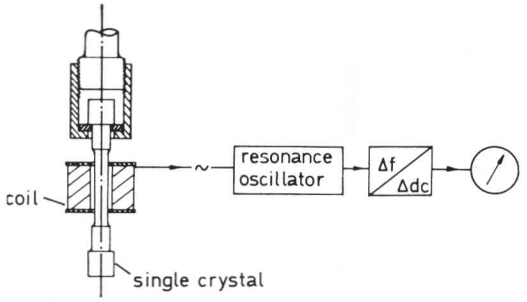

Fig. 2 Diagrammatic layout for continuously recording changes in magnetic permeability of a crystal under uniaxial deformation. Magnetic apparatus designed by K. Nevalainen.[6]

The crystals were tested in a high-precision tensile testing machine which maintained a constant rate of extension. A load cell, connected via a bridge to a pen-recorder, enabled a continuous load/extension record to be made.

Two types of magnetic measurements were carried out. In one the measuring device is essentially an electronic permeability meter.[6] The coil of a resonance oscillator enclosed the test-length of the crystal as shown in Fig. 2. The coil, which is very sensitive and must be screened from the surrounding metallic structures, was held in position independently of the specimen. Subsequent changes in magnetic permeability as the crystal undergoes deformation affect the impedance of the coil which results in a frequency change in the resonance oscillator. This change in frequency is then converted to a d.c. voltage change which is fed to a pen-recorder. In this way, changes in load on the specimen may be recorded simultaneously with changes in permeability.

In addition to the continuous permeability measurements, the magnetic moment was measured on small sections of deformed crystals cut by spark-machining. These measurements were done in a Satmagan high-sensitivity magnetic balance.[7]

Samples were also spark-cut from deformed crystals and thinned by the "window" method in a 33% nitric acid–methanol solution at $-30°$ C with a potential of 9V.

Results

Magnetic Measurements

Fig. 3(*a*) shows the orientations and final stresses and strains developed in six crystals before unloading and sectioning for magnetic measurements and examination in the electron microscope. The initial flow stress (point 7) is the average of the six crystals tested. The onset of each of the three stages of deformation was clearly defined by the load/extension record and these three stages are indicated in the figure.

The relative magnetic moments of samples taken from crystals 1–6 of Fig. 3(*a*) are shown in Fig. 3(*b*). Point 7 in Fig. 3(*b*) refers to an undeformed crystal. It is seen that while the magnetic moment of the samples increases with deformation (as expected), the greatest rate of increase occurs during Stage-II deformation. A further increase occurs during Stage-III deformation. It is also seen that even during easy glide there is a definite increase in magnetic moment, i.e. precipitates have begun to transform to the ferromagnetic martensite phase.

The continuous curves of relative magnetic permeability/extension all tended to confirm the magnetic moment measurements. An example of these tests is shown in Fig. 4 where both the load/extension and relative magnetic permeability/

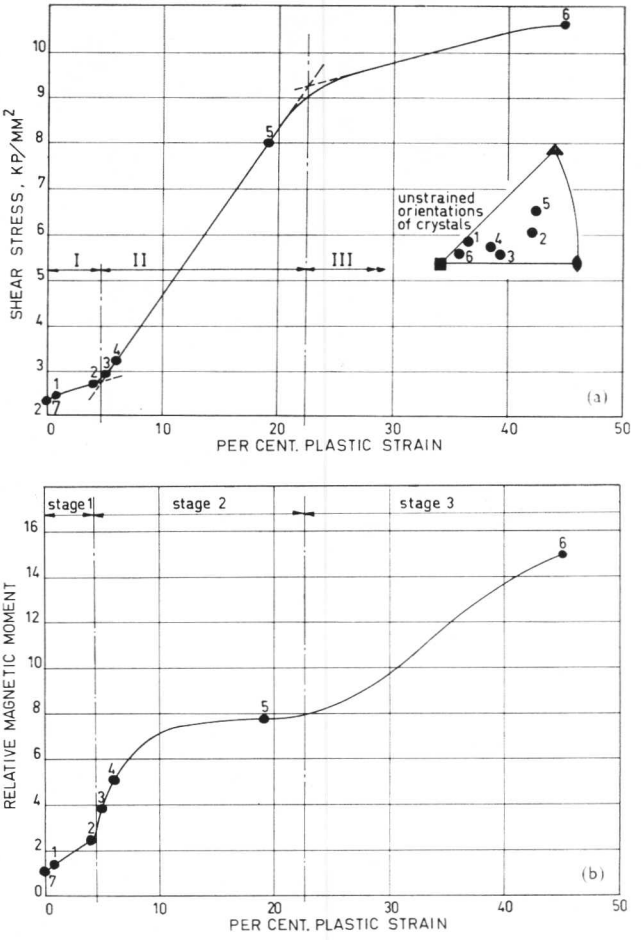

Fig. 3 (a) Shear stress/plastic strain curve for 6 single crystals of Cu–1·12% Fe deformed in tension to the strains shown. Point 7 is the average flow stress of the crystals.
(b) Relative magnetic moment/plastic strain curve for samples taken from the 6 crystals of (a). *Point 7 is from an undeformed crystal. Compare with Fig. 4.*

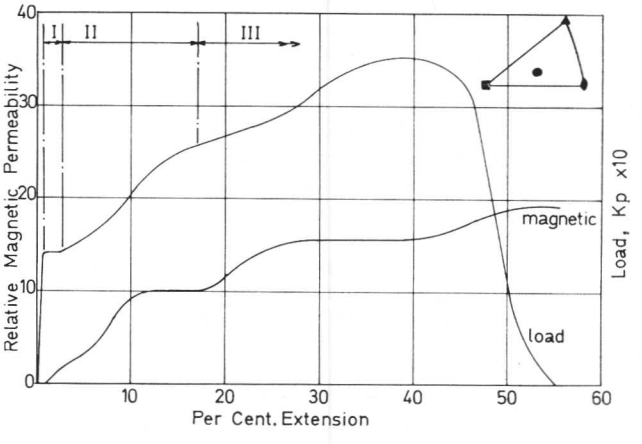

Fig. 4 Continuously recorded curves of relative magnetic permeability and load against per cent. extension. Compare with Fig. 3 (b).

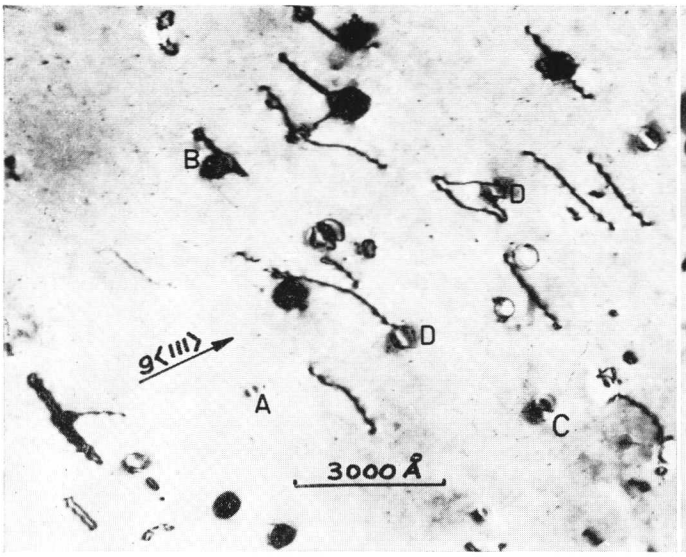

Fig. 5 Microstructure from Stage I of plastic deformation. Partially transformed precipitates are marked C and D. Beam direction [110].

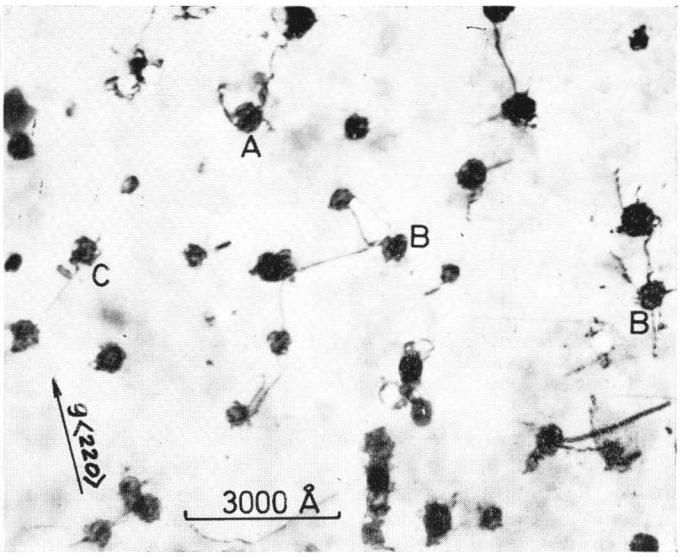

Fig. 6 Microstructure at the beginning of Stage-II deformation. Note the substantial increase in dislocations at the precipitates compared to Fig. 5. Beam direction [111].

extension curves are given. In agreement with Fig. 3(*b*), the onset of easy glide immediately causes precipitates to transform, while Stage-II deformation again causes a marked increase in the rate of precipitate transformation. A similar increase is seen to occur in Stage-III deformation and yet a further increase during necking. Thus, both sets of magnetic measurements are consistent in showing that the amount of precipitate transformed is closely related to the slip behaviour of the crystal.

It should be noted that the magnetic permeability/extension curves shown are corrected to allow for the change in cross-section of the crystal during deformation, since this also affected the impedance of the coil. To establish a calibration, tests were made on crystals of pure copper and the solution-treated copper–iron alloy (i.e. both non-ferromagnetic materials) and these exhibited a linear change in permeability between the onset of easy glide and the onset of necking.

Electron Microscopy

Samples from each of the six crystals in Fig. 3 were examined in the electron microscope after deformation. Fig. 5 is an example of the microstructure developed during Stage-I deformation. The dislocation segments seen are typical of this stage of deformation. Some fully coherent precipitates remain (e.g. at A), although several precipitates have trapped dislocations and transformed to martensite, losing their strain-field contrast (e.g. at B). In addition, some precipitates appear to have partially transformed to martensite and have still retained part of the coherency strain field, e.g. at C and D in Fig. 5. In these cases the very fine dark striations across the precipitates are interpreted to be the martensite discs since they exhibit a similar morphology to the more-completely transformed precipitate shown in Fig. 1. One of the precipitates marked D in Fig. 5 is particularly interesting since it shows a dislocation attached to a pair of these discs within a single precipitate. The tendency for martensite discs to form in pairs is very noticeable and several examples can be seen in Fig. 5.

Figs. 6 and 7 show typical microstructures at the beginning and end of Stage-II deformation. At the beginning of Stage II there is a striking decrease in the number of coherent and partially coherent precipitates (Fig. 6). The formation of parallel (A) and cross (B) grids of dislocations, and dislocation loops (C) at the surfaces of the precipitates is also evident. Later in Stage-II deformation, dislocation tangles extend from the precipitate and connect up to form a cell structure as seen in Fig. 7.

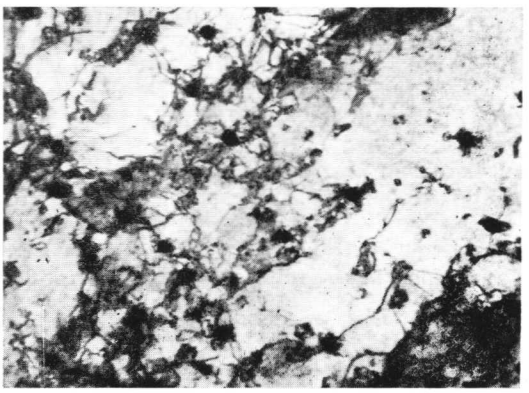

Fig. 7 Microstructure at the end of Stage-II deformation. Most precipitates now appear fully transformed. Beam direction [111].

Discussion

The elastic-strain energy associated with γ-iron precipitates can be almost entirely eliminated by transformation since the volume occupied by the martensite is only 0·23% greater than the copper matrix, whereas the volume of the parent γ is ~ 4% less than the matrix. Also at room temperature the γ-iron precipitate is several hundred degrees below the bulk-transformation temperature; thus the driving force for transformation must be unusually high. Specimens can be stressed to the elastic limit or refrigerated at liquid-helium temperature yet transformation does not occur. However, transformation can

be made to occur by relatively small amounts of plastic deformation.

The resistance to transformation would seem to be due to a nucleation problem but martensite growth is also difficult in this case since many examples of partially transformed precipitates are observed. Several observations indicate that nucleation requires the direct interaction between precipitates and mobile dislocations:

(*a*) A strong increase in magnetic moment and susceptibility of samples (i.e. proportion of transformed precipitates) occurs at the onset of and during Stage-II deformation, corresponding with a rapid increase in the density of mobile dislocations.

(*b*) Matrix dislocations are frequently attached to fully transformed or partially transformed precipitates. In some cases a direct connection between matrix dislocations and martensite discs within plates is clearly visible. On the other hand no matrix dislocations have been seen attached to untransformed precipitates.

(*c*) The resistance of precipitates to undergoing complete transformation, even when attached to a matrix dislocation, indicates that the local stress field of the nearby matrix dislocation is insufficient in itself to induce further nucleation or further growth. It appears that direct interaction between the precipitate and dislocations is necessary for nucleation to occur.

At present the electron-microscope observations are not detailed enough to determine the exact role of dislocations in the nucleation mechanism. However, the observation that martensite discs frequently occur in parallel pairs within partially transformed precipitates does suggest that nucleation is induced by dislocation segments of similar character but opposite sign formed when the dislocation begins to loop around the precipitate. The segments would be pure screw if the glide occurs along the observed $(110)_\gamma$ habit plane of the discs, which is also the glide plane of the transformation dislocations proposed by Frank.[8] Such an interpretation is consistent with the configuration shown at C and D in Fig. 5.

It is interesting to speculate on the reason why martensite discs fail to grow sideways across precipitates. Generally the two thermodynamic factors opposing the growth of martensite are the increasing elastic and surface free energies. In this case the transformation actually reduces the elastic energy of the system and thus the surface energy required for growth would seem to be the important factor. Fig. 8 shows that two types of surface are involved in the transformation: the two circular interfaces between the martensite (α') and the γ-iron and the interface between α' and the copper matrix (ε). For a martensite disc nucleated across the diameter of a precipitate the area of α'/γ interface decreases during growth, whereas the area of the α'/ε interface increases. In this case the formation of the latter type of interface would be the only factor resisting the growth of the martensite. Such a martensite disc can be seen at C in Fig. 5. However, the high degree of undercooling, the decreasing area of the α'/γ surface, and the other factors favouring transformation should be adequate to account for the required α'/ε interfacial energy.

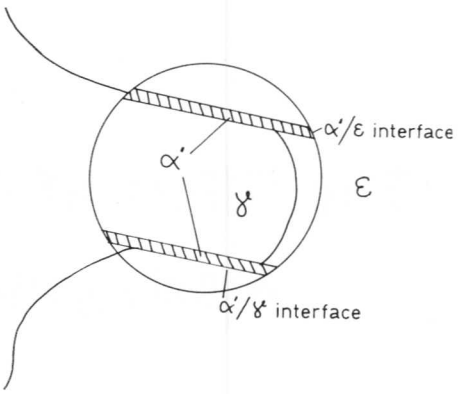

Fig. 8 Schematic interpretation of a partially transformed precipitate. Compare with the precipitates marked D in Fig. 5.

The above argument supposes that there is a mechanism available for developing the appropriate interface. In this work it was found that transformation proceeds by further interaction with matrix dislocations. Thus, it appears that the main factor resisting growth is the lack of a dislocation source associated with the precipitate to develop the appropriate α'/ε interface.

Conclusions

(1) Martensite is nucleated in defect-free precipitates of γ-iron, most probably by screw segments of matrix dislocations moving through the precipitates during deformation.

(2) Growth proceeds by the formation of thin martensite discs, apparently by the motion of screw dislocations in the $(110)_\gamma$ habit plane of the discs, in agreement with Frank's model.[8]

(3) It is deduced that growth by thickening of the discs does not readily occur owing to the lack of a suitable dislocation source at the α'/ε interface. The transformation thus continues by further interaction with other matrix dislocations.

Acknowledgements

The experimental part of this work was carried out in the Laboratory of Physical Metallurgy at the Finland Technical University. The authors are grateful to Professor H. M. Miekk-oja for providing facilities and for the lively interest he has shown in the work. The alloys were kindly provided by the Outokumpu Company. One of them (K.E.E.) acknowledges financial support in the form of a Science Research Council grant.

References

1. K. E. Easterling, Finland Technical Univ., **1965.**
2. R. B. Gordon and M. Cohen, " Age-Hardening of Metals ", p. 161. **1940:** Cleveland, Ohio (Amer. Soc. Metals).
3. J. B. Newkirk, *Trans. Amer. Inst. Min. Met. Eng.*, 1957, **209,** 1214.
4. K. E. Easterling and H. M. Miekk-oja, *Acta Met.*, 1967, **15,** 1133.
5. V. K. Lindroos and H. M. Miekk-oja, *J. Inst. Metals*, 1964-65, **93,** 513.
6. K. Nevalainen, to be published.
7. E. Laurila, *Acta Polytech. Scand.*, 1964, **Ch. 30.**
8. F. C. Frank, *Acta Met.*, 1952, **1,** 15.

The Effect of Austenitizing Conditions on Martensite Transformation by Bursts

A. R. Entwisle and J. A. Feeney

An investigation has been made of the effect of austenitizing temperature on the martensitic transformation in four Fe–Ni–C alloys. All the alloys showed " bursts" at the start of transformation. Increasing the austenitizing temperature resulted in a steady rise in M_B, but the burst size passed through a maximum corresponding to treatment at 1050° C. The burst temperature (M_B) of a given alloy appears to be determined by the heat-treatment to which it had been subjected. The burst size is a function of grain size, and the chemical driving force at M_B. By stimulating transformation above M_B with local plastic deformation, an estimate could be made of the effect of the chemical driving force, and hence of the effect of grain size, ***per se***, on the magnitude of the burst.

The effect of different austenitizing treatments on the M_s of carbon and low-alloy steels has frequently been studied. The results obtained before 1954 have been summarized by Meyerson and Rosenberg.[1] In the absence of any changes in the chemistry of the austenite (e.g. carbide dissolution) it was found that as the austenitizing temperature is increased, the M_s temperature rises. It is not clear, however, whether the changes in M_s are due to the thermal treatment *per se*, or to the associated change in austenite grain size. More recently Sastri and West[2] showed that for austenitizing times of a few minutes, the thermal treatment is the critical factor and they suggested that the number of lattice defects in the austenite (a function of thermal treatment) influences the M_s. Some evidence indicated that the progress of transformation is also sensitive to the austenitizing treatment.

In the case of isothermal transformation, increasing the austenite grain size greatly accelerates transformation[3] and there is clear evidence that the austenitizing temperature influences the transformation, first increasing and then decreasing the initial nucleation rate as the temperature rises.[4]

The experimental evidence relating to steels that commence transformation with a " burst " is limited and conflicting.[5–7]

In the work described below, an attempt is made to separate the effects of thermal treatment and austenite grain size on the transformation behaviour of steels that exhibit " bursts ".

Manuscript received 7 February 1968. A. R. Entwisle, M.A., Ph.D., is in the Department of Metallurgy, University of Sheffield, where the work was carried out. J. A. Feeney, M.Met., Ph.D., is now with Boeing Aircraft Corpn., Renton, Washington, U.S.A.

Experimental

The alloys used in this investigation were taken from vacuum-melted 28-lb ingots. After hot rolling to 0·5-in.-dia. bar, a homogenization treatment of 64 h at 1200° C was given, followed by cold swaging to 0·188-in.-dia. rod. Dilatometer specimens 0·156 in. in dia. × 0·5 in. machined from the rod were then austenitized in vacuum in sealed silica capsules. Treatments between 800 and 1200° C, with times between 15 min and 3 h, were used. Water-quenching the capsules after the austenitizing treatment was found to be necessary to prevent austenite decomposition. After stress relieving (30 min at 450° C) the specimens were ready for experiment. The compositions of the alloys are given in Table I.

TABLE I

Designation	C	Ni	Mn	Si	S	P
19N5C	0·52	19·1	0·14	0·04	0·013	0·011
24N5C	0·51	23·7	0·11	0·03	0·012	0·011
26N5C	0·48	25·7	0·10	0·02	0·015	0·009
27N5C	0·48	27·2	0·11	0·02	0·012	0·010

The transformation behaviour was investigated using a sensitive recording dilatometer,[6] where the specimen was cooled by a uniform flow of cold nitrogen gas. A cooling rate of 30 degC/min was used except as indicated otherwise. Under these operating conditions the apparatus was sensitive to 0·2% transformation to martensite. Temperature was measured by a thermocouple in contact with the specimen (± 0·5 degC). Austenite grain size was determined as the mean linear intercept $\bar{L}$, measured over ~ 400 intersections during traverses of longitudinal sections.

Results and Discussion

The Start of Transformation, M_B

Typical transformation curves for 24N5C are shown in Fig. 1. No transformation was detected before the burst, except for specimens annealed at 800° C which showed other anomalies. The bursts were accompanied by large evolutions of heat (i.e. the enthalpy of transformation) sufficient in some cases to raise the temperature of the specimen by 30 degC, transformation often recommencing before the original M_B temperature was regained. To avoid undue complexity in Fig. 1, the regions of the curves immediately following the burst have been smoothed, and the temperature excursions are not shown. The effect of time at the austenitizing temperature on M_B was relatively small

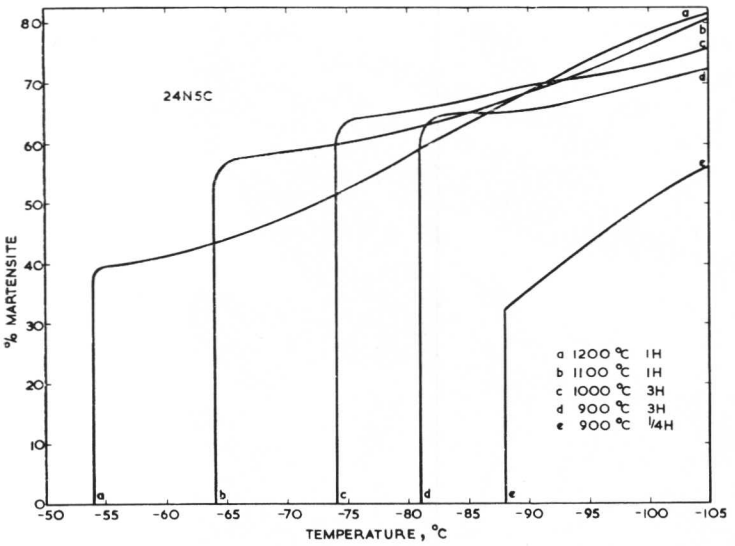

Fig. 1 *Martensite transformation curves for alloy* 24*N*5*C, showing the effects of austenitizing treatment.*

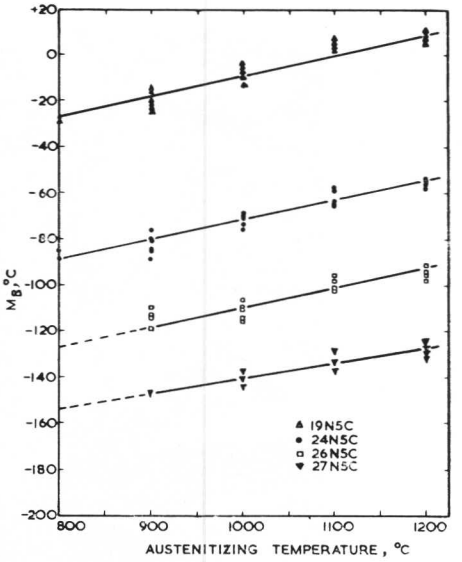

Fig. 2 *Burst temperature* M_B *as a function of austenitizing temperature.*

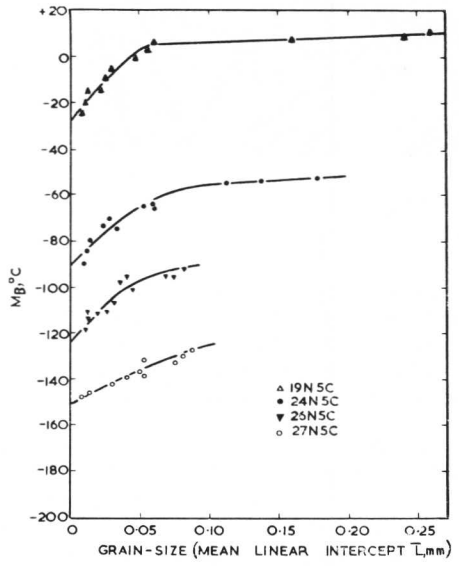

Fig. 3 *Burst temperature* M_B *as a function of austenite grain size.*

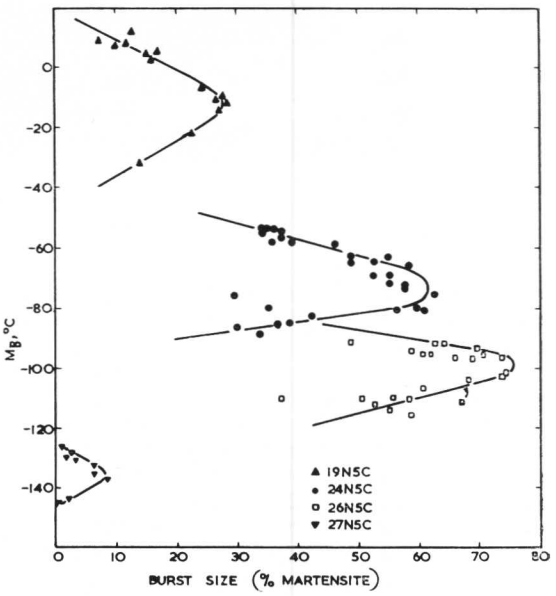

Fig. 4 *Burst size as a function of burst temperature, for spontaneous transformation.*

(a few degC) and was generally lost within the experimental scatter; for low temperatures, e.g. 900° C, the effect of time at temperature was rather more readily detected (curves d and e).

Fig. 2 shows the collected results for M_B as a function of austenitizing temperature. No results are given for the two higher-nickel alloys for 800° C, as graphitization occurred at this temperature. In contrast to the linear relationship between M_B and austenitizing temperature, the relation between M_B and grain size is more complex (Fig. 3). Here the individual grain-growth characteristics of each alloy strongly influence the curves; the almost horizontal parts of the curves for 19N5C and 24N5C arise from the rapid but somewhat variable grain coarsening that occurs above 1100° C. These results are compatible with the view of Sastri and West[2] that the austenitizing treatment is the dominating factor controlling the start of transformation, grain size merely being a dependent variable with essentially no influence on the start of transformation.

There are also conceptual difficulties in explaining any effect of grain size on M_B. In the case of the athermal transformation observed in low-alloy steels, transformation begins gradually, there being a range of 10–15 degC before the transformation curve becomes linear. A grain-size effect on M_s is conceivable in this case since the sensitivity of the measuring apparatus is important in determining the earliest stages of transformation. The M_s, in fact, represents the temperature at which some small amount of transformation is first detected and is therefore dependent on the progress of transformation to some extent.

Where bursts occur, it appears that the first successful nucleating event triggers off the whole burst, and that M_B truly represents the start of transformation. In these circumstances it is difficult to see any mechanism whereby grain

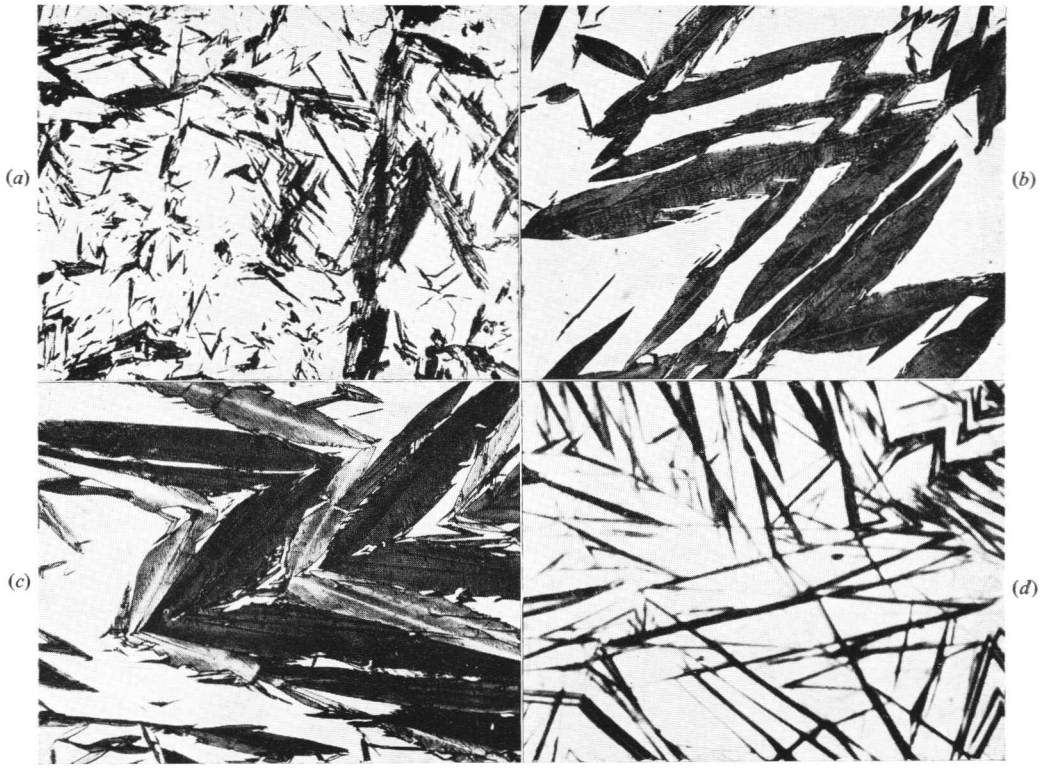

Fig. 5 Microstructures after partial transformation of (a) 19*N5C;* (b) 24*N5C;* (c) 26*N5C;* (d) 27*N5C.* × 200.

size *per se* can influence M_B. A postulated grain-boundary nucleation would be at variance with the general trend of the results shown in Fig. 3.

The Progress of Transformation

The magnitudes of the bursts observed varied systematically with the burst temperature (itself a function of the austenitizing treatment). All the alloys showed the trends exhibited in Fig. 1 and the collected results are given in Fig. 4. For each alloy the curves show a maximum burst size corresponding to an annealing temperature of ~ 1050° C (see Fig. 2). The overall burst size increases with increasing nickel content and the consequent lowering of the transformation range; alloy 27N5C is clearly anomalous.

The progress of transformation, i.e. the burst size in a given alloy depends on (*a*) the chemical driving force, since this will control the efficiency of the autocatalytic processes giving rise to the burst, and (*b*) the grain size, since this limits the volume transformed per plate. These two effects oppose each other on the curves of Fig. 4, since low M_B temperatures correspond with low austenitizing temperatures and small grain sizes, while high M_B temperatures correspond with large grain sizes. Thus, when the grain size is large, the driving force is low, and vice versa. As a working hypothesis it is assumed that grain size dominates on the lower limb of the curves and driving force dominates on the upper limb.

These curves also explain an earlier report[6] that grain size had little effect on burst size. This result was deduced from observations on two grain sizes only obtained by heat-treatment at 1200 and 900° C, and it is now clear that the experimental points would fall on opposite limbs of the appropriate curve of Fig. 4.

The differences in the magnitudes of the bursts in these alloys derive from the different morphologies observed in them. Figs. 5 (*a*)–(*d*) show the microstructures of partly transformed specimens. Alloy 19N5C has the fragmented microstructure typical of mixed (225)γ and (259)γ habit planes which is associated with moderate bursts.[6] Alloys 24N5C and 26N5C show well-formed plates with midribs typical of (259)γ habit planes and strong bursts. The anomalous alloy 27N5C showed a remarkably different microstructure, the thickness to dia. ratio of the martensite plates being nearly an order of magnitude smaller than in the other alloys. This clearly accounts for the much-reduced burst sizes observed in this alloy, despite the fact that the autocatalytic activity seems in no way reduced.

The Effect of Temperature and Grain Size on Burst Size.

In order to disentangle the opposing effects of grain size and temperature (driving force) on the observed burst size, it is necessary to examine one of these effects independently. The driving force may be varied using the effect of hydrostatic pressure[8] or magnetic fields.[9] An alternative method used in the present work is to stimulate transformation above M_B by local deformation, measuring the appropriate burst sizes and temperatures.

Specimens of similar dimensions to those used in the dilatometer were prepared, but with a machined projection 0·15 in. × 0·060 in. in dia. at one end. After thermal treatment, the specimen was lightly held by the projection in the jaws of a pair of wire-cutters, and then immersed in a suitable low-temperature liquid bath held at the desired temperature above M_B. " Tweaking " the specimen by closing the jaws

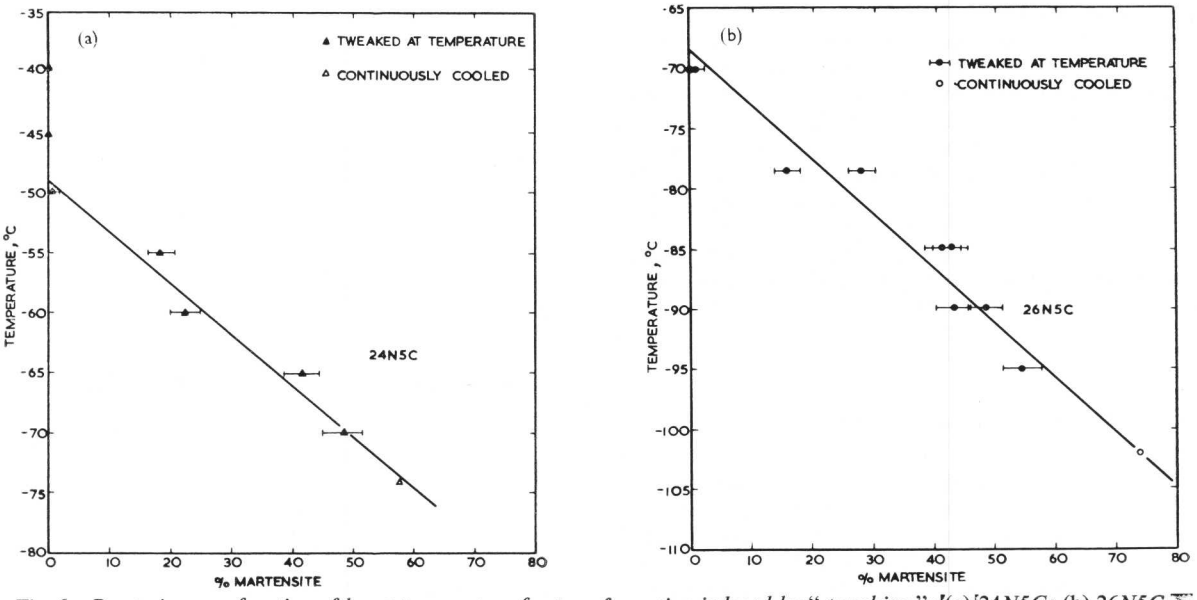

Fig. 6 Burst size as a function of burst temperature for transformation induced by " tweaking ": (a) 24N5C; (b) 26N5C. Both lines were fitted by the least-squares method

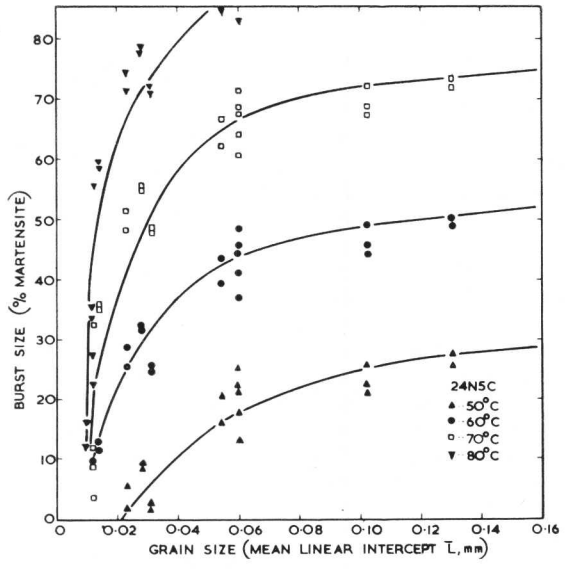

Fig. 7 The effect of austenite grain size on burst size; the data are derived from Fig. 4.

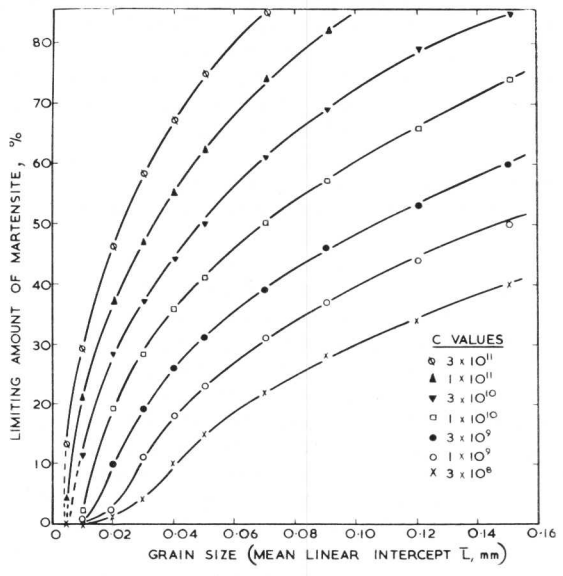

Fig. 8 Variation of the limiting amount of martensite with grain size predicted from equation (1). The autocatalytic parameter c increases as the driving force increases.

of the wire-cutters induced transformation in the projection, which then spread into the larger undeformed region of the sample. After up-quenching to room temperature, specimens were sectioned longitudinally and the amount of transformation estimated by point counting. Experiments of this type were carried out on alloys 24N5C and 26N5C and the results are presented in Fig. 6. Both alloys showed a similar linear dependence of burst size on temperature ($\sim$ 2·2% martensite/degC). Limited evidence from further specimens given different austenitizing treatments suggests that the effect is not sensitive to variations in grain size.

Assuming that the relation between burst size and temperature for the two alloys is defined by the ratio 2·2%/degC, irrespective of grain size, it is now possible to reassess the data given in Fig 4. All the values of burst size on a given curve can be corrected to some chosen temperature and any residual variation of burst size can then be attributed to differences in grain size. Fig. 7 shows the result for alloy 24N5C corrected to temperatures in the range -50 to $-80°$ C. There is considerable scatter of the experimental points and the curves drawn through them can only be regarded as indicating the general trends. The transformation appears to be very sensitive to grain size below 0·05 mm, increasingly so at lower temperatures. The results for alloy 26N5C, treated in the same way, gave very similar curves for the effect of grain size on burst size but were displaced to lower temperatures (by $\sim$ 25 degC).

The residual grain-size effect shown in Fig. 7 is qualitatively reasonable and in this sense the working hypothesis suggested above to account for the curves of Fig. 4 may be considered satisfactory. However further justification for the curves given in Fig. 7 is needed.

Theoretical Development

In a recently developed theory for the kinetics of isothermal transformation to martensite,[3] it is assumed that the untransformed austenite contains embryos (n_i per cm^3) requiring energy ΔW to be activated to form full-scale martensite plates. It is further assumed that the plates create new embryos in proportion to the volume transformed (c embryos per unit volume of martensite). The new autocatalytic embryos are presumed to require the same thermal activation energy as the original embryos. Using the formula for partitioning of the austenite by martensite plates given by Fisher *et al.*[10] it can be shown that the rate of transformation is given by:

$$\frac{dV}{dt} = [-\nu \exp -(\Delta W/RT)]\ [m(1+qc+qn_i-qcV-V^{-1/m})V^{(1+1/m)}] \quad \ldots (1)$$

where V is the volume fraction of austenite remaining after time t, m is the thickness to dia. ratio of the martensite plates ($\sim 1/30$), q is the average volume of an austenite grain, and ν is the frequency of atomic vibration. The parameter n_i is taken to be 10^7/cm^3. Numerical integration of equation (1) enables the isothermal transformation curves to be obtained. Good agreement between experiment and theory is possible if a suitable value of the only freely adjustable parameter, c, is selected. The value selected is $\sim 10^9$/cm^3 for the barely detectable isothermal transformation at relatively high temperatures, and it increases steadily as the temperature falls and the reaction rate increases

Isothermal transformation curves generally show a slow beginning, an acceleration as the autocatalytic effects dominate, and a gradual dying away, approaching a limiting amount of martensite ν_l at long times, when the partitioning of the austenite becomes the controlling factor.

An extension of this approach to low-alloy steel compositions where the transformation range is above room temperature strongly indicates that "athermal" transformation is in fact rapid isothermal transformation.[11]

In the case of alloys of the type studied here which show bursts, it is clear that the autocatalytic effect is essentially instantaneous, and one plate can be considered as directly giving rise to other plates (without thermal activation) because of the very favourable stress field around each plate.[12] If a burst is regarded as an "instantaneous" isothermal transformation in which the whole of the autocatalytic succession of plates propagates in one continuous event, then the magnitude of the burst can be identified with the limiting amount of martensite ν_l, derived from the integration of equation (1).

Fig. 8 shows the dependence of ν_l on grain size for a range of values of the parameter c. In Fig. 9 the experimental curves of Fig. 7 are compared directly with these theoretical curves. The agreement between theory and experiment is encouraging, although considerable discrepancies arise at large amounts of transformation (larger grain sizes). The values of the autocatalytic parameter c required are similar to those used in the theory of isothermal transformation, and as in that case, the values of c required increase as the temperature falls (more properly, as the driving force increases). Thus, the essential difference between isothermal and burst kinetics is that for bursts the autocatalytic embryos are operated immediately, without waiting for thermal activation. A further difference lies in the fact that for isothermal transformation, the pre-existing embryos (n_i/cm^3) play an important role in determining the shapes of the transformation curves. For bursts, it is sufficient to activate one embryo (or at most very few) to start the burst. In the integration of equation (1) n_i was taken to be 10^7/cm^3, appropriate for isothermal transformation but clearly unsuitable for bursts. This discrepancy has no bearing on the present discussion since n_i has almost no influence on the limiting amount of martensite ν_l. Provided that $c\nu_l \gg n_i$, the value of n_i is not significant.*

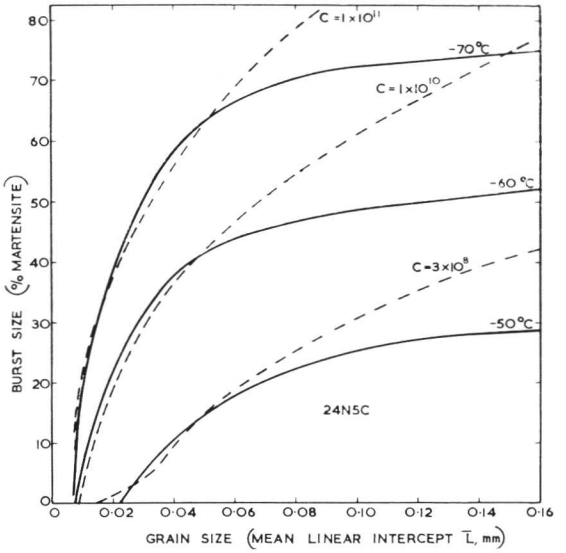

Fig. 9 Comparison of theoretical and experimental curves for the variation of burst size with austenite grain size.

The differences between the theoretical and experimental curves of Fig. 9 may arise from three sources. The predictions of the theory of isothermal transformation are less good at large volume fractions of transformation. The correction of the burst size to different temperatures may not be entirely independent of grain size. The heat evolved during a burst may play some part in limiting the burst size, particularly for large bursts. Despite these difficulties the measure of agreement obtained in Fig. 9 is considered sufficient to support the working hypothesis proposed earlier.

Conclusions

In the iron–nickel–carbon alloys studied, the burst temperature M_B is essentially a function of the thermal treatment to which the austenite has been subjected. The magnitude of the burst is a function of the austenite grain size, and the temperature at which the burst has occurred. By stimulating transformation above M_B, it has been possible to measure directly the effect of temperature on burst size. The effect of grain size on burst size can then be deduced. The relation between burst size and grain size is shown to be in reasonable agreement with predictions from a theory of transformation kinetics originally proposed to account for isothermal transformation to martensite.

---

* It follows directly from the criterion $dV/dt = 0$ that the limiting amount of martensite ν_l satisfies the equation

$$1 + qc\nu_l + qn_i - (1 - \nu_l)^{-1/m} = 0$$

and therefore, provided $c\nu_l \gg n_i$, qn_i can be neglected.

References

1. M. R. Meyerson and S. J. Rosenberg, *Trans. Amer. Soc. Metals*, 1954, **46,** 1225.
2. A. S. Sastri and D. R. F. West, *J. Iron Steel Inst.*, 1965, **203,** 138.
3. V. Raghavan and A. R. Entwisle, " Physical Properties of Martensite and Bainite ", (Special Rep. No. 93), p. 30. **1965:** London (Iron Steel Inst.).
4. S. R. Pati and M. Cohen, *Acta Met.*, 1966, **14,** 1001.
5. E. S. Machlin and M. Cohen, *Trans. Amer. Inst. Min. Met. Eng.*, 1951, **191,** 746.
6. R. Brook and A. R. Entwisle, *J. Iron Steel Inst.*, 1965, **203,** 905.
7. W. Cias, *Prace Inst. Hutnic.*, 1959, **11,** 55.
8. S. V. Radcliffe and M. Schatz, *Acta Met.*, 1962, **10,** 201.
9. K. R. Satyanarayan and A. P. Miodownik, this vol., p. 162.
10. J. C. Fisher, J. H. Hollomon, and D. Turnbull; *Trans. Amer. Inst. Min. Met. Eng.* 1949, **185,** 691.
11. V. Raghavan and A. R. Entwisle, to be published.
12. J. C. Bokros and E. R. Parker, *Acta Met.*, 1963, **12,** 1291.

The Effect of Magnetic Fields on Transformations in Steels

K. R. Satyanarayan and A. P. Miodownik

Evidence for the effects of the superimposition of a magnetic field on transformations in steels is reviewed and extended. The M_s temperature is shifted by 0·1–0·3 degC/kgauss. The shift in the M_s temperature can be accurately predicted from simple thermodynamic considerations. It can be shown that $\Delta S = H\Delta J/\Delta T$, where H is the field strength, ΔJ the difference between the saturation magnetization values of the phases concerned, ΔT the shift in M_s temperature, and ΔS the slope of the free-energy curve at the M_s. This information can be used to confirm that the rate of formation of martensite below the M_s is directly proportional to the rate of change of free energy with temperature. Heats of reaction can be measured from the heat evolved when a specific percentage of martensite is generated by the isothermal application of a field, and combination of such values with ΔS can yield the free-energy change associated with transformation at the M_s. First-stage tempering is appreciably retarded if high-carbon steels are tempered in a magnetic field, or tempered ordinarily after having been previously quenched in a magnetic field. No change in activation energy can be detected, but the results are consistent with the same basic thermodynamic model.

The possibility that a strong magnetic field influences the martensite transformation in steels was first investigated by Sadovskiy *et al.*,[1] who observed that a pulsating magnetic field of 350 kgauss applied at liquid-nitrogen temperatures induced martensite transformation in an austenitic 23% Ni–1·5 Cr–0·5% C steel.

Fokina and Zavadaski[2] studied the effect of field strength and number of pulses on the extent of martensite formation. It was found that the field had to exceed a critical value before martensite could be induced. Once the critical field strength is exceeded, the amount of martensite formed increases sharply, rising to ~ 30% for a field strength of 170 kgauss; most of the martensite is formed during the first cycle and subsequent pulses induce very little additional transformation. The effect of applying various fields at different temperatures is shown in Fig. 1. The whole M_s curve

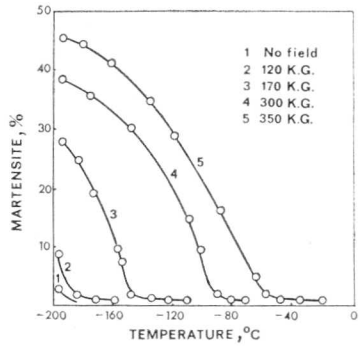

Fig. 1 The effect of pulsating magnetic fields on the course of martensite formation in a 22% Ni–2% Cr–0·5% C steel.[3]

is effectively raised to higher values, the average shift being 0·3 degC/kgauss once the critical field has been exceeded.[3] For less-highly alloyed steels the M_s shift for different alloys heat-treated in fields up to 350 kgauss falls in the range 0·10–0·25 degC/kgauss.[3,7,9,11,13,14]

The Effect of Constant Magnetic Fields

Fokina *et al.*[4] and Gridnev *et al.*[5] have shown that a constant magnetic field generated by a superconducting solenoid produced essentially the same effects as a pulsating field of the same strength. Bernshteyn *et al.*[6] followed the effect of a constant magnetic field on the martensite transformation of nickel steels covering a composition range 0·03–1·1% C and 5–16% Ni, using a field of 4·2 kgauss. No detectable change in the M_s was observed but this is not surprising in view of the small field used; as will be shown later the expected shift in M_s for 4·2 kgauss is only ~ 1 degC.

Satyanarayan *et al.*[7] have studied the effect of a magnetic field on the martensite transformation by using the Greninger–Troiano technique, which allows a direct metallographic estimation of the amount of martensite formed as the transformation proceeds below the M_s.

In agreement with previous Russian work the whole transformation curve is shifted to higher temperatures and, as a result, a greater amount of martensite is formed at any temperature below the M_s when a field is superimposed. The percentage of extra martensite varies in a characteristic manner as the total percentage of martensite increases, falling from a value of 8–9% just below the M_s to 4–5% at lower temperatures (i.e. at ~ 25–30% martensite) for both the

Manuscript received 11 March 1968. A. P. Miodownik, B.Sc., Ph.D., F.I.M., is in the Department of Metallurgy and Materials Technology, University of Surrey, where the work was carried out. K. R. Satyanarayan, M.Sc., Ph.D., has now returned to the Metallurgy Department, Engineering College, Poona, India.

alloys studied. The percentage of retained austenite at room temperature is correspondingly reduced by 5–10%.[6,10]

The Effect of Austenite Stabilization

The effect of pulsating fields on austenite previously stabilized mechanically by plastic deformation is shown in Table I. As might be expected, the critical field strength necessary to initiate martensite transformation increases with increasing amounts of plastic deformation.

TABLE I

Variation of Critical Field Strength Required to Initiate Martensite in a 22% Ni–2% Cr–0·5%C Steel[8]

Percentage before Deformation	Critical Field Strength to Produce Martensite, kgauss
20	105
35	115
50	130
70	170

The effect of a magnetic field on austenite that has been thermally stabilized was investigated using an Fe–Ni–Cr alloy (13·7% Ni–9·0% Cr–0·05% C) with a normal M_s at − 30° C. After soaking at 1100° C the austenite was stabilized at 550° C for 2 h; on subsequent cooling the M_s was reduced to − 90° C. When the alloy was cooled in a field of 350 kgauss (after being stabilized under the same conditions) the M_s increased to − 60° C. These effects are important in relation to interpreting much of the Russian work, in which the investigators have tended to use very complex alloys and heat-treatments before superimposing a magnetic field.

The Effect of Magnetic Fields on Isothermal Transformations

Relatively little work seems to have been done on the effect of magnetic fields on isothermal martensitic transformations. Estrin[9] has studied the effect of periodically applying a field of 18·6 kgauss below the M_s on the isothermal transformation of an Fe–Ni–Mn alloy (22·7% Ni–3·3% Mn–0·06% C). When a field was applied in the transformation range there was no sudden increase in the amount of martensite formed; instead an increase in the rate of martensite formation was observed. On removal of the field the rate of transformation was correspondingly reduced.

Fokina *et al.*[8] investigated the effect of strong pulsating magnetic fields on the martensitic transformation of a similar alloy containing 23·6% Ni–3·6% Mn–0·03% C at − 196 °C. When cooled from the austenitic state, transformation normally starts slowly below room temperature; the transformation rate increases up to − 130° C and then drops. At − 196° C hardly any transformation occurs, and only 4–5% martensite is formed in 24 h. A critical field of 160 kgauss, however, induced transformation at this temperature.

Intermittent Applications of a Magnetic Field below M_s

Periodic application of a magnetic field in the transformation range of a 19% Ni–0·5% C steel has been studied by Estrin.[9] When a field is applied, there is a sudden increase in the additional amount of martensite formed, the effect being more pronounced in the initial stages of the transformation. Estrin has proposed the schematic explanation illustrated in Fig. 2(*a*). If cooling curves are measured simultaneously in such an experiment,[10] a rise in temperature of

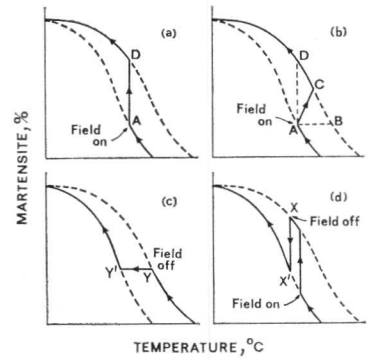

Fig. 2 Schematic illustration of the effects produced by applying a magnetic field below M_s.

~ 3 degC may be observed for a 1·5% Cr–1% C alloy, which obviously relates to the release of latent heat associated with the formation of the extra martensite. The fact that heat is evolved means that a strictly isothermal interpretation of the magnetic-field effect as postulated by Estrin is not entirely true; the actual amount of extra martensite formed is related to a change such as is illustrated by AC in Fig. 2(*b*). Investigations on the relative effect of a continuous and local application of a magnetic field on the percentage of martensite formed substantiate this analysis. The additional amount of martensite formed at 85° C when a field is applied continuously is 9%, while the same field applied instantaneously gives only 6% of extra martensite.[10]

Although the degree of recalescence and changes in the percentage of martensite produced are in reasonably good agreement, it is not possible to predict directly which particular combination of martensite and recalescence will take place within the permissible limits set by AD and AB.

The effect of removing the field during transformation is straightforward; there will be no sudden heat evolution in this case, so the only effect will be a reduction in the driving force for the transformation. Under normal circumstances further transformation will cease until a drop in temperature brings the driving force back to the value corresponding to the point where the field was removed (Fig. 2(*c*)). The case of thermoelastic martensite should be quite interesting because removal of a field could give the reaction path XX' (Fig. 2(*d*)).

The Effect of a Magnetic Field on the Reverse Transformation ($\alpha' \rightarrow \gamma$)

Malinen and Sadovskiy[11] have studied the effect of a magnetic field of 22 kgauss on the reverse transformation ($\alpha' \rightarrow \gamma$) in Fe–Ni alloys (containing 26·5–31% Ni, 0·04–0·06%C), and found that a magnetic field stabilizes the martensite so that the A_s is raised. This is entirely consistent with all the other effects that have been described, though in fact the iron–nickel alloys can show anomalous behaviour due to the presence of ferromagnetic austenite.[7]

A Theoretical Model for Magnetic-Field Effects

It is clear that the major effect of a magnetic field on a thermal martensite transformation is to displace the M_s to higher temperatures; a simple linear thermodynamic model can give a satisfactory qualitative and quantitative explanation for this effect.

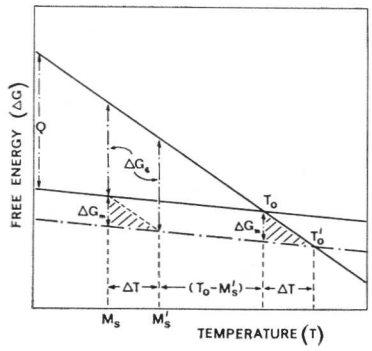

Fig. 3 Linear free-energy model illustrating the origin of the M_s shift.

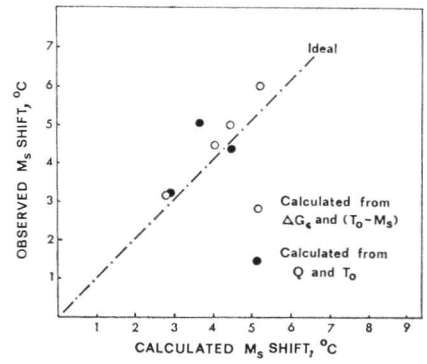

Fig. 4 Comparison of calculated and experimentally observed M_s shifts.

It is generally accepted that to initiate martensite formation an alloy has to be undercooled from T_0 (the equilibrium $\gamma \rightarrow \alpha'$ temperature) to a lower-temperature M_s, because energy has to be made available to overcome the interfacial and elastic restraints (ΔG_ε) associated with the transformation (Fig. 3). The free energy released when 1 mole of austenite transforms to martensite ($\Delta G^{\gamma\rightarrow\alpha'}$) provides the chemical driving force, so that the degree of supercooling required will be determined by the way in which $\Delta G^{\gamma\rightarrow\alpha'}$ varies with temperature. If the transformation takes place in a different environment, e.g. under pressure, P, the position of T_0 will be changed, because the basic free energy of each phase is altered in the new environment. In the case of pressure changes the shift in T_0 will be related to a term $P\Delta V$, where ΔV is the difference in molar volumes of the phases concerned. In the same way, if the transformation takes place in a magnetic field, H, the free energy of each phase is changed by an amount J_xH, where J_x is the saturation magnetization of each phase.[15] The difference in free energy $\Delta G_{mag.}$ of a given volume element in the two crystal structures is therefore

$$\Delta G_{mag.} = H \,.\, [J_{\alpha'} - J_\gamma] = H\Delta J \qquad \ldots (1)$$

where ΔJ represent the difference in saturation magnetization between martensite and austenite. In the case of pure iron and low-alloy steels, austenite is paramagnetic, hence $J_{\alpha'} \gg J_\gamma$ and

$$\Delta J \simeq J_{\alpha'} \simeq J_\alpha \qquad \ldots (2)$$

Provided the M_s temperature is $< \theta_c/2$, where θ_c is the Curie temperature, any temperature variation of J can be considered negligible.[17] The net affect of altering the free energy of martensite by an amount $H\Delta J$ is to raise T_0 to T_0' (Fig. 3). Since magnetoelastic-energy terms are small in comparison with $H\Delta J$,[6,10,12] it may be assumed that ΔG_ε is not affected to a measurable extent. Hence a shift of T_0 to T_0' by ΔT will lead to an equal shift of M_s to M_s' (by ΔT).

It can be seen by inspection that

$$\frac{\Delta T}{(T_0 - M_s)} = \frac{\Delta G_{mag.}}{\Delta G_\varepsilon} \qquad \ldots (3)$$

Alternatively, if the heat of transformation, Q, is known, then it follows that with linear free-energy curves

$$\frac{\Delta T}{T_0} = \frac{\Delta G_{mag.}}{Q} \qquad \ldots (4)$$

The latter relationship was first derived by Meyer and Tagland[16] and is the equation that has been used by Krivoglaz and Sadovskiy,[14] Estrin,[9] and other Russian workers[13] to calculate the shift in M_s due to an applied field.

A comparison of the M_s shift observed by various experimental methods with the values calculated using equations (3) and (4) is shown in Fig. 4.

The first equation is preferred by the present author because in principle it is likely to be a better approximation for non-linear free-energy curves in the vicinity of the M_s.[7,10] The good agreement between calculated and experimental results confirms that the only magnetic-energy term of any importance in the general case is $H\Delta J$. Further evidence that $H\Delta J$ is the major factor arises from the way in which the additional martensite formed below M_s changes with increasing percentage of martensite.[7]

Since the amount of martensite generated by a magnetic field is so simply related to thermodynamic parameters, it is possible to use the effect to derive thermodynamic data for the system and other ancillary information.

Results

The Rate of Martensite Formation below M_s

Brook, Entwisle, and Ibrahim[18] have proposed that the rate of martensite formation (in the region where the amount of martensite formed is linear with decrease in temperature) is a function of the variation of free energy with temperature, that is:

$$\frac{d\%M}{dT} = \frac{d\Delta G^{\gamma\rightarrow\alpha'}}{dT} = K\Delta S_T^{\gamma\rightarrow\alpha'} \qquad \ldots (5)$$

where K is a constant. Since $G_{mag.} = H\Delta J$, it is possible to determine $\Delta S^{\gamma\rightarrow\alpha'}$ experimentally from the M_s shift ΔT. Reference to Fig. 4 shows that at the M_s

$$\frac{\Delta G_{mag.}}{\Delta T} = \frac{d\Delta G^{\gamma\rightarrow\alpha'}}{dT} = \Delta S^{\gamma\rightarrow\alpha'} \qquad \ldots (6)$$

Measurements of the kind presented in Fig. 1 yield both the data required for ΔS and the rate of martensite formation ($d\%\,M/dT$). Koistenen and Marburger[19] have proposed an alternative and more complex empirical relationship for the kinetics of martensite formation of the form

TABLE II

Heats of Reaction and Other Free-Energy Data Derived from Experiments in a Magnetic Field

Alloy Composition	Heat of Reaction, H_T, cal/g-mole	Ref.	Entropy (ΔS_T)	T, °K	Experimental Free Energy ($\Delta G_T^{\gamma\rightarrow\alpha'}$), cal/g-mole	Theoretical Free Energy ($\Delta G_T^{\gamma\rightarrow\alpha'}$), cal/g-mole.
1·5% Cr–1·0% C	600 (± 100)	10	0·9	380	260 (± 100)	265 (Fe–1% C)[23] 516 (Fe–1·1% C–1·8% Cr)[24]
4% Cr–8·5% Ni–0·6% C	620 (± ?)	13	1·4	290	225 (± ?)	360 (calculated from C, Cr, & Ni content only)[10]
20% Ni–2% Cr–0·4% C	120 (± ?)	13	0·85	77	55 (± ?)	

$$(1 - V) = \exp[-A(M_s - T)] \quad \ldots (7)$$

where V is the volume fraction of martensite at a temperature T (below M_s) and A is a constant independent of carbon content in Fe–C alloys. The assumption that A is independent of carbon content can be traced back to Cohen *et al.*,[20] who assumed $\Delta S^{\gamma\rightarrow\alpha'}$ for Fe–C alloys to be constant in the region of interest. Fig. 5 shows that the experimental results are more consistent with equation (5) than with equation (7).

Magnetocalorimetry

Since appreciable thermal effects can be detected after the application of a magnetic field, it is possible to use these effects for measuring heats of transformation.

Voronchikin and Fakidov[13] evaluated the latent heat of martensitic transformations in two steels (20% Ni–2% Cr–0·4% C, 8% Ni–4% Cr–3% Si–0·6% C) by measuring the temperature rise due to the additional amount of martensite formed when a high pulsating magnetic field was applied below M_s.

Temperature peaks were obtained when the field was raised above a critical value and these were correlated with the percentage of additional martensite formed, which was measured by a magnetic method (Table II). (The particular alloys investigated show martensite burst formation which fortunately allowed synchronization of the two measurements.) The accuracy of these results is difficult to evaluate since details of the calculations are not given by the authors.

Direct analysis of the heat evolved from continuously recorded cooling curves[10] merely requires a knowledge of cooling rate in the absence of a field, if it can be assumed that the effect of a magnetic field on the thermal e.m.f. itself can be neglected.[21] The results shown in Table II must be considered a crude form of calorimetry, but it is believed that the method is capable of considerable refinement, so that the application of a magnetic field may ultimately allow accurate measurements of both the enthalpy and entropy of the transformation. Table II includes a comparison of various calculated values relating to the free-energy characteristics of the 1·5% Cr–1% C alloy.

These methods must be distinguished from estimates of the latent heat of transformation using equation (4) which are obviously entirely dependent on the validity of the linear model. Estrin[9] has calculated the latent heat for a Fe–13% Ni–0·5% C alloy on this basis, substituting $\Delta T = 6$ degC in a field, H, of 18·6 kgauss, with $J = 280$ gauss/g and $T_0 \simeq M_s + 200 = 460°$ K. The latent heat was estimated to be $\simeq 7$ cal/g or 400 cal/g-mole.

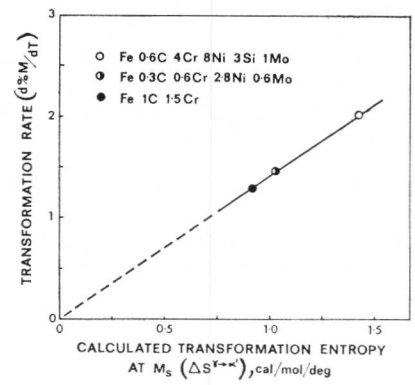

Fig. 5 Correlation between the rate of martensite formation and the entropy of transformation.

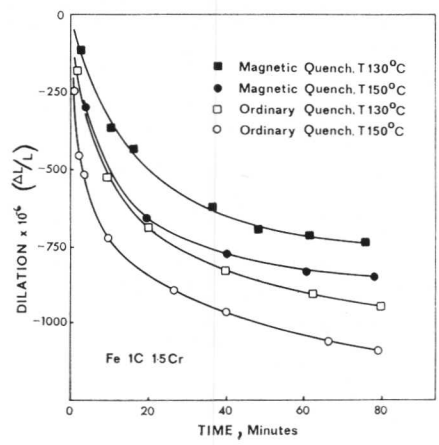

Fig. 6 The effect of prior quenching in a magnetic field (16 kgauss) on the first-stage tempering of a 1·5% Cr–1% C steel.

Changes in the Structure of Martensite Produced by the Magnetic Field

Jahn[22] has reported a refinement in martensite structure which has not been substantiated by other workers, though it may be specific to his experimental conditions. No evidence for any changes in orientation of the martensite formed in a magnetic field has been reported, nor does it seem necessary to invoke any changes in habit planes to account for any of the observed results. Nevertheless, observations on tempering behaviour suggest that the presence of a magnetic field can affect the degree of autotempering which normally accompanies the formation of martensite.

Bernshteyn[6] has reported that quenching specimens of 8% Ni–1·1% C steel in a constant magnetic field of 16 kgauss and then tempering at 175° C *without* a field delays the decomposition of martensite. This effect has been confirmed by work on 1·4% C and 1·5% Cr–1% C steels (Fig. 6). It has also been shown that the change in tempering rates is not associated with any corresponding changes in activation energy (all values fall in the range 19 ± 1 kcal/mole).[10] A similar effect is obtained by tempering in a magnetic field after a normal quench.[6]

Both results can be explained by the thermodynamic principles already outlined, if it is remembered that in the tempering of martensite it is the parent phase that has the higher saturation magnetization, and hence is energetically favoured by the presence of a magnetic field. It is therefore likely that the formation of iron carbide is retarded on tempering, though it is not possible to indicate the precise rate-controlling step. Retardation of iron carbide formation during quenching in a magnetic field is equivalent to a reduction in the degree of autotempering. Without such an hypothesis it is very difficult to see how a magnetic quench could subsequently affect tempering under ordinary conditions.

The Effect of Alloy Composition on the Formation of Martensite in a Field

It is interesting to consider what conditions are likely to lead to the greatest changes in the percentage of martensite as a result of the application of a magnetic field. Reference to Fig. 2 shows that the maximum amount of extra martensite will be produced (for a given field strength) when there is a large shift in M_s combined with a high rate of martensite formation (under normal conditions) as the temperature falls.

The magnetically induced martensite can be expressed by

$$\Delta M = \Delta T \,.\, (d\%\ M/dT) \qquad \ldots (8)$$

Substituting $\Delta T = \Delta G_{mag.}/\Delta S^{\gamma \to \alpha'}$ (equation (6)) and $d\%\ M/dT = K\Delta S^{\gamma \to \alpha'}$ (equation (5)) yields

$$\Delta M = K\Delta G_{mag.} = KH\Delta J \qquad \ldots (9)$$

Thus, though ΔT will be a function of ΔS, the percentage of magnetically induced martensite is independent of the free-energy characteristics of the steel and depends only on the field strength and the difference in the saturation magnetizations of the parent and product phases.

Acknowledgements

The authors would like to thank the B.I.S.R.A. Laboratory, Sheffield, for producing the alloys used in this research project and their colleagues at the University for stimulating discussions. One of them (K.R.S.) gratefully acknowledges the award of a British Commonwealth Scholarship without which the work could not have been carried out.

References

1. V. D. Sadovsky, N. M. Rodigin, L. V. Smirnov, G. M. Filonchik, and I. G. Fakidov, *Physics Metals Metallography*, 1961, **12,** (2), 131.
2. Ye. A. Fokina and E. A. Zavadaski, *ibid.*, 1963, **16,** (2), 128.
3. Ye. A. Fokina, L. V. Smirnov, and V. D. Sadovsky, *ibid.*, 1965, **19,** (4), 101.
4. Ye. A. Fokina, L. V. Smirnov, and A. F. Peikul, *ibid.*, 1965, **19,** (6), 121.
5. V. N. Gridnev, Yu. Ya. Meshkov, and S. P. Oshkaderov, *Akad. Nauk. Ukrain. S.S.R., Struktura Metallicheskikh Splavov*, **1966,** p. 17.
6. M. L. Bernshteyn, G. I. Granik, and P. R. Dolzhanskiy, *Physics Metals Metallography*, 1965, **19,** (6), 77.
7. K. R. Satyanarayan, W. Eliasz, and A. P. Miodownik, *Acta Met.*, in the press.
8. Ye. A. Fokina, L. V. Smirnov, and V. D. Sadovsky, *Physics Metals Metallography*, 1965, **19,** (5), 73.
9. E. I. Estrin, *ibid.*, 1965, **19,** (6), 117.
10. K. R. Satyanarayan, Ph.D. Thesis, Univ. London, **1968.**
11. P. A. Malinen and V. D. Sadovsky, *Physics Metals Metallography*, 1966, **21,** (5), 139.
12. P. A. Malinen, V. D. Sadovsky, L. V. Smirnov, and E. A. Fokina, *Fizika Metallov i Metallovedenie*, 1967, **23,** (3), 535.
13. L. V. Voronchikin and I. G. Fakidov, *Physics Metals Metallography*, 1966, **21,** (3), 119.
14. M. A. Krivoglaz and V. D. Sadovsky, *ibid.*, 1964, **18,** (4), 23.
15. C. Kittel and G. K. Galt, *Solid State Physics*, 1956, **3,** 472.
16. J. P. Meyer and P. Tagland, *J. Phys. Radium*, 1953, **14,** 82.
17. R. M. Bozorth, " Ferromagnetism ". **1955:** New York (D. Van Nostrand).
18. R. Brook, A. R. Entwisle, and E. F. Ibrahim, *J. Iron Steel Inst.*, 1960, **195,** 292.
19. D. P. Koistenen and R. E. Marburger, *Acta Met.*, 1959, **7,** 59.
20. M. Cohen, E. S. Machlin, and V. J. Paranjpe, " Thermodynamics in Physical Metallurgy ", p. 242. **1950:** Metals Park, Ohio (Amer. Soc. Metals).
21. C. Loscoe and H. Mette, " Temperature—Its Measurement and Control in Science and Industry ", Vol. 3, p. 283. **1962:** New York (Reinhold).
22. H. Jahn, *Stahl u. Eisen*, 1958, **78,** (3), 178.
23. W. Kaufman, S. V. Radcliffe, and M. Cohen, " Decomposition of Austenite by Diffusional Processes ", p. 313. **1962:** New York and London (John Wiley).
24. J. C. Fisher, J. H. Hollomon, and D. Turnbull. *Trans. Amer. Inst. Min. Met. Eng.*, 1949, **185,** 691.

Martensitic Transformations in Non-Ferrous Crystalline Solids

D. S. Lieberman

In examining a large number of transformations in crystalline solids, noting similarities and differences among them and comparing them with the " classical " martensitic transformations, such as those in " 259 " steels and AuCd, a simple system for classifying martensitic transformations and martensite-like products has been developed which is described and its adoption recommended. This system differentiates according to the degree of atomic motion for one of the components during the transformation: *orthomartensitic* if all atoms move less than an interatomic distance, as in Fe alloys; *paramartensitic* if diffusion is very short-range with no change in composition, as in ordering to AuCu(II); and *quasimartensitic* if long-range diffusion and composition changes occur, as in the transformation from β-brass to plates of α. In all these transformations, the crystallographic features associated with the shape deformation and habit plane in a partially transformed specimen which characterize and define a transformation as martensitic are exhibited. The deceptive martensite-like twinned product phase that forms by a non-martensitic transformation is termed *pseudomartensite*, as in GeTe–SnTe. Recent observations on the paraelectric to ferroelectric martensitic transition in semiconducting perovskite-type crystals are discussed with emphasis on the intimate relationship between crystal geometry, physical-property changes, and the transformation mechanism. The implications of such transformations for the phenomenological crystallographic theory of martensitic phase transformations are briefly discussed The wide variety of metallic and nonmetallic crystalline solids exhibiting this type of phase change attests to the highly interdisciplinary nature of the phenomenon.

Although a substantial fraction of all the experimental and theoretical work on martensitic or " displacive " first-order phase transformations has been on the iron-base alloys, transitions of this type in pure elements, other solid solutions, intermetallic compounds, and ceramic systems have been studied in some detail. This type of phase change is of particular theoretical interest and often practical significance when it is accompanied by (or there is a change in) some important property. As examples: in iron-base alloys, the transformation on cooling is to a ferromagnetic martensite of high hardness; in the titanates, from paraelectric to ferroelectric; in some oxides, from semiconductor to metallic conductor; in some intermetallic compounds, to an antiferromagnetic, ordered, or ferroelastic product structure.

Because of its practical importance in the steel industry and its consequent concern to many metallurgists, the austenite–martensite transformation in iron-base alloys has received a considerable amount of attention which has resulted in a rather large number of papers and articles.* This is not to say that this type of transformation was not observed and studied in other systems rather early. For example, the intermetallic phases of copper were investigated in the Cu–Al and Cu–Zn systems by Kurdjumov and his co-workers[1–4] and by Greninger[5] and the CuSn alloys by Smith[6] and by Greninger and Mooradian;[7] the order–disorder, precipitation, " massive ", and displacive transformations in Cu alloys have continued to attract interest up to the present.[8,9] The β to β′ transformation in near-equiatomic Au–Cd alloys was also studied quite early; Ölander[10] and Benedicks[11] pointed out the remarkable "rubber-like " or ferroelastic behaviour of the product phase resulting from a first-order martensitic transformation of the ordered CsCl phase. The Wechsler–Lieberman–Read (W–L–R) phenomenological theory of the crystal geometry of martensitic transformation was developed 15 years ago to describe the easily observed single-interface transformation in this alloy[12] (and in the In–Tl[13] system), but was first presented and published as applied to the austenite–martensite transformation in Fe–Ni–C[14] because of the widespread metallurgical interest in steels; its successful application to the iron-base alloys is certainly the more impressive (and in a sense, surprising) as will be discussed below.

The mechanism of martensitic transformations cannot be considered separately from consideration of the constraints of crystal geometry and physical-property changes. The examination of a transformation with generalized and often only qualitative arguments based on the W–L–R descriptive theory of martensitic transformations can provide insight into the nature of the specific transition and the probability that certain mechanisms were or were not operative. This approach is particularly enlightening when the presence of, absence of, or change in some critical physical or chemical property associated with the transformation is also taken into account. Thus, utilization of the physical principles of the *crystallographic theory* and some consideration of *properties* are necessary to elucidate the *mechanism.* A simple

Manuscript received 3 July 1968. D. S. Lieberman, is in the Department of Mining, Metallurgy, and Petroleum Engineering and the Materials Research Laboratory, University of Illinois, Urbana, Illinois, U.S.A.

* These are referenced most completely in the proceedings of the Scarborough Conference, " Physical Properties of Martensite and Bainite " (Special Rep. No. 93). **1965:** London (Iron Steel Inst.), and the proceedings recorded here. The two articles by J. W. Christian, for example, in these two proceedings contain, respectively, 136 and 168 references to work in ferrous and non-ferrous systems; no attempt will be made here to be exhaustive.

and meaningful system of designations to differentiate martensitic and closely related transitions and products is first proposed. Observations on some transformations exhibiting a remarkably wide variation of kinetic and morphological characteristics are also reported and comparisons between transformations in non-ferrous and ferrous systems are made where appropriate.

Classification of Martensitic and Martensitic-Like Transformations and Products

The use of the terms " martensite " and " martensitic " for the product phase and transformation, respectively, has been reviewed[15–17] and a fairly complete list of the many elements, alloys, and other systems exhibiting this type of transition has been compiled.[8,9,18–20]

The generally accepted geometric or crystallographic features that characterize martensitic transformations include:

(i) A *shape deformation* which results in surface upheavals in a polished reference surface of the parent or a sharp dihedral angle between parent and product indicating that, macroscopically, the transformation consists of a shear on an undistorted plane and a possible volume change perpendicular to it, i.e., an *invariant plane strain.*

(ii) The transformation is *heterogeneous* since it is accompanied by the formation of new interfaces.

(iii) The interface or *habit plane* separating parent and product in a partially transformed crystal is on the average undistorted.

(iv) The habit plane is generally *irrational* with its normal having direction cosines characteristic of the material.

(v) A lattice correspondence exists between a unit cell in the parent and one in the product, which is not necessarily unique.

(vi) There is a rather precise *orientation relationship* between principal directions and planes in the two phases on either side of the interface.

(vii) There is a discontinuous change in some parameter, such as the lattice constants, during the transformation.

(viii) Atoms frequently move less than an interatomic distance and hence nearest neighbours (or at least atomic sites) are maintained as far as possible during the change in crystal structure.

(ix) There is usually a change in crystal symmetry and most of the time no change in composition.

(x) There is frequently evidence of a fine inhomogeneous structure such as slip or twinning, in the parent or product phase (usually the latter) which does not alter the lattice, i.e. it is a *lattice-invariant shear.*

(xi) Generally there is a temperature hysteresis and the transformation is *polymorphic.* Sometimes a series of transformations of decreasing symmetry is observed as the temperature is decreased, such as cubic to tetragonal to orthorhombic in some of the actinides and in some perovskite-type crystals.

In many systems, martensitic transformations appear to occur isothermally,[17,21,22] even in the same alloys which under other conditions appear to transform under continuous cooling. In some systems, the transformation strains and consequent volume and shear restraints are so large that the transformation proceeds by the nucleation of many plates which grow very little, while in other systems the transformation goes to completion by the *growth of only a few large domains* of the product[21] (or even sometimes by the movement of a *single* interface). In the former class, the transformation may be very rapid (10^{-6} sec for each event) while in the latter, minutes or hours may be required for transformation. This type of growth may only be slow on a macroscopic scale. It is possible that the interface moves through a small distance rapidly but then must stop to allow relaxation at the interface before it can move again. The range of morphologies, rates, and behaviour is so large and varied that kinetics, for example, is not a very fruitful criterion for martensitic transformations. Hence only the geometric and crystallographic features delineated above will be considered as distinguishing characteristics since the salient ones are exhibited by all martensitic transformations.

The shape deformation (i) is a *necessary* condition for any martensitic phase change and rather implies most of the other criteria and features as will be emphasized below. Certainly if the geometric and crystallographic features are to be observed and determined, measurements must be made of the interface and of both phases in the immediate vicinity of the interface. This is possible only if (1) the interface can be preserved, as in the cubic to tetragonal transformation in iron-base alloys where the martensitic plates grow to a finite size and retained austenite and martensite can be examined on either side of the habit plane boundary,[23] or (2) the transformation goes to completion but where the interface can be stopped or started at will, as in the single-interface CsCl to orthorhombic transformation in a near-equiatomic Au–Cd alloy,[12,13] or (3) the macroscopic interface velocity is low during the transformation. Unless the interface and hence both phases can be observed and studied together, it cannot be demonstrated that the transformation was indeed martensitic even though the product phase may be deceptively like martensite.

The classification system herein proposed differentiates according to the relaxation of item (viii) on the movement of the atoms of at least one of the species. If no atoms move more than an interatomic distance, the transformation is here designated as *orthomartensitic.* If some atoms can move an interatomic distance or so (very-short-range diffusion) while atomic sites are maintained and composition remains invariant (as in ordering), then the transformation is called *paramartensitic.* If at least one of the species moves over large distances and long-range diffusion occurs to produce a composition change, the transformation is termed *quasi-martensitic.* In all these cases the crystallographic features characteristic of a martensitic transformation are exhibited, however. These three general categories can be assigned an L number indicating this degree of atomic movement, which would be $L = 0$, $L \simeq 1$, and $L \gg 1$, respectively. Finally, there are transformation products that look like martensite even though the transformation mechanisms producing them are not martensitic; these products will be called *pseudo-martensite* to emphasize their deceptive or false nature. This classification system is discussed in some detail here. Only a few examples are given here of each category—others will be found in the extensive literature referred to previously. Christian's[17] way of describing and classifying transformations will be related to that presented here where appropriate.

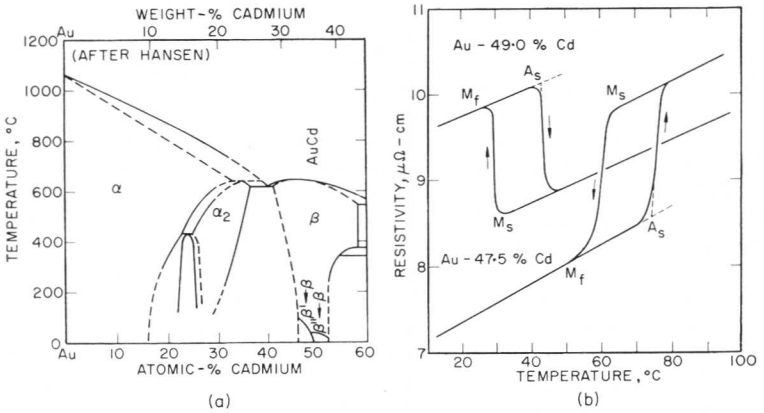

Fig. 1 Part of the Au–Cd phase diagram showing (a) *the two transformations in the narrow* β *field and* (b) *the two reversible martensitic phase changes. Note that the* ~20% *change in resistivity is in opposite directions for the two transformations.*[65,67]

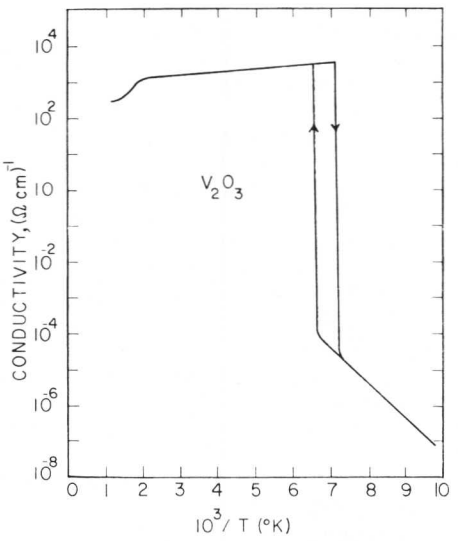

Fig. 4 Conductivity vs. temperature for a single-crystal sample of V_2O_3.[38]

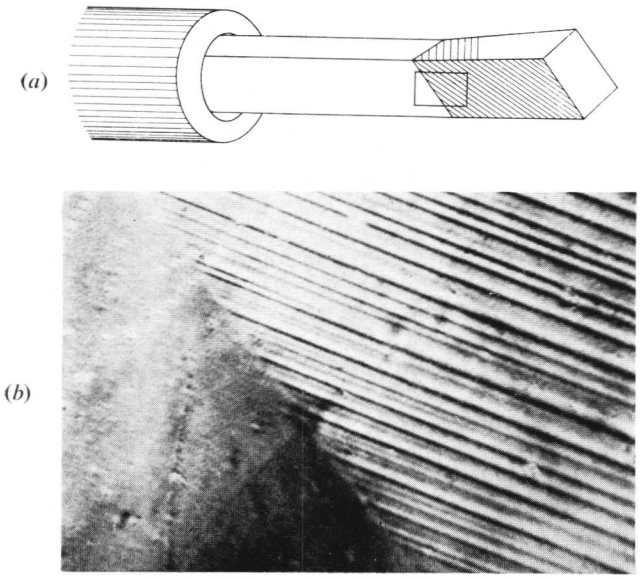

Fig. 2 A single-interface transformation in AuCd. (a) *The power to the heater at extreme left has been adjusted so that the* β′ *twinned orthorhombic phase has nucleated at the right-hand end and is moving toward the left.* (b) *Photomicrograph of the interface with the parent CsCl single crystal on the left and the transformed twinned orthorhombic phase on the right.* × ~ 300. (*Micrograph courtesy of B. S. Subramanya.*)

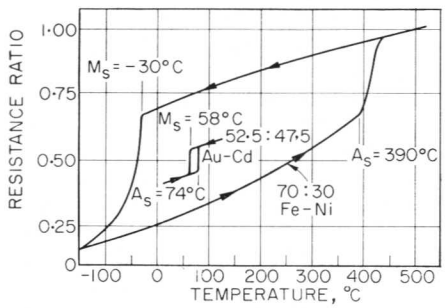

Fig. 3 Electrical-resistance changes during the cooling and heating of an Fe–Ni and an Au–Cd alloy, illustrating the hysteresis between the martensitic reaction on cooling and the reverse transformation on heating.[21]

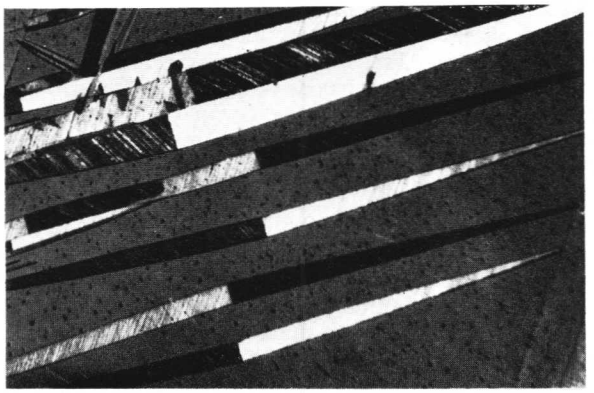

Fig. 5 Microstructure showing sub-bands, "diamond" figures, and habit plane in an AuCu specimen transformed for 18 *h at* 400° *C.*[41] *Polarized light.* × 150.

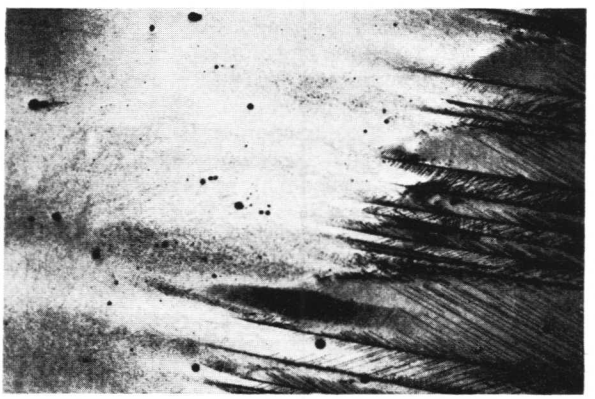

Fig. 6 Transition zone between the cubic structure and the twinned tetragonal structure in a single crystal of AuCu quenched after partial transformation in a temperature gradient.[41] × 50.

Orthomartensite

The f.c.c. austenite → twinned b.c.t. martensite transformations in iron-base alloys (particularly those exhibiting the so-called "259"-type habit) obviously satisfy the criteria listed above and hence must be considered as *orthomartensite*. Among the other metallic systems, the CsCl phase in near-equiatomic Au–Cd alloys (Fig. 1 (*a*)) is one of the most attractive for studying phase changes (as well as point defects[25,26] and diffusion[27] in ordered alloys) and the $\beta \rightarrow \beta'$ transformation is one of the clearest examples of this category. Alloys having compositions near 47·5 at.-% Cd transform to the β' twinned orthorhombic phase at $\sim 60°$ C on cooling, while alloys having near-equiatomic compositions transform at 30° C to a β'' phase which also has a lower symmetry than the parent structure. Fig. 1(*b*) shows typical plots of resistivity against temperature for these transformations. Chang and Read[28] first reported that the transformations go to completion and exhibit relatively narrow temperature hysteresis widths of ~ 15 deg C. The transition region of a few degrees between the beginning and end of the $\beta \rightarrow \beta'$ transformation on cooling in the 47·5 at.-% Cd alloy indicates that this reversible transformation occurs only with continuous temperature change; the behaviour appears to be independent of the rate of variation of the temperature. A common mode of transformation (and the easiest one to analyse) is that by the movement of a single interface[12,13,28,29] which is clearly visible because of the dihedral angle between the single-crystal parent and twinned product phases at the undistorted interface separating the two, as shown in Fig. 2. Since the transformation can be stopped at will[12,29] and does not proceed isothermally, all the geometric features associated with the parent, product, interface habit plane, and fine structure can easily be determined with X-ray, optical microscopy, and interference fringe studies; these were found to agree with the values calculated using the W–L–R theory to within experimental error.[12]

These two cases epitomize the extremes of morphology and something of the range of kinetic behaviour exhibited by orthomartensitic transformations and support the argument that such a variation militates against kinetics being a fruitful criterion for characterizing such transitions. Kaufman and Cohen[21] in an early review article compared in some detail these rather important differences in terms of the significance of nucleation in the iron-base alloys, for example, and growth of existing plates or domains in the systems exemplified by Au–Cd. Christian[17] has also discussed these types. Fig. 3 shows the comparison in the widths of the hysteresis loop for the two cases. The sizeable discrepancies in the amount of undercooling and superheating required are directly associated with the magnitudes of the transformation strains involved: a contraction of 18–20% and a (perpendicular) expansion of ~ 12% in the f.c.c. → b.c.t. transformation in Fe alloys[14,23] and a contraction of 5% and expansions of 3·5 and 1·3% in the cubic → orthorhombic transformation in Au–Cd.[12,30] It was argued that the large shear and volume constraints and considerable strain energy involved in the former inhibit the growth of plates and produce a nucleation-controlled transformation. However, as will be discussed later, even here minimization of the strain energy at the interface must be the dominant factor since this is the term considered in the simple phenomenological crystallographic theories which successfully account for all of the features in the " 259 "-type cases at least.[14,17,23,24,31]

There is a type of martensitic transformation in metallic systems that occurs only between close-packed structures and that Christian[17] has called " fully coherent ". He points out that " . . . such a transformation is expected in f.c.c. alloys with low stacking-fault energies " and gives as examples the transformation in cobalt and its alloys and ε-martensite formation in some steels. The invariant habit plane here is the close-packed plane in each structure and the two structures match in this plane. Christian[17] describes it as " the most disciplined of all transformations "; it satisfies the general geometric and crystallographic criteria and is *orthomartensitic*. Generally, martensitic transformations require some additional lattice-invariant shear to permit matching across the interface boundary as the ones herein described, which would therefore be " semi-coherent ".

Many non-metallic systems, particularly oxides of various types, exhibit sequences of phase transformations to products of decreasing symmetry as the temperature is decreased, many of which have been reported to be first-order and probably are martensitic. Indeed, at least one phase change *to* an oxide has been shown to be martensitic.[32–34] A comprehensive study of these transformations is now in progress and no attempt at a bibliography will be made in this paper. However, first-order transformations have been observed in $MgMn_2O_4$[35] and $NiCr_2O_4$;[36,37] in both cases a temperature hysteresis is reported with both phases simultaneously observed (by X-rays) in a certain temperature region; the X-ray lines of one phase become more intense while the lines of the other phase decrease in intensity as the transformation proceeds. Although no observations *per se* have been reported of the interface nor of bands or twins in the tetragonal phase, nevertheless the evidence is strong that these are *orthomartensitic* transformations. The first-order cubic → tetragonal transformation in semi-conducting $BaTiO_3$ and KTN will be discussed later while the semiconductor to metal transformation, as in V_2O_3[38] shown in Fig. 4, is currently receiving a considerable amount of attention.[34,39,40]

Paramartensite

In the orthomartensitic transformation discussed above, criterion (viii) obtains *strictly*; atoms are considered to move less than an interatomic distance in a shear-like manner, nearest neighbours are maintained as far as possible and hence the degree of order existing in the parent is preserved in the product. It is now suggested that if there is no change in overall composition during a transformation and that if only criterion (viii) is relaxed while the other criteria are satisfied (particularly simultaneous observation of both phases separated by an invariant plane interface) then the transformation be designated as *paramartensitic*. Christian[17] discusses this type of transformation where " . . . the formation of a superlattice from a solid solution is accompanied by a change of shape and has the crystallography expected of a martensitic reaction ". The short-range diffusion required to accomplish the ordering still permits Christian to " . . . describe the situation approximately by stating that there is a correspondence of atomic *sites*, although migration of individual atoms over a few interatomic distances on these sites can take place ".

Examples of paramartensitic transformations are the isothermal cubic → twinned ordered orthorhombic structure AuCuII in the range 380–400° C[41,42] and probably the similar transformation in CoPt at between 815 and 822° C.[41] The former, shown in Fig. 5, has been analysed in detail by Smith and Bowles,[41] who employed the Bowles–Mackenzie formulation of the crystallographic theory[31] to account for the crystallographic features. Other examples of this type will probably be found in systems which are similar to AuCu or CoPt.

Quasimartensite

If the condition that there be no change in composition is now relaxed so that *long-range diffusion* of at least one of the species is permitted, then the transformation may still involve a shape change and deformation and the other crystallographic features associated with martensite formation. If so, the resemblance to such a transition is close enough for the process to be termed appropriately *quasimartensitic*. Christian[17] has discussed some transformations falling into this category using the term " quasi-military " and his description is adopted here as part of the definition of this designation: " Considering an alloy in which the two components occupy different sets of sites ... it may happen that ... one component is sufficiently mobile for long-range diffusion to take place, while the other is relatively immobile. The whole transformation may then consist in the diffusion of the mobile component to form phases of different composition combined with a rearrangement of the atomic configuration of the other component by a martensitic type transformation. There will then be a lattice correspondence for the slow-moving component. . . .".

Thus, whereas a shape deformation as shown by surface upheavals or a dihedral angle between phases at the interface (a *necessary* condition for all martensitic transformations) implies most of the other geometrical features (and hence may be *sufficient* as well), the converse is not true. For example, while the shape deformation implies an orientation relation between directions and planes in the two phases on either side of the interface, an orientation relationship does not imply a shape deformation. Certainly, from simple energetic arguments, it is reasonable that close-packed planes and directions will remain approximately parallel during any kind of transformation. It may also be possible to use discrepancies between the observed orientation relationship and that predicted by theory of martensitic transformations to deduce something about the nature of the transformation.

A few illustrations of quasimartensitic transformations can be given. Bowles and Tegart[43] reported that the geometric features of the early stages of the diffusion-controlled precipitation of b.c.c. CuBe from f.c.c. alloys containing 1·80–1·95 wt.-%Be seemed to be described consistently by the Bowles–McKenzie formulation of the phenomenological theory of martensite formation. Long-range diffusion must occur during this transformation, which thus appears to be quasimartensitic.

Another example is the transformation of β-brass to plates of α whose slow isothermal growth is apparently controlled by the diffusion of zinc away from the transforming region. Garwood[44] first suggested that this transformation in a 41·3 at.-% Zn alloy be called " bainitic " when he reported that the plates adopt the same habit planes as the martensitic transformation product in the same alloys and that the formation of the plates is accompanied by a surface-relief effect in which the transformed volume appears to undergo a homogeneous shear. More recently,[45] he used the graphical formulation of the W–L–R theory[46] to analyse this transformation and found good agreement between predicted values of the crystallographic features and experimental results; it therefore seems reasonable to denote this process as quasimartensitic. The question as to which bainitic transformations can properly be included in this classification will not be discussed in detail. It is probably correct for some transformations in other copper alloys and for lower bainite in iron-base alloys, since Garwood[45] found similar effects where lower bainite forms as supersaturated ferrite by a diffusionless martensitic-type reaction followed by carbide precipitation behind the moving interface with the growth velocity limited by carbon diffusion. Christian,[17] in discussing the relation between bainitic and his " quasi-military " transformations, points out that this transformation has also been considered as interface-controlled isothermal growth. Srinivasan and Wayman[47,48] have reported on isothermal transformations in Fe–7·9%Cr–1·1%C and suggest that " ... lower bainite forms by a shear mechanism not unlike martensite ", while upper bainite forms by a different mechanism.

Pseudomartensite

The three previously described transformation classes exhibit all the crystallographic features in partially transformed specimens which characterize true martensitic transformations and were differentiated only on the basis of the degree of atomic interchange for one of the components. However, the martensite-like *appearance* of the product of a transformation, such as a banded surface indicating surface upheavals among twin-related regions of the product, is no proof that it was formed by a martensitic transformation unless surface upheavals were observed between parent and product across an interface during transformation. Products of a transformation that is not martensitic (as defined by the characteristic crystallographic features) exhibiting this deceptive appearance will be termed *pseudomartensite*.

Systems such as Au–Cu may exhibit true martensitic behaviour as well as pseudomartensitic behaviour in the same alloy, depending on thermal history. The paramartensitic cubic → twinned orthorhombic transformation at 380–400° C has already been mentioned above.[41] When, however, ordering occurs isothermally below 380° C, the transformation product is a twinned tetragonal structure but the transformation is *not* martensitic. No sharp interface exists between the two phases; rather, as shown in Fig. 6, there is a gradual increase in the degree of order and tetragonality over an appreciable region. Smith and Bowles[41] conclude that " ... for the conditions studied, the tetragonal phase does not form at the expense of the cubic phase by the advancement of a well-defined interface. The results are consistent with the view that the bands are mechanical twins which form after some degree of order and tetragonality has developed". When the transformation is complete, the surfaces of the crystal and the product are not inconsistent with their formation by a martensitic phase change; hence the name *pseudomartensite* is appropriate for this product.

A continuous cubic → rhombohedral transformation in GeTe–SnTe alloys was reported by Bierly *et al.*,[49] who observed that the angle α varied continuously from 90° at T_c = 400° C to 88·25° at T_c = 20° C. Markings resembling those produced by twinning were observed in the surface of the rhombohedral material at room temperature; the authors suggest that these are twins produced at temperatures below T_c as a result of the strains set up by the continuously increasingly rhombohedral distortion with decreasing temperature. The product is pseudomartensite but the transformation, like the one described above, is second order with no discontinuity in the lattice parameters at T_c.

The cubic → twinned tetragonal transformation in V_3Si has been extensively studied,[50–61] at least partly because of its transition to a superconductor just below the completion of this structural transformation. The transformation has been reported as continuous by some workers,[54] while others conclude that it is martensitic.[61] If it is the former, the product is probably a pseudomartensite with the twins forming to relieve the stresses set up as c/a increases on cooling; this will be discussed elsewhere.[34]

(*a*)

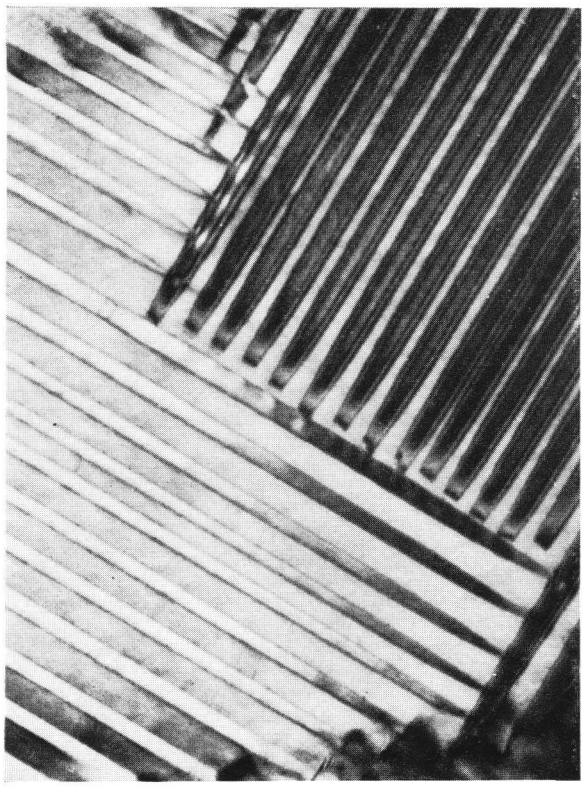

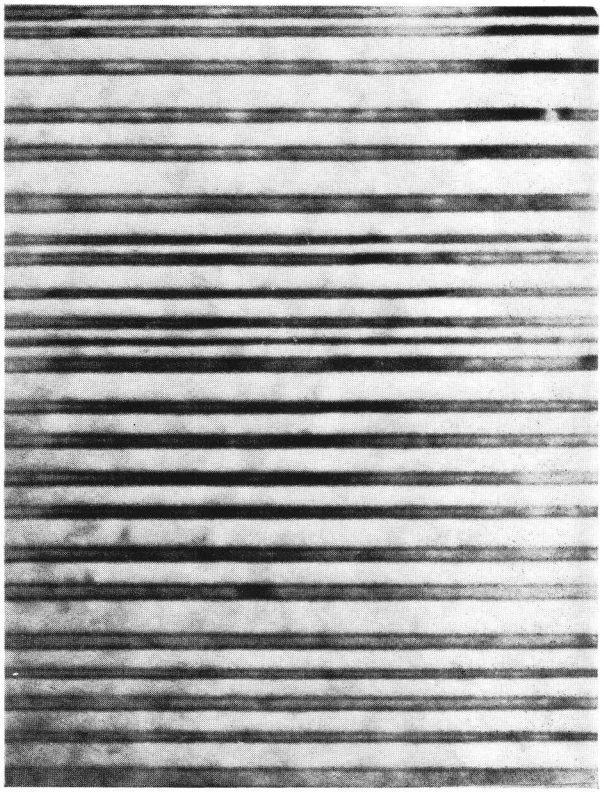

(*b*)

Fig. 7 (a) *Twinned structure of the ordered NiMn alloy transformed by slow cooling*;[9] *note twinning on several* $\{110\}_t$ *planes.*[62] × 100,000.

(b) *Parallel twins in quenched NiMn; the interfaces in the* $(111)_t$ *planes are parallel to the electron beam.*[63] × 400,000. (*Micrographs courtesy of S. Amelinckx.*)

Transformation Behaviour Changes and the Relation Between Crystal Geometry, Physical Properties, and Probable Mechanisms

Although there is unquestionably an intimate relationship among property changes, mechanism, and modes of transformation in all phase changes, it is usually not obvious. Applying an external field or stress, quenching, or changing the thermal history, altering the conditions or state of the parent phase or altering the composition very slightly, may profoundly affect the transformation. Observations of such effects do not always contribute to the understanding of the basic phenomena but they can provide clues as to the nature of the mechanisms if examined within the framework of the phenomenological theory, as will be shown by a few examples.

Phase Transformations in NiMn

Even when data and observations are incomplete, qualitative arguments based on the W–L–R phenomenological theory may provide some insight into the modes of transformation that could have been operating in a specific system and may suggest the direction of further investigation. Two interesting transmission electron microscopy studies of the product phases in NiMn, following transformation under two different sets of cooling conditions, have been reported by Kraševec *et al.*[62,63] When the bulk specimen was *slowly cooled* from the high-temperature CsCl phase before thinning, order twins and anti-phase boundaries in antiferromagnetic tetragonal NiMn were observed. However, when an alloy of the same nominal composition was *quenched* from the high-temperature parent phase before thinning, a superstructure due to periodic twinning in the ordered f.c.t. structure was found. The critical point for this discussion is that Kraševec *et al.* reported that although the crystal structures of the product phases are apparently the same* i.e. f.c.t. with $c/a = 0{\cdot}96$, the twin planes are quite different: $\{110\}_t$ in the slow-cooled specimen shown in Fig. 7(*a*) and $(111)_t$ in the quenched specimen shown in Fig. 7(*b*). Using the simple ideas and model of the W–L–R theory, it will now be shown that whereas the $(111)_t$ twinned f.c.t. structure was very probably produced by an orthomartensitic transformation from the CsCl phase on quenching, what appears to be the same f.c.t. structure twinned on $(011)_t$ produced on slow cooling was not a result of the same type of transformation.

The lattice correspondence between the product tetragonal and parent CsCl phases is shown in Fig. 8; the Bain distortion which transforms the CsCl parent lattice into the product f.c.t. lattice can be viewed as from a f.c.t. cell having $c/a = 1/\sqrt{2} = 0{\cdot}707$, delineated within the parent CsCl lattice in Fig. 8(*a*), to the observed product f.c.t. cell with $c/a = 0{\cdot}96$, as shown in Fig. 8(*b*). Examination of Fig. 8(*a*) shows that $(011)_t$ comes from $(112)_c$ and $(111)_t$ comes from $(101)_c$, respectively, during this transformation distortion. The Bain distortions $\eta_1 = \dfrac{a}{a_0\sqrt{2}} = 0{\cdot}888$ in the x–y plane and $\eta_2 = \dfrac{c}{a_0} = 1{\cdot}192$ perpendicular to this plane have been

* That the product crystal structure is apparently the same for such widely different heat-treatments is not unique, as shown by the Au–Cd system, where the same specimen seems to transform to the same product crystal structure under different conditions and with markedly different kinetics and morphology.[64] It will be assumed that this is the case for NiMn since there is no evidence to the contrary.[62,63,65,66]

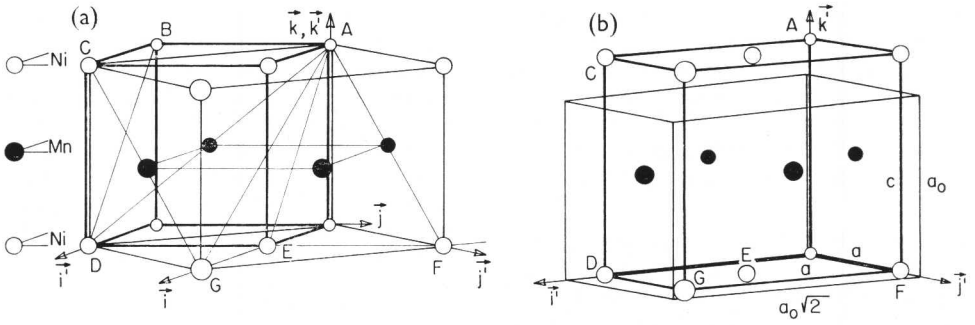

Fig. 8 (a) *Geometrical relationship*[63] *(lattice correspondence) between the CsCl parent structure* (c) *and the tetragonal product structure* (t) *in NiMn.* $(112)_c = AGF = ACGF \rightarrow (011)_t$ *and* $(101)_c = ABDE = ADF \rightarrow (111)_t$. (b) *The Bain distortion takes the tetragonal cell with lattice constants* a_0 *and* $\sqrt{2}a_0$ *into the product cell with* c *and* a.

calculated from the average room-temperature lattice constants of the tetragonal phase and the CsCl lattice constant at 745° C.*[65,66] In this alloy one of the distortions is greater than unity and two are less than unity. Hence, since none is *exactly* unity, there must be an additional lattice-invariant shear in the transformation distortion if the transformation is martensitic with an interface or habit plane between the two phases which is undistorted, thus permitting the strain energy associated with the transformation to be minimized.

Using the graphical method,[46] it was found that whereas the Bain cone (containing vectors that are unchanged in length owing to the transformation distortion implied in Fig. 7) intersects $(101)_c$ (which becomes $(111)_t$), it does not intersect $(112)_c$ (which becomes $(011)_t$), although it is close to it. Since it has been shown that one of the conditions for the existence of an undistorted habit plane is that the plane of the lattice invariant shear part of the total transformation distortion must intersect the Bain cone if a solution for a undistorted habit plane is to exist, we conclude that the transformation in NiMn to a $(111)_t$ twinned product is *orthomartensitic* while the transformation to an $(011)_t$ twinned product is probably not. Then the $(011)_t$ twinned product is *pseudomartensite* and the transformation is probably second-order. However, as recently suggested by Amelinckx,[68] the compositions of the two alloys could be different and ordering might be occurring with a different sequence of structures. In that case, the twinned product could be *paramartensite* or *pseudomartensite*, as in the AuCu system described earlier. However, the essence of the argument is that an idea of the possible nature of the transformation and fruitful directions for future work can be deduced from even limited or incomplete observations examined within the framework of the phenomenological theory.

The Paraelectric to Ferroelectric Transformation in Perovskite-Type Crystals

The transformation from the high-temperature paraelectric (cubic) phase to the ferroelectric (tetragonal) phase in semiconducting $BaTiO_3$ and $KTa_{0.65}Nb_{0.35}O_3$ (KTN), as reported by DiDomenico and Wemple,[69] is a striking example of the interrelationship among physical properties, crystal geometry, and mechanism. Fig. 9 shows that the transformation in KTN is first-order martensitic. The explicit expressions for the direction cosines of the habit plane normal predicted by the

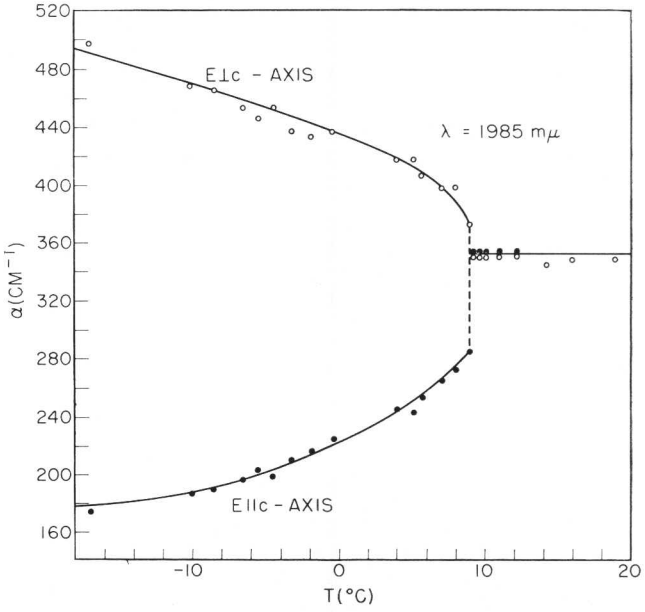

Fig. 9 *Optical absorption coefficient* α *as a function of temperature in KTN at* λ = 1985 *mμ for light polarized perpendicular to* ($E \perp$ c) *and parallel to* ($E \parallel$ c), *the crystal* c *axis.*[69]

W–L–R theory, as published for the similar transformation in InTl[13] (which involves the same type of Bain distortions), were used to calculate the direction cosines of the habit plane. They were found to be in excellent agreement with the measured values, the predicted angles relative to cube axes being 90°, 49·7°, and 40·3° and the measured angles 89–90°, 50±1°, and 40±1°.

Equally good agreement is reported for semiconducting $BaTiO_3$[69] but more important for the understanding of mechanism is the fact that in *insulating* $BaTiO_3$, preliminary observations indicate a habit plane very close to $(110)_c$,[70] ~ 5° from the irrational habit plane exhibited when the crystal is *semiconducting*. This significant difference, as the authors point out,[69] is associated with the fact that in semiconducting crystals, the free charges present can neutralize the bound polarization charge inside the crystal, whereas in highly insulating crystals the absence of free charges imposes restrictions on the paraelectric/ferroelectric boundary and the ferroelectric domain configuration. Thus, the minimization

* These lattice parameters are the only ones available at this time, but a reasonable conjecture based on the behaviour in other systems leads to the proposal below and makes it more plausible.[34]

of the strain energy at the interface and matching considerations can be the factor which determines the nature of the transformation and the interface boundary in semiconducting crystals, but not in insulating crystals where electrostatic and electrostrictive terms must be considered. The transformation strains are quite small, $\sim 10^{-4}$, and hence it is not surprising that the theory is able to describe the former transformation so well.

The phenomenological theories have generally ignored considerations other than minimum interfacial strain energy. That they have been applied with reasonable success to iron-base alloys with their large transformation strains, where the product is ferromagnetic and where there are appreciable volume and shear restraints, suggests that, at least in the initial stages of growth, these are secondary effects as is suggested by the experimental scatter of habit planes reported in a single alloy.[14] Some of the crystallographic features (such as $\vec{\mathbf{d}}_1$, the direction of the macroscopic shear) may be much more sensitive than others to such factors and to details of the growth of the plates which are not incorporated in the present crystallographic theories.[71] That other forces are probably operative in determining the mode of a transformation can sometimes be inferred from the discrepancy between the crystallographic features to be expected on the basis of the simple theory and that observed, as in the paraelectric to ferroelectric case cited.

Finally a topic which can be mentioned only briefly is the softening of certain vibrational modes well above the transformation, indicating an instability as if in anticipation of the structural transformation. Zener[72] first incorporated a consideration of the anisotropy constant $\frac{2C_{44}}{C_{11} - C_{12}}$ in a mechanism for diffusionless phase transformations in b.c.c. metals and Robertson[73] has discussed martensite transformations in terms of elastic moduli. Zirinsky[74] reported an appreciable softening in β-AuCd well above the transformation temperatures in both the 47·5 and 50 at.-% Cd alloys. More recently, softening has been reported well above the transformation temperature in the cubic → tetragonal transformation in V_3Si.[52,55,56,58] However, it is interesting to note that whereas the products are martensite in AuCd the product in V_3Si may be pseudomartensite and the transformation is second-order.

Summary

In examining and comparing a number of transformations, a simple, reasonable and easily remembered system of classifying martensitic transformations and martensite-like products has been developed based on geometric criteria. Although the present phenomenological crystallographic theory is useful in that it can sometimes differentiate between possible modes, as illustrated here for NiMn and KTN, it will have to be revised to take into account electrical, magnetic, electrostrictive, piezoelectric, and other effects as well as property changes if it is to make its maximum contribution to the determination and understanding of fundamental mechanisms of transformations in crystalline solids.

Acknowledgements

The author wishes to acknowledge many helpful discussions with colleagues and graduate students and particularly the critical reading of the manuscript by H. Ledbetter; the continued support of the U.S. Atomic Energy Commission under Contract AT(11-1)-1198 is sincerely appreciated.

References

1. V. Gawranek, E. Kaminsky, and G. Kurdjumov, *Metallwirtschaft*, 1936, **15**, 370.
2. G. Gridnev and G. V. Kurdjumov, *ibid.*, 1936, **15**, 437.
3. I. Isaitchev, E. Kaminsky, and G. Kurdjumov, *Trans. Amer. Inst. Min. Met. Eng.*, 1938, **128**, 337.
4. I. Isaitchev, E. Kaminsky, and G. Kurdjumov, *ibid.*, p. 361.
5. A. B. Greninger, *ibid.*, 1939, **133**, 204.
6. D. W. Smith, *ibid.*, 1933, **104**, 48.
7. A. B. Greninger and V. G. Mooradian, *ibid.*, 1938, **128**, 337.
8. "Physical Properties of Martensite and Bainite" (Special Rep. No. 93). **1965:** London (Iron Steel Inst.).
9. "The Mechanism of Phase Transformations in Crystalline Solids". **1969:** London (Inst. Metals).
10. A.Ölander, *Z. Krist.*, 1932, **83A**, 145.
11. C. Benedicks, *Arkiv. Astron. Fysik*, 1940–41, **27A**, (18), 1.
12. D. S. Lieberman, M. S. Wechsler, and T. A. Read, *J. Appl. Physics*, 1955, **26**, 473.
13. M. W. Burkhart and T. A. Read, *Trans. Amer. Inst. Min. Met. Eng.*, 1953, **197**, 1516.
14. M. S. Wechsler, D. S. Lieberman, and T. A. Read, *ibid.*, p. 1503.
15. J. K. Mackenzie, *J. Australian Inst. Metals*, 1961, **6**, 90.
16. J. W. Christian, "The Theory of Transformations in Metals and Alloys". **1965:** Oxford, &c. (Pergamon Press).
17. J. W. Christian, Ref. 8, p. 1.
18. A. G. Crocker, "Deformation Twinning" (edited by R. E. Reed-Hill *et al.*), Vol. 25, p. 272. **1964:** New York, &c. (Gordon and Breach).
19. J. W. Christian, T. A. Read, and C. M. Wayman, "Intermetallic Compounds", p. 428. **1967:** New York and London (John Wiley).
20. R. P. Reed and J. F. Breedis, "Behaviour of Materials at Cryogenic Temperatures" (ASTM. Spec. Tech. Pub. No. 387), p. 60. **1966:** Philadelphia (Amer. Soc. Test. Mat.). (Article includes 702 references.)
21. L. Kaufman and M. Cohen, *Progress Metal Physics*, 1958, **7**, 165.
22. V. Raghavan and A. R. Entwisle, Ref. 8, p. 29.
23. C. M. Wayman, Ref. 8, p. 153.
24. J. W. Christian, this vol., p. 129.
25. M. S. Wechsler, *Acta Met.*, 1957, **5**, 150.
26. W. J. Sturm and M. S. Wechsler, *J. Appl. Physics*, 1957, **28**, 1509.
27. D. Gupta, D. Lazarus, and D. S. Lieberman, *Phys. Rev.* 1967, **153**, 863.
28. L. C. Chang and T. A. Read, *Trans. Amer. Inst. Min. Met. Eng.*, 1951, **191**, 47.
29. L. C. Chang, *J. Appl. Physics*, 1952, **23**, 725.
30. L. C. Chang, *Acta Cryst.*, 1951, **4**, 320.
31. J. S. Bowles and J. K. Mackenzie, *Acta Met.*, 1954, **2**, 129, 138, 224.
32. R. E. Pawel, J. V. Cathcart, and J. J. Campbell, *ibid.*, 1962, **10**, 149.
33. J. Van Landuyt and C. M. Wayman, *ibid.*, 1968, **16**, 803, 815.
34. D. S. Lieberman, to be published.
35. R. Mănăilă and P. Păuşescu, *Physica Status Solidi*, 1965, **9**, 385.
36. P. Wojtowizc, *Phys. Rev.*, 1959, **116**, 32.
37. P. Păuşescu, *Acta Cryst.*, 1966, **21**, A204.
38. J. Feinlieb and W. Paul, *Phys. Rev.*, 1967, **155**, 841.
39. Proceedings of the first "International Conference on the Metal–Nonmetal Transition", *Rev. Modern Physics*, 1968, **40**, 673.
40. D. S. Lieberman, discussion in Ref. 39.
41. R. Smith and J. S. Bowles, *Acta Met.*, 1960, **8**, 405.
42. J. S. Bowles and A. S. Malin, *J. Australian Inst. Metals*, 1960, **5**, 131.
43. J. S. Bowles and W. J. McG. Tegart, *Acta Met.*, 1955, **3**, 590.
44. R. D. Garwood, *J. Inst. Metals*, 1954–55, **83**, 64.
45. R. D. Garwood, Ref. 8, p. 90.

46. D. S. Lieberman, *Acta Met.*, 1958, **6,** 680.
47. G. R. Srinivasan and C. M. Wayman, *Trans. Met. Soc. A.I.M.E.*, 1968, **242,** 79.
48. G. R. Srinivasan and C. M. Wayman, *Acta Met.*, 1968, **16,** 609, 621.
49. J. N. Bierly, L. Muldawer, and O. Beckman, *ibid.*, 1963, **11,** 447.
50. B. W. Batterman and C. S. Barrett, *Phys. Rev. Letters,* 1964, **13**, 390.
51. M. J. Goringe and U. Valdrè, *ibid.,* 1965, **14,** 823.
52. L. R. Testardi, T. B. Bateman, W. A. Reed, and V. G. Chirba, *ibid.*, 1965, **15,** 250.
53. J. E. Kunzler, J. P. Matta, H. J. Levenstein, and E. J. Ryder, *Phys. Rev.*, 1966, **143,** 390.
54. B. W. Batterman and C. S. Barrett, *ibid.*, 1966, **145,** 296.
55. S. R. Patel and B. W. Batterman, *ibid.*, 1966, **148,** 662.
56. L. R. Testardi and T. B. Bateman, *ibid.*, 1967, **154,** 402.
57. J. R. Patel and B. W. Batterman, *J. Appl. Physics*, 1966, **37,** 3447.
58. E. R. Vance and T. R. Finlayson, *ibid.*, 1968, **39,** 1980.
59. J. Labbe and J. Friedel, *J. Physique*, 1966, **27,** 153.
60. B. W. Batterman and J. Wanagel, *Bull. Amer. Phys. Soc.*, 1968, **13,** 444.
61. H. U. King, F. H. Cocks, and J. J. A. Pollock, *Physics Letters*, 1967, **26A,** 77.
62. V. Kraševec, P. Delavignette and S. Amelinckx, *Mat. Research Bull.*, 1967, **2,** 77.
63. V. Kraševec *et al.*, *ibid.*, p. 1029.
64. J. A. Mullendore and D. S. Lieberman, to be published.
65. M. Hansen and K. Anderko, " Constitution of Binary Alloys ", p. 938. **1958:** New York and London (McGraw-Hill).
66. R. P. Elliott, " Constitution of Binary Alloys, 1st Suppl.", p. 605. **1965:** New York and London (McGraw-Hill).
67. S. G. Fishman, R. S. Karz, and D. S. Lieberman, to be published.
68. S. Amelinckx, private communication.
69. M. Di Domenico, Jr., and S.H. Wemple, *Phys. Rev.*, 1967, **155,** 539.
70. M. S. Wechsler, *U.S. Atomic Energy Commission Rep.* **(NYO-3968),** 1954.
71. D. S. Lieberman, *Acta Met.*, 1966, **14,** 1723.
72. C. Zener, " Elasticity and Anelasticity of Metals ", p. 37. **1948:** Chicago (Univ. Chicago Press).
73. W. D. Robertson, Ref. 8, page 26.
74. S. Zirinsky, *Acta Met.*, 1956, **4,** 164.

The Crystallography of Martensitic Transformations in Uranium and Its Alloys

A. G. Crocker and N. D. H. Ross

The importance of both the $\beta \rightarrow \alpha$ and the $\gamma \rightarrow \alpha$ transformations in uranium and its alloys as critical tests of theories of martensite crystallography is first emphasized. It is then shown that many possible correspondences exist relating the β and α structures but further detailed experimental information is necessary before definite conclusions can be drawn about their operation in practice. Such information is available for the $\gamma \rightarrow \alpha$ transformation but in this case it is demonstrated that for some observed cases the theories have no real solutions. This shows that current theories of martensite crystallography are inadequate. A new theory of transformation shears is therefore being developed and a preliminary account of this is given.

The Institute of Metals Symposium on the Mechanism of Phase Transformations in Metals held in 1955 included the first general review[1] of what are still the current theories of martensite crystallography. In addition, two papers were presented[2,3] on the $\beta \rightarrow \alpha$ transformation in uranium and its alloys. Since that time transmission electron microscopy and other techniques have confirmed some of the basic hypotheses of the theories. However, these techniques have not been successfully applied to the uranium transformation. This is in part due to technological interest being diverted first to alloys with a higher solute content, in which the β phase is suppressed so that it is the $\gamma \rightarrow \alpha$ transformation which becomes of interest and then, more recently, to the use of ceramic nuclear-fuel elements. This is unfortunate as the unique parent and product crystal structures associated with the $\beta \rightarrow \alpha$ transformation in uranium provide an ideal opportunity for testing the crystallographic theories of martensite. It is certainly important that this should be done since observations on other systems have shown that in many ways these theories are inadequate. Indeed, as we shall demonstrate in this paper, the most striking example of the failure of the theories occurs in the $\gamma \rightarrow \alpha$ transformation in uranium alloys for which, fortunately, there is recent detailed experimental information.

The established theories of martensite crystallography[1,4] resolve the total shape deformation into a rotation, a pure strain, and a simple lattice invariant shear. The data required to apply the theories are then the lattice parameters of the parent and product structures, a correspondence relating directions in these structures, and the shear plane and direction of the simple shear. The lattice parameters and correspondence define the pure strain and impose restrictions on the choice of shear elements.[5] Furthermore, in the case of twinned martensite,[6] if the two product orientations are to be related to the parent material by means of crystallographically equivalent correspondences, the twin or shear plane must be associated with a mirror plane of the parent.

When applying these theories to the uranium transformations, difficulties arise because the choice of correspondence is not obvious as in the case of other transformations. This is particularly true of the $\beta \rightarrow \alpha$ transformation where the parent phase has a complex tetragonal unit cell containing thirty atoms. The γ phase is body-centred cubic and the α phase is, at least approximately, base-centred orthorhombic. The lattice parameters vary slightly with alloy content. We shall here use the values $A = 10{\cdot}590$ Å; $C = 5{\cdot}634$ Å; $a = 2{\cdot}855$ Å; $b = 5{\cdot}862$ Å; $c = 4{\cdot}961$ Å for the $\beta \rightarrow \alpha$ transformation, and $a_0 = 3{\cdot}465$ Å; $a = 2{\cdot}854$ Å; $b = 5{\cdot}869$ Å; $c = 4{\cdot}955$ Å for the $\gamma \rightarrow \alpha$ transformation. These parameters are appropriate for transformations in U–1·4 at.-% Cr and U–5 at.-% Mo alloys, respectively. A second difficulty in applying the theories is that a large number of simple shears, particularly twinning shears, are available and need to be considered.

In the present paper we shall first discuss the choice of correspondence for the $\beta \rightarrow \alpha$ transformation. So many possibilities arise, however, that without further guidance from detailed experimental information it seems unwise at present to use these correspondences as data for the theories. We therefore proceed to consider correspondences for the $\gamma \rightarrow \alpha$ transformation and conclude that the only one likely to occur in practice is that deduced recently[7] from complex electron-diffraction patterns. This correspondence is then used as data for the theories and it is shown that for several experimentally observed simple shears the theories have no real solutions. This result clearly demonstrates some inadequacy of the theories and has prompted us to examine the basic problem of transformation shears in lattices. The last section of the paper discusses the new theory of martensite crystallography that is now being developed from this analysis. Some details of the algebraic procedures involved in handling correspondences are given in the Appendix.

Manuscript received 23 February 1968. A. G. Crocker, Ph.D., and N. D. H. Ross, B.Sc., are in the Department of Physics, University of Surrey.

The β → α Transformation in Uranium and Its Alloys

At the 1955 Symposium, Butcher and Rowe[2] reported their experimental results on the habit planes and orientation relationships associated with the β → α martensite transformation in a U–1·4 at.-% Cr alloy. This paper was followed by a theoretical discussion by Lomer[3] of the possible correspondences between the two structures. He had examined 1600 different ways in which one β cell containing 30 atoms could transform into $7\frac{1}{2}$ α cells each containing 4 atoms and found only one correspondence involving particularly small strains. He did, however, report a second correspondence with larger strains and deduced from the experimental evidence two further correspondences relating two β cells to fifteen α cells. Later, Crocker[8] used Lomer's correspondences as data for the theories of martensite crystallography but, because of the large choice of possible lattice invariant shear modes and the lack of experimental information on any operative shears, no very definite conclusions could be drawn about their validity. In addition we have now discovered that many other correspondences with comparatively small strains exist. The physical criteria governing which correspondence occurs in practice are, of course, critical to our understanding of this and other phase changes and we therefore consider it important to report these correspondences here.

The procedure for determining the principal strains associated with a correspondence is described in the Appendix In particular we note that it is convenient[9] to classify correspondences in terms of a quantity Q giving the sum of the squares of the principal distortions η_i ($i = 1, 2, 3$). For a correspondence involving zero strains we have $\eta_i = 1$, so that $Q = 3$ and as the strains increase Q also increases. As it seems likely that correspondences involving small strains will be preferred in practice, we have looked for correspondences between one β cell and $7\frac{1}{2}$ α-uranium cells having $Q < 3{\cdot}1$. Nine such correspondences have been found and these are given in Table I, together with the associated values of Q and the principal strains ($\eta_i - 1$).

Correspondences 1 and 7 in Table I are the two deduced by Lomer,[3] who did not report the other seven correspondences. The two more complex correspondences he gave, involving two cells of β-uranium, have Q values of 3·024 and 3·089. Because a large number of atoms is involved in these correspondences it is not convenient in general to represent them diagrammatically. However, correspondences 3, 4, and 9 in Table I are comparatively simple as they involve the $(001)_\beta$ plane and the $[001]_\beta$ direction becoming the $(001)_\alpha$ plane and the $[001]_\alpha$ direction. Therefore, in Fig. 1 we have outlined the three parallelograms in the $(001)_\alpha$ plane that arise from the square bases of three possible tetragonal β cells as a result of the deformations associated with these correspondences. Atomic positions have been deliberately omitted from Fig. 1 as the β-uranium structure is so complex. Indeed, for the correspondences listed in Table I only one atom in thirty moves directly to its correct product site, the remainder having to shuffle. The relative magnitudes and directions of these shuffles provide a second means of classifying the correspondences and may be the controlling factor in deciding which correspondences are likely to arise in practice. In particular the three correspondences shown in Fig. 1 may well be favoured in practice because of their simplicity. However, as yet, no comprehensive study of the shuffles associated with these correspondences has been carried out. In fact it seems unwise at present to embark on a more detailed examination of the correspondences and to use them as data for the theories before further experimental information becomes available. It is clear, however, that this phase change may well make use of several mechanisms although at the moment the primary correspondence due to Lomer[3] is probably the most efficient way of accomplishing the transformation.

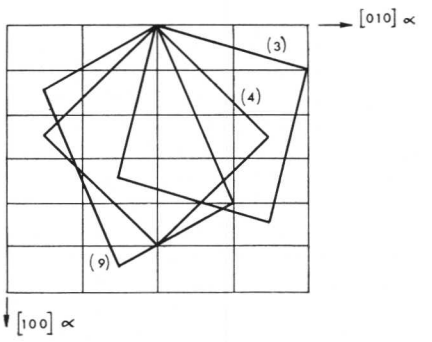

Fig. 1 Correspondences 3, 4, and 9. The deformed bases of the tetragonal β cells are outlined on the corresponding (001) plane of α-uranium.

TABLE I
Possible Correspondences for the β → α Uranium Transformation

	Correspondence ($_\alpha C_\beta$)			Q	Principal Strains		
1	$\bar{1}71$	$\bar{3}\bar{1}1$	202	3·004	0·019	0·076	− 0·101
2	333	$\bar{1}\bar{3}1$	$4\bar{2}0$	3·039	0·023	0·117	0·138
3	720	$\bar{1}40$	002	3·041	− 0·028	− 0·119	0·143
4	550	$\bar{3}30$	002	3·063	− 0·047	− 0·119	0·174
5	632	$\bar{2}30$	$\bar{2}02$	3·065	0·052	0·125	− 0·167
6	$4\bar{5}1$	231	$\bar{2}02$	3·070	− 0·051	− 0·122	0·183
7	630	012	$2\bar{4}0$	3·074	0·045	0·153	− 0·164
8	522	$\bar{1}40$	$\bar{2}02$	3·081	0·083	0·114	− 0·182
9	380	$\bar{3}20$	002	3·098	− 0·077	− 0·119	0·212

The elements of the correspondence matrices $_\alpha C_\beta$, which are defined in the Appendix, have all been multiplied by two. The three rows of each matrix are given as a single row in the table, bars indicating negative elements.

The γ → α Transformation in Uranium Alloys

The most detailed experimental investigation of the crystallography of the γ → α transformation is that by May[7] using a U–5 at.-% Mo alloy. Following detailed examination of transmission electron micrographs and electron-diffraction patterns taken from twinned martensitic products in this alloy, May[7] deduced a correspondence and demonstrated the presence of {130} and {021} twins. There was also good evidence for {112} twins and some evidence for a {111} twin.

We shall first discuss May's correspondence and compare it with that adopted by Christian[10] in an earlier theoretical analysis of the transformation. This latter correspondence is in fact equivalent to that associated with the well-known cubic → orthorhombic transformation in gold–cadmium alloys.[11] The two correspondences are defined using the notation described in the Appendix, by the correspondence matrices

$$(_\alpha C_\gamma)_M = \tfrac{1}{4}\begin{pmatrix} 3 & 3 & 2 \\ 1 & 1 & \bar{2} \\ \bar{2} & 2 & 0 \end{pmatrix}; \quad (_\alpha C_\gamma)_C = \tfrac{1}{2}\begin{pmatrix} 0 & 0 & 2 \\ 1 & 1 & 0 \\ \bar{1} & 1 & 0 \end{pmatrix}$$

where the suffixes M and C refer to May and Christian, respectively. In both cases the $(1\bar{1}0)_\gamma$ plane and $[1\bar{1}0]_\gamma$ direction become the $(001)_\alpha$ plane and $[001]_\alpha$ direction. Therefore in Fig. 2 we illustrate and compare the two correspondences, in this case relative to the parent structure, by projecting them on to the $(1\bar{1}0)_\gamma$ plane. It is clear from this figure that the parent γ-uranium cells defined by the correspondences of Christian[11] and May[7] and which become on applying the pure strain the base-centred orthorhombic cell of α-uranium, are respectively base-centred orthorhombic and base-centred monoclinic. Also the atomic positions are shown so that the magnitudes of the atomic shuffles, which must accompany any transformation from a single- to a double-lattice structure, are easy to deduce. Again the principal directions of the pure strain associated with Christian's correspondence are seen to be parallel to the edges of the product cell and the magnitudes of these strains are thus simple to derive. This is not the case for May's correspondence for which the procedure outlined in the Appendix has to be adopted. We thus obtain the principal strains, principal directions, and shuffle magnitudes, which are summarized in Table II. Of particular importance here are the magnitudes of the strains, which are ~ 1%, − 18%, and 20%, and 1%, 9%, and − 10% for Christian's and May's correspondences, respectively. In addition, the shuffle magnitudes for Christian's correspondence are greater than May's by a factor of > 2. These magnitudes are calculated on the assumption that the shuffles occur before the deformation. In practice, of course, the deformation and shuffle components of the change of structure will occur simultaneously but the values in Table II are considered to be a significant measure of the transformation energy associated with the shuffles. In this connection it should be noted that conventionally in Fig. 2 each atom has to shuffle an equal distance, neighbouring atoms moving in opposite directions as indicated by the alternative signs in the table. This minimizes the sum of the squares of the shuffle magnitudes and hence, we assume, the energy associated with these shuffles.

Summarizing, May's correspondence is associated with much smaller shuffles and much smaller strains than that of Christian and this is likely to be favoured on theoretical grounds, as indeed it is in practice. We have in fact made a systematic study of correspondences between the γ- and α-uranium structures and found that the two discussed here involve the smallest possible strains. However, an interesting correspondence between γ- and faulted α-uranium, which has been suggested by Stobo[12] as a possible nucleus for the product structure, has principal strains intermediate between those of May's and Christian's correspondences.

Thus we adopt May's correspondence and consider which twinning planes may be used as data for the theories of martensite crystallography. As explained in the introduction we restrict these shear planes to those arising from mirror planes in the parent phase. There are nine such planes in the b.c.c. γ-uranium structure with indices belonging to the forms $\{100\}_\gamma$ and $\{011\}_\gamma$. These planes (m_γ) and the corresponding planes (m_α) in the α phase are summarized in Table III. It is now seen that planes 2, 6, and 9 are crystallographically equivalent to planes 1, 5, and 8, respectively, and need not be considered further. Of the remaining six possible shear planes, one, the $(001)_\alpha$ plane, is a mirror plane of the α-uranium structure and is thus unable to operate as a twinning plane. The other five planes {112}, {130}, {110}, {111}, and {021} will now be considered as possible transformation twinning planes. Indeed, these are all well established as

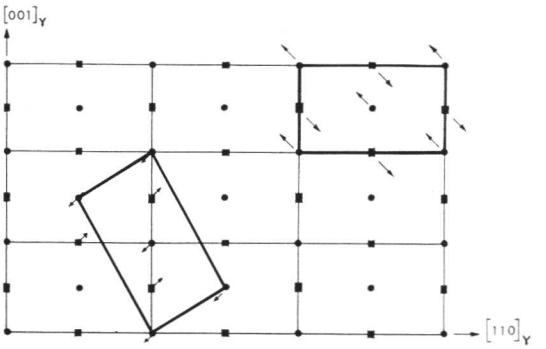

Fig. 2 The correspondences of Christian (top right) and May (bottom left) illustrated by outlining two-dimensional cells in the $(1\bar{1}0)$ plane of γ-uranium. These become the centred bases of α-uranium cells following the appropriate deformations. The atomic shuffles that must accompany the deformations are also indicated.

TABLE II
Comparison of the Two Correspondences for the γ → α Uranium Transformation

Correspondence	Principal Strains	Principal Directions	Shuffle Magnitudes
Christian	0·011 −0·176 0·198	$[\bar{1}10]_\gamma$ $[001]_\gamma$ $[110]_\gamma$	$\pm 0{\cdot}289a_0$
May	0·011 0·092 −0·097	$[\bar{1}10]_\gamma$ $[1, \bar{1}, 0{\cdot}681]_\gamma$ $[1, \bar{1}, \bar{2}{\cdot}9\bar{3}\bar{6}]_\gamma$	$\pm 0{\cdot}121a_0$

TABLE III
The Possible Twinning Systems for the γ → α Uranium Transformation

	(m_γ)	(m_α)	(l_α)	(l_γ)	m_i	l_i	M,L
1	100	$11\bar{2}$	+0·408 −0·882 −0·237	0 +0·297 −0·955	+0·707 −0·637 −0·307	+0·210 +0·603 −0·769	
2	010		≡ 1	—	—	—	—
3	001	$1\bar{3}0$	310	110	0 +0·434 −0·901	0 −0·901 −0·434	*M*
4	110	110	$1\bar{1}0$	001	0 −0·901 −0·434	0 +0·434 −0·901	*L*
5	101	$1\bar{1}\bar{1}$	+0·264 −0·537 +0·801	−0·632 −0·448 −0·632	+0·500 −0·144 −0·854	−0·764 +0·391 −0·513	
6	011	$1\bar{1}1$	≡ 5	—	—	—	—
7	$1\bar{1}0$	001	—	—	—	—	—
8	$10\bar{1}$	$02\bar{1}$	−0·996 −0·038 −0·077	−0·512 +0·690 +0·512	+0·500 −0·757 −0·420	+0·126 +0·544 −0·830	*L*
9	$01\bar{1}$	021	≡8	—	—	—	—

crystallographically possible deformation twinning planes of α-uranium,[13] although in practice only {130} and {112} twins have been reported. However, deformation twins have been observed on the irrational planes " {172} " and " {176} ". which are reciprocal to {112} and {111}. In addition $\{1\bar{1}0\}$ is the reciprocal twinning plane to {130}. The effective shear directions $[l_\alpha]$ associated with these twinning planes may be deduced from the fact that directions normal to the mirror planes (m_γ) become the conjugate twinning directions in the product phase. Standard crystallographic formulae[14] may then be used to deduce the twinning directions $[l_\alpha]$, which are also given in Table III, together with the parent directions $[l_\gamma]$ from which they are derived using the correspondence. The directions $[l_\alpha]$ are in fact the well-known deformation twinning directions[13] associated with these twinning planes. Note that in the case of {112}, {111}, and {021} planes these directions are irrational.

We now consider the restrictions imposed on the twinning planes and directions by the crystallographic theories. These restrictions are the conditions for real roots of the quadratic equations defining first the directions of the dislocation lines in the interface and secondly the normal to this interface. They may be written[5]

$$m_1^2(1-\eta_2^2)(1-\eta_3^2)+m_2^2(1-\eta_3^2)(1-\eta_1^2)+m_3^2(1-\eta_1^2)(1-\eta_2^2)\leqslant 0$$

$$l_1^2\eta_1^2(1-\eta_2^2)(1-\eta_3^2)+l_2^2\eta_2^2(1-\eta_3^2)(1-\eta_1^2)+l_3^2\eta_3^2(1-\eta_1^2)(1-\eta_2^2)\leqslant 0$$

Here $(\eta_i - 1)$, $i = 1, 2, 3$, are the principal strains defined by the correspondence and m_i and l_i are the components of vectors perpendicular to the plane (m_γ) and parallel to the direction $[l_\gamma]$ respectively. These components must be given relative to an orthonormal basis defined by the principal directions of the pure strain. For the case of May's correspondence the strains $(\eta_i - 1)$ are given in Table II and the components of m_i and l_i in Table III. The results of substituting these values in the two restrictions are given in the final column of Table III, the symbols M and L indicating that the twinning mode violates the restriction on the shear plane and direction respectively. Only the {112} and {111} twinning modes satisfy both restrictions. The {130} mode violates the restriction on the twinning plane and the {110} and {021} modes the restriction on the twinning direction.

Thus these modes, two of which have been shown conclusively by May to be operative in practice, produce imaginary solutions when used with the crystallographic theories. It is therefore apparent that the basic hypotheses on which the theories are based are not satisfied in the case of this transformation. Indeed, the results suggest that a major revision of the theories is necessary. This would appear particularly appropriate at this time when an increasing amount of experimental evidence suggests that the existing theories are inadequate.

Discussion

In this paper we have examined the possibility of applying the phenomenological theories of martensite crystallography to the phase changes in uranium alloys and found that several major difficulties arise. In particular, for the case of the $\gamma \rightarrow \alpha$ transformation, the theories do not give real solutions for the crystallographic features. This demonstrates conclusively that these theories are not suitable for universal application to all transformations with martensitic characteristics. Indeed, it may indicate that some of the apparent successes of the theories are in fact fortuitous. It therefore seems desirable to develop at this stage a new, largely mechanistic, theory of martensite crystallography to replace the present phenomenological theories. Such a theory should clearly be based on structural changes produced by shears. In the first instance we have considered the fundamental problem of shearing a given lattice into any other lattice. The treatment is similar to that given recently by Bevis and Crocker[15] for the case of twinning shears, where it was shown that both the twinning plane and the twinning direction can in general have irrational indices. For the case of transformation shears, occurring at interfaces between two phases and thus not specifically associated with either parent or product structure, such irrational shear elements would appear to be particularly apposite.

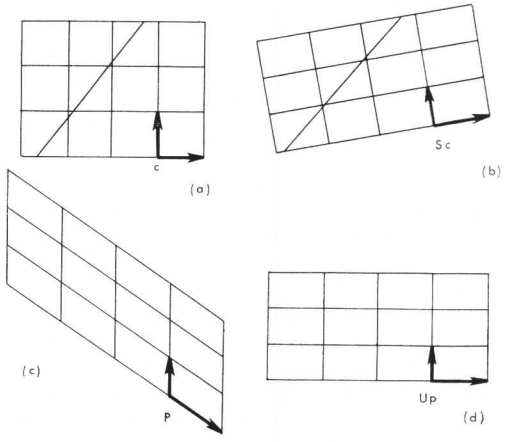

Fig. 3 Illustrating the derivation of the equation **Sc = RUp** *that forms the basis of the new theory of transformation shears at present being developed.*

The analysis is illustrated schematically in Fig. 3 for the two-dimensional case of a square lattice shearing into a rectangular lattice. Diagram (*a*) shows the parent lattice together with the shear direction and shear strain. The resulting rectangular product lattice is shown in (*b*) but this will not in general be in the required orientation, indicated at (*d*). In addition, although the lattice points in (*d*) form a rectangular array an infinite number of unit cells may be used, such as that shown in (*c*). Algebraically we have the parent lattice vectors **c** in (*a*) becoming **Sc** in (*b*), where **S** is a shear matrix. Similarly the product lattice vectors **p** in (*c*) become **Up** in (*d*), where **U** is a unimodular matrix, i.e. its determinant is equal to unity. Apart from a rotation these lattices are identical so that **Sc = RUp**. The rotation matrix **R** can be eliminated from this equation by multiplying both sides by their transposes. The resulting equation enables the transformation shears to be determined in terms of the unimodular matrix **U** and the lattice parameters. In practice matrices **U** are chosen which produce shears of small magnitude for given lattices. For the example shown in Fig. 3 a rectangle of axial ratio n^2 is obtained by a shear strain $(n - n^{-1})$ in the direction $[1, n]$, n being chosen to be 1·2 in this case. Thus a square lattice can be sheared into any rectangular lattice with cells of the same area, but even in this elementary example both the normal to the shear plane and the shear direction are irrational.

In general we find that, if two different lattices are to be related by a simple shear, the lattice parameters are subjected to several restrictions. The first of these is, of course, that the parent and product cells must have the same volume. Indeed, in a martensite theory based on shears any volume change has to be accommodated by an additional deformation such as a strain perpendicular to the interface. However, the other restrictions on the lattice parameters make a single-shear theory impractical and we are therefore at present developing a multiple-shear analysis of transformation crystallography. In this we are interested in determining the minimum number of shears, if necessary on irrational planes in irrational directions, and the smallest shear strains that will transform a given parent lattice to a given product. We believe that this analysis will then form the basis of a new theory of martensite crystallography which will explain the characteristics of a wide range of transformations including those that, like the phase changes in uranium alloys discussed in the present paper, appear at the moment to be anomalous. However, in order to apply any theory successfully to these transformations further experimental information is necessary and we hope that the publication of the present paper will stimulate new interest in this field.

Acknowledgements

One of the authors (A.G.C.) carried out part of the work on the $\gamma \rightarrow \alpha$ transformation in uranium alloys at The International Research and Development Co., Ltd., and would like to thank Dr. H. M. Finniston for support and encouragement, and also Mr. G. H. May and Dr. J. J. Stobo for valuable discussions. Financial assistance from the Science Research Council is acknowledged by N.D.H.R.

References

1. B. A. Bilby and J. W. Christian, " The Mechanism of Phase Transformations in Metals ", p. 121. **1956:** London (Inst. Metals).
2. B. R. Butcher and A. H. Rowe, *ibid.*, p. 229.
3. W. M. Lomer, *ibid.*, p. 243.
4. J. W. Christian, " The Theory of Transformations in Metals and Alloys ". **1965:** Oxford (Pergamon Press).
5. A. G. Crocker and B. A. Bilby, *Acta Met.*, 1961, **9,** 992.
6. A. G. Crocker, " Deformation Twinning ", p. 272. **1964:** New York (Gordon and Breach).
7. G. H. May. *Internat. Research Develop. Co. Research Rep.* **(IRD 66-71).** 1966: Newcastle upon Tyne (The Company).
8. A. G. Crocker, Ph.D. Thesis, Univ. Sheffield, **1959.**
9. A. G. Crocker, *Acta Met.*, 1962, **10,** 113.
10. J. W. Christian, *Atomic Energy Research Estab. Rep.* **(AERE M/R 1811),** 1955.
11. D. S. Lieberman, M. S. Wechsler, and T. A. Read, *J. Appl. Physics*, 1955, **26,** 473.
12. J. J. Stobo, *Internat. Research Develop. Co. Research Rep.* **(IRD 64-95).** 1966: Newcastle upon Tyne (The Company).
13. A. G. Crocker, *J. Nuclear Mat.*, 1965, **16,** 306.
14. B. A. Bilby and A. G. Crocker, *Proc. Roy. Soc.*, 1965, [A], **288,** 240.
15. M. Bevis and A. G. Crocker, *ibid.*, 1968, [A], **308,** 127.

Appendix

On Lattice Correspondences*

A correspondence specifies which vectors of the parent transform into given vectors of the product. The deformation implied by this change of structure is then characterized by the pure strain associated with the correspondence. This pure strain, which we represent by the symmetric matrix $\mathbf{P}$, leaves certain vectors $\mathbf{z}$ unchanged in direction so that $\mathbf{Pz} = \eta\mathbf{z}$ where η is a scalar. Thus

$$(\mathbf{P}^2 - \eta^2\mathbf{I})\,\mathbf{z} = 0 \qquad \ldots (1)$$

where $\mathbf{I}$ is the unit matrix. Equation (1) has non-zero solutions only if the determinantal equation

$$|\,\mathbf{P}^2 - \eta^2\mathbf{I}\,| = 0 \qquad \ldots (2)$$

is satisfied. If $\mathbf{P}^2$ is known the cubic equation (2) may be solved for η_i $(i = 1, 2, 3)$, which are known as the principal distortions and hence the principal strains $(\eta_i - 1)$ obtained. The principal directions $\mathbf{z}_i$ can then be derived from equation (1). In addition the quantity $Q = \eta_1^2 + \eta_2^2 + \eta_3^2$, a convenient measure of the deformation associated with a correspondence, is the coefficient of $-\eta^4$ in equation (2) and is thus given by the sum of the elements of $\mathbf{P}^2$.

To determine $\mathbf{P}^2$ for a given correspondence we choose two orthonormal bases fixed relative to the parent and product lattices, respectively. These are related by a rotation matrix θ so that the components of any vector $\mathbf{y}$ referred to the parent basis are given by

$$\mathbf{y}' = \theta\mathbf{y} \qquad \ldots (3)$$

when referred to the product basis. Using the parent basis as our reference, the lattice deformation $\mathbf{D}$, which may be resolved into a rotation $\mathbf{R}$ and the pure strain $\mathbf{P}$, transforms a parent lattice vector $\mathbf{x}_1$ into a product lattice vector $\mathbf{y}_2$ given by $\mathbf{y}_2 = \mathbf{RPx}_1$. Thus, using equation (2) we obtain

$$\mathbf{y}_2' = \theta\mathbf{RPx}_1 \qquad \ldots (4)$$

The Miller indices $[x_1]$ and $[y_2']$ of the vectors $\mathbf{x}_1$ and $\mathbf{y}_2'$ are now given by

$$[x_1] = \mathbf{M}_1\mathbf{x}_1\,;\,[y_2'] = \mathbf{M}_2\mathbf{y}_2' \qquad \ldots (5)$$

Here $\mathbf{M}_1$ and $\mathbf{M}_2$ are matrices whose columns give the Miller indices, relative to the parent and product lattices respectively, of the basic vectors of the orthonormal bases. Thus, combining equations (4) and (5) we obtain

$$[y_2'] = \mathbf{M}_2\theta\mathbf{RPM}_1^{-1}[x_1]$$

But $[y_2'] = ({}_2C_1)\,[x_1]$ where $({}_2C_1)$ is the correspondence, so that

$$\theta\mathbf{RP} = \mathbf{M}_2^{-1}({}_2C_1)\mathbf{M}_1 \qquad \ldots (6)$$

Multiplying both sides of equation (6) by their own transposes and using the fact that θ and $\mathbf{R}$ are orthogonal and $\mathbf{P}$ symmetrical, we obtain an expression for $\mathbf{P}^2$ as required. For the transformations in uranium it is of course convenient to place the orthonormal bases parallel to the orthogonal cell edges so that $\mathbf{M}_\alpha$, $\mathbf{M}_\beta$, and $\mathbf{M}_\gamma$ are all diagonal having elements a^{-1}, b^{-1}, c^{-1}; A^{-1}, A^{-1}, C^{-1}; a_0^{-1}, a_0^{-1}, a_0^{-1}, respectively.

*The presentation here is similar to but more general than that given previously by Lomer[3] and Christian.[10]

The Morphology and Crystallography of Massive Martensite in Iron–Nickel Alloys

R. G. Bryans, T. Bell, and V. M. Thomas

The groups of parallel shear markings observed on previously polished surfaces of iron-based alloys containing < 29% nickel have been related to the sub-surface structure of massive martensite. The sub-structure of these slabs consists of bundles of laths with their long axes approximately parallel to the slab interfaces. The habit plane of both the surface shear markings and the slab interfaces has been measured as $\{111\}_\gamma$ or a plane very close to it. Hot-stage optical metallographic studies have shown that massive martensite forms in a self-accommodating fashion, generally in groups of at least two plates, and that a homogeneous deformation is often associated with the transformation. Detailed interferometric studies have revealed that the interface between pairs of self-accommodating plates is usually undistorted. The magnitude and direction of the shape deformation have been measured using a simple shear model. Finally, a model is proposed to explain the observed magnitude and direction of the shape deformation and the self-accommodating nature of massive martensite.

Iron–nickel alloys, after transformation to massive martensite, exhibit tilts on surfaces polished before austenitizing. These tilts, which correspond to shear plates, form in packets with all the plates parallel or occasionally interlacing[1,2] (Fig. 1(*a*)). There has been some confusion in the literature as to whether these surface tilts correspond to the bulk transformation observed in polished and etched sections, or whether they are surface martensite phenomena such as those discussed by Klostermann and Burgers[3] and by Honma.[4] Careful progressive polishing, etching, and photographing of sections in an Fe–22 wt.-% Ni alloy (Fig. 1(*a*)) leaves no doubt that the individual packets of plates observed on the surface correspond to the underlying structure (Fig. 1(*b*)). The metallographic structure of massive martensite beneath the surface consists of rectangular regions, often with jagged boundaries. A consistent structure exists throughout the thickness of the specimen. This is very clearly illustrated in Fig. 2, which is a composite photomicrograph of an Fe–22% Ni alloy showing the slab-like appearance of massive martensite grains on two polished and etched orthogonal surfaces.

Manuscript received 24 May 1968. R. G. Bryans, B.Eng., T. Bell, B.Eng., Ph.D., A.I.M., and V. M. Thomas, B.Sc., F.I.M., are in the Department of Metallurgy, University of Liverpool.

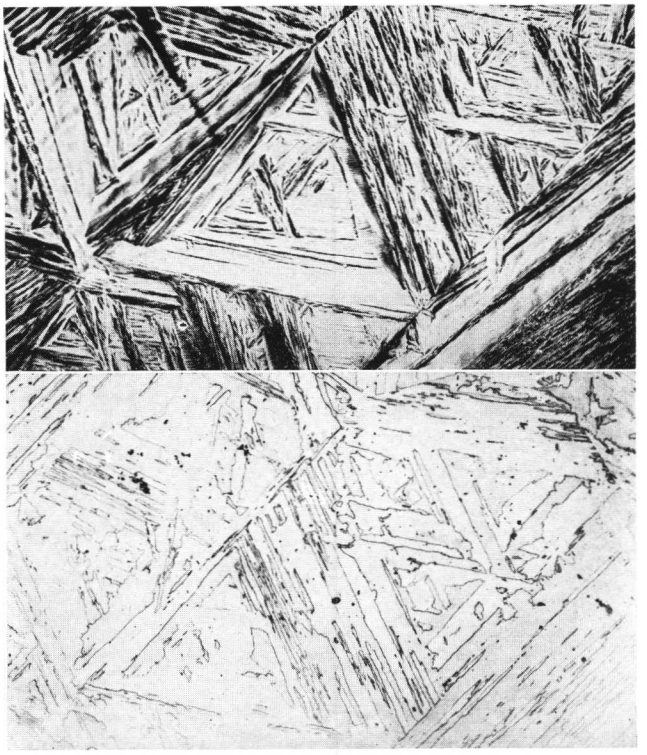

(*a*)

(*b*)

Fig. 1 (a) *A typical field of surface shear markings produced on a prepolished surface of an Fe–22% Ni–0·01% C specimen annealed at* 1200° *C and quenched to room temperature.* (b) *The microstructure revealed by polishing and etching a surface* 4 μm *below the surface seen in* (a). *Etchant* 5% *nital. Both* × 120.

Thin-film electron microscopy studies of those ferrous systems that exhibit the massive martensite transformation have all revealed that the substructure of the slabs is made up of " bundles " or " sheaves " of approximately parallel laths,[1,2,5–7] as seen in Fig. 3. The laths, which do not always have completely planar interfaces, dovetail together to fill space and are usually several μm long, varying in width between 0·3 and 2·0 μm.

Hot-stage optical metallographic studies were performed to demonstrate that the tilts formed on prepolished surfaces are not associated with " reverse " transformation markings arising from the martensite–austenite transformation. Such

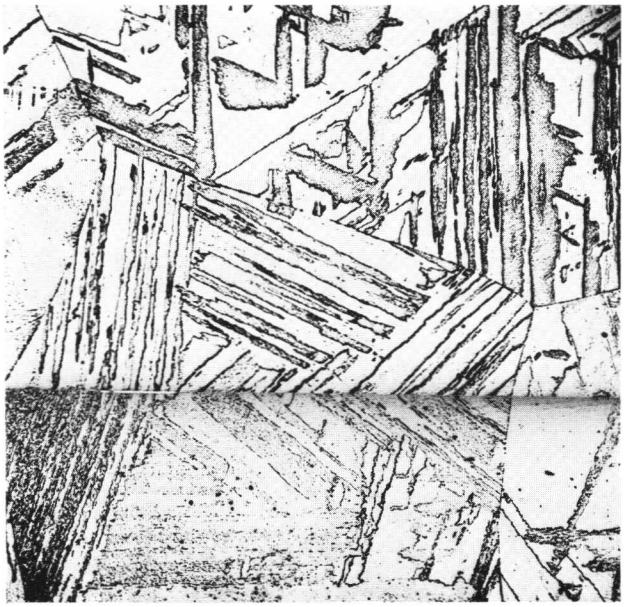

Fig. 2 A composite micrograph showing the massive martensite microstructure as revealed by polishing two intersecting orthogonal surfaces of an Fe–22·0% Ni–0·01% C specimen. Etchant 5% nital. × 84.

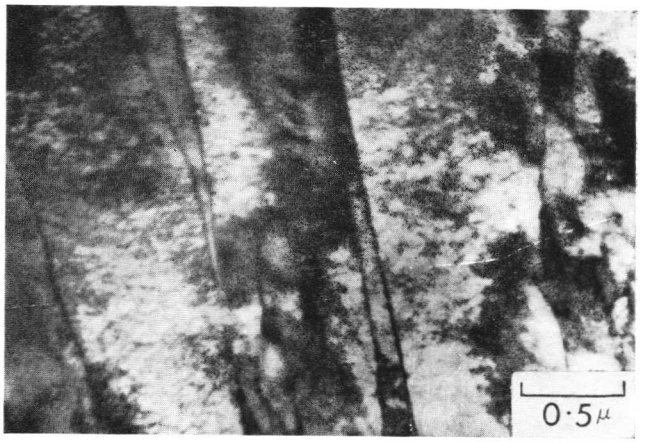

Fig. 3 An electron micrograph of massive martensite laths in an Fe–19·6% Ni–0·09% C specimen.

markings have been observed by Krauss[8] in acicular iron–nickel martensite. Specimens of an Fe–21·6% Ni–0·06% C alloy were carefully prepared and examined in vacuum on a high-temperature microscope. At 750° C the grains at the surface started to etch by thermal grooving of the grain boundaries. The grains were allowed to grow at 925° C for 45 min. The specimen was then cooled to 675° C and held at this temperature. As can be seen from Fig. 4(*a*), no

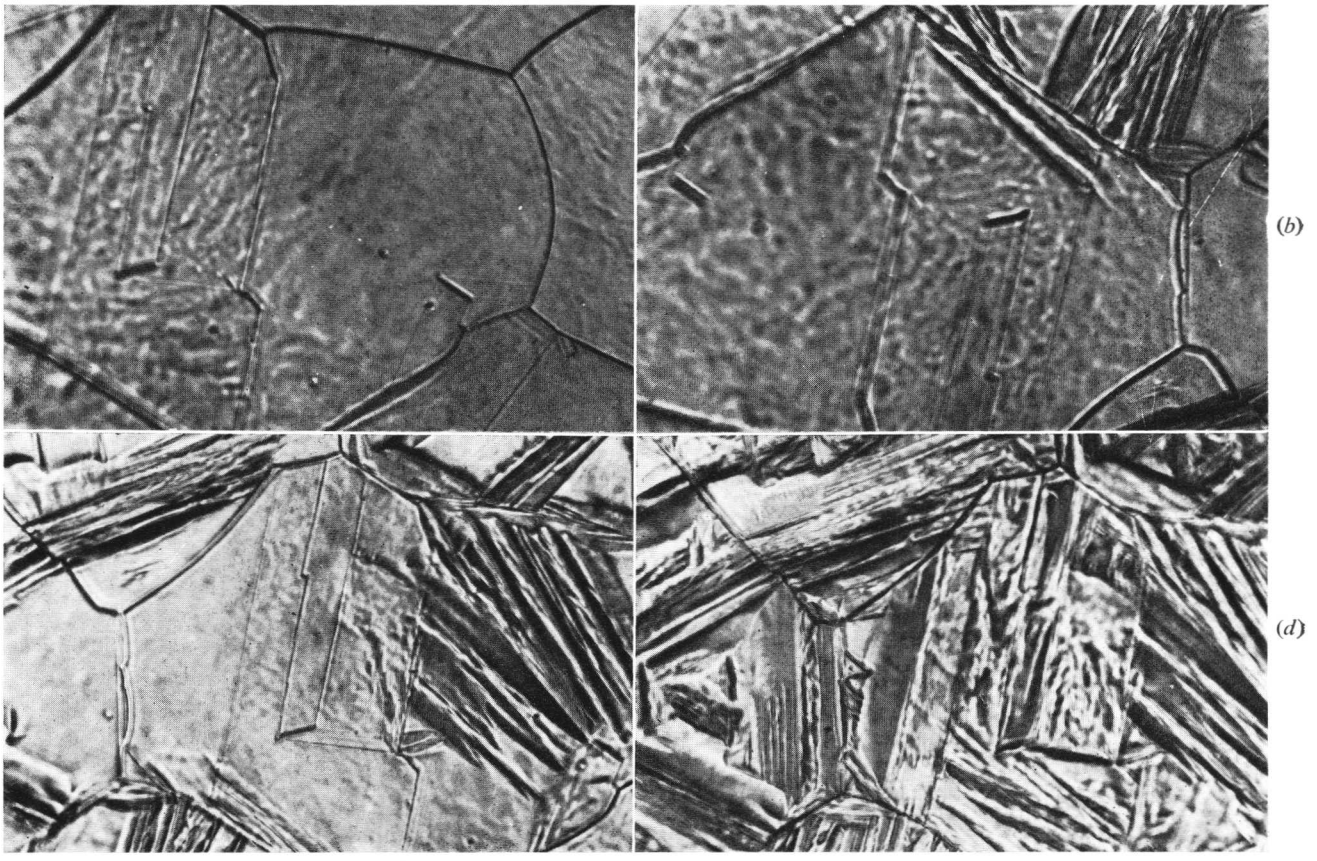

Fig. 4 Transformation sequence from austenite to massive martensite on a prepolished surface of an Fe–21·6% Ni–0·06% C specimen, annealed in vacuum at 925° C for 45 min after polishing and before transformation. × 330. (a) After cooling from 925 to 675° C. (b) After cooling from 675 to 152° C (the surface had transformed 10%). (c) After cooling from 152 to 145° C (the surface had transformed 45%). (d) After cooling from 145 to 97° C (the surface had transformed 100%).

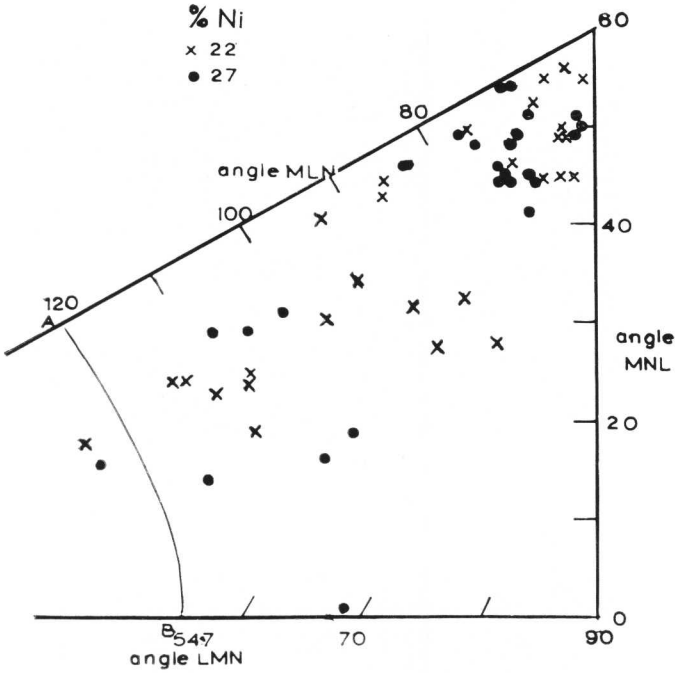

Fig. 5 The inter-trace angles of the surface of randomly sectioned massive martensite specimens, plotted in ternary diagram form from measurements of the non-parallel habit plane traces observed on the surface. The angle $M\hat{L}N$ > the angle $L\hat{M}N$ > the angle $M\hat{N}L$. The line AB marks the limit of the inter-trace angles consistent with the traces being of $\{111\}_\gamma$ planes.

significant " reverse " surface markings were observed during this heat-treatment cycle. After 15 min at 675° C the specimen was allowed to cool. The progress of the transformation is illustrated in Figs. 4(*b*)–(*d*). The massive martensite plates grew in bursts, the first occurring at 157° C and further bursts taking place at temperature intervals down to 97° C in the area observed. The burst generally consisted of one or more regions of parallel plates. Initially the plates formed along or at small angles to annealing twins, or at the remains of the boundaries from previous grains; subsequent transformation was more random within the grains.

Crystallography

Habit Plane

No more than four different surface traces of the shear plates are ever found within any volume formed from an individual austenite grain, suggesting that the shear plates form on $\{111\}_\gamma$ planes. The habit plane of massive martensite must in fact be the plane along which the shape deformation occurs to produce the surface markings, i.e. the plane whose trace is the edge of the shear plates. However, for the present experiments, the plane investigated was that represented by the long edge of the slabs seen in polished and etched massive martensite specimens (e.g. Fig. 2). An advantage of this method is that measurements of the slab edge, which has been shown to be parallel to the surface shear markings, eliminates any errors caused by measuring the edge of plates of surface martensite. It was assumed that the habit plane is the $\{111\}_\gamma$ plane corresponding to the longitudinal edge of the massive martensite slabs. The habit plane of two Fe–Ni massive martensites (22% and 27·4% Ni) were determined using a powerful indirect single-surface crystallographic analysis based on a technique developed by Crocker *et al.*,[9] which involves measuring

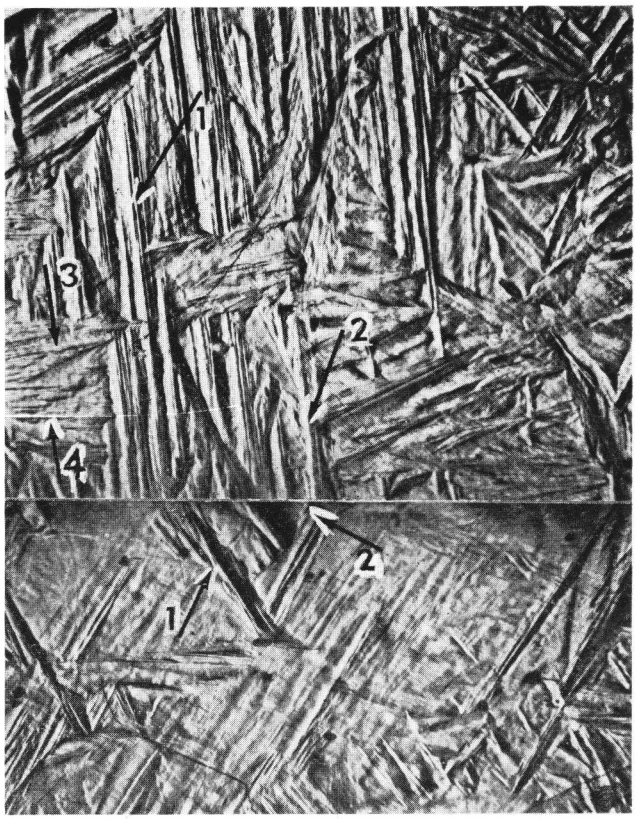

(*a*)

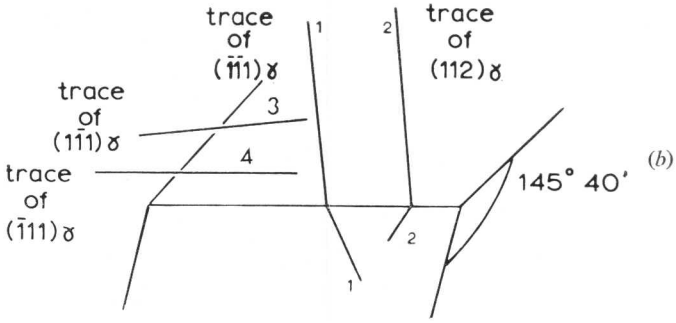

(*b*)

Fig. 6 (a) *A composite micrograph of the surface shear markings on a prepolished Fe–27·4% Ni–0·01% C specimen. The two surfaces intersect and are* 145°45′ *to each other.* × 190. (b) *A diagram of the traces of the habit planes of the plates marked in* (a).

the angles between the habit plane traces of massive martensite slabs in individual austenite grains. Approximately 30 different fields in both alloys were examined. All but two sets of angles were found to produce points on the ternary diagram in Fig. 5 to the right of line AB, where AB indicates the limiting values for the inter-trace angles if the traces are $\{111\}_\gamma$ planes. A very small scatter from a $\{111\}_\gamma$ habit plane would account for the anomalous results. By using the result that the habit plane of the slab interfaces is $\{111\}_\gamma$, the angle between two precision-polished orthogonal surfaces showing three habit-plane traces was calculated in several instances to be within 30′ of 90°, confirming the result of the single-surface analysis that the habit plane is $\{111\}_\gamma$ or a plane very close to it. The habit plane of the surface shear markings of massive martensite was also determined as $\{111\}_\gamma$ by two-surface analysis. Recently McDougall[10] has

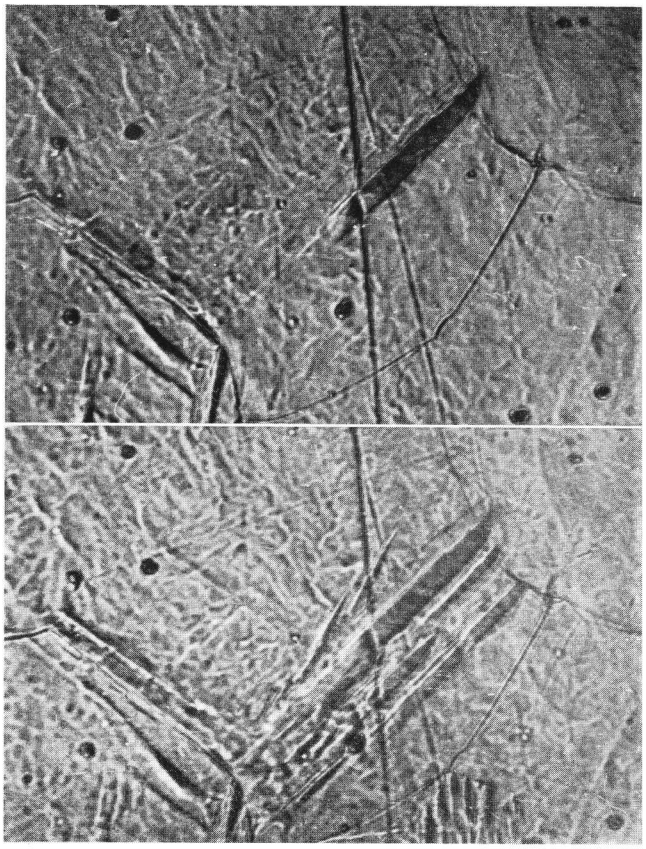

Fig. 7 (a) *The transformation markings that appeared initially on the surface of an Fe–22·0% Ni–0·01% C specimen at 230° C. Note the change in direction of the scratches caused by the surface upheavals.* (b) *The same field as in* (a) *after further transformation had occurred at 180° C. Both* × 380.

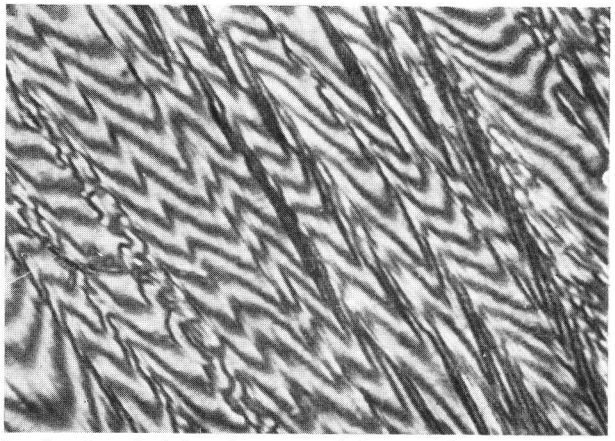

Fig. 8 A typical interferogram of the transformation markings on the surface of an Fe–22·0% Ni–0·01% C specimen. This shows the shape of the tilts associated with a homogeneous shape deformation. Taken with mercury light, $\lambda = 0{\cdot}54$ *μm.* × 340.

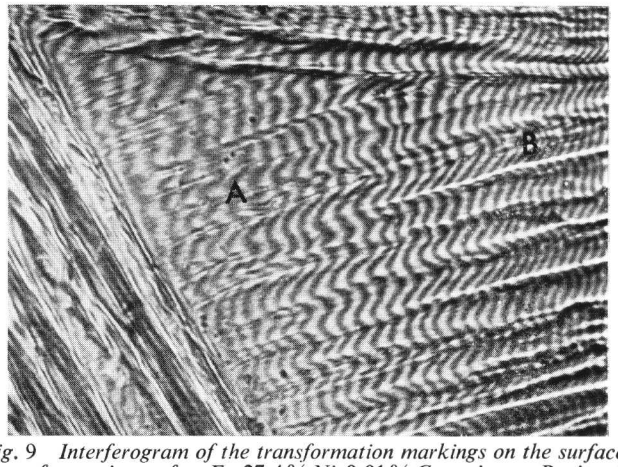

Fig. 9 Interferogram of the transformation markings on the surface of a specimen of an Fe–27·4% Ni–0·01% C specimen. Region A is an area of curved markings, whereas region B is a typical example of an area containing pairs of self-accommodating markings. Taken with mercury light, $\lambda = 0{\cdot}54$ *μm.* × 450.

carried out a selected-area electron-diffraction study of an Fe–24% Ni–0·1% C alloy containing a small amount of retained austenite at room temperature, and has shown that the habit plane of the individual laths within the slabs is $\{111\}_\gamma$. Therefore, the habit plane of the massive martensite slabs, the surface shear markings, and the substructural laths is $\{111\}_\gamma$.

Occasionally in the Fe–22% Ni alloy, surface markings did not correspond to $\{111\}_\gamma$ traces and did not penetrate more than ~ 4 μm into the bulk of the material. The amount of this surface martensite increased considerably as the nickel content increased towards the transition to acicular martensite (29% Ni). These surface martensite plates are very similar to the surface shear markings of massive martensite (Fig. 6) and can be distinguished from them on free surfaces only by measurement of the habit plane. The habit plane was found by two-surface trace analysis to be close to $\{112\}_\gamma$, confirming the single-surface result of Klostermann and Burgers.[3]

Shape Deformation

A further series of hot-stage microscopy experiments was performed to determine the nature of the shape deformation producing surface shear markings. This was done by scratching the surface before placing the specimens in the hot stage and observing the subsequent deflection of the scratches due to the formation of the surface shear markings. The deviation of the scratches produced by the initially formed plates was quite easy to follow (Fig. 7(*a*)), but plates produced later in the transformation could not be examined in this fashion because the scratches were too distorted as a result of earlier surface upheavals (Fig. 7(*b*)). A close study of the mode of formation of massive martensite using the hot stage has shown that only in exceptional circumstances does an individual shear marking appear. They are generally, as in Fig. 7(*a*), in groups of at least two self-accommodating plates[11] and such an arrangement appears to be connected at least partly with the accommodation of the martensite by the austenite. From Fig. 7(*a*) it can be seen that the scratches remain straight on crossing the tilts and are continuous on crossing the austenite/martensite interface, i.e. the transformation markings have been formed by a tilting of the original surface about the interface between the transformed region and the austenite. It can therefore be concluded that the initial shear markings have been formed by a homogeneous deformation process, but it is not possible to say that the austenite/martensite interface is undistorted.

Interferometric studies at room temperature on fully transformed specimens have revealed that the interface between pairs of self-accommodating plates is usually undistorted. A typical interferogram of surface shear markings

in an Fe–22% Ni specimen is shown in Fig. 8. The form of the interference fringes crossing the pairs of massive martensite plates clearly demonstrates that the shape deformation associated with massive martensite is homogeneous. However, in a number of fields, particularly in the Fe–21·6% Ni–0·06% C and Fe–27·4% Ni specimens, it became noticeable that there were fewer homogeneous deformation profiles and that some profiles had become curved (A in Fig. 9). A feature of some of these plates was that one end (B) had regular deformation profiles as found with self-accommodating pairs, while at the other end there was a curved profile, associated with a single plate. It has been shown that massive martensite forms in such a manner as to fill space completely and this would suggest that in those regions of austenite near to previously transformed martensite the internal elastic and plastic strains are sufficiently large to prohibit normal self-accommodating growth. Consequently, to minimize the strain energy of the plates they attempt to accommodate themselves *internally* and take on this curved shape. Such profiles are clearly not associated with homogeneous distortions and no attempt will be made to fit a theory of martensite crystallography to these curved plates.

Magnitude and Direction of Shape Deformation

The other two parameters, in addition to the $\{111\}_\gamma$ habit plane, necessary to define the shape deformation are its magnitude and direction. These were measured in the manner described by Greninger and Troiano.[12] This method assumes that the shape deformation is a shear (called the shape shear) on the habit plane and neglects the volume change necessary for a complete description of the austenite to martensite transformation. The determination of the shear direction was performed stereographically and normally would give a result accurate to within 3°. However, the accuracy of the present work was improved by measuring a shear direction with respect to each of the two surfaces on which tilting due to the measured plate was seen. Then one of these directions was rotated, so that it was given with respect to the reference surface for the other direction, and the mean value of these directions was taken as the measured value. These results are shown in Fig. 10. The magnitude of the shape shear was calculated from the measurements on each surface and the two values were always to within 1°. The mean of these values is shown in Table I.

The relationship between the magnitude and direction of the shear and the magnitude and direction of the true shape deformation is shown in Fig. 11(*a*). To assess the error involved in Greninger and Troiano's assumption, the volume ratio between the austenite and the martensite was determined. With this information calculations were made of the differences between the measured magnitude of the shape shear (γ') and the real magnitude of the shape deformation (γ), also between the directions AC and AB, the measured and real directions of the shape deformation. The maximum error in the magnitude of the shape deformation was negligible compared with the measured value (if $\gamma' = 7°$ the difference between γ and γ' is $\sim 12'$). However, the error between the measured shear direction and the true shape-deformation direction is not negligible It is also very sensitive to changes in γ', e.g. the angle BÂC in Fig. 11 varies by 8° for a change of 2° in γ'. The positions of the true shape-deformation directions are shown in Fig. 10(*a*). From the results for the Fe–22% Ni alloy it can be seen that, like the shear directions, the corresponding shape-deformation direc-

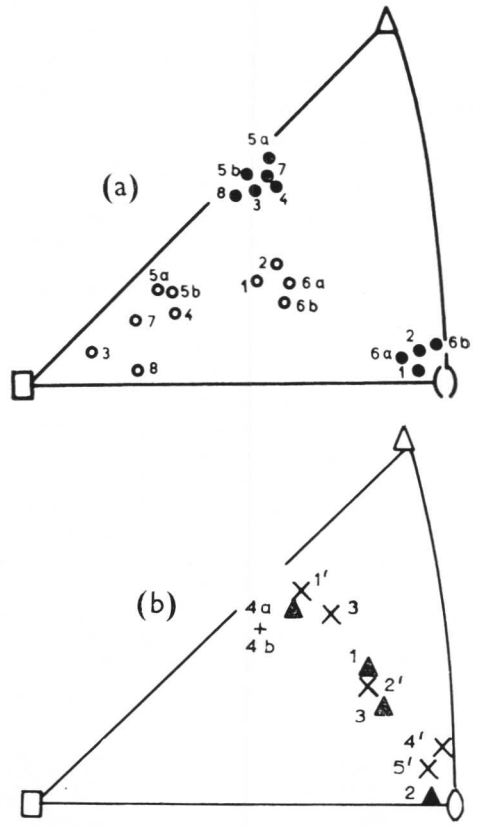

Fig. 10 (a) *The measured directions of the shape shears and the calculated shape-deformation directions associated with the production of the transformation markings on the surfaces of Fe–22% Ni–0·01% C specimens.* ○ *Shape-deformation directions.* ● *Shape-shear directions.* (b) *The measured directions of the shape shears associated with the production of the transformation markings on the surfaces of Fe–21·6% Ni–0·06% C and Fe–27·4% Ni–0·01% C specimens.* ▲ *Fe–27·4% Ni–0·01% C.* × *Fe–21·6% Ni–0·06% C.*

TABLE I

The Magnitude of the Shape Shear γ' Calculated from Experimental Measurements on Specimens of Massive Martensite

Fe–22% Ni–0·01% C		Fe–21·6% Ni–0·06% C		Fe–27·4% Ni–0·01% C	
Plate No.	Average γ'	Plate No.	Average γ'	Plate No.	Average γ'
1	5·5°	1	8·0°	1	8·5°
2	5·0°	2	6·5°	2	5·0°
3	4·0°	3	7·0°	3	7·5°
4	8·0°	4	5·5°	4a*	10·0°
5a*	7·5°	5	7·5°	4b*	7·5°
5b*	7·0°				
6a*	6·5°				
6b*	5·5°				
7	6·5°				
8	8·0°				

*Self-accommodating pairs of massive martensite plates.

tions lie in two discrete regions. For the other two alloys, where the scatter in the measured shear directions is appreciable, the scatter becomes accentuated when the true shape-deformation directions are evaluated and for the purpose of clarity these have not been plotted. As there is no significant difference between the magnitude of the shape deformations for any of the three alloys studied, the increased scatter cannot be attributed to changes in γ. It is likely that this change is due to slight deviations in the habit plane from $\{111\}_\gamma$, which can occur at alloy concentrations approaching the transition to acicular martensite.

Orientation Relationship

A specific orientation relationship between a lath of massive martensite and the parent austenite, which is necessary for the application of phenomenological theories of martensite formation, is normally unobtainable by conventional orientation techniques. This is because of the small size of the laths and the fact that at room temperature there is usually no retained austenite. However, Mehl and Derge[13] have found that a Fe–29% Ni alloy which transformed to massive martensite near room temperature, and thus contained some retained austenite, had a Kurdjumov–Sachs[14] orientation relationship, while in an Fe–24% Ni–0·1% C alloy, also containing a little retained austenite, McDougall has shown by electron diffraction that a K–S relationship existed between the martensite laths and the surrounding austenite.[10]

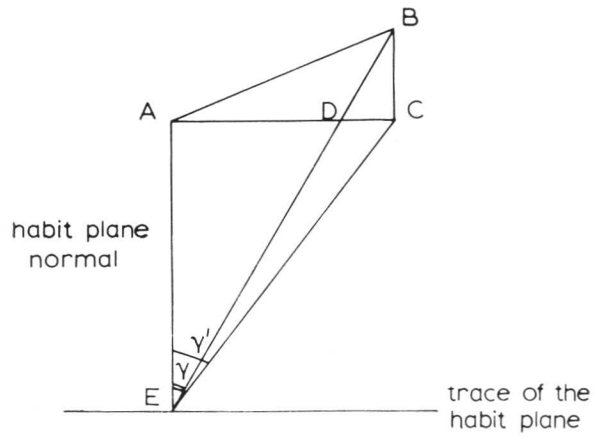

Fig. 11 *The relationship between the true magnitude of the shape deformation* γ *and the measured magnitude of the shape shear* γ'*, and between the true and measured shape-deformation directions AB and AC, respectively.*

In the present work it was decided to obtain a specific orientation relationship by comparing the orientation of large austenite grains with the orientation of laths in thin foils prepared as nearly as possible parallel to the parent austenite grain. In the light of the above evidence pointing

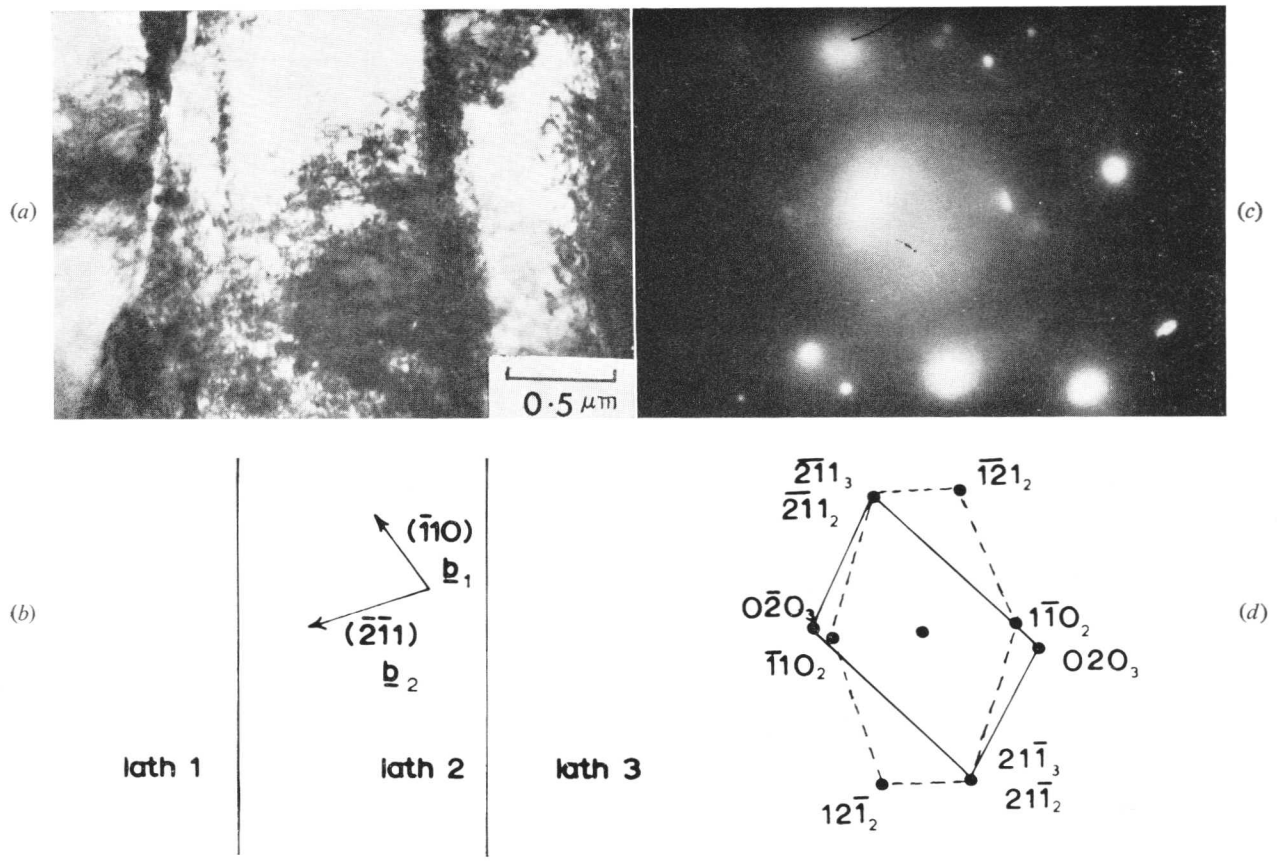

Fig. 12 (a) *An electron micrograph of a thin foil from a single crystal of austenite of known orientation, showing three separate laths.* (b) *Schematic representation of the three laths labelled* 1, 2, *and* 3. (c) *The combined diffraction pattern from laths* 2 *and* 3. (d) *The solution to the diffraction pattern in* (c).

to a K–S relationship, together with the fact that Speich and Swann[2] have shown that the lath interface is a close-packed $\{110\}_\alpha$ plane, it was decided to restrict the infinite number of possible relations that could exist between a martensite lath and a parent austenite grain. Only those orientations relationships known to exist for ferrous alloys in which a close-packed plane in the austenite is parallel to one in the martensite were considered. It was reasoned that any two laths of different orientations must bear the same type of orientation relationship with respect to the austenite grain within which they were formed. Therefore, if the orientation of one of the laths is considered to give a particular relationship with respect to the austenite, this would be valid only if the orientation of the second lath, which is fixed with respect to the first, exhibited the same type of relationship with the austenite as with the first lath.

A single crystal of austenite in an Fe–22% Ni alloy, after transformation to massive martensite, was oriented precisely using $\{111\}_\gamma$ slab interfaces which extended on to two orthogonal surfaces and found to be $(\overline{2.003}, 2.003, 1.353)_\gamma$. This individual grain was then carefully grown until 0·003 in. thick and finally electropolished to produce a thin foil. The field to be considered is shown in Fig. 12(*a*) and is schematically represented in Fig. 12(*b*). The diffraction pattern from lath 1 was identical to that from lath 3 and in Fig. 12(*c*) the combined diffraction pattern from laths 2 and 3 is given. The solution to the diffraction pattern is presented in Fig. 12(*d*). Standard stereographic analysis of these results reveals the following relationships:

For laths 1 and 3: $(\bar{1}\bar{1}1)_\gamma \parallel (\bar{1}01)_{\alpha'}$
$[011]_\gamma \wedge [1\bar{1}1]_{\alpha'} = 2^\circ$

For lath 2: $(\bar{1}\bar{1}1)_\gamma \parallel (\bar{1}01)_{\alpha'}$
$[\bar{1}10]_\gamma \wedge [111]_{\alpha'} = 2^\circ$

Although these relationships are not quite Kurdjumov–Sachs, the relationship between laths, which is a rotation of 10° about the interface pole, is such that a Kurdjumov–Sachs orientation is a possibility. The difference between the quoted and the Kurdjumov–Sachs relationship may be due to unavoidable experimental inaccuracies.

Application of the Phenomenological Theories of Martensite Formation to the Massive Martensite Reaction

The major phenomenological theories of martensite formation,[15–18] based on the equation

$$\mathbf{E} = \mathbf{S}\,\mathbf{R}\,\mathbf{P}$$

where **E** is the total shape deformation, **R** the orientation rotation, **S** the correspondence strain, and **P** the lattice inhomogeneous shear, have failed to account for the experimental $\{111\}_\gamma$ habit plane and an average total shape deformation of 6·5° for massive martensite.

In the present work the approach of Jaswon and Wheeler[19] has been adopted. They derived a matrix, δ, which on operating upon the individual atomic positions in the austenite lattice produces corresponding atomic positions on the martensite lattice, referred to the austenite lattice. The value of δ has been calculated as detailed by Jaswon and Wheeler for the case of massive martensite in an Fe–22% Ni alloy with the following orientation relationship:

$$(\bar{1}\bar{1}1)_\gamma \parallel (\bar{1}01)_{\alpha'}$$

$$[011]_\gamma \parallel [1\bar{1}1]_{\alpha'}$$

which approximates to the orientation relationship discussed in the previous section. The austenite lattice parameter used was 3·576 Å, obtained by extrapolation of the data of Bradley, Jay, and Taylor,[20] while the martensite parameter was obtained by standard diffractometry as 2·875 Å.

The matrix was found to be

$$\delta = \begin{pmatrix} 0.791 & \overline{0.060} & 0.134 \\ 0.074 & 1.133 & 0.074 \\ \overline{0.194} & \overline{0.060} & 1.120 \end{pmatrix}$$

As a result of the operation of this matrix upon atom positions lying in all planes, vectors in only $(\bar{1}\bar{1}1)_\gamma$ and $(\bar{2}\bar{2}5)_\gamma$ planes do not rotate. There is, however, a change in their length, i.e. the distortion corresponding to δ is not an invariant plane strain. The observed *invariant plane* between the *martensite laths* can be explained by considering the following experimental orientation relationships between adjacent laths.

(*a*) The orientation of lath 1 is related to that of lath 2 by a rotation of 70° 32′ about the normal to the interface, to produce twin related laths.[2]

(*b*) The orientation of lath 1 is related to that of lath 2 by a rotation of 10° about the interfacial normal.

(*c*) The orientation of lath 1 is approximately the same as lath 3. For case (*a*) it can be seen, by calculating two values of δ such that twin related laths are formed, that the atoms in the interface that are initially displaced from their original positions by the formation of the first plate are hardly affected by the formation of the second plate next to the first. This results in the formation of an effectively undistorted interface plane, the large strains that would have been apparent in the austenite/martensite interface if just one plate had been formed being practically cancelled out by the formation of the second plate alongside it. Calculations using the theory in case (*b*) show that an invariant interface plane between the laths can be produced in the same way as for case (*a*). Case (*c*) is more difficult to explain, since the action of the same distortion upon the interface twice does not produce an undistorted interface between two laths of the same orientation. However, if the orientation of the first lath is related to that of the second lath by a rotation of 180° about the normal to the interface, the diffraction patterns of two laths with a $\{110\}_\alpha$ interface would be indistinguishable. If in fact this relationship between the laths is present, the action of the two distortions upon the interface will give an approximately invariant plane between the laths. Consequently, for the three cases examined the observed invariant interface plane of self-accommodating massive martensite plates is, for the purposes of calculation, directly comparable to an invariant habit plane between austenite and martensite. In the following discussion a model is proposed that explains the observed magnitude and direction of the shape deformation of self-accommodating pairs of massive martensite plates that have an invariant $\{111\}_\gamma$ interface plane.

The deformation corresponding to the matrix δ derived by Jaswon and Wheeler[19] takes into account the volume

change between the austenite and massive martensite. However, the results from the shape-deformation experiments are more readily analysed when the simple shear model of Greninger and Troiano[12] is considered. Therefore, the magnitude and direction of the deformation derived from δ have been modified so that they correspond to the experimental shear results. When the orientation relationships between the martensite and the austenite were

$$(\bar{1}\bar{1}1)_\gamma \parallel (\bar{1}01)_{\alpha'}$$
$$[011]_\gamma \parallel [1\bar{1}1]_{\alpha'}$$

and the undistorted interface plane was $(\bar{1}\bar{1}1)_\gamma$, the direction of the modified distortion δ' was $[0.438\ \overline{0.098}\ 0.340]_\gamma$ and the magnitude of the shear was 16·5°. Clearly this does not correspond to the experimental results and the assumption that $E = \delta$ or E' (the shape shear) $= \delta'$ alone is not permissible.

However, consider now the case where $E' = \delta' P$, where P is a shear occurring on the undistorted interface plane. This will not alter the interface plane or the orientation relationships, but the shape shear now becomes the result of the two shears δ' and P. The calculation of the magnitude and direction of the new shape shear becomes analogous to the solution of a triangle of forces. The sides of the triangle are made up of vectors representing the magnitudes and directions of the three shears E', δ', and P, which in the case of massive martensite may be considered as occurring in the interface plane. Since the resultant shape shear has been experimentally determined, the problem reduces to the selection of possible combinations of P and δ', which together with the experimental shape shear will produce three vectors such that the sum of the angles between the vectors will be 180°. For the specific case stated above the following elements of P were considered:

$[011]_\gamma$ $(\bar{1}\bar{1}1)_\gamma$, $[1\bar{1}0]_\gamma$ $(\bar{1}\bar{1}1)_\gamma$, $[\bar{1}10]_\gamma$ $(\bar{1}\bar{1}1)_\gamma$, $[101]_\gamma$ $(\bar{1}\bar{1}1)_\gamma$, $[\bar{1}0\bar{1}]_\gamma$ $(\bar{1}\bar{1}1)_\gamma$, $[0\bar{1}\bar{1}]_\gamma$ $(\bar{1}\bar{1}1)_\gamma$.

The angles between these directions and $[0.438, \overline{0.098}, 0.340]$ were determined and possible overall shape shears with the experimental shear directions $\langle 112\rangle_\gamma$ and $\langle 110\rangle_\gamma$ fitted to see if geometrical consistency between the directions could be obtained. When such directions were obtained, their length, i.e. the value of tan γ', was calculated together with the magnitude of P. Possible results are given in Table II. It can be seen that some of these values are very nearly in agreement with the experimentally measured shape shear. As a check on the simple shear model, the ideal $[112]_\gamma$ and $[110]_\gamma$ shear directions were translated into true shape-deformation directions (as outlined earlier) and the closest possible rational index directions assigned to them; these were $[128]_\gamma$ and $[\bar{1}24]_\gamma$, respectively. The corresponding magnitudes of the true shape deformations were found to be 4° 36′ and 4° 42′, thus confirming the results of the simple shear model.

An interesting feature of this theory of massive martensite is that it predicts the experimental observation that massive martensite laths should be self-accommodating. If this does not happen, an intolerable strain will exist in the austenite/martensite interface and the reaction will cease. The size of a group of self-accommodating massive martensite laths is governed by the number of occasions on which self-accommodation can occur. When a lath fails to nucleate alongside the lath formed immediately before it, the strain across the martensite/austenite interface becomes so great that coherency is lost and the group will not propagate further. A possible reason for the failure of a lath to nucleate at the edge of a massive martensite group is the build-up of strain in the austenite due to the formation of previous laths in the group. When this occurs, as has been shown by hot-stage metallography, a considerable drop in temperature must occur before nucleation in the region of the group can take place.

TABLE II

The Theoretical Magnitude and Direction of the Shape Shear E', together with the Corresponding Elements of the Lattice-Invariant Shear P, for a Massive Martensite Lath with a $(\bar{1}\bar{1}1)_\gamma$ Habit Plane

The orientation relationship between the martensite and the austenite is given by: $(\bar{1}\bar{1}1)_\gamma \parallel (\bar{1}01)_{\alpha'}$; $[011]_\gamma \parallel [1\bar{1}1]_{\alpha'}$

Plane of P	Magnitude of P	Direction of P	Magnitude of E'	Direction of E'
$(\bar{1}\bar{1}1)$*	14·0°	$[\bar{1}0\bar{1}]_\gamma$	4·3°	$[1\bar{1}0]_\gamma$
$(\bar{1}\bar{1}1)$*	15·5°	$[\bar{1}0\bar{1}]_\gamma$	4·0°	$[1\bar{2}\bar{1}]_\gamma$
$(\bar{1}\bar{1}1)$	14·0°	$[\bar{1}10]_\gamma$	12·5°	$[112]_\gamma$
$(\bar{1}\bar{1}1)$	4·5°	$[\bar{1}10]_\gamma$	14·5°	$[101]_\gamma$

*Results fit experimental facts.

Acknowledgements

The authors wish to thank their colleagues Professor W. S. Owen and Dr. M. J. Bevis for many helpful and stimulating discussions.

References

1. W. S. Owen, E. A. Wilson, and T. Bell, " High-Strength Materials " (edited by V. F. Zackay) (Proc. 2nd Berkeley Internat. Mat. Conf.), p. 167. **1965:** New York and London (John Wiley).
2. G. P. Speich and P. Swann, *J. Iron Steel Inst.*, 1965, **203**, 450.
3. J. A. Klostermann and W. G. Burgers, *Acta Met.*, 1964, **12**, 355.
4. T. Honma, *J. Japan Inst. Metals*, 1957, **22**, 122.
5. J. A. Lund and A. M. Lawson, *Trans. Met. Soc. A.I.M.E.*, 1966, **236**, 581.
6. P. M. Kelly and J. Nutting, *Proc. Roy. Soc.*, 1960, [A], **259**, 45.
7. T. Bell and W. S. Owen, *J. Iron Steel Inst.*, 1967, **205**, 428.
8. G. Krauss, *Acta Met.*, 1963, **11**, 499.
9. A. G. Crocker, F. Heckscher, and M. Bevis, *Phil. Mag.*, 1963, **8**, 1863.
10. P. McDougall, " Physical Properties of Martensite and Bainite " (Special Rep. No. 93), p. 164. **1964:** London (Iron Steel Inst.).
11. J. W. Christian, *ibid.*, p. 1.
12. A. B. Greninger and A. Troiano, *J. Metals*, 1940, **1**, 590.
13. R. F. Mehl and G. Derge, *Trans. Amer. Inst. Min. Met. Eng.*, 1937, **125**, 482.
14. G. Kurdjumov and G. Sachs, *Z. Physik*, 1930, **64**, 325.
15. M. Wechsler, D. S. Lieberman, and T. A. Reid, *Trans. Amer. Inst. Min. Met. Eng.*, 1953, **197**, 1503.
16. J. S. Bowles and J. Mackenzie, *Acta Met.*, 1954, **2**, 129.
17. R. Bullough and B. A. Bilby, *Proc. Phys. Soc.*, 1956, [B], **69**, 1276.
18. A. G. Crocker and B. A. Bilby, *Acta Met.*, 1961, **9**, 678.
19. M. A. Jaswon and J. A. Wheeler, *Acta Cryst.*, 1948, **1**, 216.
20. A. R. Bradley, A. H. Jay, and A. Taylor, *Phil. Mag.*, 1937, **1**, 545.

Research Note

Transformation in Stressed Cobalt–Nickel Crystals

Emmanuel deLamotte and Carl Altstetter

Close-packed planes of atoms may be stacked in several different ways so that either a face-centred cubic or a hexagonal lattice may be formed. For simple crystal structures a change from one structure to another may occur by the shifting of the planes over one another in a regular fashion. The formal similarity between transformation, f.c.c. twinning, and slip suggests that transformation occurs by the glide of dislocations over the close-packed planes. Indeed, shear displacements are observed to occur upon transformation of cobalt, cerium, and lanthanum, as well as in alloys of these and other metals. The f.c.c. $\rightleftharpoons$ h.c.p. transformation in cobalt and its alloys may be accomplished by an $a/6\ \langle 112\rangle$ ($a/3\ \langle 10\bar{1}0\rangle$) dislocation passing over every second $\{111\}$ ((0002)) plane of the cubic (hexagonal) crystal. In addition, the interatomic distance in the plane, as well as the interplanar spacing, must change in order to account for the observed lattice parameters. The present work seeks to determine the mechanism through which dislocations are produced on or transferred to the required planes so that the transformation interface is propagated from plane to plane. Single-crystal specimens were stressed in tension and then cooled and heated through the transformation-temperature range, both with and without the stress applied. Product morphology, surface shears, lattice rotation, and macroscopic strain were measured both before and after transformation as a function of the applied stress.

A cobalt alloy containing 30·5% nickel was chosen for study, because the transformation hysteresis loop is centred around room temperature. Either structure could then be studied at room temperature depending on whether the specimen had just been cooled or just been heated to room temperature. The alloy was vacuum induction-melted from $>$ 99·99% purity metals in an alumina crucible. Seven crystals 5 mm in dia. by up to 25 cm in length were produced from swaged rod by electron-beam floating-zone levelling at 10^{-6} torr. From one crystal as many as five tensile specimens having $^3/_{32}$-in.-square cross-sections and 1-in. gauge-lengths were spark-machined. Electropolishing and chemical polishing were used to remove the spark damage and to make metallographic and X-ray observation easier.

In the unstressed crystals the alloy transformed on the four possible $\{111\}$ planes, but the transformation did not go to completion even after cooling to −196°C. This behaviour is in marked contrast to that of pure cobalt crystals, which may transform within an interval of a few degrees to a hexagonal single crystal.[1] Under zero load the transformation in the alloy was rather difficult to detect by dilatometry because the anomaly was so small and spread over a broad temperature interval. This indicates that the shear strains very nearly averaged to zero by passage of equal numbers of dislocations having the three possible $\langle 112\rangle$ directions in a given transformation plane. Interferograms of surfaces which were polished and then partially transformed showed that fringes suffered little net displacement across a transformation band, though

Manuscript received 3 July 1968. Professor Carl Altstetter, Sc.D., is in the Department of Mining, Metallurgy, and Petroleum Engineering, University of Illinois, Urbana, Ill., U.S.A. Emmanuel deLamotte, Ph.D., is now at McMaster University, Hamilton, Ontario, Canada.

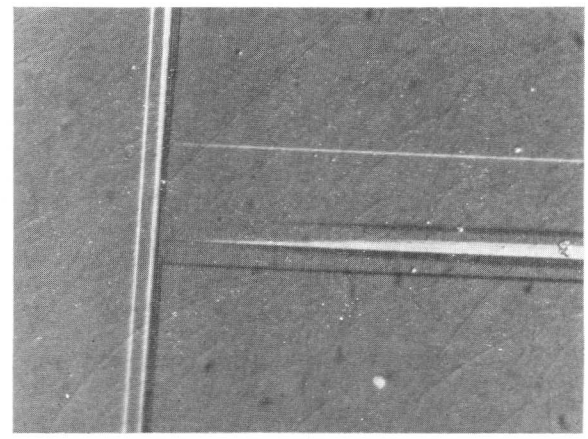

Fig. 1 Surface relief due to bands of h.c.p. in f.c.c. matrix. Co–30·5% Ni alloy. Nomarski contrast. ×750.

at places within the bands the shear strain approached the theoretical value of 0·35. Mostly, however, the averaging of the shear strains to zero takes place within distances of the order of 1000 Å.[2]

Small elastic tensile stresses applied while cooling did not force transformation on the most highly stressed plane in the alloy, nor in pure cobalt.[1] Obviously, no critical resolved shear stress criterion determines the shear system for transformation as it does for slip. The length change on transformation did show a slight effect of applied elastic stress. On cooling the length usually increased abruptly as the transformation started. On heating, the length usually decreased, in opposition to the applied tensile stress, but the magnitude was less than on cooling, so that the hysteresis loop did not close. On cooling, the orientation of the tensile axis tended to rotate toward a $\langle 112\rangle$ direction in each of the regions of product phase. On heating, the axis moved in the opposite direction, tending toward its original orientation. Fig. 1 illustrates the likely reason for this: the transformation dislocations which must exist at the tapered end of the horizontal band merely reverse their direction of motion upon heating. Single crystals resulted from one cycle around the hysteresis loop. Very little transformation occurred on cooling these crystals to −196°C a second time, and they recrystallized upon heating to 800°C. The amount of lattice damage done by the transformation is certainly considerable.[3]

At increased applied tensile stress, approaching the yield stress of the material, the effect of stress became more pronounced. The hysteresis loop narrowed, there was an increase in the amount transformed, and a tendency toward a single orientation of product. The specimens increased in length by several per cent. on cooling and *increased* in length nearly this much on heating.

The most dramatic effect of stress occurred when the yield stress was exceeded. As expected, a critical resolved shear stress criterion determined the slip system and the specimen axis rotated toward a $\{110\}$ direction. A single orientation of slip lines was observed, but there was no transformation at

room temperature, except for specimens stressed into work-hardening Stage II. Single-slipped f.c.c. crystals transformed to single h.c.p. crystals on cooling, either with or without applied stress during cooling. With applied stress, the axial elongation and specimen axis rotation indicated shear strains approaching the theoretical value of 35%. The specimen axis rotated toward a ⟨112⟩ direction, but not invariably toward the most highly stressed one. Without applied stress during cooling the macroscopic shear strain was very small. Upon heating the single h.c.p. crystals, the transformation shear strains approached 35% if stress was applied during heating, otherwise the strains were small. The rotation of the specimen axis upon heating under stress was generally not toward a rational crystallographic direction. In fact, most commonly the specimen axis rotated toward the most highly stressed (non-crystallographic) direction in the habit plane. Frequently the f.c.c. crystal resulting from one cycle of transformation under a high tensile stress was the twin of the starting crystal. In effect, after one cycle, an $a/6$ ⟨112⟩ partial dislocation had swept over each close-packed plane so that the crystal completely twinned under the action of the applied stress and temperature cycle.

The data described here and other recent data from the authors' laboratory[4] have been used to test some of the existing models of interface propagation. Without going into the details here, it was concluded that some extension or synthesis of existing models could better explain the recent findings. The following mechanism is proposed. Dislocations existing in the virgin crystals, or introduced by stressing, are widely dissociated near the transformation temperature. The stacking faults that join the partial dislocations act as surfaces near which additional loops of partial dislocation may be nucleated on parallel planes two layers away. The nucleation is made possible by the free-energy difference between the phases and the applied plus internal stress. It is suggested that the elastic energy of a dislocation loop at the f.c.c./h.c.p. interface may be smaller than that for a loop having the same Burgers vector, but which is not at an interface. This is partly due to the fact that the dislocation helps to accommodate the difference in interatomic distances between the two phases: it is an interface dislocation. In addition, it seems reasonable to expect that along the interface the shear modulus has a lower value than in the bulk. At the M_s temperature the supercooling has reached a critical value at which the dislocation loop nucleation rate becomes very large.

Though the dislocations are quite glissile, so that the "growth" rate may be very high, transformation does not go to completion because of the back-stresses that develop. Also, the driving force is diminished by the production of point defects, accommodation slip dislocations, stacking faults, and elastic strains in the parent and product phases as the transformation proceeds. The enthalpy increase due to these defects which remain in the specimen has been measured to be ~15% of the enthalpy difference (100 cal/mole) between the two crystalline forms of cobalt. Further work to measure the number and distribution of transformation-induced defects is currently under way.

Acknowledgements

This work was sponsored by the U.S. Army Research Office (Durham), whose support is gratefully acknowledged. The use of some of the facilities of the Materials Research Laboratory of the University of Illinois is also appreciated.

References

1. J. Nelson and C. Altstetter, *Trans. Met. Soc. A.I.M.E.*, 1968, **242,** 139.
2. M. Gedwill, C. Altstetter, and C. Wayman, *ibid.*, 1964, **230,** 463.
3. R. Adams and C. Altstetter, *ibid.*, 1968, **242,** 139.
4. E. deLamotte and C. Altstetter, *Trans. Met. Soc. A.I.M.E.*, to be published.

Research Note

Remarks on the Factors Controlling the Lattice-Orientation Relationship and Habit Orientation in Martensitic Transformation Processes

W. G. Burgers

In the theories of martensite formation, as developed in particular by Bowles and Mackenzie[1] and by Wechsler, Lieberman, and Read,[2] the transformation process is treated in a purely phenomenological way without the necessity to consider the precise atomic movements that bring about the transformation. Given the parameters of the original and the transformed lattices, the correspondence and the crystallography of the lattice invariant shear (or twinning) have been assumed; then the undistorted plane (the "habit plane"), the lattice-orientation relationship, and the shape deformation follow from the matrix calculation.

The fact that the experimental observations for a given metal or alloy, though approximately corresponding to the calculated data, deviate rather considerably in various cases, may be accounted for by the introduction of a "free" parameter in the theory, e.g., an isotropic dilatation of the undistorted plane, a different choice of the crystallographic character of the lattice invariant shear, or eventually the assumption of a multiple shear.

Another approach to the problem of the orientation relationships occurring in martensite formation would be to start from what happens precisely in the act of nucleation. Considerations of the activation energy required for nucleation (see e.g. Refs. (3) and (4)) make it practically certain that nucleation can occur only in regions of the matrix where sufficient surplus free energy, presumably as pile-ups of suitable dislocations, is available. Under such circumstances the course of the actual nucleation process might be expected to depend on the local pattern and activity of available dislocations, i.e. whether they are distributed over one or over intersecting sets of parallel planes, and moving simultaneously or

Manuscript received 3 July 1968. Professor W. G. Burgers, Dr. Chem., is in the Laboratory for Metallurgy, Technological University, Delft, The Netherlands.

one after the other. Such factors, we think, may play a predominant part in determining what lattice planes and/or directions of the original lattice will finally be parallel to corresponding planes and/or directions in the transformed lattice. Such a conception comes close to a statement by Lieberman,[5] according to which the introduction of certain arrays of dislocations into a metal or alloy *before* transformation predetermines the "pattern of inhomogeneity" and hence the transformation mechanism.

A reasoning along these lines was given[6] when considering the transformation of a close-packed stack of spheres into a body-centred cubic arrangement by applying shears along close-packed planes in easy (f.c.c. ⟨112⟩) directions.[7] Depending on what plane or direction in such a model is kept fixed with respect to the surrounding matrix, the various orientation relationships can be obtained at will. Experimentally this could be realized[8] by producing martensite domains in nickel–iron single crystals purely by isothermal compression. If the compression took place parallel to an austenite ⟨100⟩ direction, shear occurred simultaneously along all octahedral planes in approximately equal intensity and the true Bain orientation relationship resulted. If, however, a crystal of the same composition was compressed parallel to the austenite ⟨110⟩ direction, the model predicted (and the experiment confirmed) that the same type of shears, although activated according to a different pattern, gave rise to the Pitsch orientation. This is an experimental example that the final orientation relationship is not constant for one material.

The habit plane comes into the picture only after the nucleus has grown to certain dimensions. In fact, according to Bilby and Christian[9] the first-formed part of a martensitic domain "... does not necessarily possess any true habit". Its interpretation in the sense of the phenomenological theories would require it to be a macroscopically flat plane running throughout the test-piece. This is, rather exceptionally, observed in definite single-interface transformations. Mostly, however, within martensite domains of limited extension, the true interface is not flat but is curved or corrugated, showing straight sections in different directions, or is even smooth on one side and rough on the other.[10–12] In such cases there may be a straight midrib, which is then often considered to be (a trace of) the habit plane. In these instances one is more or less at a loss to explain what precise feature of the habit plane the phenomenological theory refers to.

In view of such difficulties it may be suggested that the interface is in the first place a plane of optimal fit on an *atomic* scale so that the interfacial energy is as small as possible. This view was brought forward by Klostermann[12] when studying the formation of surface martensite in nickel–iron. Klostermann found that the martensite needles are bounded by f.c.c. {112} planes,* which, by the Bain correspondence of the variant in question, were transformed into b.c.c. {123} planes. The closest-packed atom rows in both planes, f.c.c. ⟨110⟩ and b.c.c. ⟨111⟩, were approximately parallel. As the distance between successive corresponding rows in these two planes is practically the same, in this case at least the interface seems to be one of close atomic fit. Growth in the length direction of the domains would require only a "reshuffling" of the close-packed rows without change in direction.

The above considerations suggest that what has been called the "available pattern of dislocations" determines the nucleation event and the relative orientation of matrix and new lattice at its first moment. Then, during further growth, the new phase selects the best atomic fit between the two lattices. In this reasoning the occurrence of a certain scatter in orienttation relations may perhaps be unavoidable and must even be expected.

In this connection attention must be drawn to a recent paper by Pitsch.[15] He distinguishes between truly "diffusionless" or "martensitic" processes, for which the phenomenological theories are apparently held to be applicable, and "diffusion-directed nucleation and growth transformations". For the latter type of process direct lattice correspondence is involved only during nucleation but further growth is governed by the requirement of best atomic fit (minimum interfacial energy). This is attained by postulating that in the interface two corresponding planes of possibly similar atomic structure adjoin in such a way that the corresponding closest-packed directions are parallel. This requirement concerning the interface corresponds to what is said above concerning the interface of martensite domains as found by Klostermann. Pitsch shows that his hypothesis allows for a certain scatter in the orientation relationship, to the same degree as postulated by Bogers and Burgers.[6] (In the case of f.c.c. → b.c.c. transformations the scatter is centred around the ideal Bain orientation.)

Finally a few words may be said about the object of the present remarks. It seems that papers on martensite transformation often contain two sets of information data: one set, derived by application of the hypotheses of the phenomenological theory, able to interpret with a certain degree of accuracy the crystallographic character of what is taken to be the habit plane (midrib, length direction of a martensitic plate, &c.); and another set concerning the many complicated features of the domains (e.g. the interface actually observed, the presence or absence of a midrib or twins) for which various, often plausible, reasons are given. One has, however, the impression that both sets of data are considered more or less on their own and that generally no attempt is made to explain them on a common basis. This seems understandable on account of the different starting points. However, we think that it will be necessary to shift attention from a continued adaptation of the phenomenological theories to a consideration of the atomic processes occurring during nucleation and growth, notwithstanding the lack of precision with which these can be made.

* Cf. also in this connection the findings of Patterson and Wayman[13] and of Reed.[14]

References

1. J. S. Bowles and J. K. Mackenzie, *Acta Met.*, 1954, **2,** 129.
2. M. S. Wechsler, D. S. Lieberman, and T. A. Read, *Trans. Amer. Inst. Min. Met. Eng.*, 1953, **197,** 1503.
3. H. Knapp and U. Dehlinger, *Acta Met.*, 1956, **4,** 289.
4. M. Cohen, *Trans. Met. Soc. A.I.M.E.*, 1958, **212,** 171.
5. D. S. Lieberman, *Acta Met.*, 1958, **6,** 680.
6. A. J. Bogers and W. G. Burgers, *ibid.*, 1964, **12,** 255.
7. S. Dash and N. Brown, *ibid.*, 1966, **14,** 595.
8. A. J. Bogers, *ibid.*, 1962, **10,** 260; Thesis, Univ. Delft, **1962.**
9. B. A. Bilby and J. W. Christian, *J. Iron Steel Inst.*, 1961, **197,** 122.
10. R. B. G. Yeo, *Trans. Amer. Soc. Metals*, 1964, **57,** 48.
11. J. A. Klostermann and W. G. Burgers, *Acta Met.*, 1964, **12,** 355.
12. J. A. Klostermann, "Physical Properties of Martensite and Bainite" (Special Rep. No. 93), p. 20. **1965:** London (Iron Steel Inst.).
13. R. L. Patterson and C. M. Wayman, *Acta Met.*, 1966, **14,** 347.
14. R. P. Reed, *ibid.*, 1967, **15,** 1287.
15. W. Pitsch, *Arch. Eisenhüttenwesen*, 1967, **38,** 853.

Research Note

The $\alpha \rightarrow \gamma$ Martensite Transformation in Crystalline Mercury

J. S. Abell and A. G. Crocker

Recently several short reports have been published concerning a new stress-induced phase transformation occurring in crystalline mercury. In particular, Doidge and Eastham[1] adduced evidence of a transformation based on a change in the superconducting properties of α-Hg when crystals were deformed in tension at liquid-helium temperatures. They labelled the new phase γ. This work prompted Weaire[2] to report a possible product crystal structure which he had predicted using the pseudopotential theory of metals. He proposed that the normal α phase, having a face-centred rhombohedral structure of axial angle 98° 22′, would transform to a structure with the same symmetry but having an axial angle of ~ 82°. The present authors[3] have also published an account of some metallographic observations and concluded that the phase change is martensitic in character, the habit plane and macroscopic shear direction being $\{\bar{1}13\}$ and $\langle 110\rangle$, respectively. An account of the orientation-dependence of the occurrence of the transformation was also given,[3] together with a preliminary application, based on the product structure suggested by Weaire, of the stereographic version of the theories of martensite crystallography developed by Lieberman.[4] It should be noted that it is now considered to be well established[3] that γ-Hg and the previously reported β-Hg[5] are distinct phases.

The present note reports direct experimental information on the transformation in the form of micrographs of plates of γ-Hg. In addition, quantitative results on the shear-strain magnitude deduced from surface-tilt measurements are presented and discussed, and progress on the experimental determination of the crystal structure of this new phase described.

The typical appearance of the transformation product on a surface of a single crystal of square cross-section that has been deformed at 4·2° K up to 5% is shown in Fig. 1. This micrograph was taken at 200° K, the crystal being covered by a layer of alcohol to prevent frosting of the surface. It demonstrates that, though the bulk of the specimen has reverted back to the α phase at ~ 50° K, appreciable surface-relief effects still remain. A similar behaviour is observed for deformation twins in mercury after recrystallization. Two sets of traces are present in Fig. 1. Indeed, plates of γ-Hg are nearly always produced in complementary pairs, the two operative variants of the $\{\bar{1}13\}$ habit plane being those containing the common $\langle 110\rangle$ shear direction. The shears associated with these plates are in the same sense, and thus accommodate each other satisfactorily, when the two variants meet at an obtuse angle, as shown in Fig. 2. The common plane of the two plates, which is well defined in this figure, is then the mirror plane $\{1\bar{1}0\}_\alpha$. Acute-angled intersections have not been observed.

The surface tilts of four plates of γ-Hg were measured by a technique described elsewhere[6] and the associated macroscopic shear-strain magnitudes deduced by a stereographic

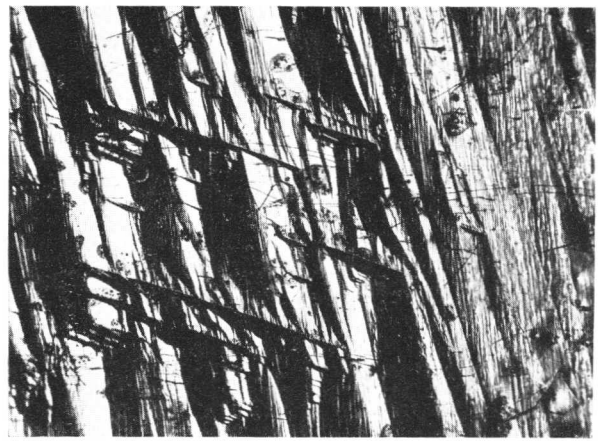

Fig. 1 Surface-relief effects associated with plates of γ-Hg on two variants of the $\{\bar{1}13\}$ habit plane. × 80.

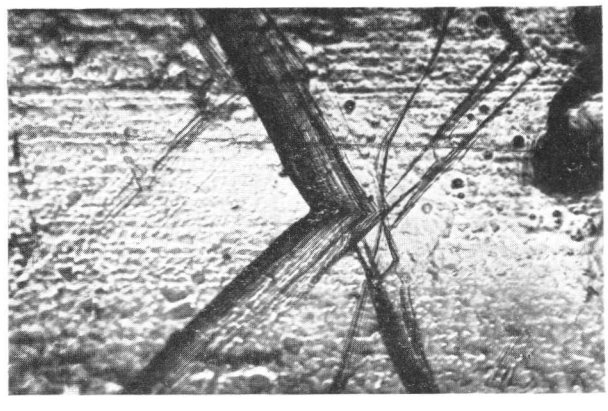

Fig. 2 A complementary pair of martensite plates meeting each other at an obtuse angle. × 80.

procedure.[6] The values obtained were 0·46, 0·50, 0·48, and 0·56. These strains are remarkably large compared with those for other martensitic transformations. Thus, in order that the mercury transformation be energetically favourable, the atomic mechanism involved is likely to be particularly simple. Indeed, the fact that the transformation is stress-induced suggests that it might be instructive to compare it with deformation twinning of α-Hg[6] where the shear strain of 0·63 is also large. No atomic shuffling following the twinning shear is necessary for this mode and this is also true of the transformation if the product structure suggested by Weaire[2] is adopted. This structure may be related to the parent structure by means of two particularly simple distinct correspondences. These relationships are illustrated schematically in Fig. 3. In the first, illustrated by diagrams (*a*), (*b*), and (*c*), the parent unit cell is simply extended in the unique $[111]_\alpha$ direction. The associated correspondence formed the basis of the preliminary and unsuccessful analysis of the crystallo-

Manuscript received 3 July 1968. J. S. Abell, B.Sc., and A. G. Crocker, Ph.D., are in the Department of Physics, University of Surrey.

graphy of the transformation reported earlier.[3] The second relationship may be described by an extension in the $[111]_\alpha$ direction until a f.c.c. structure is obtained, followed by a further extension in one of the three directions derived from $\langle 11\bar{1}\rangle_\alpha$. This sequence is illustrated by Figs. 3(*a*), (*b*), and (*d*). For the case of a face-centred rhombohedral product angle that is exactly the supplement of the parent angle, the correspondence implied by this second mechanism may be shown to be equivalent to that associated with a simple shear on a parent $\{100\}_\alpha$ plane. An additional strain is necessary if, as is likely, this relationship does not hold. The principal strains associated with these two correspondences are smaller than those for all alternatives, if atomic shuffles are not allowed. They have been determined by the procedure described by Crocker and Ross[7] and, for a product rhombohedral angle of 82°, are found to be (0·34, − 0·14, − 0·14) and (0·16, − 0·14, −0·00), respectively. Thus, if the choice of correspondence is governed by a criterion of minimum strain, the second relationship is clearly to be preferred. However, two of the principal strains associated with this correspondence are still large, which suggests that the associated macroscopic shear strain might also be large. This suggestion and other crystallographic features of the transformation are at present being investigated quantitatively[8] using an algebraic version[9] of the theories of martensite crystallography.

Unfortunately, our understanding of this transformation is at present hindered by the lack of direct experimental information on the crystal structure of the γ phase. A determination of this crystal structure has been attempted using a modified version of the X-ray cryostat developed by King and Preece.[10] The modification, which will be described in detail elsewhere,[11] enables a strain to be applied at low temperatures to a specially cast tensile specimen while under direct observation in the cryostat. It has proved possible to induce strains of up to 100% in the 8-mm gauge-length and in some cases the specimen has fractured as a result of inhomogeneous deformation and large local strains. Some experiments performed at 77° K showed that the diffraction peaks corresponding to the initial α-Hg structure usually broaden significantly when the stress is applied, confirming that the strain is successfully imparted to the gauge-length under X-ray observation. Preliminary work at 20° K, the lowest temperature attained to date, has confirmed this effect and in some cases new peaks have been observed. In particular, a peak has been detected that is consistent with the $\{11\bar{1}\}$ reflection of the structure proposed by Weaire[2] for this new phase. We have thus confirmed by a direct X-ray method that a new phase is present and have obtained some preliminary information about its crystal structure. A complete determination of the structure thus appears imminent and this will enable a full assessment of the crystallographic features of the transformation to be carried out.

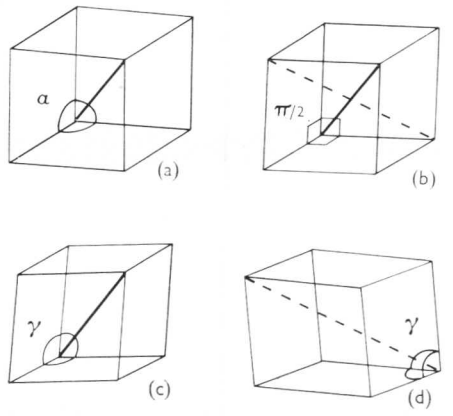

Fig. 3 Schematic representation of the two correspondences relating the parent α-Hg structure and the predicted γ-Hg structure. The face-centred rhombohedral parent cell of axial angle 98° 22′ shown in (*a*) *is first extended along the three-fold axis* (*heavy line*) *until it becomes the f.c.c cell shown in* (b). *Further extension along the original three-fold axis then gives the product face-centred rhombohedral cell of axial angle ~ 82° shown in* (c), *whereas extension along one of the alternative three-fold axes of the cubic cell, e.g. the heavy broken line in* (b), *results in the crystallographically equivalent product cell shown in* (d).

Acknowledgements

The authors are greatly indebted to Professor J. G. Ball of the Metallurgy Department, Imperial College, for providing facilities and to Dr. H. W. King for help and guidance with the low-temperature X-ray work. Discussions with Mr. D. Weaire of the University of Cambridge and with colleagues at the University of Surrey, in particular Mr. N. D. H. Ross, are gratefully acknowledged. One of the authors (J.S.A.) would like to thank the University of Surrey for financial support.

References

1. P. R. Doidge and A. R. Eastham, *Phil. Mag.*, in the press.
2. D. Weaire, *ibid.*, in the press.
3. J. S. Abell and A. G. Crocker, *Scripta Met.*, in the press.
4. D. S. Lieberman, *Acta Met.*, 1958, **6**, 680.
5. J. E. Schirber and C. A. Swenson, *ibid.*, 1963, **10**, 511.
6. D. M. M. Guyoncourt and A. G. Crocker, *ibid.*, 1968, **16**, 523.
7. A. G. Crocker and N. D. H. Ross, this vol., p. 176.
8. N. D. H. Ross and A. G. Crocker, to be published.
9. R. Bullough and B. A. Bilby, *Proc. Phys. Soc.*, 1956, [B], **69**, 1276.
10. H. W. King and C. M. Preece, *Advances in X-Ray Analysis*, 1967, **10**, 354.
11. J. S. Abell and H. W. King, to be published.

Research Note

The Crystallography of the Martensitic Transformation in an Fe–32% Ni Alloy

P. C. Rowlands, E. O. Fearon, and M. Bevis

Christian[1] has pointed out that one of the outstanding problems of martensite crystallography in steels is the scatter observed in the experimentally determined habit planes. With more precise determinations of habit planes for particular alloy compositions it has become evident that the scatter in the results is not entirely due to experimental errors.

The object of this research note is to report on work now in progress to determine the factors that cause a variation in the martensite habit planes of acicular martensite in Fe–Ni alloys.

An Fe–32%Ni single crystal (1 × 0·5 × 0·3 cm) was used in the experiments. The magnitude and direction of the shape deformation of martensite plates were determined using the procedure described by Bowles and Morton.[2] The martensite habit planes were determined from a two-surface trace analysis and the orientations of martensite and austenite crystals were determined by a back-reflection Kossel technique.[3] Martensite plates with widths as small as 5 μm may be orientated rapidly using this technique.[4] A typical martensite Kossel pattern is shown in Fig. 1. The crystal orientation was obtained from the patterns by plotting the diffracting-plane normals using charts developed by Rowlands and Bevis.[5] Up to ten poles were plotted for each pattern and the overall accuracy of orientation relationships determined in this way was estimated to be 0·50. Planes defined by etch traces related to the lattice invariant shear were determined from two-surface analysis with respect to the martensite basis.

The results for 12 of the 23 plates in one austenite grain initially selected for analysis are shown in Fig. 2. The habit planes are plotted in the unit triangle defined by the (010), (011), and (111) austenite poles. The directions of the shape deformations **d** are plotted in the corresponding unit triangle. The habit-plane poles of the plates 2, 4, 5, 6, 10, and 15, which all lie within a cone of 2° angular dia. are the poles of martensite plates which extend across the whole cross-section of the crystal and are considered to be the first-formed plates. In Fig. 2 a broken line has been drawn around these poles. The directions of the shape deformation of plates 4 and 6 are shown, and are within 3° of the theoretical shape-deformation direction for an Fe–30%Ni alloy. Direct comparison of experimental results with theoretical predictions for the alloy being considered here cannot be made until we have completed the determination of the martensite and austenite lattice parameters using a transmission Kossel technique. The average magnitude of the shape deformation for plates 4 and 6 is 0·216.

Manuscript received 3 July 1968. P. C. Rowlands, B.Eng., E. O. Fearon, B.Eng., and M. Bevis, B.Sc., Ph.D., are in the Department of Metallurgy and Materials Science, University of Liverpool.

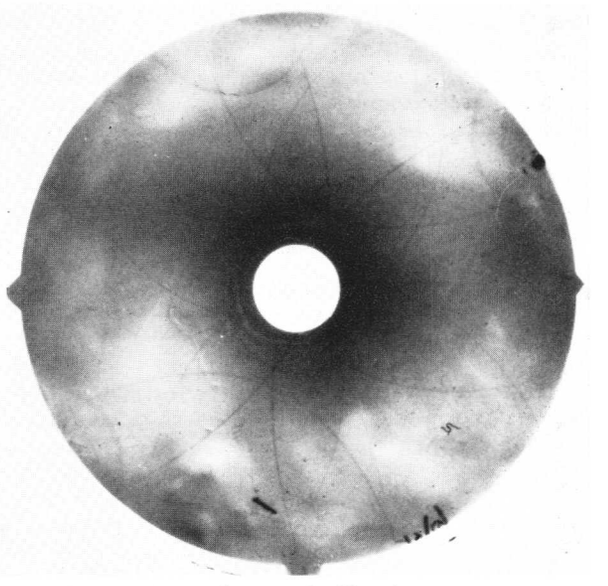

Fig. 1 A typical martensite Kossel pattern.

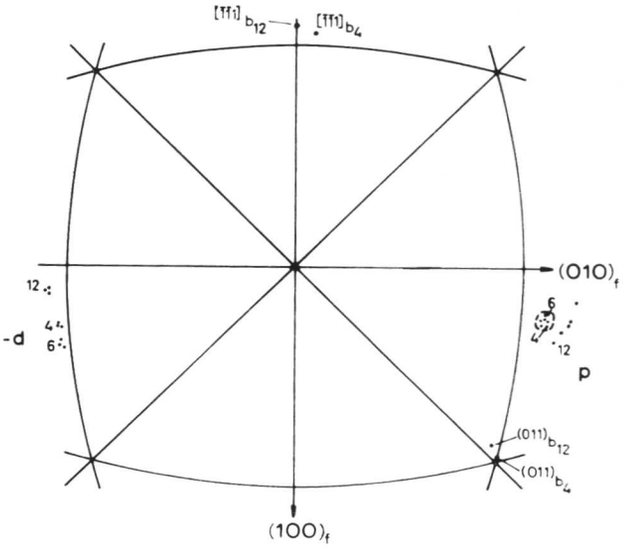

Fig. 2 The (001) austenite stereographic projection, showing the martensite habit planes **p**, *shape-deformation direction* **d**, *and orientation relationships.*

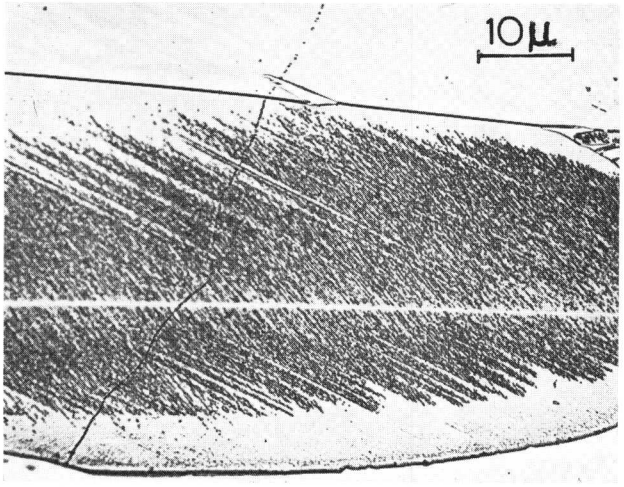

Fig. 3 Optical micrograph of a martensite plate showing complex substructure.

The orientation relationships for plates 2, 4, 5, 6, 10, and 15 were indistinguishable from one another so that only one, that for plate 4, has been plotted in Fig. 2. For this case $(111)_f \parallel (011)_b - 1°$; $[\bar{1}01]_f \parallel [\bar{1}\bar{1}1]_b - 3{\cdot}5°$. The planes defined by the etch traces within these plates lie within 2° of the $(112)_b$ pole, which is the correct variant of the lattice invariant shear for the particular correspondence used. It is clear that once the lattice parameters of martensite and austenite have been determined there should be good agreement between theory and the results presented above.

The remainder of the martensite plates analysed so far exhibited a large scatter in habit planes. When examined, all these plates had fine structures which consisted of two sets of etch traces. A typical example is shown in Fig. 3. For plate 12 the plane of one trace is 8° from the nearest $(112)_b$ pole, the other trace defining a plane 5° from the $(011)_b$ pole. As can be seen from Fig. 2, the shape-deformation direction has rotated 8° towards the $(0\bar{1}1)_f$ pole, though the magnitude of shear of 0·227 is comparable with those of plates 4 and 6. Coupled with the scatter in habit planes for these plates there is an associated scatter in the orientation relationships. For plate 12 the relationship is

$$(111)_f \parallel (011)_b - 2{\cdot}5°; [\bar{1}01]_f \parallel [\bar{1}\bar{1}1]_b - 3°$$

and this was the maximum observed deviation from the accepted orientation relationships.

These results suggest that in some martensite plates a multiple-shear lattice-invariant shear mechanism is operative as the inhomogeneous shear component of the transformation. This proposal is supported by our electron-microscopy observations. Fig. 4 is an electron micrograph showing the "block-like" transformation twins.[6] In this particular example the pole of the interface plane is 8° from the nearest $(112)_b$ pole and supports the suggestion[6] that the twins have been sheared.

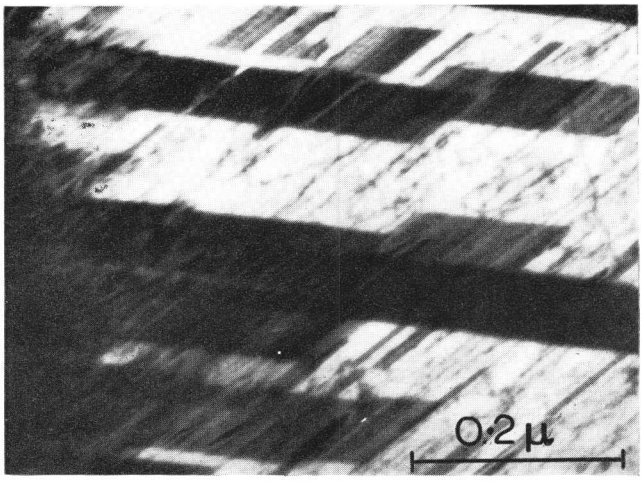

Fig. 4 Electron micrograph of sheared transformation twins.

In conclusion, we are of the opinion that the results presented in this note are evidence that multiple-shear lattice-invariant deformations are operative in some martensite plates in steels, and that we have been able to correlate the changes in martensite habit and orientation relationship with the mode of the lattice invariant shear. A generalized theory of martensite crystallography[7] is now being used in an attempt to explain the results presented above.

Acknowledgements

This research has been sponsored in part by the Air Force Materials Laboratory, Research and Technology Division, AFSC, through the European Office of Aerospace Research, OAR United States Air Force, under Contract AF61 (052)-920. The authors also wish to thank Mr. A. F. Acton for valuable discussions.

References

1. J. W. Christian, this vol., p. 129.
2. J. S. Bowles and A. J. Morton, *Acta Met.*, 1964, **12,** 629.
3. M. Bevis and N. Swindells, *Physica Status Solidi*, 1967, **20,** 197.
4. P. C. Rowlands, E. O. Fearon, and M. Bevis, *Trans. Met. Soc. A.I.M.E.*, 1968, **242,** 1559.
5. P. C. Rowlands and M. Bevis, *Physica Status Solidi*, 1968, **26,** K25.
6. K. Shimizu, *J. Phys. Soc. Japan*, 1962, **17,** 508.
7. A. F. Acton and M. Bevis, *Air Force Materials Lab. Scientific Rep. No.* **(5),** 1968: USAF Contract No. AF61 (052)-920.

Research Note

A Note on the Dependence of the Low-Temperature Martensitic Transformation in Nb_3Sn on Composition

H. W. King

The martensitic transformation from the β-W cubic structure to a tetragonal structure in the superconductors V_3Si and Nb_3Sn is of interest because of its extreme sensitivity to the composition of the alloy. Batterman and Barrett,[1] for example, found that not all single crystals cut from the same bar of V_3Si transformed on cooling, while Mailfert, Batterman, and Hanak[2] and King, Cocks, and Pollock[3] have shown that the transformation in Nb_3Sn can be related to the room-temperature lattice parameter of the β-W structure.

Nb_3Sn alloys of varying composition were prepared by hot pressing mixtures of predetermined amounts of powdered Nb and Sn at 1350–1450° C for periods of up to 3 h, followed by a 2-h annealing treatment at 900° C. All alloys were single-phase, with the β-W structure, when examined by X-ray diffraction at room temperature. Since the sintering operation invariably involves some loss of Sn, the room-temperature lattice parameter of the β-W structure was used as an indicator of the composition of the alloys, pending a chemical analysis.

The diffraction patterns of all the alloys were recorded at 6·5° K using a modified version of the X-ray cryostat described by King and Preece,[4] mounted on a General Electric S.P.G. Spectrogoniometer. Broadened profiles indicative of the tetragonal martensite were observed only in alloys with room-temperature lattice parameters between 5·2867 and 5·2908 Å (λ Cu $K_{\alpha 1}$ = 1·54051Å). The reverse transformation, i.e. from the martensite to the β-W structure, was followed by warming the samples from 6·5° K at a rate of 0·25 degK/min and repeatedly scanning the 432 diffraction-line profile, as described by King, Cocks, and Pollock.[3] The results are shown in Fig. 1, where A_s and A_f refer to the start and finish of the reverse transformation. The probable variation of the M_s temperature is indicated by the broken line drawn through the single point reported by Mailfert, Batterman, and Hanak.[2]

The composition scale at the bottom of the diagram is based on lattice-parameter results reported in the literature. These indicate a linear increase in the a up to the stoichiometric composition (a = 5·2902Å),[5–8] followed by a sharp rise when excess Sn is present,[9] so that the composition scale in Fig. 1 is discontinuous beyond this point. The results in Fig. 1 show that, although the β-W structure is present from ~ 20 to 26 at.-%Sn, the martensite is limited to a narrower range of composition from 22·7 to 25·1 at.-%Sn.

The asymmetry of the A_s and A_f curves about the stoichiometric composition can be understood by considering the different environments of the sites for the Nb and Sn atoms. In a fully ordered stoichiometric alloy with the β-W structure,

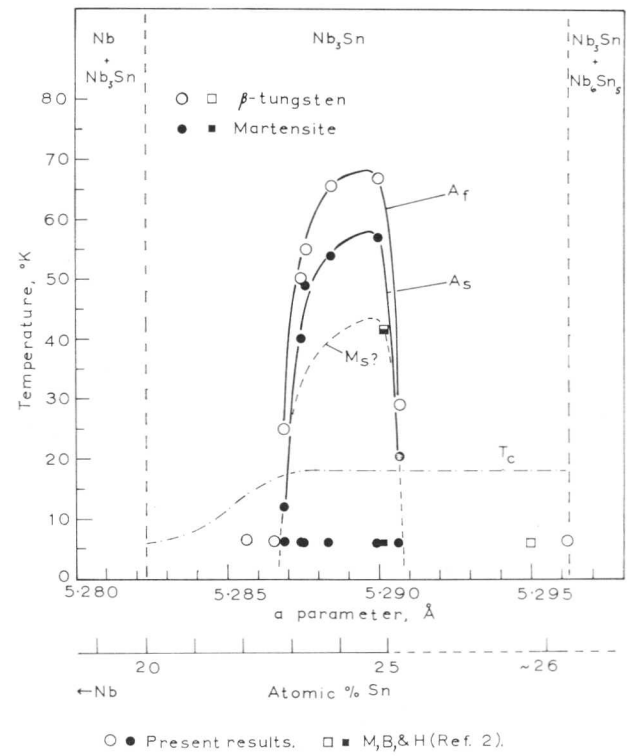

Fig. 1 Martensitic transformation temperatures, A_s and A_f, and superconducting transition temperatures, T_c, as functions of the room-temperature lattice parameters of β-W–Nb_3Sn alloys. The composition scale is derived from published lattice-parameter data.[5–9]

the Sn atoms occupy positions at 0, 0, 0 and $\frac{1}{2}$, $\frac{1}{2}$, $\frac{1}{2}$ on a b.c.c. lattice, while the Nb atoms are located at $\frac{1}{4}$, 0, $\frac{1}{2}$; $\frac{1}{2}$, $\frac{1}{4}$, 0; 0, $\frac{1}{2}$, $\frac{1}{4}$; $\frac{3}{4}$, 0, $\frac{1}{2}$; $\frac{1}{2}$, $\frac{3}{4}$, 0; and 0, $\frac{1}{2}$, $\frac{3}{4}$, which are in fact the tetrahedral interstices of the b.c.c. lattice.[10] If it is considered that the Nb atoms are in contact with each other and form chains that keep the Sn atoms apart,[5,11] the holes occupied by the Nb atoms are found to be ~ 25% smaller than the sites occupied by the Sn atoms. An assessment of the elastic strains due to atomic misfits and differing elastic properties among the elements has shown that the insertion of a large solute atom into a small hole in a solvent matrix causes a greater lattice strain than the equivalent case of a small atom introduced into a large interstice.[12] Further, since in the elemental form of these metals the Sn atom is larger than the Nb atom, it follows that the elastic strains in the matrix lattice will be greater when excess Sn is present, as opposed to excess Nb, so that the composition range of

Manuscript received 3 July 1968. H. W. King, B.Sc., Ph.D., is in the Metallurgy Department, Imperial College, London. This work was performed while the author was on leave of absence at the Inorganic Materials Research Division, University of California Lawrence Radiation Laboratory, Berkeley, California, U.S.A.

the β-W structure and, even more so, that of the martensite are asymmetric about the stoichiometric composition.

It is also interesting to compare the dependence on composition of the martensitic transformation with the known trends in superconducting transition temperature, T_c, in Nb_3Sn alloys. As may be seen in Fig. 1, the absence of the martensitic transformation has no effect on the high values of T_c observed in Sn-rich alloys, yet the drop in T_c found on the Nb-rich side of stoichiometry occurs only in alloys that do not undergo the martensitic transformation. The relationship between the martensite and the superconducting properties is being examined further by studying its effect on magnetization and current-carrying capacity.

Acknowledgements

The author is grateful to M. F. Merriam, E. R. Parker, and V. F. Zackay for helpful suggestions and discussions, and to B. Arnold and G. M. Gordon for their assistance with the X-ray measurements. The work was supported in part by the United States Atomic Energy Commission.

References

1. B. W. Batterman and C. S. Barrett, *Phys. Rev.*, 1965, **145**, 296.
2. R. Mailfert, B. W. Batterman, and J. J. Hanak, *Phys. Letters*, 1967, **22**, 315.
3. H. W. King, F. H. Cocks, and J. T. A. Pollock, *ibid.*, 1967, **26A**, 77.
4. H. W. King and C. M. Preece, *Advances in X-Ray Analysis*, 1967, **10**, 354.
5. T. B. Reed, H. C. Gatos, W. J. LaFleur, and J. T. Roddy, " Metallurgy of Advanced Electronic Materials " (edited by G. E. Brock), p. 71. **1963:** New York and London (Interscience Publishers).
6. J. J. Hanak, K. Streter, and G. W. Cullen, *R.C.A. Rev.*, 1964, **25**, 342.
7. L. J. Vieland, *ibid.*, 1964, **25**, 366.
8. H. Pfister, *Z. Naturforsch.*, 1965, [A], **20**, 1059.
9. J. J. Hanak and H. S. Berman, " International Conference on Crystal Growth " (Suppl. *J. Chem. Physics Solids*), p. 249. **1967:** Oxford, &c. (Pergamon Press).
10. W. B. Pearson, " Handbook of Lattice Spacings and Structures in Metals and Alloys ". **1958:** Oxford, &c. (Pergamon Press).
11. F. Laves, " Theory of Alloy Phases ", p. 124. **1956:** Cleveland, Ohio (Amer. Soc. Metals).
12. H. W. King, " Alloying Behaviour and Effects in Concentrated Solid Solutions " (edited by T. B. Massalski), p. 85. **1965:** New York (Gordon and Breach).

Research Note

Martensite Produced by Deformation in Monocrystals of Beta-Brass

Horace Pops and M. Ahlers

The b.c.c. β phase in the Cu–Zn system is unstable at low temperatures and, depending on composition, transforms spontaneously during cooling into a thermoelastic or a burst-type martensite phase[1] or undergoes a strain-induced martensitic transformation.[2,3] We have plastically deformed single crystals of β-brass in tension and compression for the composition range between 43 and 48 at.-% zinc. In this range, martensite forms only by plastic deformation. Habit planes and macroscopic shear directions were determined for several different orientations spanning the stereographic unit triangle.

Fine slip markings are always observed in conjunction with a stress-induced martensite. The slip system varies with both composition and method of deformation: $\{211\}\langle 111\rangle$ occurs only for low solute contents by compressive loading, whereas $\{110\}\langle 111\rangle$ occurs in all alloys deformed in tension. Spontaneous martensite, which forms in low-zinc-content alloys, has a habit plane lying in the vicinity of $\{2, 11, 12\}_\beta$.[1] For slight deformation, habit planes were observed between $\{2, 11, 12\}_\beta$ and $\{110\}_\beta$, but the $(2, 11, 12)_\beta$ family of habit planes was also observed in the 45 and 48 at.-% Zn alloys after heavy deformation. A $\{112\}_\beta$ habit plane occurs in alloys containing 43 and 45 at.-% Zn. Generally, only one variant was obtained for both tensile and compressive loading. The observed martensite and slip systems have the highest resolved shear component of stress. Although the M_D temperature decreases with increasing zinc content,[3] martensite forms most easily (lowest resolved critical shear stress) in the 48 at.-% Zn alloy.

Manuscript received 3 July 1968. H. Pops and M. Ahlers are at the Mellon Institute, Carnegie–Mellon University, Pittsburgh, Pa., U.S.A.

In a previous investigation[2] the inhomogeneous lattice shear, habit plane, and macroscopic shear direction were calculated for martensite arising from plastic deformation, using a phenomenological model similar to the one developed by Wechsler, Lieberman, and Read (WLR)[4] for spontaneous martensite. $\{110\}\langle 110\rangle$ secondary-shear systems have been predicted when the habit plane and macroscopic shear directions are $\{110\}$ and $\langle 110\rangle$, respectively. A $\{110\}\langle 113\rangle$ secondary-shear system was predicted for the $\{211\}$ habit plane. When the alloy containing 48 at.-% Zn was deformed in tension, the macroscopic shear direction within the $\{110\}$ habit plane was not $\langle 110\rangle$ but lay between $\langle 010\rangle$ and $\langle 111\rangle$. From the phenomenological theory, the $\{110\}\langle 113\rangle$ system was expected.

Planes and directions mentioned above are indexed in terms of the b.c.c. phase. When the secondary-shear systems are translated to an f.c.t. (martensite) lattice (M), the $\{110\}_\beta\langle 113\rangle_\beta$ and $\{110\}_\beta\langle 110\rangle_\beta$ systems are equivalent to the $\{111\}_M\langle 112\rangle_M$. The growth of stress-induced martensite is therefore most probably associated with slip that is produced by $\langle 112\rangle_M$ partial dislocations.

To test the validity of the predicted secondary-shear systems, foils were prepared from deformed samples of several different alloys and examined by transmission electron microscopy. In the Cu–43 at.-% Zn sample, foils were spark-cut with their surfaces nearly normal to the predicted secondary-shear plane, $\{110\}_\beta$, i.e. $\{111\}_M$, and also parallel to a $\{100\}_\beta$ plane, i.e. $\{110\}_M$. Fig. 1 is taken from a region within a single plate of martensite that has a $\{211\}$ habit plane. The selected-area diffraction pattern is representative of a twinned f.c.c. lattice that has a $\langle 110\rangle_M$ foil normal. The straight lines in this figure are produced by the intersection of $\{111\}_M$

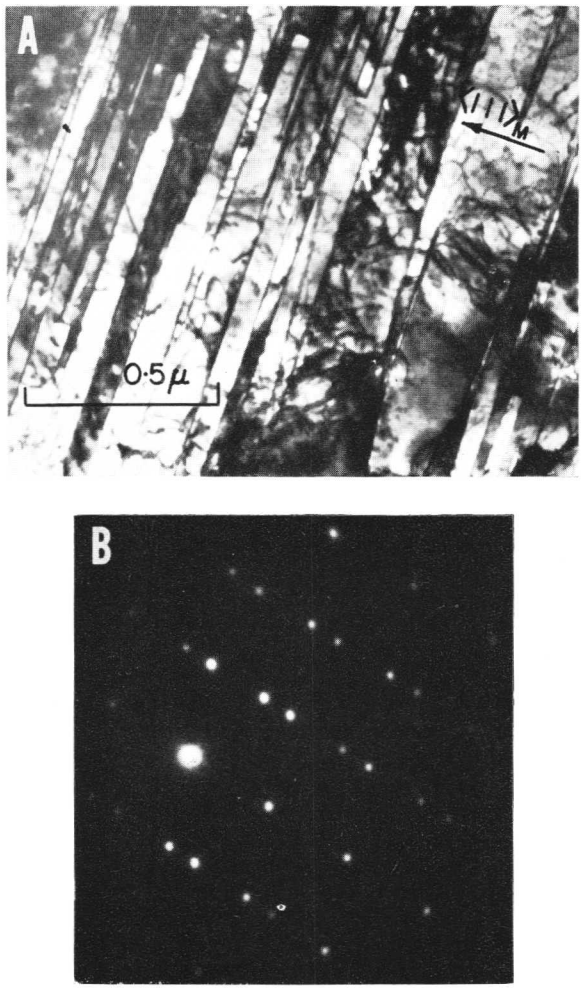

Fig. 1 Stress-induced martensite in a Cu–43 at.-% Zn alloy having the habit plane $\{112\}_\beta$. The $\{110\}_M$ secondary-shear plane is normal to the foil. (A) Area within a single martensite plate; the normal to the secondary-shear plane is indicated by the arrow. (B) Selected-area diffraction pattern of the same plate showing twin-related spots from an f.c.c. lattice.

twin planes with the foil surface, thereby indicating that these planes are the predicted secondary-shear planes. They are also parallel to the observed $\{110\}_\beta$ slip planes in the matrix.

In the Cu–48 at.-% Zn alloy foils were cut in a similar manner to those of the 43 at.-% Zn alloy. In this case, however, straight lines were not present and only b.c.c. diffraction spots were obtained. Nevertheless, by tilting the foil numerous striations were observed on the $\{110\}_\beta$ planes, as seen in Fig. 2. The absence of contrast effects when these planes are normal to the foil suggests that the contrast effects are most probably due to the presence of very thin layers of a martensitic phase. This suggests that the observed structure may be a transition structure between the parent

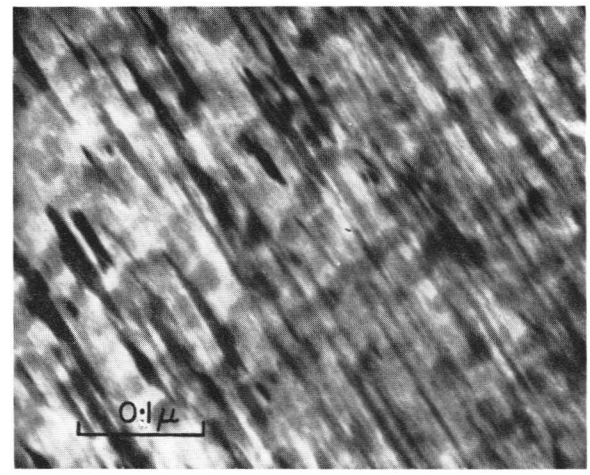

Fig. 2 Fault fringes in a deformed Cu–48 at.-% Zn alloy.

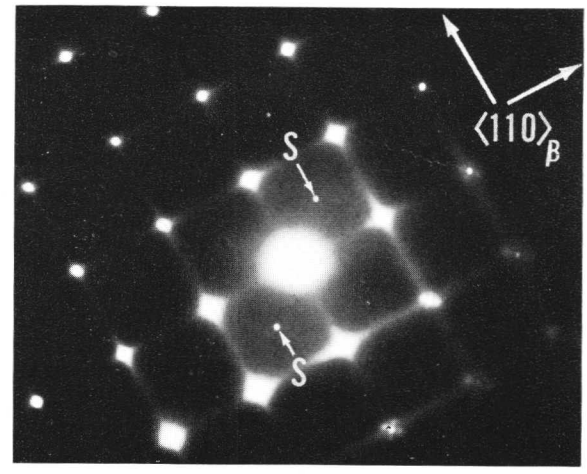

Fig. 3 Selected-area diffraction pattern for a Cu–43 at.- % Zn alloy deformed slightly in compression. Martensite is not visible. Some superlattice reflections (S) are shown.

and product phases. This idea is supported by the fact that the habit plane and the macroscopic shear change continuously with increasing amounts of strain.[2]

When samples were deformed slightly and examined before strain-induced martensite could be detected, diffraction streaks appeared in $\langle 110 \rangle_\beta$ directions, as shown in Fig. 3. These streaks may be associated with the nucleation of strain-induced martensite which must therefore be very fine.

References

1. Horace Pops and T. B. Massalski, *Trans. Met. Soc. A.I.M.E.*, 1964, **230**, 1662.
2. M. Ahlers and Horace Pops, *ibid.*, 1968, **242**, 1267.
3. T. B. Massalski and C. S. Barrett, *Trans. Amer. Inst. Min. Met. Eng.*, 1957, **209**, 455.
4. M. S. Wechsler, D. S. Lieberman, and T. A. Read, *ibid.*, 1953, **197**, 1503.

Dr. T. BELL (University of Liverpool): I should like to ask Dr. Klostermann how confident he is of the depth of 30 μm for surface martensite.

Dr. J. A. KLOSTERMANN (Technische Hogeschool Twente, Enschede, Netherlands): This depth is correct. It will, of course, depend on the type of needle. There are also some very narrow needles and in that case it appears that the depth is less. If you have a lower nickel content, the depth is greater.

Dr. BELL: Our experience would seem to be the reverse: the lower the nickel content the smaller is the depth of the surface martensite.

Professor B. A. BILBY (University of Sheffield): What are the dimensions? The needle is 30 μm deep but how long and wide is it?

Dr. KLOSTERMANN: It is ~ 25–30 μm wide. This depends on the specific variant. There are variants that are small and variants that are large. This can be seen in Fig. 4 of the paper, where there are narrow and broad needles.

Dr. P. M. KELLY (University of Leeds): Could I ask Dr. Klostermann two questions? First, he described surface martensite as needles. Have these needles one dimension very much longer than the other two dimensions, or are they in fact sections of plates or laths?

Dr. KLOSTERMANN: They are needles. The length dimension is, in many cases, a thousand or ten thousand times the width.

Dr. KELLY: In that case, I am not at all surprised that the invariant-plane-strain theories do not apply since there is *no* invariant plane, only an invariant line. My second question is: In trying to fit the invariant plane theory to this invariant line did Dr. Klostermann attempt to use a dilatation?

Dr. KLOSTERMANN: On the first question, I said that the invariant-plane-strain theory was tried on the supposition that the needle is, in fact, a narrow lath and this is supported by the fact that we have a habit plane, not a direction. As regards the second question, a dilatation was not observed. Surely it is zero.

Professor D. HULL (University of Liverpool): How do you know?

Dr. KLOSTERMANN: Because a very small dilatation in the direction of the needle would be observed in our experiments.

Dr. H. I. AARONSON (Ford Motor Co., Dearborn, U.S.A.): On an atomic scale, do you believe that your slow-growing martensite is still growing slowly?

Dr. KLOSTERMANN: No. I believe that there are three factors affecting growth: (1) the heat of the transformation, (2) carbon, and (3) dislocation tangles. The last of these is the most important. Needles can form in less than one hundredth of a second. It depends on the dislocation arrays present.

Dr. AARONSON: I mean on a very fine scale. When it does grow, do you believe it grows rapidly for as far as it is able to grow before it is blocked?

Dr. KLOSTERMANN: Yes, but less rapidly than in the case of low-temperature martensites.

Dr. A. BAR-OR (Israel Atomic Energy Commission, Negev, Israel): Can you determine the activation energy of the slow growth?

Dr. KLOSTERMANN: I have not attempted to determine it but it will be fairly difficult to do so.

Professor J. W. CHRISTIAN (University of Oxford): Referring back to Dr. Aaronson's question, is it quite certain that atomic mobility over the surface will not explain the growth of the martensite?

Dr. KLOSTERMANN: I think it is unlikely that it can do so because such vast movements are involved.

Dr. H. MCI. CLARK (University of Illinois, U.S.A.): Dr. Klostermann mentioned scratch displacements across the needles. Does one, in fact, get a genuine displacement of the scratch from one side of the needle to the other, or merely a displacement of the scratch within the needle?

Dr. KLOSTERMANN: Just within the needle.

Dr. CLARK: Displacement from one side to the other seems quite characteristic of martensites.

Dr. KLOSTERMANN: Ours is a displacement that occurs gradually. In the case of plate martensite you have the condition shown in Fig. D.IV.1, i.e. a displacement of the surface. For surface martensite both sides of a needle are on the same level and this means that one has a prior accommodation and this deformation is more or less opposite to the total deformation of the martensite.

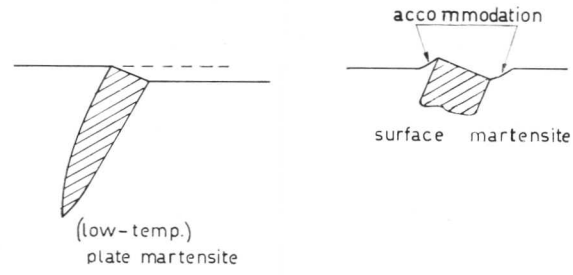

Fig. D.IV.1 *A comparison between plate and surface martensite showing the accommodation in the latter case.* (Klostermann.)

Dr. CLARK: If the growth starts at one side and proceeds so that the widening occurs in one direction, you would, nevertheless, expect a displacement of the scratch across the plate. I agree you could get the curvature shown in Fig. 3(*b*) of the paper because there is a lot of accommodation. I think it is an important point whether you also get a genuine displacement across the plate.

Dr. A. R. ENTWISLE (University of Sheffield): Could Dr. Easterling tell us the copper content of the particles? Only the copper content of the alloy is given.

Dr. K. EASTERLING (Imperial College, London): By interpolation from the equilibrium diagram it should be ~ 2½% at the ageing temperature and we found the M_s temperature for bulk Fe–2·5% Cu to be ~ 600° C.

Dr. BAR-OR: Why do you call it martensite and not a polymorphic transformation?

Dr. EASTERLING: Because the transformation occurs at room temperature, where diffusion is extremely slow, and we feel that it must be a diffusionless martensitic transformation.

Mr. N. E. RYAN (University of Oxford): I notice in Fig. 5 of the paper by Dr. Easterling that there appears to be a possibility that cross-slip is taking place with a prismatic loop associated with the particles. It may be that you are not, in fact, passing the dislocation through the particle, but virtually stress-inducing the transformation within the particles.

Dr. EASTERLING: We have considered this possibility. I assume by this that what we are calling striations you are calling dislocation loops at the interface.

Mr. RYAN: No, rather that the transformation is triggered off by the strain field as the dislocation comes up against the particle, not necessarily passing through the particle.

Professor HULL: Are you suggesting homogeneous nucleation?

Mr. RYAN: Of the martensite in the particle, yes, but stress-induced nucleation.

Dr. EASTERLING: The metallographic evidence so far obtained indicates that the dislocations pass through the precipitates. For example, in Fig. 1 of our paper the precipitates are clearly elongated in the direction of rolling. Furthermore, although many dislocations are present near precipitates in quenched samples, they do not appear to be able to initiate the transformation unless the specimen is further strained. There are quite a lot of dislocations in the matrix moving around, but they are not able to penetrate the precipitates. We have presumed that the reason for this, apart from the strain field of the precipitates, is that the shear modulus in the precipitate is about twice that of the copper matrix, so that it repels the dislocations coming near the precipitates.

Professor J. W. CAHN (Massachusetts Institute of Technology, Cambridge, U.S.A.): We have had at least one suggestion that a simple screw dislocation nucleates martensite and yet many experiments, (for instance Professor Turnbull's experiment with Cech*), show that you cannot nucleate martensite in some of the small iron–nickel spheres. Could it be that an iron precipitate in copper is so highly undercooled that the simple dislocation is a nucleus, whereas in ordinary martensites the M_s is determined by some much more complex defect?

Professor CHRISTIAN: I think this is quite likely. I was impressed by what Mr. Ryan said. Work at Oxford suggests that, in copper alloys like this, dislocations will tend to go round rather than through the particles, and I wonder how certain Dr. Easterling is that the dislocations do go through his precipitates. Also, I am not very clear as to the evidence he has that the striations are individual plates of martensite, and that the whole thing has not transformed. It does seem to me very odd that the whole particle does not transform once it starts.

Professor B. A. BILBY (University of Sheffield): I do not know whether I have understood this point but I did not see any evidence that when the stress is there before transformation it disappears afterwards. If this is the case it surely has a great influence on the situation in the copper alloys and should not be ignored. Do you possess evidence that the strain field disappears when the transformation takes place?

Dr. EASTERLING: We have micrographs where we can see striations across precipitates and the strain field of the precipitate is still there. There are several examples in our paper (Fig. 5).

Professor HULL: I would like to know what happens when you get a plate of martensite in the sphere. Does this martensite then grow to fill up that sphere?

Dr. EASTERLING: This seems to be difficult. We observe striations in the austenite spheres which we interpret as thin martensite discs. We suggest that for the transformation to be completed new interaction between precipitates and dislocations is necessary.

Dr. L. DELAEY (University of Leuven, Belgium): Could the discs observed in the precipitates be twins? If the precipitates are in dark contrast might the twins be normal to the electron beam?

Dr. EASTERLING: In some precipitates these could possibly be twins, but again I would refer you back to the fact that the precipitates have thin discs across their diameter. The strain-field contrast is still there, which certainly means that some austenite is left. Fully transformed spheres can be recognized in the electron microscope because they do not exhibit strain-field contrast.

Professor CHRISTIAN: Is it true that if you transform a particle into a single crystal the strain-field contrast will disappear? It will disappear only if the transformation strains are uniform in all directions.

Dr. EASTERLING: I understand that if you transform a sphere of austenite into a single crystal of martensite then it becomes an ellipsoid, and strain-field contrast would be observed. The micrographs of precipitates in heavily deformed crystals indicate that transformation occurs in several directions and the strain-field contrast vanishes.

Mr. D. HARVEY and Professor J. BURKE (University of Swansea) (*written discussion*): The experiments of Easterling and Swann demonstrate that the stability of metastable austenite in the form of isolated particles is greatly in excess of the same material in bulk form. Some surprise has been expressed at the failure of the particles to transform fully to martensite after the change had been initiated by dislocations in the copper matrix, in view of the considerable chemical free-energy driving force that must have been available at room temperature, bearing in mind that M_s in the bulk material is probably greater than 300° C. This may simply reflect the fact that one martensite nucleus transforms only a limited volume of austenite, as the diameter of a plate is determined by the distance between growth obstacles and the thickness by the coherency strains and the elastic constants of the two phases. We would thus interpret these observations on the basis that the matrix dislocations at the strains imposed are capable of activating only a limited number of martensite nuclei in the particles.

Some results of a study of strain-induced martensite in a series of Fe–Ni–Mo–C alloys in which the M_s temperature is below room temperature may be of significance. We have found that the amount of strain-induced martensite formed by cold rolling can be related to the difference between M_s and the working temperature T_w. For example, after 90% reduction the volume fraction, V, of retained austenite remaining can be expressed by the empirical equation

$$1 - V = A \exp - K (T_w - M_s)$$

where K is a constant $= 1{\cdot}8 \times 10^{-2}$ for our alloys and A is ~ 1. On the assumption that the fraction transformed is determined only by the number of nuclei activated, it follows that the effectiveness of dislocations as nucleation catalysts is related to the amount of thermodynamic driving force available at the deformation temperature.

* R. E. Cech and D. Turnbull, *Trans. Amer. Inst. Min. Met. Eng.*, 1956, **206**, 124.

In Easterling and Swann's system the effective M_s is less than 4° K, while M_0 exceeds the ambient. We think that the driving force at room temperature for the Fe–Cu austenite is greater than in our alloys. If this is so, plastic deformation is less effective in the absence of lattice defects in the parent austenite. It would be of considerable interest if Easterling and Swann's observations were extended to cover deformation between room temperature and 4° K to test whether strain-induced martensite in small particles follows the same pattern as in our bulk samples.

Dr. AARONSON: I have a question on the paper by de Lamotte and Altstetter. How does the surface relief look around the single martensite plate?

Dr. CLARK: One does not in general get a single martensite plate because of the operation of three shear directions on one habit plane. A single martensite plate was illustrated in Fig. 1 of the paper, in so far as it showed a single habit-plane variant. Because the shear strain is so large, one does not get a single shear direction variant operating, but we have seen plates in which there is a quite clear displacement of the fringes. This displacement is usually rather narrow. Of course, quite a lot of accommodation is going on, so that one does not measure the theoretical shear strain.

Professor CHRISTIAN: What kind of change in accepted parameters did you have to make to get the energy of formation of the dislocation loop down to a reasonable value?

Professor C. J. ALTSTETTER (University of Illinois, U.S.A.) (*written reply*): A reduction of the shear modulus at the interface to 0·1–1% of that of the bulk material would achieve this.

Dr. KLOSTERMANN: I should like to ask Dr. Entwisle why the transformation occurs at a higher temperature with a higher austenitizing temperature.

Dr. ENTWISLE: We assume that this is because we are altering the defects in the austenite.

Dr. T. BROOM (Central Electricity Research Laboratories, Leatherhead): What happens if you austenitize at a high temperature to produce a coarse grain size and then drop the austenitizing temperature to, say, 900° C before transformation?

Dr. ENTWISLE: We have not made this particular experiment. There are problems with these steels. You have to be very careful to avoid graphitization and this does impose some limitation on this kind of experiment. That is why we have not worked with the high-nickel alloys at 800° C, for instance.

Professor J. NUTTING (University of Leeds): In view of the fact that the micrograph in Fig. 5 of the paper by Entwisle and Feeney shows that the martensite plate size is considerably smaller than the austenite grain size, why do you try to relate your burst size to the austenite grain size?

Dr. ENTWISLE: This is true only in the 19% Ni alloy, which is two-phase. I think you will find that, in general, the first plates to form do go across the whole grain. The point is that the smaller the grain size, the smaller is the amount of transformation per plate.

Mr. W. K. C. JONES (University of Sheffield): We have observed in an Fe–25·7% Ni–3% Cr alloy,* and Brownrigg has done so in an Fe–26% Ni–2% Mn alloy,† that completely isothermal transformation, with a (225) habit plane, is obtained in the temperature range − 50 to − 150° C, with a maximum initial nucleation rate at ~ − 135° C. Below − 150° C the alloys transform by bursting, with an accompanying change in habit plane to (259).

If the appropriate numbers are inserted in the Kaufman–Cohen embryo model‡ an M_B below 0° K is predicted. This suggests that there are two embryos present in the austenite, one which promotes isothermal transformation of martensite at the higher temperatures, and one for the burst transformation at lower temperatures: this does not seem reasonable when one remembers that burst transformation can be obtained in materials that do not exhibit isothermal transformation. It may be that adjustments must be made to the Kaufman–Cohen model but it is difficult to see quite how, as it does not make allowance for change in habit plane.

It may be that a martensite embryo can choose either habit plane, the particular one selected being dependent on the physical conditions to which the embryo is subjected.

Dr. D. R. F. WEST (Imperial College, London): I would like to ask Professor Christian if he could comment on a point that is relevant to the papers by Klostermann and by Entwisle and Feeney. If one tries to take into account dislocation density in the austenite, is it correct to consider the yield stress as a parameter in the nucleation theory?

Professor CHRISTIAN: I tried to comment on this in the paper. It seems that there are really two opposing effects. There is the introduction of defects that possibly help nucleation, and there is also, as Dr. West says, the strain-hardening of the matrix which may oppose the growth of the plate. There are many papers which show both these effects working but the interaction is very complex, I think.

Dr. KELLY: Could I support Professor Lieberman in making a plea that we drop the term " massive martensite "? Can we agree on another term?

Dr. T. BELL (University of Liverpool): The origin of this term was when Professor Owen§ observed these metallographic structures about six or seven years ago. I feel that the term " massive martensite " is adequate, and has served its purpose. Now that we have looked at the transformation in much more detail we could perhaps follow a suggestion made initially by Professor Christian a couple of years ago that the term " massive martensite " (while being an adequate description for the optical metallographic appearance) should be changed to " self-accommodating martensite ".

Dr. KLOSTERMANN (*written discussion*): In his paper Lieberman proposes a system for classifying martensitic transformations. Perhaps it is a drawback of this classification that several types of martensite with a self-accommodating character, e.g. surface martensite,‖ angle-profile martensite,¶ martensites with a lath habit or with a massive** appearance, and eventually deformation martensites,†† are not covered. These types of martensite can form at rather low temperatures, e.g. in iron–nickel alloys at below − 30 or − 50° C,‡‡ and one needle or lath can form in $< 10^{-2}$ sec. Thus, it is probable that nearly all atoms move less than an interatomic distance and this condition will be disturbed only to a minor extent by dislocations moving on slip planes, performing the lattice-invariant deformation. For these types of martensite, however, surface upheavals are slight and the lattice deformation is to a large extent compensated by the lattice-

* W. K. C. Jones and A. R. Entwisle, to be published.
† A. Brownrigg, Ph.D. Thesis, Univ. Sheffield, **1966.**

‡ L. Kaufman and M. Cohen, *Progress Metal Physics,* 1958, **7,** 165.
§ A. Gilbert and W. S. Owen, *Acta Met.,* 1962, **10,** 45.
‖ J. A. Klostermann and W. G. Burgers, *ibid.,* 1964, **12,** 355.
¶ J. A. Klostermann, " Physical Properties of Martensite and Bainite " (Special Rep. No. 93), p. 43. **1965:** London (Iron Steel Inst.).
** R. G. Bryans, T. Bell, and V. M. Thomas, this vol., p. 181.
†† A. J. Bogers, Thesis, Univ. Delft, **1962.**
‡‡ R. Huizing and J. A. Klostermann, *Acta Met.,* 1966, **14,** 1695.

invariant deformation (which is not an invariant plane strain).

The self-compensating types of martensite are an important class. Moreover, self-compensating aspects will often result in deviations from the crystallography " predicted " by the I.P.S. theory in many transformations.

To cover the self-compensating types of martensite, condition (vii) of the paper by Lieberman must be relaxed. It is proposed in this remark to define a martensite transformation by the condition that the atoms move less than an interatomic distance, excepting the relative displacement of the atoms performed by dislocations moving in their slip planes. In this way conditions (ii) and (iii) in the paper by Lieberman are automatically satisfied. Conditions (iv) and (vi) will very probably be fulfilled; however, condition (v) will in certain cases essentially not be met, e.g. for the h.c.p. $\rightarrow$ f.c.c. transformations.

Professor D. S. Lieberman (University of Illinois, U.S.A.) (*written reply*): I prefer not to get into a semantic discussion of " massive martensite " but would rather suggest that the massive transformation is not a martensitic one since the geometric criteria are not satisfied. As I discussed in the paper, the h.c.p. $\rightarrow$ f.c.c. transformation is, of course, a special martensitic transformation in which the invariant habit plane is the close-packed plane in each structure and no additional lattice-invariant strain (twinning or slip) is required for matching and minimizing the energy at the interface. Of course, the habit plane for this (in a sense degenerate) case is not irrational; you will note that I prefaced this point in my paper with the word " generally ".

The very important additional energy considerations associated with the several types of " martensite " mentioned by Dr. Klostermann (surface, angle-profile, lath, deformation) were not incorporated at all in the original phenomenological theory as formulated by Wechsler, Read, and myself and by Bowles and Mackenzie. At that time, only the requirement that the strain energy at the interface be a minimum and that the interface be one of zero *average* distortion was used to develop the matching conditions and relations among the crystal geometric features. Thus, it would certainly be most surprising if such a simple approach were to describe these cases without some modification.

Dr. Entwisle: Could I just raise a small point with Dr. Crocker? The criterion that he used for looking at the strains was $\Sigma\eta_i^2$. Why did he choose that? It seems to me it may be more favourable to take into account the sign and the magnitude of strains. His analysis completely ignores the fact that we may have a large extension one way and two small compressions the other way.

Dr. A. G. Crocker (University of Surrey): The magnitude of the scalar quantity is simply a convenient means of classifying correspondences. In addition, as explained in the Appendix to our paper, it may be obtained directly from the elements of the correspondence matrix, without solving the cubic determinantal equation. In practice we do, of course, also obtain the individual principal strains. As Dr. Entwisle remarks, it is useful to consider the magnitudes and signs of all three principal strains independently; these are not ignored.

Dr. J. E. Kittl (Argentine Atomic Energy Commission, Buenos Aires, Argentine): I want to comment on the same question. The stresses that can be set up in the inner grains in a specimen using Dr. Crocker's equation also depend on what is happening in the neighbouring grains. You will appreciate this if you consider bent specimens containing stress-induced martensite. The transformation reverses the bending, and therefore changes the stress conditions. If we then cool the specimen, we can observe in certain grains that we change the compression just to enable the grains to transform. It is a complex case, and martensite and grains are being produced at the same time, so what stresses are acting?

Professor Hull: I think this, in fact, supports Dr. Entwisle's concern about the generalization made by Dr. Crocker.

Mr. A. F. Acton (University of Liverpool): I have some general comments with reference to the operation of multiple shears in martensite transformations. Dr. Bevis and I have been working on a new analysis of the crystallography of martensite transformations which is based on a previous analysis by Dr. Crocker, but is much more general. In essence, this analysis consists of combining two simple shears in any crystal system with a rigid body rotation to give a single simple shear. The elements of this equivalent single shear are determined and used as the lattice-invariant shear plane and shear direction in the Bowles–Mackenzie type of analysis. We believe this work is significant, as I hope the following three important points may illustrate. First, selecting two simple shear modes operative in any crystal system at random, then, except in certain very special cases, they will combine to give a resultant simple shear, and so long as one shear is not unidirectional they will always combine to give a resultant simple shear. Secondly, these combinations of unrelated shear modes usually involve some restrictions on the magnitudes of the component shears, but these restrictions are not excessive since such combinations may result in physically realizable and acceptable lattice-invariant shears. Thirdly, two-component shear modes, (e.g. two twinning modes) must be compatible and must be able to coexist in the same matrix, and this point is kept in mind on application of the analysis. Work such as that presented by Mr. Rowlands can be handled by this analysis, and investigation of the combinations of these multiple shears is under way. The more definitive results recently published by Oka and Wayman* can also be analysed. We are sure, in fact, that the variants of the $(112)_{\text{b.c.t.}}$ and $(101)_{\text{b.c.t.}}$ twinning modes suggested by Wayman to be operative in high-carbon steels do not give a solution for the martensite habit plane. However, the operation of a different $(101)_{\text{b.c.t.}}$ twinning mode with a higher shear does give rise to a solution for the habit plane that is consistent with the experimental results.

Dr. Crocker: The approach described by Mr. Acton is quite different from that which we are at present pursuing. Thus, in the Bevis and Acton treatment the lattice-invariant shear of the basic crystallographic theories is replaced by a rotation and two shears and these are in fact very restricted because they have to be equivalent to a single shear. We are developing a new theory based on a lattice deformation consisting of two unrestricted homogeneous shears.

Dr. Bilby: May I just ask where you put in the volume change?

Dr. Crocker: As yet no volume change has been introduced. To incorporate a volume change we should have to introduce a dilatation parameter.

Professor Christian: Is there a lattice-invariant shear?

Dr. Crocker: No, the shears are not lattice-invariant. They are homogeneous shears of the lattice and we first looked at the following problem: Given a parent lattice, is it possible to shear it into a given product lattice? In general,

* M. Oka and C. M. Wayman, *Trans. Met. Soc. A.I.M.E.*, 1968, **242**, 337.

the answer was No. We are now asking: Is it possible to transform the parent lattice into the product lattice by a combination of two shears? In general, we believe the answer will be Yes. This is because any shear involves four independent parameters so that with two shears we have eight parameters. In addition any lattice deformation, without a volume change, is defined by eight quantities. Thus, in principle, it should be possible to transform from one lattice to another by using two shears of this kind. If not, we shall consider introducing further shears.

Professor CHRISTIAN: So you are abandoning the invariant-plane-strain condition altogether?

Dr. CROCKER: At this stage, yes. However, once we have completed our analysis of multiple lattice-deformation shears we may incorporate it in a theory involving an invariant plane strain.

Dr. M. BEVIS (University of Liverpool) (*written discussion*): In the paper by Crocker and Ross and in the discussion by Acton two ways of generalizing the martensite crystallography theories have been briefly described. Both analyses are being developed to explain the anomalous crystallographic features of some martensitic transformations. The paper by Crocker and Ross introduces for the first time a new mechanistic theory of martensite crystallography. The development of this analysis is important, as no systematic study has been made of the changes in parameters of a lattice that undergoes a simple shear or a combination of simple shears. The value of the analysis with respect to the crystallography of martensite will depend on the way in which the resultant lattice deformation is related to experimentally observed crystallographic features such as the invariant-plane-strain condition, volume change, and transformation twinning and slip. The reason for developing this analysis was in part the lack of success of the phenomenological theories in explaining the $\gamma \rightarrow \alpha$ transformation in an U–5 at.-% Mo alloy. The experimentally determined transformation twinning modes in this alloy were not used as a multiple-shear, lattice-invariant shear in the martensite theories. It would therefore be interesting to see if the crystallographic features of the $\gamma \rightarrow \alpha$ transformation could be explained by applying to this problem the analysis discussed by Acton which retains the essential features of the current theories. The further development and assessment of martensite crystallography theories would be enhanced by precise experimental determination of the internal structure of martensite plates and the role this structure plays in the transformation process. It is unfortunate that this precise information is so difficult to obtain experimentally.

Dr. A. P. MIODOWNIK (University of Surrey): Could I say something about the considerable ambiguity that exists concerning the energy of the interface between austenite and martensite, and suggest, backed by a still tentative but interesting hypothesis, that there might be quite a large temperature-dependent component of this interfacial energy? This has never really been considered. We usually have a surface-energy term, and a free-energy term, to a variety of powers that are dependent on whether one is trying to determine a critical radius or a critical free energy for the embryo. In general, the free-energy term is known to be temperature-dependent, and this results in a considerable variation of the critical nucleus size. The surface-energy term is always, so far as I can make out, treated as temperature-independent, and one runs into tremendous difficulties, because people use different values. Now, it has already been suggested in Christian's paper that there are

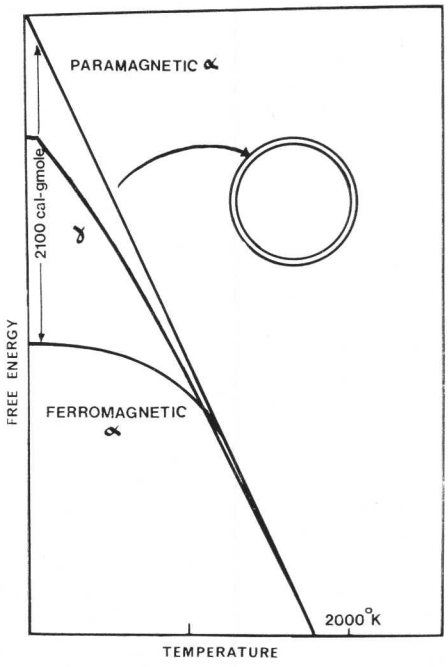

Fig. D.IV.2 *The free-energy difference between austenite and ferrite as a function of temperature.* (Miodownik.)

a number of components in this surface-energy term, and one component that might be significant in the particular case of an austenite/martensite interface is the magnetic component $H\Delta J$. The free-energy difference between austenite and ferrite is shown in Fig. D.IV.2, and if one takes out the magnetic component, one would find that the relative stability of α and γ becomes completely reversed from the normal situation. Now, at the surface of a particle of α, it seems quite feasible, bearing in mind work done on very small particles of iron, that there is a layer one atom deep which is not ferromagnetic.

The coupling forces change so rapidly when you get to the extreme surface of the particle that, if you conduct the free-energy analysis in the normal way, you can take in this factor as a magnetic surface-energy term in addition to the normal surface energy. The maximum value you get out of this is of the order of 100–200 ergs cm^{-2}. It is temperature-dependent, because $H\Delta J$ continually changes with temperature near the Curie point. You therefore have a large magnetic component of surface energy at low temperatures, and a small one at high temperatures. This may resolve some of the difficulties we have seen in the literature.

Professor CHRISTIAN: The 200 ergs cm^{-2} one puts into the nucleation of martensite in iron is merely a structural, or misfit, energy which comes from the semi-coherent nature of the interface, and I do not think there can be much temperature-dependency in that.

Professor R. B. NICHOLSON (University of Manchester): I do not see that Miodownik's idea is going to solve the problem on nucleation generally, because so many of these transformations occur in materials that are not magnetic at all. I still feel the evidence is very much in favour of nucleation that is aided by some form of elastic stress. I think that what Professor Christian said about the frequent occurrence of sympathetic nucleation . . .

Professor CHRISTIAN: Auto-catalytic. Sympathetic nucleation sometimes means something else. I prefer not to use that term.

Professor NICHOLSON: . . . auto-catalytic nucleation, is significant. The relation between dislocations and martensite nuclei in Easterling's paper is also relevant. It seems to me that the problem of the nucleation of martensite is more likely to be solved in terms of a general mechanism than that suggested by Dr. Miodownik.

Professor ENTWISLE: I am not sure whether the distinction between a structure imperfection and a region of high stress is particularly vital, but let me give you an indication of the result of an experiment that we performed to settle this point, which was totally unsuccessful. We argued that, in steels that undergo isothermal transformation, there was a sensitive way of looking at the effect of deformation. We take material which is austentic, deform it a little, and observe its isothermal transformation behaviour at low temperatures. The real object of this is to put numerous embryos into the material. You find that the general result of deformation in the range 2–10% is to suppress transformation very drastically. This greatly surprised us and we are not sure of the detailed interpretation. The only acceleration of transformation is for extremely small deformations (the sort of deformation you get by loading up to 90% of yield stress). This we can account for in terms of macroscopic internal stresses, but all the other evidence seems to suggest that microscopic internal stresses put in by deformation (e.g. dislocation pile-ups) greatly suppress nucleation. We do not understand this.

Professor C. S. BARRETT (University of Chicago, U.S.A.): Are Abell and Crocker able to cold work the mercury specimen as well as to apply a tensile strain?

Mr. J. S. ABELL (University of Surrey): Yes, although I have not yet found it necessary to use this facility to produce the new phase. This can be done with simply a tensile strain.

Professor BARRETT: I thought perhaps the reason you were not presenting the structure here was that you did not have enough of the new phase to give a good diffraction effect.

I would also like to ask Dr. King if it is possible to extend the region of the Nb–Sn diagram that transforms to an M_d curve instead of an M_s curve by cold work.

Dr. H. W. KING (Imperial College, London): We used powder samples for this work, which rules out cold work. In any case Nb_3Sn is extremely brittle, as evidenced by the fact that it is not necessary to strain-relieve powdered specimens. We could, however, examine the effect of elastic stresses on a polycrystalline specimen by using the straining jig for our cryostat that was referred to by Abell and Crocker.

Mr. P. R. KRAHÉ (École Nationale Supérieure des Mines, Paris, France): I understand the relation between the surface tilts and the etched boundaries in the paper by Bryans *et al.*, but I would like to know how they interpret the substructure inside these plates, and what is the relation between the laths and the plates?

Dr. BELL: The dimensions of the laths are completely different from the dimensions of the plates or slabs, as we prefer to call them. We have, in fact, taken individual grains of austenite and transformed them to massive martensite, and then polished them away to produce thin foils. We were able to orient the actual grain from the massive martensite traces on the surface. We were able to see groups of individual traces under the electron microscope, which corresponded with the actual markings on the surface.

Dr. KLOSTERMANN: I should like to comment on the same paper. I disagree that a matrix δ results in a (111) or (225) plane that contains only vectors that do not rotate, and I cannot see how rotation in this way is compensated in their model. They add a shear in the same plane and accommodation rotations by choosing a stack of alternating orientation variants. These variants indeed compensate the rotation about the axis but not the rotation in the length direction.

Mr. R. G. BRYANS (University of Liverpool): There are, in the paper by Speich and Swann,* four different ways in which you can achieve a Kurdjumov–Sachs relationship, and yet get a relationship between the martensite plates themselves. One of these is to have a rotation of 10° at the interface, assuming the interface between the individual massive martensite laths is $(110)_{\text{martensite}}$. Others are 49, 60, and 70°. In each of these cases, we worked out an individual shape deformation in the same form as you see in the paper. I have considered the effect of these on the atoms in the interface between the two plates. Our experimental results have shown that one would expect the interface between adjacent plates to be undistorted. You will find in other cases that if you apply the next shape deformation to the atom positions in this interface, nothing happens after the intermediate position when the first plate is formed. That is, we compensate for the initial rotation, arising from the formation of the first plate.

Dr. KELLY: Might I join in this argument? These points have been misinterpreted by the authors. If you have a martensite plate which obeys a Kurdjumov–Sachs relationship to the matrix and has $(101)_{\text{martensite}} \parallel (111)_\gamma$ as a habit plane, there are six Kurdjumov–Sachs variants which share this same parallelism. These are related by various angles, and include one which is an identical twin. By using the Jaswon–Wheeler matrix it is possible to predict an invariant plane *between martensite laths* as Bryans *et al.* have done, but *not* between martensite and the parent austenite. It is the latter plane which is important.

Mr. BRYANS: These lath relationships are based on one experimental result. I am not seeking to apply a single experiment and a single result to all the cases, but these shape deformations apply to this one case where the rotation is 10° from the interface normal.

Mr. R. D. GARWOOD (University of Cardiff): In the original Jaswon–Wheeler analysis, certain directions in the predicted $(225)_\gamma$ habit plane underwent rotations of as much as 19°. This may produce a change in surface relief consisting of a tilt along the length of a plate. In your analysis, are there similar rotations of directions in the predicted $(111)_\gamma$ habit plane?

Mr. BRYANS: Yes, the vectors in the $(111)_\gamma$ and $(225)_\gamma$ planes rotate within these planes but not out of them.

Mr. KRAHÉ: In Fig. 4 of the paper by Bryans *et al.* there are several annealing twins. Do you think this has an effect on the nucleation of the plates?

Dr. BELL: The twins often act as nuclei for the martensite plates, but do not always do so. This is what Yeo† found also.

Mr. KRAHÉ: Could I throw the discussion back to Kelly? If you have a (111) plane, could you give me an idea of how you form the first lath, and then how you get the others, because if you make a diffraction analysis you will find both high- and low-angle boundaries between laths?

Professor HULL: What is the nature of the boundaries between the laths?

Dr. KELLY: I will answer this question from my own

---

* G. R. Speich and P. R. Swann, *J. Iron Steel Inst.*, 1965, **203**, 480.
† R. B. G. Yeo, *Trans. Amer. Soc. Metals*, 1964, **57**, 48.

experimental work, because I do not want to put words into the mouths of Bryans, Bell, and Thomas. The relationship between the laths in a stack is either a small tilt (I would have estimated $< 3°$ and nothing like 10°), or else it is a twin relation. Again, the twin relationship may not be perfect, and could be tilted by up to 3°.

Mr. KRAHÉ: Marder* reports that some laths are separated by high-angle boundaries. How does this happen?

Dr. KELLY: Some peculiar things do happen. The paper by Bryans, Bell, and Thomas reports an angle of 10° between adjacent laths. For example, examine the diffraction pattern in their Fig. 12, showing the orientation difference between laths 2 and 3, which are supposed to be 10° apart. The pattern shows a (110) reflection of lath 2, and an (020) reflection of lath 3. Now, the angle between these two planes in a cube is 45°. On the pattern these two reflections are 6° apart, showing that the misorientation is at least $> 39°$ (i.e. $45 - 6°$). I suggest that it might be a good idea to re-examine this pattern and I suspect that it will turn out to be close to a twin orientation, as it certainly does *not* represent a 10° misorientation.

Dr. BELL (*written discussion*): We are confident of the result given in Fig. 12.

Mr. KRAHÉ (*written discussion*): With reference to the paper by Bryans *et al.*, up to now the study of lath martensite has been by conventional polishing and etching techniques, observation of surface reliefs, and thin-film electron microscopy. Few authors have used the three techniques to study the morphology of the transformation product. From these data, it seems that the structure can be described in terms of three structural units of very different cross-sections, i.e. sheaves or blocks of parallel shear plates, shear plates, and laths. The term lath should be reserved for the unit seen with the electron microscope.

Simple calculations using the available data, including the work discussed, will show that the shear plates have a cross-section several times larger than laths. From Speich and Swann's work on Fe–Ni alloys† and our own work on Fe–C–Ni alloys,‡ the average difference in cross-section is about tenfold.

Bryans *et al.* say with reference to the structural units observed in the electron microscope (laths), that their common interfaces are invariant planes. This cannot be inferred from the interferometric evidence, which only suggests that some particular interfaces between adjacent laths (e.g. the plane between a self-accommodating pair of shear plates) is an invariant plane. Fortunately, these are the invariant planes needed to apply the formal theory of crystallography. However, it is difficult to see how a simple shear parallel to the habit plane, when combined with the correspondence strain and the orientation rotation, will leave this plane invariant.

Finally, although the authors state that shear plates nucleate parallel to or at small angles to austenite annealing twins, Fig. 4 shows a group which nucleated at $\sim 49°$ to a twin interface. This is in agreement with data* on Fe–C alloys and our own observations on Fe–C–Mn lath martensites.

Dr. BELL (*written discussion*): In reply to the points raised by Dr. Krahé, there is no evidence that laths are some form of substructure of shear plates, as he implies. In view of the fact that lath widths can vary by a factor of 10, it would seem to us that there is reasonably good correspondence between the dimensions of surface tilts and substructural laths. We are not sure what further evidence Dr. Krahé would require to convince him that a lath and tilt do in fact correspond, short of taking an individual lath, measuring its tilt, and preparing a thin foil from it.

Finally, we should like to emphasize the point made in the paper that we do not get an invariant plane between the austenite and the martensite in our theory. What we do aim to get is an undistorted plane between two laths of martensite which must bear a specific orientation relationship to each other. By using different variants of **S** in **E** = **S.R.P.** we produce two adjacent laths with the right orientation relationship to each other which match across their common interface. The **P** is used to modify **S** because **S** by itself does not predict the correct experimental shape deformation.

Dr. AARONSON (*written discussion*): My remarks are concerned with Professor Christian's considerations on the mechanistic implications of the appearance of shape changes in conjunction with phase transformations involving a change in composition.

In an earlier treatment of this problem, he concluded that a shape change is improbable in this situation when both matrix and precipitate are substitutional solid solutions.§ The appearance of these changes in the $\beta \rightarrow \alpha$ reaction in Cu–Zn‖ apparently contradicted this conclusion; however, there was possibly some uncertainty as to whether or not a composition change actually occurred in this situation. The electron-probe analyses subsequently performed by Repas and Hehemann¶ prove that zinc does partition to β during growth. Garwood's** attempt to repair this contradiction by proposing that an α plate has the same composition as the parent β for a short distance behind the advancing α/β boundary is not admissible, as this would require that zinc is removed from the interior of an α plate by diffusion up an activity gradient. In the present review, the impression is given that the martensitic nature of the shape change at issue has yet to be established in a quantitative manner. However, Garwood** has successfully accounted for the shear angle produced at a free surface by α plates in Cu–Zn by means of the theory of martensite crystallography.

In discussing the study of Laird and Aaronson†† on the dislocation structure of the broad faces of γ plates in Al–15% Ag, Christian questions their adoption, for the interphase-boundary situation, of the view of Cottrell and Bilby‡‡ that the Shockley partials which make up this structure cannot climb. However, in a subsequent study of the growth of γ plates in the same alloy, Laird and Aaronson§§ readily demonstrated that the observed growth kinetics is wholly inconsistent with a dislocation-climb mechanism. This point may have been stressed by Christian because he notes that " semi-coherent particles would also be produced by the orderly addition or removal of planes of atoms from the product without further rearrangement ". However,

* A. R. Marder and G. Krauss, *Trans. Amer. Soc. Metals*, 1967, **60**, 651.
† G. R. Speich and P. R. Swann, *J. Iron Steel Inst.*, 1965, **203**, 480.
‡ P. R. Krahé, Ph.D. Thesis, Ecole Nationale Supérieure des Mines, **1967**.

§ J. W. Christian, " The Decomposition of Austenite by Diffusional Processes ", p. 371. **1962:** New York and London (Interscience Publishers).
‖ R. D. Garwood, *J. Inst. Metals*, 1954–55, **83**, 64.
¶ P. E. Repas and R. F. Hehemann, " Formation of Bainite in Beta Brass ", ONR Report on Contract No. Nonr 1141(15), **1967**.
** R. D. Garwood, " Physical Properties of Martensite and Bainite " (Special Report No. 93), p. 90. **1965:** London (Iron Steel Inst.).
†† C. Laird and H. I. Aaronson, *Acta Met.*, 1967, **15**, 73.
‡‡ A. H. Cottrell and B. A. Bilby, *Phil. Mag.*, 1951, **42**, 573.
§§ C. Laird and H. I. Aaronson, *Acta Met.*, in the press.

electron-probe analysis has proved that long-range interdiffusion of aluminium and silver accompanies the growth of γ plates.*

Christian also states that Laird and Aaronson failed to distinguish properly between misfit and transformation dislocations. The point of the Laird–Aaronson argument, however, is that a misfit dislocation can be so placed that, although it compensates misfit only inefficiently, it serves simultaneously as a transformation dislocation. In their subsequent investigation, Laird and Aaronson obtained direct experimental confirmation of this deduction.† They observed that Shockley partials can migrate across the broad faces of γ plates when the Burgers vectors of adjacent partials are parallel; these dislocations must be stepped relative to one another to preserve the correct packing order.‡ When such partials enter a region of a γ plate where they can join a network of other partials with different Burgers vectors of the form $a/6\langle 112\rangle$, their movement stops as the ledges disappear, planarity is locally restored to the boundary, and the Shockleys make the transition from misfit-and-transformation dislocations to misfit dislocations alone.

The movement of those partials which act as ledges across the broad faces of γ plates usually proceeds at a diffusion-controlled rate.† Attachment of atoms to the edges of these ledges thus takes place in an " unguided " manner across the region of local atomic disorder provided by the bounding Shockley partial. Neither this process nor the equally disorderly long-range interdiffusion process is consistent with the concept " that a lattice correspondence is maintained during growth ". On the other hand, this growth process *simulates*, in a crystallographic sense, a martensitic transformation with one vital feature of such a mechanism clearly omitted. This feature is the transport by glide of " labelled " atoms from specific sites in the matrix to specific sites in the product phase. As Laird and Aaronson†‡ have suggested, this simulation is physically manifested by the presence of a dislocation interphase boundary and is sufficient to give a martensite-like shape change. They chose to term this effect a " geometric " surface relief or shape change to avoid the assumption of a one-to-one " correspondence " between the presence of a shape change and the atomic mechanism of transformation. It has now become clear that a shape change is a necessary, but not sufficient, condition for describing the mechanism of a phase transformation as martensitic.

Finally, it should be noted that Christian§ has predicted that the shape change accompanying diffusional transformation would disappear as soon as it formed. That this is not observed probably results from the formation and the disappearance of this change by different mechanisms, propelled by different driving forces.

* H. I. Aaronson, unpublished work.
† C. Laird and H. I. Aaronson, *Acta Met.*, in the press.
‡ C. Laird and H. I. Aaronson, *ibid.*, 1967, **15**, 73

§ J. W. Christian, " The Decomposition of Austenite by Diffusional Processes ", p. 371. **1962:** New York and London (Interscience Publishers).

Interstitial Order–Disorder Transformation in the Titanium–Oxygen System

M. Hirabayashi, M. Koiwa, and S. Yamaguchi

Electron-diffraction studies and calorimetric measurements have been carried out on a series of titanium–oxygen specimens with compositions from O/Ti = 0·09 to 0·40. It is shown that over this range oxygen atoms distribute themselves regularly in every second layer of the octahedral interstitial planes normal to the *c* axis of the hexagonal metal lattice at temperatures lower than 400–500° C, depending on oxygen content. Thus, an interstitial order–disorder transformation is found over the whole composition range. The transformation is characterized by a two-stage process accompanied by a broad λ-type peak and a subsidiary shoulder in curves of specific heat vs. temperature. The structural changes during these processes are elucidated with the aid of electron-diffraction patterns of single-crystal specimens.

It is well known that α-modifications of titanium, zirconium, and hafnium are characterized by a high solubility of oxygen atoms which occupy the octahedral interstitial sites in the h.c.p. lattice. The fact that oxygen atoms dissolved in α-zirconium distribute themselves regularly in certain sites of the octahedral interstices over a wide range of oxygen contents was recently revealed by one of the present authors.[1] Such atomic order is sometimes called interstitial order or sub-lattice order.

In the titanium–oxygen solid solution, interstitial order has been observed only at relatively high oxygen contents. At a composition given by an atomic ratio O/Ti ≡ $x = 0{\cdot}5$ (Ti_2O), Andersson *et al.*[2] found that oxygen atoms are situated exclusively in every second layer of octahedral interstices extending normal to the *c* axis, and thus all the interstices in these planes are filled while those in the alternate planes are empty. This structure is illustrated in Fig. 1. Similar types of ordered arrangement have been reported by Holmberg[3] in the range $x = 0{\cdot}33$ to 0·5 at relatively low temperatures around 400° C.

A phase transformation of the order–disorder type related to the oxygen distribution has been suggested for the range $x = 0{\cdot}33$ to 0·45 from X-ray diffraction results by Holmberg and from measurements of electrical resistivity by Wasilewski.[4] Moreover, the existence of two sub-oxide compounds, Ti_3O and Ti_6O, has been proposed by Kornilov and Glazova[5] on the basis of metallographic observations as well as measurements of various physical properties. According to their results, the compound Ti_3O is stable up to the melting point (~ 1900° C), while the maximum temperature of stability for Ti_6O is 820–830° C. Previous investigations on the extent of the Ti–O primary solid solution have been reviewed in some detail by Wahlbeck and Gilles.[6]

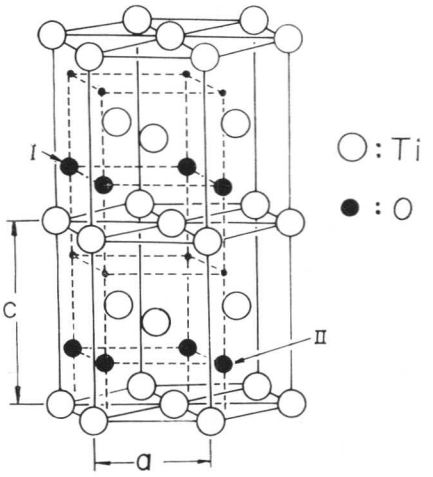

Fig. 1 Interstitial sites in α-titanium. Open circles are titanium atoms. Closed circles and black dots indicate available and forbidden sites for oxygen in the ordered states. All the former are occupied for the structure Ti_2O, and the sites I and II are supposed to be vacant for the ordered structure Ti_3O.[3]

Thus, no general understanding of this interstitial solution has been established despite the accumulation of considerable experimental data. In the present work, therefore, alloys in the composition range $x < 0{\cdot}5$ were studied by means of electron diffraction as well as by calorimetric measurements to clarify the atomic arrangement of oxygen atoms and the nature of the phase transformation that occurs over this range. The results to be described show that oxygen atoms are regularly distributed, even in dilute solutions as low as 9 at.-% O, in every second layer of the octahedral interstices at relatively low temperatures. An order–disorder transformation relating to the interstitial sub-lattice takes place in two distinct steps in the range between ~ 300 and 600° C, depending on oxygen content. The present paper is part of a general study of the Ti–O system and a brief preliminary note has been published elsewhere.[7]

Manuscript received 1 April 1968. Professor M. Hirabayashi, D.Sc., M. Koiwa, D.Eng., and S. Yamaguchi, M.Sc., are in the Research Institute for Iron, Steel, and Other Metals, Tohoku University, Sendai, Japan.

TABLE I

Impurities (wt.-%) Detected in Titanium

Fe	Mg	Mn	Si	Cl	N	C	H
< 0·07	< 0·02	< 0·01	< 0·01	< 0·03	< 0·02	< 0·01	< 0·01

TABLE II

Oxygen Content of the Specimens

at.-% O	8·6	8·8	10·3	13·6	15·4	17·8	21·1	21·8	24·0	26·3	28·4
O/Ti Ratio	0·094	0·097	$0·11_5$	$0·15_8$	$0·18_2$	$0·21_7$	$0·26_8$	$0·27_9$	$0·31_6$	$0·35_7$	$0·39_7$

Experimental Procedure

Specimens were prepared by melting appropriate mixtures of titanium metal and titanium dioxide (99·9%) under an argon atmosphere in an arc furnace of the non-consumable type with a tungsten electrode.* Impurities detected in the titanium metal are listed in Table I. Eleven alloys in the range $x = 0·09$ to 0·40 were studied. Oxygen contents of specimens, given in Table II, were determined from the increase in weight on oxidation to form TiO_2 by heating in air. Calorimetric measurements and electron diffraction were carried out in the same way as described previously elsewhere.[1,8] Bulk specimens of ~ 20–50 g were used for the calorimetry under vacuum up to ~ 700° C. Electron-diffraction patterns were taken by using small chips of single-crystal specimens prepared from the same ingots as were used for the calorimetry.

Results

Calorimetric Measurements

The calorimetric results for a specimen with $x = 0·18$ are shown in Fig. 2. Curve A, measured on a specimen quenched from 600° C, shows a heat evolution which starts at ~ 250° C and subsequently a heat absorption with a maximum at ~ 450° C. After the measurements, this specimen was annealed at 300–400° C for ~ 1 week and then cooled slowly to room temperature. A second calorimetric experiment on the annealed specimen gave the result shown by curve B in Fig. 2, indicating a relatively large amount of heat absorption with a broad maximum at ~ 460° C. These features are quite typical for an order–disorder transformation, and can reasonably be interpreted as a result of rearrangement of interstitial oxygen atoms. In fact, this was ascertained by electron-diffraction studies, as will be described later in detail.

Another example of heat-capacity measurements is shown in Fig. 3 for a well-annealed specimen of $x = 0·28$. This figure shows a curious variation of heat absorption over a wide range of temperatures; double peaks appear at ~ 500 and 540° C.† Similar anomalies were also found in measurements

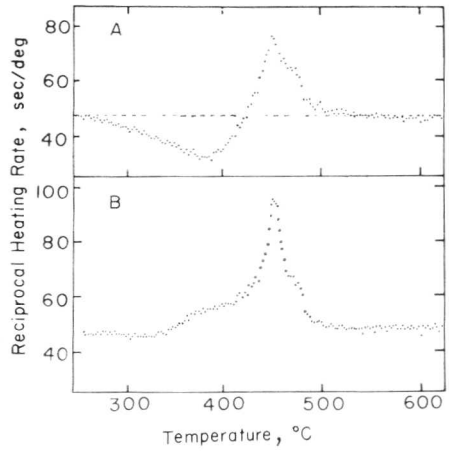

Fig. 2 Thermal-analysis curves on heating the specimen x = 0·18. (A) *After quenching from* 600° *C. The broken line corresponds to the specific-heat value of* 6 *cal/mole/deg.* (B) *After annealing at* 300–400° *C for* 1 *week.*

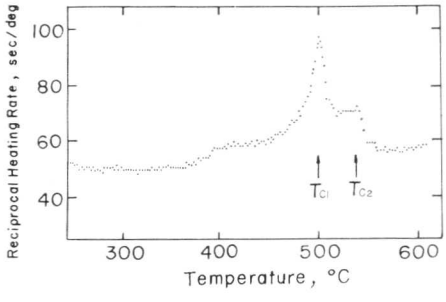

Fig. 3 Thermal-analysis curve on heating the specimen x = 0·28 *after annealing at* 300–400° *C for* 1 *week.*

on other specimens, e.g. a subsidiary peak may be seen in curve B of Fig. 2 at a higher temperature (~ 480° C) than that of the main peak. The temperatures of the main peak and of the sub-peak will be expressed as T_{c1} and T_{c2}, respectively, and the phases that are stable below T_{c1} and T_{c2} are designated α'' and α', respectively, to distinguish them from the random solution α.

* Contamination of the ingots from the electrode was ~ 0·05%.

† Another singularity may be seen as a subsidiary peak at ~ 400° C, but its nature is not yet clear.

The observed values of T_{c1} and T_{c2} are plotted as a function of oxygen content in Fig. 4. The curve of T_{c1} shows a maximum near 510° C at a composition $x = \sim 0{\cdot}30$, while T_{c2} seems to increase with oxygen content. The temperature difference between T_{c1} and T_{c2} decreases with reduction in oxygen content and finally becomes undetectable at concentrations $< \sim x = 0{\cdot}15$. A kink (530° C) observed in heat-content measurements by Mah *et al.*[9] for an alloy with $x = 0{\cdot}334$ seems to lie between T_{c1} and T_{c2}.

The changes in energy and entropy associated with the phase transformation from α'' to α were deduced from a series of calorimetric measurements on specimens with various oxygen contents. It was found that the variation of transformation energy as a function of concentration has two maxima of 400–500 cal/mole at $x = \sim 0{\cdot}17$ and $\sim 0{\cdot}30$, and that corresponding values of the entropy change are nearly equal, being $\sim 0{\cdot}6$ cal/mole/deg.†

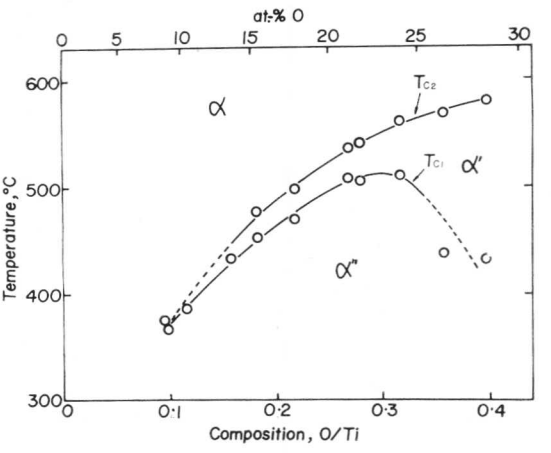

Fig. 4 Transition temperatures T_{c1} *and* T_{c2} *determined by calorimetry.*

Electron Diffraction

Ordered Structure of the α'' Phase

In addition to the fundamental reflections of the metal lattice, a number of extra reflections which arise from the ordered arrangement of the oxygen atoms were observed in electron-diffraction patterns of specimens annealed at between 300 and 400° C for 1 week. Some examples of electron-diffraction patterns are shown in Fig. 5. The superlattice spots may be seen even at the lowest oxygen content, $x = 0{\cdot}094$, and are marked by arrows in Fig. 5(*a*).

These reflections can be indexed, as illustrated in Fig. 6, in terms of a large hexagonal superlattice cell with lattice constants $A = \sqrt{3}\,a$ and $C = 2\,c$, where a and c are the lattice constants of the h.c.p. lattice of the metal atoms. The superlattice reflections are a series of spots in rows with H and K not divisible by 3, and spots with H and K divisible by 3 and $L = 4n + 2$. Other spots such as 00.1 and 00.3 observed in the photographs are due to double diffraction, since they vanish on tilting the specimen around the c^* axis. There are

† These values were calculated for masses containing 1 g-atom of titanium, while the values reported in a preliminary note[7] were for masses containing a total of 1 g-atom of titanium and oxygen.

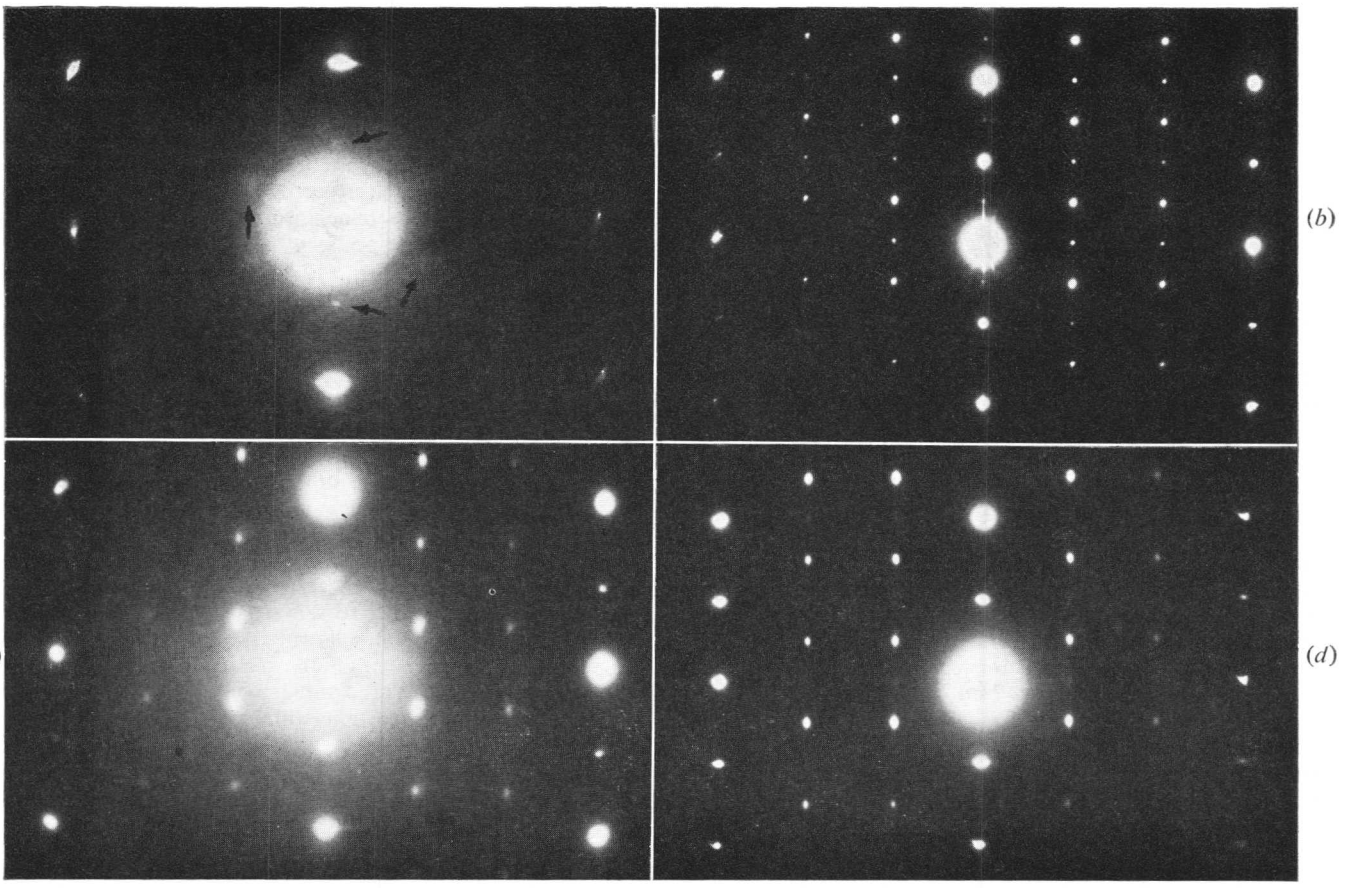

Fig. 5 Electron-diffraction patterns of specimens with various compositions annealed at 300–400° *C for* 1 *week. Reciprocal lattice plane corresponding to* (11.0) *for the original hexagonal lattice of titanium.* (a) x = 0·094; (b) x = 0·18; (c) x = 0·28; (d) x = 0·32.

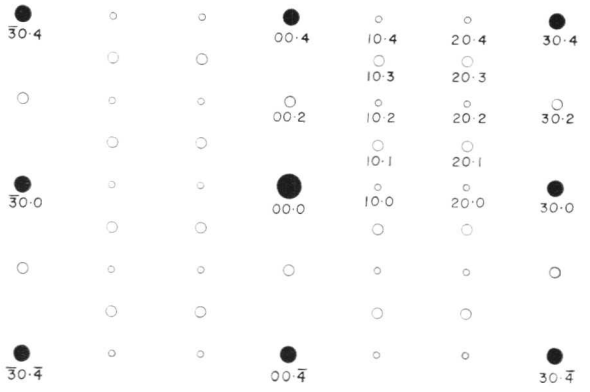

Fig. 6 Schematic interpretation of the electron-diffraction patterns of Fig. 5. Indices are referred to the large unit cell of the superlattice. Closed and open circles correspond to the fundamental and superlattice spots, respectively.

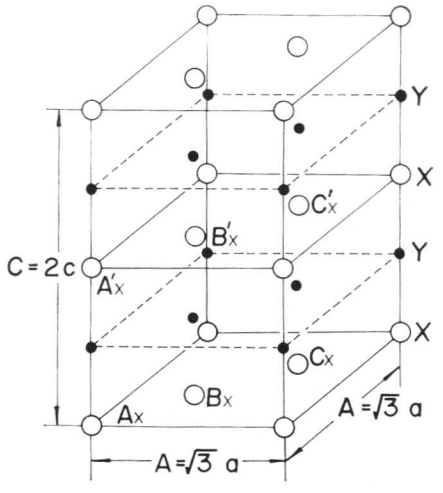

Fig. 7 Sub-lattices for the arrangement of oxygen atoms. Open and closed circles correspond to available and forbidden sites in the ordered α″ phase, being in the planes X and Y, respectively. Metal atoms are ignored.

two kinds of superlattice reflections of odd and even L in a series of spots with H and K not divisible by 3. It is observed that the spots with L odd are generally stronger than those with L even, and that the latter are hardly visible in the patterns of the specimens with $x = 0{\cdot}094$ and $x = 0{\cdot}28$. These features can be explained by considering the ordered distribution of oxygen atoms in the octahedral interstices.

To describe the distribution of oxygen, it is necessary to specify the interstitial sites in the hexagonal lattice. Twelve octahedral interstices are involved in the unit cell of the superlattice, but half of them are forbidden for the ordered arrangement of oxygen. Thus, the available sites for oxygen are considered to consist of 6 sub-lattices of the simple hexagonal cell with the lattice parameters $A = \sqrt{3}a$ and $C = 2c$, as illustrated in Fig. 7, in which the positions of the metal atoms are disregarded for simplicity. The 6 sub-lattice sites are designated A_x, B_x, C_x, A'_x, B'_x, and C'_x in this figure. The notations X and Y will also be used to describe the planes of interstitial sites normal to the c axis, which are respectively occupied and unoccupied by oxygen atoms in the ordered structure.

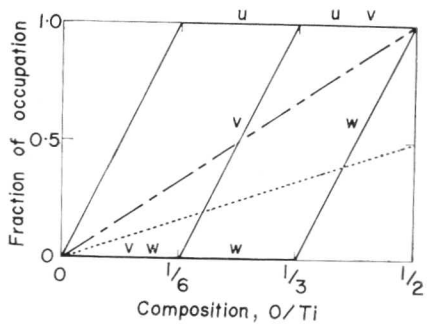

Fig. 8 Occupied fractions of interstitial sub-lattice sites in the plane X. Full, broken, and dotted lines correspond to the distribution of oxygen in the α″, α′, and α phases, respectively.

The following distribution of atoms among these sites was deduced from comparison of the calculated intensities of superlattice reflections with the intensities observed for the well-annealed state corresponding to the α'' phase. In the dilute range up to the composition $x = 1/6$, oxygen atoms only enter into the sub-lattices A_x and B'_x, and these sites are filled at the limiting composition $TiO_{0{\cdot}166}$, while the other sub-lattices remain empty. Next the sites of sub-lattices C_x and C'_x begin to be occupied by oxygen and these are completely filled at $x = 1/3$. This structure coincides with the model Ti_3O proposed by Holmberg[3] (Fig. 1). The sites of sub-lattices B_x and A'_x are gradually filled with oxygen in the range $x = 1/3$ to $1/2$. Finally the superlattice of Ti_2O determined by Andersson *et al.*[2] is realized when these sites are fully occupied at $x = 1/2$. The distribution of oxygen over the range of the α'' phase is illustrated schematically in Fig. 8, in which the occupied fractions of the interstitial sites A_x and B'_x, C_x and C'_x, and B_x and A'_x are expressed by three parameters u, v, and w, respectively. The details of the structure analysis will shortly be published elsewhere.

Disordering Processes

For comparison with the calorimetric measurements, the change in the atomic distribution of oxygen with temperature was investigated by electron diffraction using specimens quenched from various temperatures. The random solution α was obtained when specimens were quenched from temperatures higher than T_{c2}, and an intermediate structure α'' with imperfect order was found in specimens quenched from temperatures between T_{c1} and T_{c2}. Fig. 9 shows electron-diffraction patterns corresponding to both states of the specimen with $x = 0{\cdot}32$. There are no superlattice reflections in the pattern (Fig. 9(*a*)) taken from the specimen quenched from the α region except for very weak and diffuse 00.2 reflections which may be due to short-range order in the oxygen distribution. In the diffraction pattern corresponding to the α' region (Fig. 9(*b*)) it is noticeable that the superlattice reflections with H and K divisible by 3 and $L = 4n + 2$ are accompanied by diffuse streaks normal to the c^* axis, while a few other superlattice reflections are very faint and are slightly extended parallel to this axis. These characteristics can be explained by the following model. The ordered arrangement of oxygen within the basal planes X normal to the c axis (referred to as the in-plane order) almost disappears in the α' phase, while the interstitial sites in the basal planes Y remain vacant. In other words, each sub-lattice site in the planes X is statistically occupied with the same value $2x$ for the parameters u, v, and w as depicted by the broken line in Fig. 8, so that only inter-plane order exists in the intermediate phase α' between T_{c1} and T_{c2}.

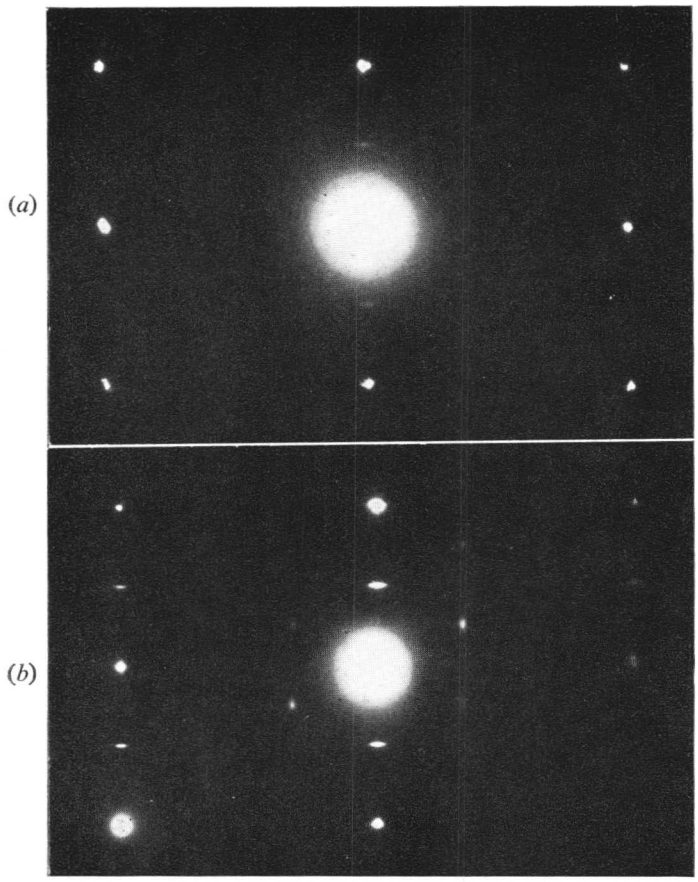

Fig. 9 *Electron-diffraction patterns of the specimen* x = 0·32, *quenched from* (a) 700° *C;* (b) 530° *C.*

It is also deduced that the coherent regions in which inter-plane order is present, are restricted to small columns extending parallel to the *c* axis, as illustrated schematically in Fig. 10. The evidence for this is the fact that the diffuse scattering in the electron-diffraction pattern consists of discs normal to the c^* axis, since the streaked reflections 00.2 and 00.6 appear independent of the foil rotation about the [00.1] axis. Similar diffuse scattering was observed by Sabine *et al.*[10] and was interpreted in terms of stacking faults in the interstitial lattice.

It is concluded, therefore, that the disordering processes take place in the following way with rising temperature: first the in-plane order gradually decreases in the α'' phase and disappears at T_{c1}, then the degree of inter-plane order decreases with temperature in the α' phase, and finally the long-range order disappears at T_{c2}, though short-range order probably remains in the α phase.

Conclusions

It has been established that the ordered arrangement of oxygen atoms and the transformation to the random solution is realized over nearly the whole composition of the solid solution, and that the distribution of oxygen at any concentration in the ordered state α'' is specified by the three occupation parameters given in Fig. 7. It is quite unreal, therefore, to consider the existence of the stoichiometric compounds Ti_3O and Ti_6O as proposed by Kornilov and Glazova,[5] since these alloys are better recognized as ordered solid solutions with special compositions.

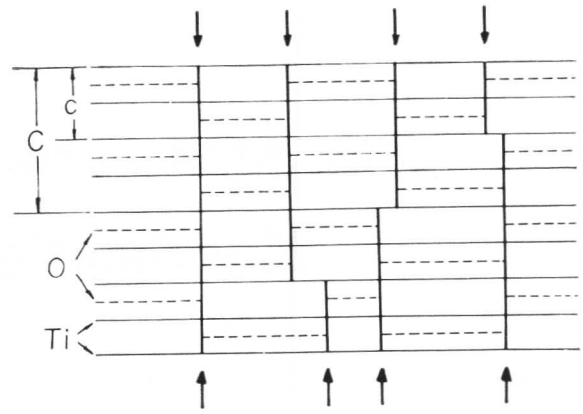

Fig. 10 *Schematic illustration of oxygen distributions in the intermediate region* α′. *Full and broken horizontal lines indicate atomic planes of Ti and O normal to the* c *axis, respectively. Vertical lines marked by arrows correspond to anti-phase domain boundaries in the oxygen distribution.*

A theoretical consideration of the interstitial order–disorder transformation in the present system was made under the assumption that the oxygen atoms repelled each other. Simple calculations based on the Bragg–Williams approximation gave composition-dependences of the critical temperatures T_{c1} and T_{c2} and a value of the transformation energy which are in a fairly good agreement with the experimental results. The details of these calculations will be published elsewhere.

The main results obtained in this study can be summarized as follows. There are two types of ordered arrangement of interstitial oxygen atoms in the primary solution of α-titanium. One of them is stable in the low-temperature phase α'' where oxygen atoms populate every second layer of the octahedral interstitial planes in a regular fashion. This type of ordered arrangement exists over a range from < 9 at.-% O up to the solubility limit. Another type of arrangement is identified in the intermediate temperature range of the α' phase where oxygen atoms are randomly distributed within the planes mentioned above but the interleaving layers are still empty. The random solid solution is stable only at relatively high temperatures. These conclusions were recently confirmed by a neutron-diffraction study at elevated temperatures which will be reported elsewhere.

References

1. S. Yamaguchi, *J. Phys. Soc. Japan*, 1968, **24,** 855.
2. S. Andersson, B. Collén, U. Kuylenstierna, and A. Magnéli, *Acta Chem. Scand.*, 1957, **11,** 1641.
3. B. Holmberg, *ibid.*, 1962, **16,** 1245.
4. R. J. Wasilewski, *Trans. Met. Soc. A.I.M.E.*, 1962, **224,** 8.
5. I. I. Kornilov and V. V. Glazova, *Doklady Akad. Nauk S.S.S.R.*, 1963, **150,** (2), 313.
6. P. G. Wahlbeck and P. W. Gilles, *J. Amer. Ceram. Soc.*, 1966, **49,** 180.
7. S. Yamaguchi, M. Koiwa, and M. Hirabayashi, *J. Phys. Soc. Japan*, 1966, **21,** 2096.
8. M. Hirabayashi, M. Koiwa, and N. Ino, *Sci. Rep. Research Inst. Tohoku Univ.*, 1966, [A], **18,** (Supplement), 337.
9. A. D. Mah, K. K. Kelley, N. L. Gellert, E. G. King, and C. J. O'Brien, *U.S. Bur. Mines Rep. Invest.* **(5316),** 1957.
10. T. M. Sabine, D. J. H. Corderoy, and A. E. Jenkins, *Acta Met.*, 1967, **15,** 519.

The Structure of the Low-Temperature Modification of Titanium Monoxide

A. W. Vere and R. E. Smallman

An investigation has been made of the transformation from high-temperature NaCl-type TiO to the low-temperature modification, using the techniques of transmission electron microscopy and electron diffraction. The results obtained indicate that the low-temperature modification is a highly faulted structure in which the oxygen vacancies are ordered in such a way that every third {110} plane in the cubic structure contains a high concentration of constitutional vacancies. It has been found that the structure of the phase varies continuously with increasing oxygen content and that this variation is reflected in the variation of fault width and density. This variation has been explained in terms of the distortion of the original NaCl-type unit cell due to the incorporation of varying concentrations of constitutional vacancies on specific {110} planes, and is considered to arise through the operation of a strain-relieving mechanism.

The structure of the titanium monoxide phase at temperatures above ~ 1000° C has been shown to consist of an f.c.c. titanium lattice in which the oxygen atoms are incorporated in the octahedral interstices.[1] The phase is stable over the composition range TiO_x, where $(0{\cdot}67 < x < 1{\cdot}22)$, and this wide phase range is achieved by the inclusion of a high proportion of titanium and oxygen vacancies, e.g. up to 30% vacant sites in the lattice. While the addition of constitutional vacancies to the lattice in general lowers the free energy of the compound, if they are added in significant quantities the vacancy-interaction energy may become so large that the resultant clustering of vacancies initiates a phase transformation. Hoch[2] has shown, however, that the vacancy-interaction energies in NaCl-type TiO are particularly low, an observation which correlates with the abnormally wide composition range and high concentration of constitutional point defects.

A similar reaction would be expected on decreasing the temperature of the compound and thus reducing the thermal energy. The structure stable at the high temperature becomes unstable and must transform, either by means of a classical phase change or by an ordering reaction, to a compound of lower free energy.

The work of previous authors[3,4] has shown that in several non-stoichiometric compounds this decrease in free energy is achieved by the ordering of the constitutional point defects, frequently giving rise to shear structures of the type found in the Ti_nO_{2n-1} series. The aim of this paper, however, is not to determine absolutely the structure of the low-temperature. modification of TiO, but to show that the structure originally proposed by Watanabe[5] may be classified as a shear structure of this type in which the unit cell is a distortion of the high-temperature NaCl-type structure, the degree of distortion and the thickness of the shear lamellae being dependent upon the deviation from the stoichiometric composition.

Manuscript received 20 February 1968. Professor R. E. Smallman, B.Sc., Ph.D., is in the Department of Physical Metallurgy and Science of Materials, University of Birmingham, where the work was carried out. A. W. Vere, B.Sc., Ph.D., is now at the Royal Radar Establishment, Malvern, Worcs.

Experimental Technique

The study of the structural transformation and its variation with oxygen content was made from transmission electron micrographs and associated selected-area diffraction patterns recorded on an A.E.I. EM6. Single-crystal specimens of $TiO_{1{\cdot}13}$ were used in the initial studies on the transformation from the high-temperature NaCl-type material to the low-temperature modification; the variation of the transformed structure as a function of composition was qualitatively examined by beam-heating the specimens in situ in the electron microscope to increase the oxygen content by absorption. The disadvantages in the use of the latter technique are that other gaseous impurities, e.g. carbon and nitrogen, are also absorbed. Since these elements are soluble in TiO and are accommodated on the interstitial sites of the titanium lattice in the same way as the oxygen atoms, they exert a similar effect upon the structure. However, since the final composition of the specimen is relatively unimportant in the study described here, the effect of beam-heating single-crystal TiO may be regarded simply as increasing the oxygen content of the material. A more serious deficiency of the technique is the inadequacy of the temperature control available. Attempts to improve this by the use of hot-stage microscopy were largely unsuccessful owing to the rapid formation of surface oxides.

More accurate measurements of the effects of variations in oxygen content were obtained from diffraction patterns taken from foils thinned from bulk specimens of polycrystalline TiO of the following oxygen contents: $TiO_{0{\cdot}7}$, $TiO_{1{\cdot}03}$, $TiO_{1{\cdot}13}$, and $TiO_{1{\cdot}19}$. Although optical micrographs revealed features resembling large-angle grain boundaries in these specimens, the X-ray and electron-diffraction patterns taken from sections cut perpendicular to the growth axis showed that this section was nevertheless a predominantly {110} face. These crystals were, in fact, prepared from {110} seeds using a modified zone-refining technique.

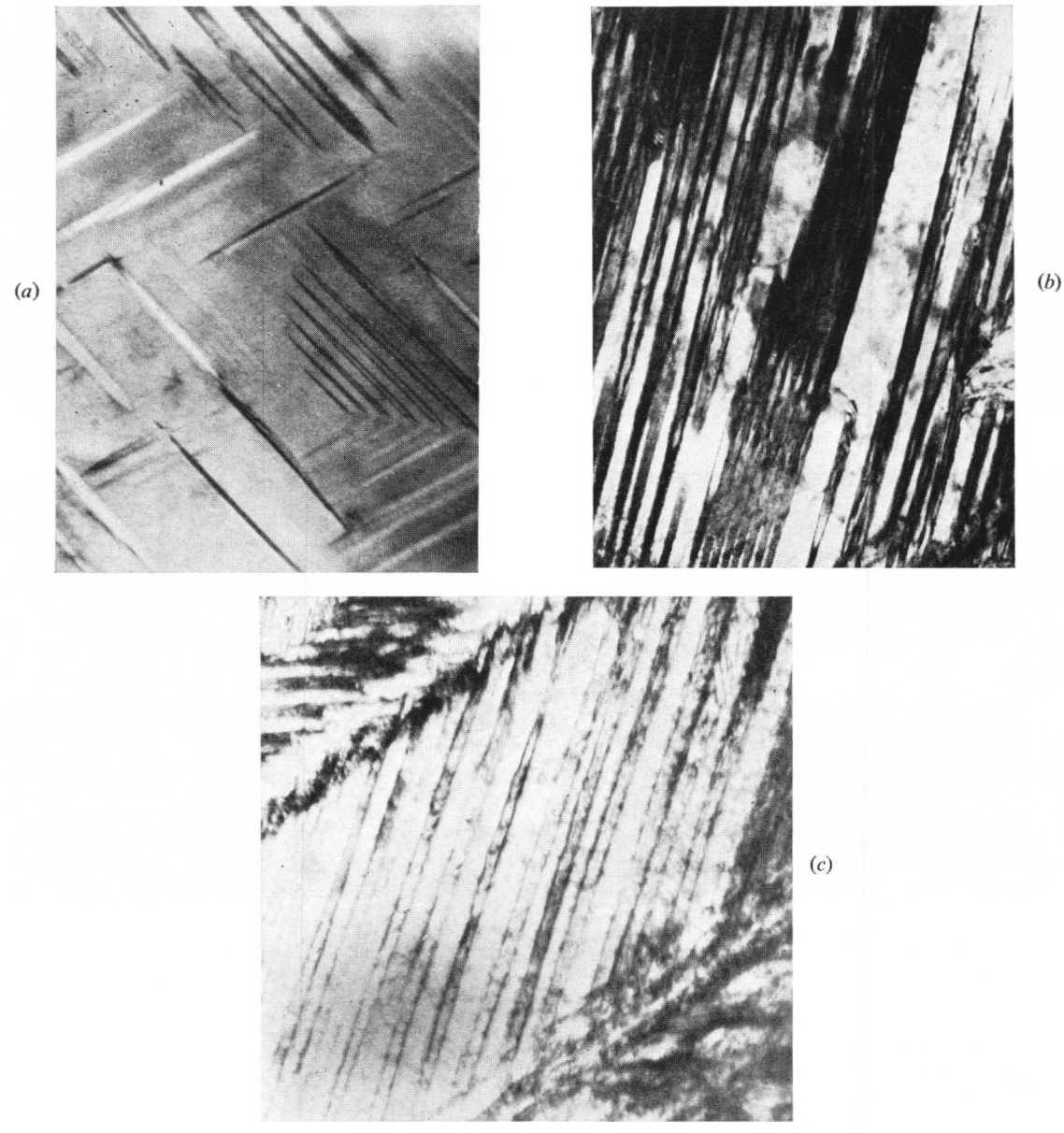

Fig. 1 Stages in the transformation from the high-temperature NaCl-type TiO phase to the low-temperature modification. (a) *Partially transformed.* × 32,000. (b) 100% *transformed.* × 48,000. (c) *Showing typical banded or domain structure containing one set of parallel lamellae.* × 36,000.

Thin foils were prepared for electron-microscopy observations from 0·5-mm slices cut in specified crystallographic orientations. These were first cut into discs 3·0 mm in dia. to fit the specimen holder of the microscope and were then chemically thinned in hot phosphoric acid. Final polishing was achieved either by electropolishing in a solution of 3 parts HNO_3, 1 part HF, and 1 part glacial acetic acid at 4 V and 40 mA, or by chemical polishing in a solution of 10% HF in concentrated nitric acid.

Since the measurements made involved the comparison of many diffraction patterns, the camera constant of the microscope was always evaluated and an internal silver standard was frequently employed. To avoid angular distortion of the diffraction pattern measurements were always made with the foil plane normal to the incident radiation.

Experimental Results

When single-crystal foils of $TiO_{1\cdot13}$ with {110} orientation are cooled through ~ 1000 degC, the high-temperature NaCl-type phase undergoes a transformation in which fine bands of a new structure are nucleated. Initially these are in the thin areas at the foil edge; they then move rapidly across the foil in ⟨111⟩ directions until they assume the appearance of a fine basket-weave structure, as shown in Fig. 1. The transformation ultimately divides the foil into domains such as that in Fig. 1(*c*), ~ 3μm wide, each domain containing one set of parallel fine lamellae ~ 200 Å in width.

The diffraction pattern taken from one domain of this structure is shown in Fig. 2(*b*). It is seen that the pattern contains all the reflections of the original NaCl-type material

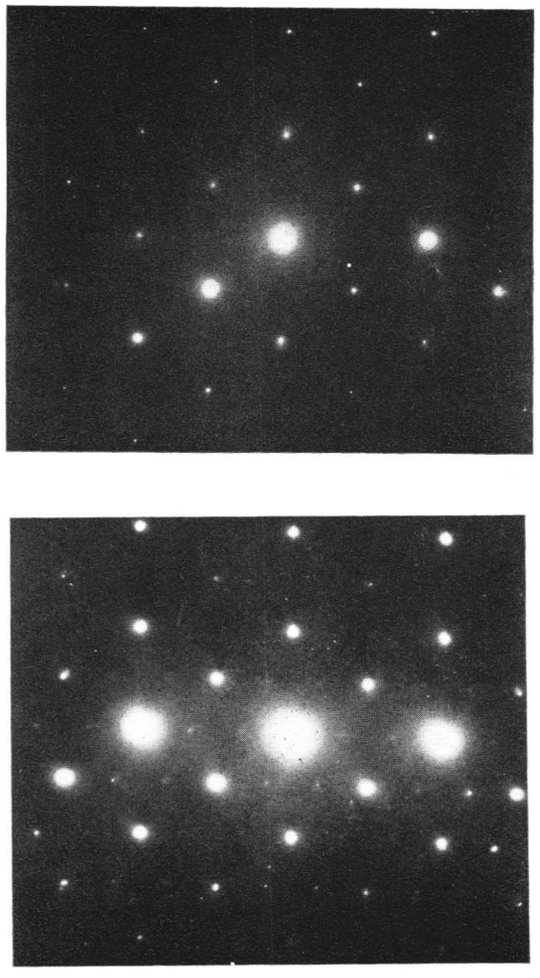

Fig. 2 Electron-diffraction patterns: (a) *from* a (110) *plane of NaCl-type TiO and* (b) *after transformation to the low-temperature modification.*

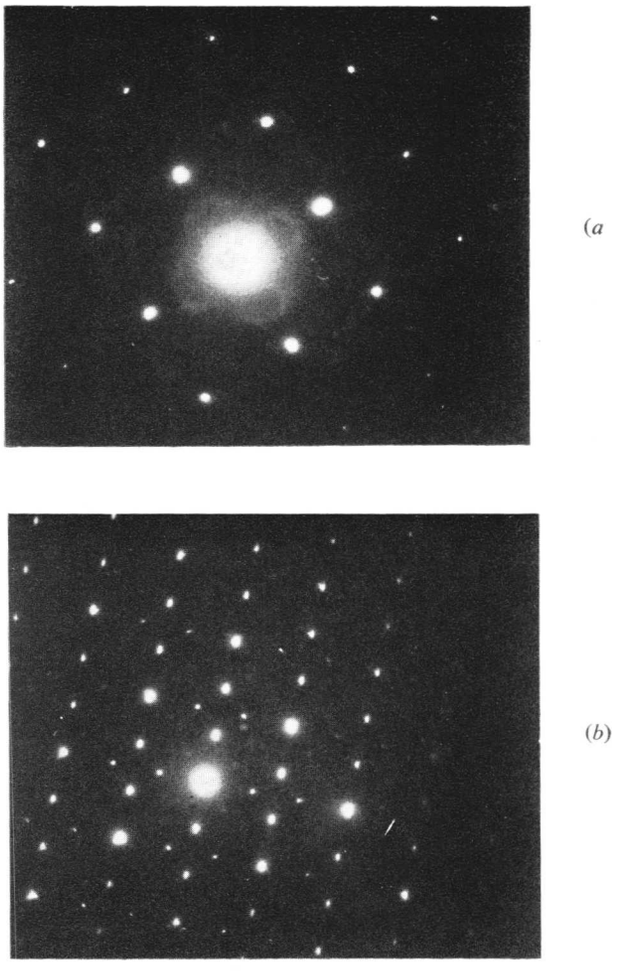

Fig. 3 Electron-diffraction patterns: (a) *from a* (100) *plane of NaCl-type TiO and* (b) *after transformation to the low-temperature modification.*

(Fig. 2(*a*)) but additional relpoints occur at one-third of the normal 220 spacing. The corresponding change in the {100} diffraction pattern is shown in Fig. 3. These patterns are identical to those obtained by Watanabe[5] in his study of $TiO_{0\cdot7}$. From exhaustive electron diffraction studies of the nature of the reciprocal lattice of the low-temperature modifications in the composition range $TiO_{0\cdot7}$–$TiO_{0\cdot9}$, these workers showed that the equilibrium structure of $TiO_{0\cdot7}$, below $\sim$ 1000° C, may be described as a NaCl-type structure in which the titanium vacancies are randomly distributed; the oxygen vacancies are ordered in such a way that all the oxygen sites on every third atomic plane parallel to the (110) plane of the original high-temperature NaCl-type structure are vacant. The proposed structure is shown in Fig. 4. Clearly this form of ordering gives rise to extremely high-energy boundaries through the juxtapositioning of adjacent $(110)_{NaCl}$ planes of titanium atoms, but this energy increase is thought to be compensated by the decrease in the free energy due to the formation of the perfect, ordered NaCl-type structure in the intermediate region. The structure may therefore be defined as ordered NaCl-type material divided on every third (110) plane by a high-energy barrier plane composed almost totally of oxygen vacancies.

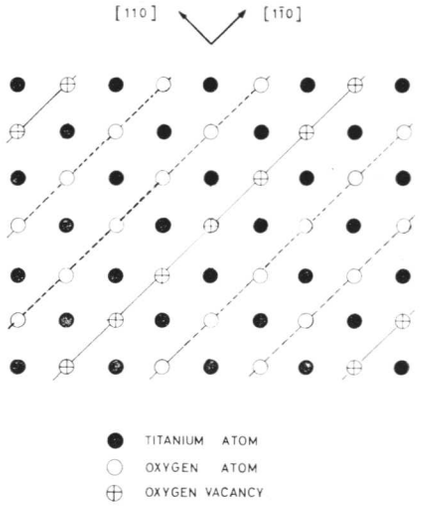

Fig. 4 Schematic structure of the low-temperature modification of $TiO_{0\cdot7}$

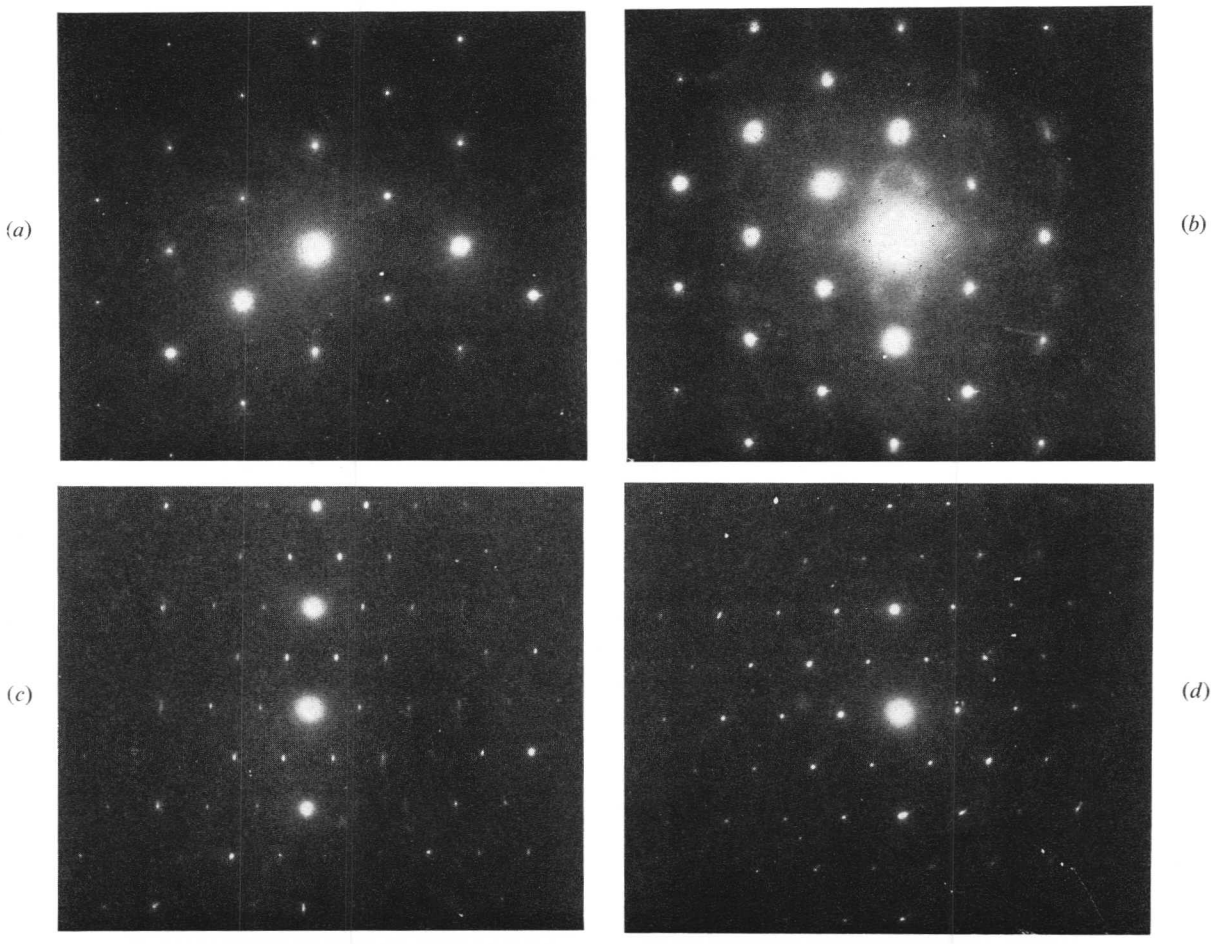

Fig. 5 Variation in (110) *diffraction pattern during beam-heating, after* (a) 0 *sec,* (b) 5 *sec,* (c) 15 *sec, and* (d) 25 *sec.*

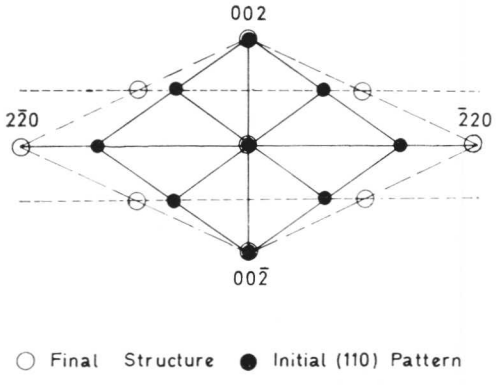

Fig. 6 Schematic diagram showing the change in diffraction pattern during annealing in the electron microscope.

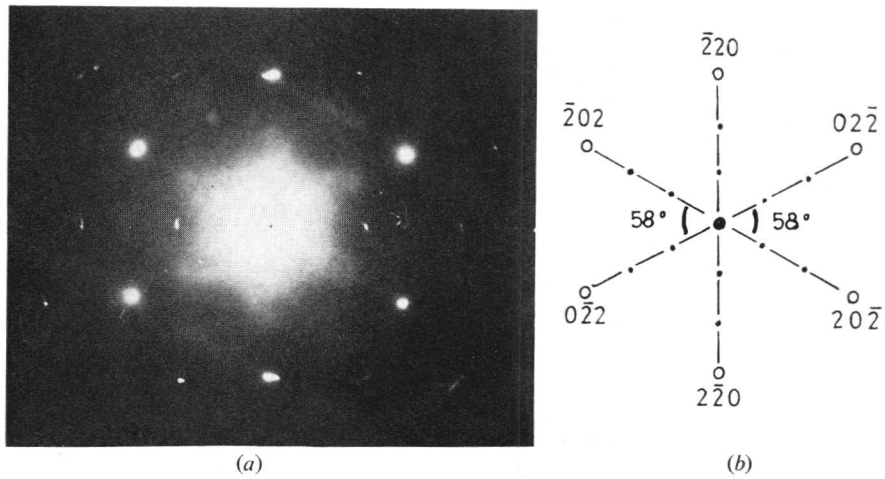

Fig. 7 (a) (111) *diffraction pattern showing streaking due to the formation of the low-temperature ordered structure;* (b) *schematic diagram showing the distortion of the original* (111) *NaCl-type section.*

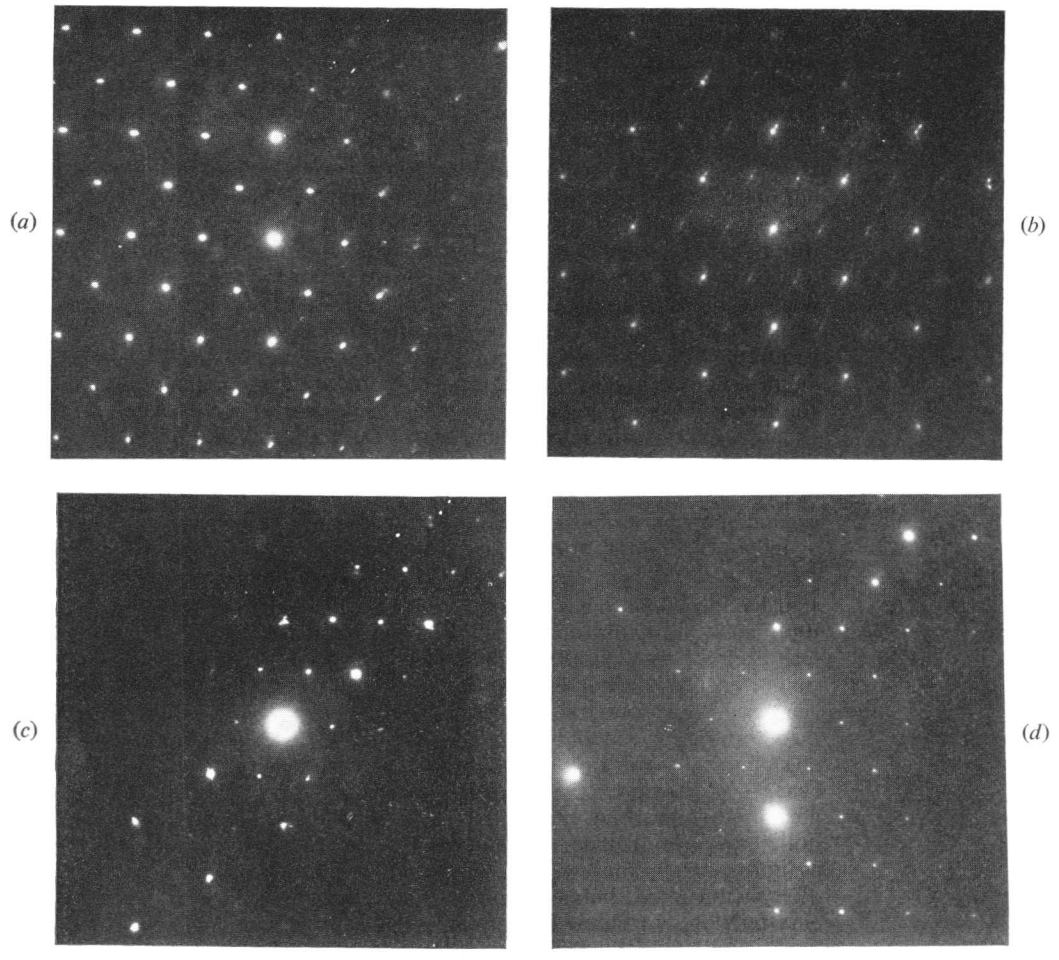

Fig. 8 (110) *diffraction patterns from specimens of various oxygen contents:* (a) $TiO_{0\cdot7}$, (b) $TiO_{1\cdot03}$, (c) $TiO_{1\cdot13}$, *and* (d) $TiO_{1\cdot19}$.

While this explanation may be valid for $TiO_{0\cdot7}$ in which almost all the titanium sites are occupied while approximately one-third of the oxygen sites are vacant, it cannot, without modification, explain the situation in $TiO_{1\cdot20}$ in which virtually all the oxygen sites are occupied while the titanium sublattice contains ~ 20% vacancies. Despite this reservation, diffraction patterns taken from foils with compositions throughout the phase range $TiO_{0\cdot7}$–$TiO_{1\cdot19}$ show the same basic characteristics in the diffraction patterns of the low-temperature modification. However, slight changes in the angular relationships were recorded between patterns taken from {110} foils of materials of differing oxygen content, and a gradual change in angular relationships was also noted during prolonged electron-beam heating of the low-temperature modification in foils of nominal composition $TiO_{1\cdot13}$. As indicated in the previous section this variation implies a structural change with changing oxygen content since strenuous efforts were made to avoid errors due to misalignment of the reflecting planes in relation to the incident beam; moreover the variation is of a systematic nature.

Fig. 5 and the schematic diagram of Fig. 6 illustrate the variation in the {110} diffraction pattern during prolonged electron-beam heating. Initially, as shown in Fig. 5, the pattern is that of the 110 reciprocal lattice plane of the quenched-in NaCl high-temperature modification. On heating the foil, diffuse superlattice reflections occur at one-third of the 220 spacing as shown in Fig. 5(*b*). On further heating (Figs. 5(*c*) and (*d*)) this spacing increases continuously while the 002 spacing remains constant. Despite these angular changes in diffraction, the micrographs of the low-temperature modification corresponding to Figs. 5(*c*) and (*d*) show no significant differences. The nature of this variation is shown more clearly in Fig. 6, in which the superlattice reflections have been omitted to show the effect on the basic {110} NaCl pattern. In contrast, the {100} diffraction pattern shows no variation in geometry after completion of the initial transformation, despite prolonged heating. In an effort to obtain a third section through the reciprocal lattice of the low-temperature structure, a {111} foil was prepared but this foil plane is considerably more difficult to polish and appears to be subject to extremely rapid oxidation, making transformation studies particularly difficult. Nevertheless, the diffraction pattern obtained after beam-heating for 20 sec (Fig. 7(*a*)) again shows traces of superlattice reflections occurring at one-third 220 spacing and a similar distortion of the reciprocal lattice section; the details are illustrated schematically in Fig. 7(*b*).

This variation in the {110} diffraction pattern with increase in oxygen content was also confirmed by patterns taken from specimens thinned from bulk samples of different compositions, which had previously been annealed for 24 h at 700° C and furnace-cooled to room temperature (Fig. 8). However, since these compositions range from $TiO_{0\cdot7}$ to

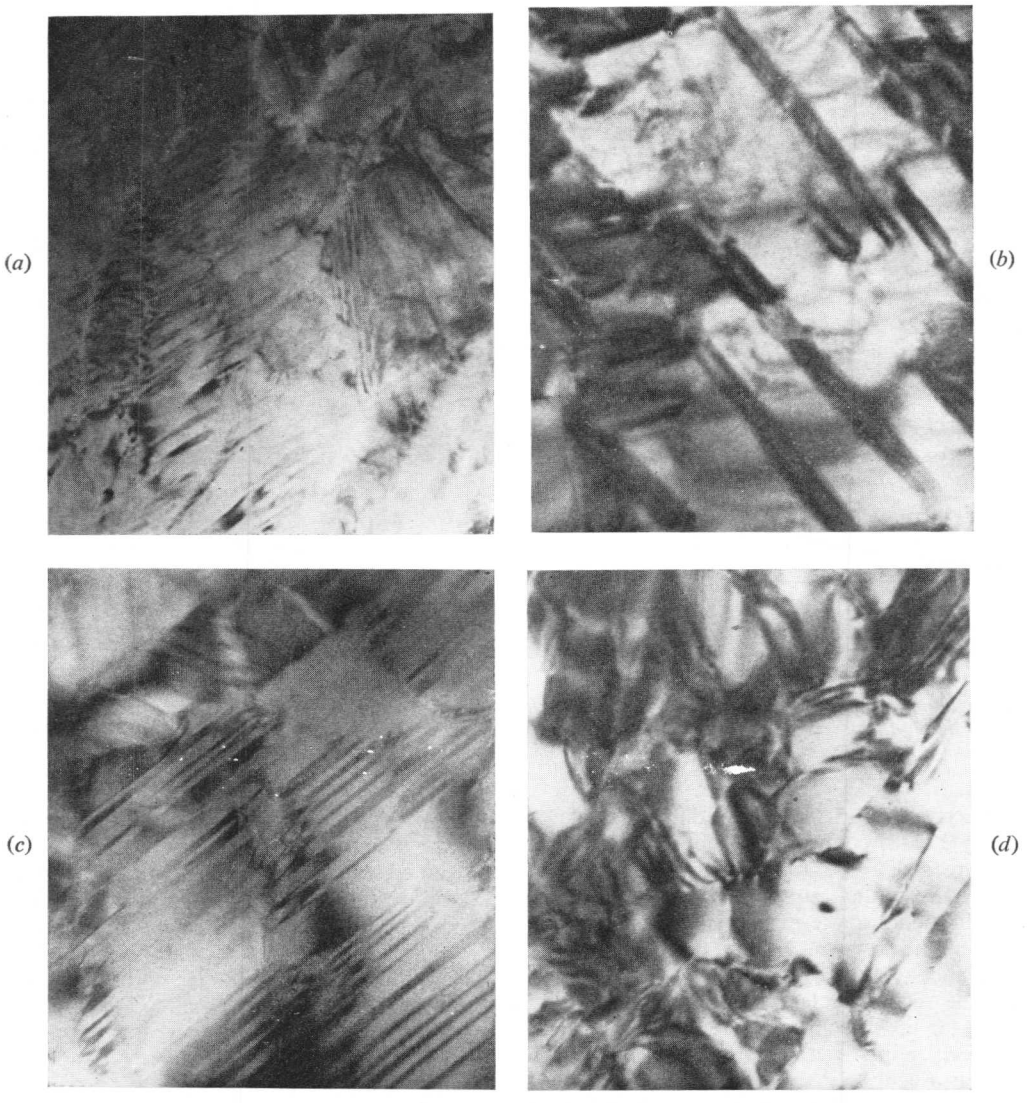

Fig. 9 Typical electron micrographs corresponding to (a) $TiO_{0\cdot7}$, (b) $TiO_{1\cdot03}$, (c) $TiO_{1\cdot13}$, *and* (d) $TiO_{1\cdot19}$. × 32,000.

$TiO_{1\cdot19}$, it is also possible to study the effect of hyperstoichiometric deviations in composition. From this it is observed that the distortion of the {110} NaCl-type pattern also increases with hyperstoichiometric deviation, so that the distortion is a minimum at the stoichiometric composition. The 002 spacing remains constant throughout.

The corresponding electron micrographs (Fig. 9) illustrate that the morphology of the low-temperature phase is of the same form irrespective of whether the transformation takes place before or subsequent to the preparation of thin foils. This eliminates the possibility that the highly faulted structure is a thin-foil artifact.

Although the morphology of the low-temperature modification is of the same form across the whole phase range, examination of the micrographs of Fig. 9 reveals that the incidence of faulting and the width of the fault lamellae varies considerably. Thus, the structure of $TiO_{0\cdot7}$ is one of small, heavily faulted domains or subgrains, whereas that of $TiO_{1\cdot03}$ exhibits a much larger subgrain size, each subgrain containing fewer, coarser lamellae. In the hyperstoichiometric material $TiO_{1\cdot13}$ the incidence of faulting again increases, but the lamellae are wider than in $TiO_{0\cdot7}$ (200 Å as opposed to 100 Å in $TiO_{0\cdot7}$) and the subgrain size remains large ($\sim$ 2 μm). The microstructure of the grossly hyperstoichiometric $TiO_{1\cdot19}$ is somewhat different to that observed previously, showing a reduction in subgrain size $\sim$ 0·75 μm) by comparison with $TiO_{1\cdot13}$ but an almost complete absence of internal faulting. Inspection of the subgrain structure, however, shows this to be delineated by short sections of straight boundary with sharply defined angles between the boundaries suggesting that the subgrains may be individual coarse faults. This structure also contains many regions of high internal stress. This variation in the low-temperature structure as a function of composition may therefore be summarized in terms of subgrain size and lamellar width. This variation in structure is of importance in controlling the mechanical behaviour of the TiO_x phase, and hence a comprehensive study of the mechanical properties of both the high- and low-temperature modification has been made and will be reported elsewhere.[6]

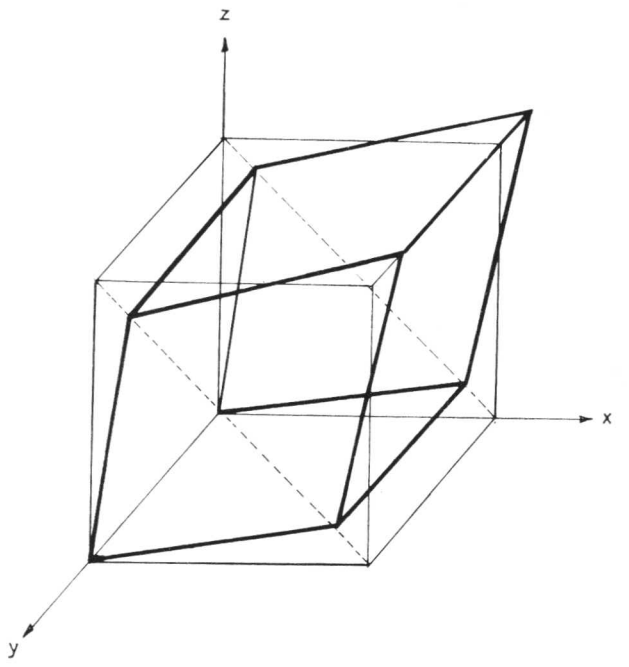

Fig. 10 Schematic diagram showing the transformation of the B_1-type unit cell to that of the ordered low-temperature structure.

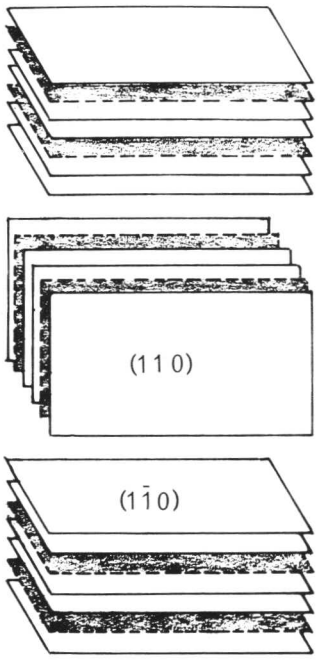

Fig. 11 Schematic diagram showing the stacking of {110} planes in adjacent lamellae of the low-temperature modification of TiO. Vacancy planes shaded.

Discussion

The electron micrographs of Fig. 1 and the associated diffraction patterns (Fig. 2) confirm earlier observations that the high-temperature NaCl-type TiO phase transforms to a highly complex heavily faulted structure on cooling below $\sim$ 1000° C. The diffraction patterns further indicate a close relationship between the low-temperature modification and the parent phase, and a study of the alteration of various sections through the reciprocal lattice with deviation from stoichiometry leads to the conclusion that the distortion of the original cubic cell results in a rhombohedral unit cell in the manner shown in Fig. 10.

Let us now examine possible explanations of the origin of the distortion. The most straightforward explanation of this variation in the structure arises directly from a consideration of Watanabe's model of the low-temperature modification of $TiO_{0.7}$.[5] Since this model invokes the concept of oxygen-vacancy planes parallel to (110) in the original NaCl-type lattice, it is expected that the [110] *d*-spacing, i.e. perpendicular to the vacancy planes, will differ from that in the [1$\bar{1}$0] direction. Moreover, as oxygen atoms are added to the structure, the oxygen-vacancy concentration on these high-energy vacancy planes decreases and the bond strength across these planes more nearly approximates to that in the direction parallel to the plane. Consequently the distortion of the 110 reciprocal lattice section, and hence of the {110} diffraction pattern, should decrease as the composition becomes more nearly stoichiometric, as is observed.

The results obtained in hyperstoichiometric material, indicating that the distortion again increases with increasing deviation from stoichiometry, may be explained on the assumption that the same mechanism operates but that in this case the increasing distortion is due to the increasing titanium-vacancy concentration on every third plane parallel to (110) in the original NaCl-type lattice.

A further interesting feature of the results is the indication that the maximum degree of lattice distortion is experienced in the composition $TiO_{0.7}$ rather than in $TiO_{1.19}$. This fact, together with the asymmetric location of the stoichiometric composition in relation to the position of the phase boundaries, suggests, as might be expected, that the distortion produced by the removal of a titanium atom from the lattice is much greater than that resulting from the removal of an oxygen atom. Thus the structure can only accommodate a comparatively low titanium-vacancy concentration and hence a moderate lattice distortion, before transformation to a completely new high-oxygen-content phase.

This distortion of the high-temperature NaCl-type lattice may also explain the occurrence of the characteristic lamellar structure of the low-temperature modification. Clearly a structural distortion of the type shown in Fig. 10 will produce a high internal strain in the [110] direction and the amount of strain produced is proportional to the vacancy concentration on every third (110) plane. It will therefore be greatest at the phase boundaries and least at the stoichiometric composition. Since the faulted structure of the low-temperature modification is composed of (110) lamellae it is postulated that it arises from the juxtapositioning of (110) and (1$\bar{1}$0) lamellae so that the [110] direction in each lamella is parallel to the [1$\bar{1}$0] direction in the adjacent lamella, giving rise to the structure illustrated schematically in Fig. 11. It can be seen from this model that the width of the lamellae will be determined by the amount of strain that can be accommodated without the necessity for massive reorientation, and hence will be dependent on the vacancy concentration of the high-energy planes. From such considerations the lamellar width should be a maximum at the stoichiometric composition and decrease with increasing deviation from this point. This is borne out by the observations on the variation of fault width and density as a function of compo-

sition, although no particularly satisfactory explanation can be advanced at the present time for the somewhat uncharacteristic morphology of $TiO_{1\cdot19}$.

This theoretical model for the accommodation of the high concentration of constitutional vacancies required to stabilize such wide composition variations is based on the formation of shear structures of the type proposed by Magnéli.[4] This type of transformation has been observed by Andersson in the compound Ti_5O_9,[7] and by Eikum and Smallman[8] during the reduction of rutile to compositions within the Ti_nO_{2n-1} series. The latter workers showed that the basic rutile structure is retained but contains a high density of stacking faults which produce additional relpoints on the diffraction patterns obtained. Eikum[9] further showed that the density of the faults could be related to the deviation from stoichiometry.

Summary and Conclusions

The experimental results obtained from a study of the structural transformation occurring at $\sim$ 1000° C are in accordance with the theory that the equilibrium concentration of constitutional vacancies present in a random array above this temperature is stabilized at lower temperatures by the clustering of vacancies on every third {110} NaCl-type plane. It has been shown that this increase in vacancy concentration on specific crystallographic planes produces a distortion of the parent lattice, the maximum distortion occurring in the ⟨110⟩ directions perpendicular to the vacancy plane. The internal stresses generated by the differences in bond strength across the vacancy planes by comparison with that across intermediate atomic planes are relieved by the formation of a shear structure in which the vacancy planes in adjacent lamellae are oriented at 90° to each other, so that the direction of expansion in one lamella corresponds to the direction of contraction in the adjacent lamella. The lattice distortion is proportional to the deviation from stoichiometry. The width of the lamellae is determined by the number of vacancy planes that can be accommodated before the internal stress reaches a point at which stress relief by reorientation occurs. Consequently the structure changes with stoichiometric deviation in such a way that the incidence and fineness of the fault structure increases as the phase boundaries are approached.

Acknowledgements

The authors would like to record their thanks to Professor G. V. Raynor, F.R.S., for provision of research facilities in the Department of Physical Metallurgy and Science of Materials, and one of them (A.W.V.) is grateful to U.K.A.E.A., Harwell, for financial support.

References

1. P. Ehrlich, *Z. Elektrochem.*, 1939, **45,** 362.
2. M. Hoch, *J. Phys. Soc. Japan*, 1963. [II], **18,** 147.
3. J. S. Anderson and A. D. Wadsley, "Non-Stoichiometric Compounds" (Adv. in Chem. Series No. 39), **1963:** Washington, D.C. (Amer. Chem. Soc.).
4. A. Magnéli, *Acta Cryst.*, 1953, **6,** 495.
5. D. Watanabe, "Proceedings of International Conference on Electron Diffraction and Lattice Defects". **1965:** Melbourne (Australian Acad. Science).
6. A. W. Vere and R. E. Smallman, to be published.
7. S. Andersson, *Acta Chem. Scand.*, 1960, **14,** 1161.
8. A. K. Eikum and R. E. Smallman, *Phil. Mag.*, 1965, **11,** 627.
9. A. K. Eikum, "Faulted Structures in Non-Stoichiometric Rutile". Unpublished Ph.D. Thesis, Univ. Birmingham, 1965.

Research Note

The Ordered Structure of $TiO_{1\cdot25}$

D. Watanabe, O. Terasaki, A. Jostsons, and J. R. Castles

The phase TiO, which has a NaCl-type structure, is known to exist over a wide range of composition depending on temperature, e.g. from $TiO_{0\cdot7}$ to $TiO_{1\cdot25}$ at 1400° C and $TiO_{0\cdot9}$ to $TiO_{1\cdot25}$ at temperatures below ~ 990° C,[1,2] and its crystal structure has varying proportions of both titanium and oxygen vacancies.[3–5] The structure of the low-temperature form of TiO, which is stable in the composition range $TiO_{0\cdot9}$–$TiO_{1\cdot1}$ below 990° C, is similar to that of NaCl but has an ordered array of vacant lattice sites.[6] Evidence of another ordered structure has been detected[6] in oxygen-rich alloys where there is an excess of titanium vacancies relative to oxygen vacancies.

This paper reports the results of a structure analysis of the ordered form of $TiO_{1\cdot25}$ based on observations made by electron microscopy and diffraction and X-ray powder techniques. Alloys were prepared from iodide titanium and high-purity TiO_2 in an atmosphere of purified argon in a tungsten-arc furnace. Cast alloys were homogenized at 1400° C for 50 h before heat-treatment. Thin foils suitable for electron microscopy were obtained by chemical polishing.[6] The interplanar spacings were determined from Debye–Scherrer photographs taken with CuK_α radiation.

Electron-diffraction patterns from specimens of 55·5 at.-% O ($TiO_{1\cdot25}$) quenched from temperatures above 1000° C contained a distribution of diffuse scattering, indicative of the existence of some short-range order of vacancies, in addition to the fundamental reflections of the NaCl-type structure (Fig. 1). Superlattice reflections were observed, however, on electron-diffraction patterns (Fig. 2), as well as X-ray powder patterns from specimens annealed for long periods below 800° C.

The lattice parameter of the high-temperature disordered form of the 55·5 at.-% O alloy was found to be 4·1681 ± 0·0005Å, but after ordering the lattice parameter of the fundamental unit cell was $a_0 = 4\cdot1707 \pm 0\cdot0005$Å. Thus, ordering in $TiO_{1\cdot25}$ is not accompanied by lattice distortions that cause changes in symmetry of the parent cubic cell as is the case in TiO.[6]

Analysis of the diffraction patterns shows that the unit cell of the ordered $TiO_{1\cdot25}$ structure is tetragonal and 2·5 times as large as the fundamental cell, the lattice parameters being $a = a_0\sqrt{10}/2 = 6\cdot594$Å, $c = a_0 = 4\cdot171$Å. A comparison of the calculated and observed interplanar spacings is shown in Table I. Systematic absences of reflections hkl when $h + k + l$ is odd suggest that the space group is I4/m. Although the unit cell contains 10 oxygen and 10 titanium sites, the observed electron- and X-ray-diffraction patterns can be explained by assuming that two titanium atoms are missing from the tetragonal cell. This assumption is consistent with the fact that ordered $TiO_{1\cdot25}$ has ~ 22% of its titanium sites vacant, as estimated from a comparison of the density calculated from the lattice parameters of the tetragonal cell and the observed pycnometric density.[4,5] The positions of atoms in the proposed structure (Fig. 3) are as follows:

TABLE I

Observed and Calculated Values of Interplanar Spacings in $TiO_{1\cdot25}$

hkl_{cubic}	$hkl_{\text{tetrag.}}$	$d_{\text{calc.}}$, Å	$d_{\text{obs.}}$, Å
	110	4·662	4·670
	101	3·525	3·520
	200	3·297	3·312
111	211	2·408	2·405
	220	2·331	—
200	310, 002	2·085	2·085
	301	1·983	—
	112	1·903	—
	202	1·762	—
	321	1·675	1·677
	400	1·649	—
	330, 222	1·554	—
	411	1·493	—
220	420, 312	1·474	1·474
	103	1·360	—
	510, 402	1·293	—
311	501, 213, 431	1·257	1·257
	332	1·246	—
222	422	1·204	1·203
400	004, 620	1·043	1·042
331	503, 433, 631	0·9568	0·9561
420	314, 622, 710, 550	0·9328	0·9324
422	424, 712, 552	0·8511	0·8511

8 O in 8(h): $(0, 0, 0; \frac{1}{2}, \frac{1}{2}, \frac{1}{2}) + x, y, 0; \bar{x}, \bar{y}, 0; \bar{y}, x, 0; y, \bar{x}, 0$

$$\text{with } x = \frac{3}{10},\ y = \frac{1}{10}$$

$$8\text{ Ti in 8(h): with } x = \frac{6}{10},\ y = \frac{2}{10}$$

2 O in 2(b); $0, 0, \frac{1}{2}; \frac{1}{2}, \frac{1}{2}, 0.$

Superlattice reflections of both $TiO_{1\cdot25}$ and the TiO ordered structures were observed in X-ray powder and electron-diffraction patterns (Fig. 4) of specimens of TiO_x ($1\cdot1 < x < 1\cdot25$) annealed for long periods below 700° C. It is interesting to note that when both ordered structures are present the superlattice reflections are markedly elongated along $\langle 210\rangle_c$* directions. This observation suggests that the ordered phases coexist as alternate thin layers of TiO and $TiO_{1\cdot25}$ parallel to $\{210\}_c$ planes. Even specimens of

Manuscript received 3 July 1968. Professor D. Watanabe, D.Sc., and O. Terasaki, M.Sc. are in the Department of Physics, Tohoku University, Sendai, Japan. A. Jostsons, Ph.D., is now in the Materials Division, A.A.E.C. Research Establishment, Sutherland, N.S.W., Australia; J. R. Castles, M.Sc., is at the School of Physics, University of Melbourne, Parkville, Victoria, Australia.

* The subscript c is used to designate Miller indices referred to the cubic axes of the NaCl-type structure.

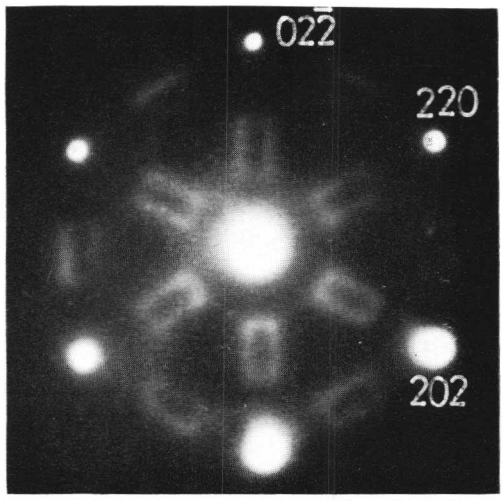

Fig. 1 Electron-diffraction pattern of Ti–55·5 at.-% O alloy quenched from 1000° C.

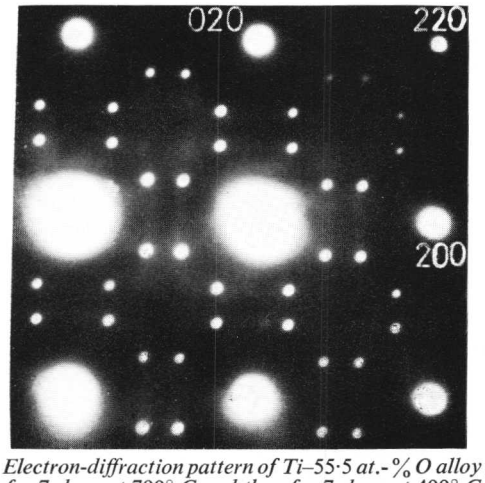

Fig. 2 Electron-diffraction pattern of Ti–55·5 at.-% O alloy annealed for 7 days at 700° C and then for 7 days at 400° C.

55·5 at.-% O occasionally contained regions of TiO structure as deduced from electron-diffraction patterns. The amount of TiO was not sufficient, however, to enable us to detect it in X-ray powder patterns. It is concluded that the $TiO_{1·25}$ structure is stable over a very narrow range of composition near 55·5 at.-% O and that it coexists with the ordered TiO phase in alloys of composition TiO_x ($1·1 < x < 1·25$).

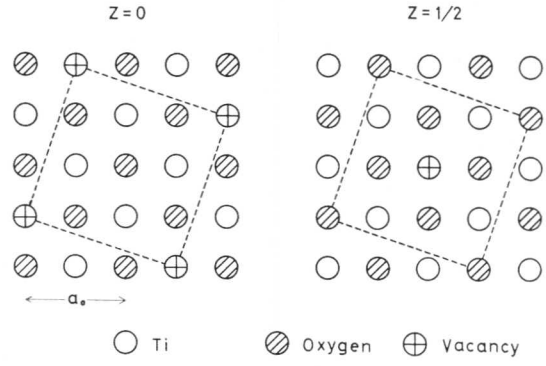

Fig. 3 Structure of ordered $TiO_{1·25}$.

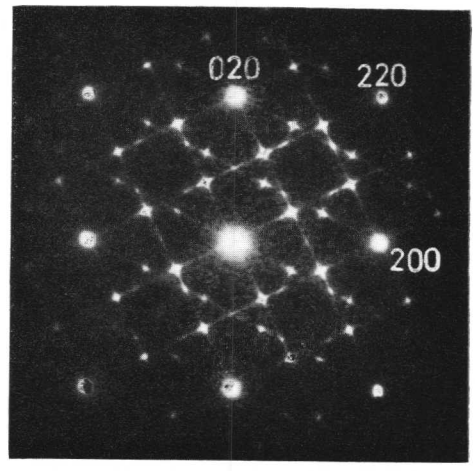

Fig. 4 Electron-diffraction pattern of Ti–54·3 at.-% O alloy annealed for 300 h at 600° C.

References

1. M. Hansen and K. Anderko, " Constitution of Binary Alloys ". **1958:** New York and London (McGraw-Hill).
2. A. Jostsons and P. McDougall, paper presented at International Conference on Titanium (London, 1968).
3. P. Ehrlich, *Z. anorg. Chem.*, 1941, **247**, 53.
4. S. Andersson, B. Collen, U. Kuylenstierna, and A. Magnéli, *Acta Chem. Scand.*, 1957, **11**, 1641.
5. S. P. Denker, *J. Physics Chem. Solids*, 1964, **25**, 1397.
6. D. Watanabe, J. R. Castles, A. Jostsons, and A. S. Malin, *Acta Cryst.*, 1967, **23**, 307.

Research Note

Some Interstitial Order–Disorder Transformations

K. H. Jack

Whenever the number of non-metal atoms in an interstitial alloy is less than the number of available interstices there is the possibility of order or disorder. The tendency for interstitial atoms to avoid one another might be expected to increase with their increasing concentration and to be particularly marked at simple atom ratios when a definite fraction of the number of interstices is filled. Since a non-metal atom always expands the interstice that it occupies, minimization of lattice strain is another factor in promoting order, and so also is the difference in electronegativity

Manuscript received 3 July 1968. Professor K. H. Jack, M.Sc., Ph.D., is in the Department of Metallurgy, University of Newcastle upon Tyne.

between metal and non-metal atoms. Strain minimization is undoubtedly the reason for the fully ordered nitrogen-atom arrangement in the tempered nitrogen–martensite α'' phase;[1] and if nitrogen atoms each carry a small positive charge their weak repulsive interaction is a plausible explanation[2] for order in the f.c.c. γ' phase Fe_4N and for the absence of order at lower interstitial-atom concentrations in nitrogen–austenite.[3] Such factors are insufficient to explain a variety of interstitial-atom ordering transformations of which the following are only two examples.

The close-packed hexagonal ε phase of the iron–nitrogen system has a range of homogeneity extending at low temperatures (400–500° C) from about Fe_3N almost to Fe_2N. Throughout the range, the nitrogen atoms are completely ordered[4] and at Fe_2N one-half of the octahedral holes are filled. However, almost exactly at this composition there is an abrupt redistribution of the nitrogen atoms—a change from one ordered arrangement to a completely different but equally ordered arrangement.

In a h.c.p. metal-atom lattice of dimensions a and c, where $c/a \simeq 1{\cdot}63$, the octahedral holes themselves form a simple hexagonal lattice with dimensions

$$a' = a,\ c' = c/2,\ c'/a' \simeq 0{\cdot}82$$

Thus, layers of holes lie directly above and below each other and the shortest distance between holes ($0{\cdot}82a$) is in the c' direction. Throughout the ε-phase concentration range the interstitial atoms achieve maximum separation and the nearest holes above and below each nitrogen atom always remain unoccupied. For ε-Fe_2N, one-third of the holes are filled in odd planes and two thirds are filled in even planes, so that the sequence is $\frac{1}{3}\ \frac{2}{3}\ \frac{1}{3}\ \frac{2}{3}\ \ldots$

The nitrogen-atom rearrangement giving ζ-Fe_2N is such that successive layers of holes each become one-half filled, $\frac{1}{2}\ \frac{1}{2}\ \frac{1}{2}\ \frac{1}{2}\ \ldots$ In each layer the nitrogen atoms are distributed in zig-zag chains parallel with the orthohexagonal b direction. The iron atoms retain their same relative positions but are pushed apart more in this b direction. Thus, there is an anisotropic distortion of the lattice that lowers the symmetry from hexagonal to orthorhombic. The formation of the new ζ phase is a direct consequence of the interstitial-atom rearrangement.

In the cobalt–nitrogen system there is a similar transition.[5] Gamma-cobalt nitrides (the difference in nomenclature is unfortunate) are isostructural with ε-iron nitrides and at the Co_2N composition there is again a redistribution of nitrogen atoms accompanied by an anisotropic distortion of the cobalt lattice. This time, however, the expansion is in the a direction of the orthohexagonal cell, because the nitrogen atoms of the new phase, δ, pack most closely in this a direction.

It is surprising that ζ-Fe_2N and δ-Co_2N have not the same structures, since they arise by small distortions of structures that *are* identical. The respective interstitial-atom rearrangements are therefore characteristic of specific metal–non-metal atom interactions. Directive valency forces, suggesting some covalent character, exist at the composition M_2X but are not evident at lower nitrogen concentrations.

On nitriding, a 50 : 50 iron : cobalt alloy gives a close-packed hexagonal phase isostructural both with ε-iron nitride and γ-cobalt nitride. Again there is a structural discontinuity at the expected composition FeCoN. This time there is no lowering of symmetry, but the superlattice X-ray reflections due to nitrogen-atom ordering disappear

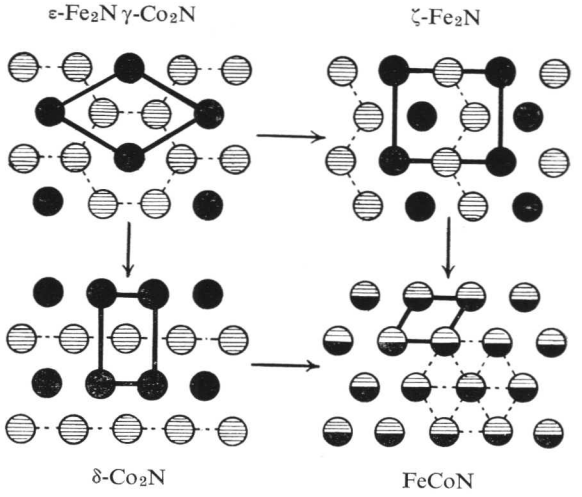

Fig. 1 Nitrogen-atom rearrangements at the composition M_2X in iron, cobalt, and iron–cobalt interstitial nitrides.

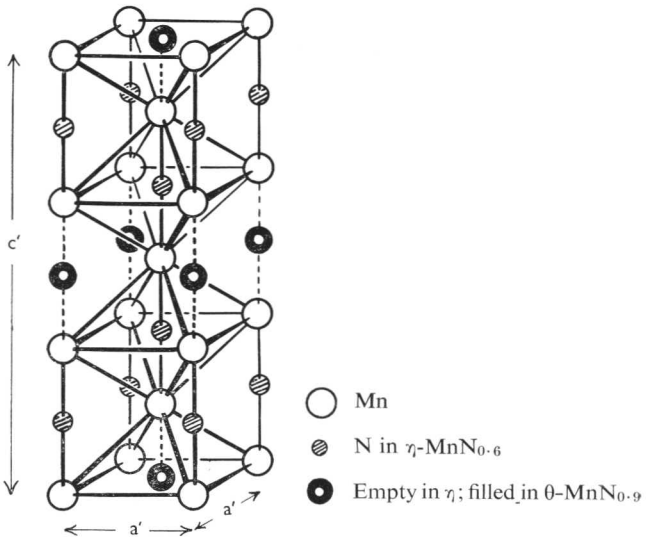

Fig. 2 The crystal structures of η-$MnN_{0{\cdot}6}$ and θ-$MnN_{0{\cdot}9}$.

completely. The two opposing directive effects, that between iron and nitrogen and that between cobalt and nitrogen, appear to cancel each other and the change is from interstitial order to disorder. These changes are shown in Fig. 1.

Ordering in manganese nitrides is equally remarkable. According to previous workers it is uncertain whether the highest manganese nitride has a composition near Mn_3N_2 or near MnN. In any case, the metal-atom arrangement is face-centred tetragonal with axial ratios somewhat less than unity; the unit cell can be described equally well as body-centred tetragonal with $c/a < 1{\cdot}414$. Two body-centred tetragonal phases, θ and η, separated by a miscibility gap and with respective axial ratios of ~ 1·39 and 1·36, are claimed in the most recent work.[6] It is now shown[7] that θ approximates to a sodium-chloride structure where the octahedral holes of a f.c.c. Mn-atom packing are completely filled, whereas in η only two-thirds are filled in an ordered manner. Moreover, in forming θ from η the additional nitrogen atoms are much less strongly bonded than those originally present.

When nitrided in ammonia at 500° C, manganese shows a weight increase corresponding to the formation of $MnN_{0\cdot9}$ (θ) but only two-thirds of this nitrogen is detected by chemical analysis. By thermal decomposition in vacuum at 500° C the " non-chemical " nitrogen is evolved as molecules to give η-$MnN_{0\cdot6}$ with the chemically determined nitrogen remaining unchanged.

The η phase shows a superlattice with dimensions

$$a' = a \text{ and } c' = 3c$$

where a and c are the dimensions of the body-centred tetragonal cell. Complete structure refinement shows that the nitrogen atoms, and hence the vacant interstices, are fully ordered (see Fig. 2).

In θ-$MnN'_{0\cdot6}N''_{0\cdot3}$ the interstitial atoms exist in two distinct chemical states, N′ and N″. Nitrogen atoms of each type, N′ or N″, occupy a different superlattice and must be bonded to manganese by valency forces with different directional characteristics.

References

1. K. H. Jack, *Proc. Roy. Soc.*, 1951, [A], **208,** 216.
2. K. H. Jack, *ibid.*, 1948, [A], **195,** 34.
3. K. H. Jack, *ibid.*, 1951, [A], **208,** 200.
4. K. H. Jack, *Acta Cryst.*, 1952, **5,** 404.
5. J. Clarke and K. H. Jack, *Chemistry and Industry*, **1951,** 1004.
6. F. Lihl, P. Ettmayer, and A. Kutzelnigg, *Z. Metallkunde,* 1962, **53,** 715.
7. M. A. Beever, P. Grieveson, and K. H. Jack, to be published.

Research Note

The Order–Disorder Transformation in Fe_3Al Alloys

M. R. Lesoille and P. M. Gielen

The order–disorder transition in Fe_3Al has been extensively studied by Taylor[1] using conventional X-ray techniques. The problem is not simple but might be of great technological importance in connection with Alnico alloys.[2]

Recently several authors[3–8] have investigated Fe_3Al by means of the Mössbauer effect. By making measurements at 550°C, Cser[8] found a ferromagnetic and a paramagnetic contribution on his spectra which should correspond to the existence of two phases, though he gave a different interpretation. To elucidate the problem, we have started a Mössbauer investigation on Fe–Al alloys ranging from 20 to 28 at.-% Al. In this note we shall report only the general results obtained.

All the spectra were taken with a commercial Elron Mössbauer spectrometer* of a constant-acceleration type, and a source of ^{57}Co diffused into copper. The alloys were prepared by melting Armco iron and 99·99% pure aluminium in an induction furnace under an argon atmosphere. Thin foils having the desired thickness of 0·001 in. were obtained by cold rolling the alloys in the disordered state. Compositions of the alloys were determined by chemical analysis.

In the disordered alloys, obtained by water-quenching from 1000°C, the spectra were very complex, showing broad and unresolved peaks. These spectra were computer analysed and the centre of gravity of the peaks could then be determined with great accuracy. A very slight mean electric quadrupole interaction was obtained and has been found to be proportional to the aluminium content of the alloys. This quadrupole interaction is probably due to the presence of some directional order in the disordered alloys, following the ideas of Néel.[9] As far as we know, this effect had never been shown before by Mössbauer spectroscopy.

In the ordered alloys, the spectra were remarkably clear, allowing an easy resolution of Fe atoms with, respectively, 4, 5, and 8 Fe nearest neighbours. In the composition range near 25 at.-% Al, two ordered phases were definitely observed, both of which were ferromagnetic, ferrimagnetic, or antiferromagnetic. One of the phases was found by X-ray diffraction to be the well known ferromagnetic DO_3-type Fe_3Al phase. In this ordered structure each Al atom is surrounded by 8 Fe nearest-neighbour atoms and 6 Fe next-nearest-neighbour atoms, the Al atoms being admitted only in the third co-ordination shell. This phase shows no electric quadrupole interaction because of the cubic symmetry of the immediate surroundings of the Fe atoms and the special relationship between the easy axis of magnetization and the principal axis of the electric-field gradient tensor. The other phase seems to be unknown and we shall call it $Fe_3Al(C)$ for reasons that will appear in the next paragraph. It shows an effective magnetic field of ~265 kgauss and a strong electric quadrupole interaction; it was present up to 50% in the alloys that were closest to the stoichiometric composition of 25 at.-% Al.

Following a suggestion of Taylor,[1] it was supposed that the unknown phase was isomorphous with the ternary Fe_3AlC compound which has been studied by Morral.[10] This compound has the Cu_3Au structure with carbon atoms occupying all the octahedral voids and hence each aluminium atom has 12 Fe nearest-neighbours and 6 Al next-nearest neighbours, thus admitting Al atoms in the second co-ordination shell. We prepared an Fe_3AlC compound from the same materials as already mentioned plus spectroscopically pure graphite. Chemical analysis revealed that it was not stoichiometric (24% Al and only 2% carbon). The compound was used in the form of a very fine powder for both Mössbauer spectroscopy and X-ray diffraction.

Fe_3AlC could be effectively indentified by X-ray diffraction from the ASTM cards. The Mössbauer spectrum revealed that the powder was probably superparamagnetic. A paramagnetic doublet appeared very clearly showing a strong electric quad-

* Elron, Electronic Industries, Haifa, Israel.

Manuscript received 3 July 1968. M. R. Lesoille and P. M. Gielen, Chargé de Cours Associé, are at the Université Catholique de Louvain, Laboratoire de Métallurgie Physique, Heverlee, Belgium.

rupole interaction $\frac{e^2qQ}{2} = 1{\cdot}30$ mm/sec. Such an interaction is exactly the same as in the unknown phase $Fe_3Al(C)$, if we suppose the easy axis of magnetization to be [110] in this phase. The quadrupole interaction is certainly due to the fact that in the Cu_3Au type of structure, each Fe atom has nearest neighbours consisting of 4 Al atoms situated in the same plane (001), plus 8 Fe atoms not situated in this plane, so that there is a non-cubic symmetry for the immediate surroundings of the atom. If we suppose that Al is positively ionized in the alloy, the planar environment of Al atoms gives a strong negative electric field gradient tensor q_{lat} at the position of Fe, and by the same token a strong electric quadrupole interaction.

However, X-ray diffraction pictures of $Fe_3Al(C)$ could not be identified with those of Fe_3AlC, in disagreement with Taylor's finding.[1] The majority of beams on the diffraction pattern could be accounted for only by using a giant tetragonal unit cell with lattice parameters $a = 16{\cdot}37$ Å and $c = 7{\cdot}15$ Å. Nevertheless, our Mössbauer results suggest that the structure of $Fe_3Al(C)$ should be quite similar to that of Fe_3AlC; only there is probably some kind of contraction of the lattice due to the absence of carbon. On the other hand a careful interpretative analysis of the lattice parameters determined by X-ray diffraction suggests there should be some kind of epitaxial relationship between Fe_3Al and $Fe_3Al(C)$, the habit plane being (001).

Our measurements of strong quadrupole interactions in Fe–Al alloys show that Al is probably highly ionized when alloyed with Fe. It is likely that Al is present as an Al^{3+} ion and the presence of such great ionization gives a better understanding as to why highly involved order – disorder transitions occur in Fe–Al alloys. To minimize the Coulomb interaction energy with other Al ions, each Al atom prefers to be surrounded exclusively by Fe atoms; in the DO_3 structure Al appears only in the third co-ordination shell, while in the Cu_3Au structure it is present in the second co-ordination shell but 12 Fe atoms are in the first shell.

Hume-Rothery has already suggested that order–disorder transformations occur when electronegativity differences appear between the different kinds of atoms present in the alloy. Maybe this is not the only reason to be invoked for the appearance of order; atomic sizes should also be taken into account. However, this certainly gives the main driving force for ordering reactions and our measurements of electric quadrupole interactions give support to Hume-Rothery's suggestions. It would be interesting to look for other order–disorder transitions in Fe-base alloys; Fe_3Si for example, like Fe_3Al, also has the complex DO_3-type structure. It is stable at even higher temperatures than Fe_3Al, probably because Si is still more highly ionized (we suspect it might be Si^{4+}). On the other hand, order transitions in Fe–Co and Fe–Ni alloys show less-complex ordered structures, probably because electro-negativity differences between the different elements are not so great.

Acknowledgement

This work has been supported in part by the Fonds National de la Recherche Scientifique (FNRS), Belgium.

References

1. A. Taylor and R. M. Jones, *J. Physics Chem. Solids*, 1958, **6**, 16.
2. L. M. Magat *et al.*, *Physics Metals Metallography*, 1966, **22**, 101.
3. P. A. Flinn and S. L. Ruby, *Phys. Rev.*, 1961, **124**, 34.
4. K. Ono, Y. Ishikawa, and A. Ito, *J. Phys. Soc. Japan*, 1962, **17**, 1747.
5. E. A. Friedman and W. J. Nicholson, *J. Appl. Physics*, 1963, **34**, 1048.
6. M. B. Stearns, *ibid.*, 1964, **35**, 1095.
7. G. P. Huffman and R. M. Fischer, *ibid.*, 1967, **38**, 735.
8. L. Cser, J. Ostanevich, and L. Pal, *Physica Status Solidi*, 1967, **20**, 581, 591.
9. L. Néel, *J. Phys. Radium*, 1954, **15**, 225.
10. F. R. Morral, *J. Iron Steel Inst.*, 1934, **130**, 419.

Research Note

The Mechanism of Formation of the $L1_0$ Superlattice

H. N. Southworth and B. Ralph

The results of a parallel X-ray and field-ion microscope investigation into the development of order in PtCo suggest that the mechanism of ordering is considerably more complex than has previously been believed.[1] A question debated at one time was whether the thermodynamic order of the reaction was of the first or the second kind.[2] The conclusion was reached that, providing equilibrium was maintained, the transformation was of the first order, and thus probably one of the nucleation and growth of ordered particles at the expense of the disordered matrix.[2,3] The alternative mode would be one of continuous increase in the degree of order by a homogeneous process and within a single phase. However, the above condition as regards equilibrium fails to be satisfied in most practical cases, and it is suggested here that homogeneous ordering plays a major role in the mechanism of the reaction.

Superlattice formation in PtCo takes place with a change in lattice symmetry from a disordered f.c.c. lattice to an ordered f.c.t. structure of the $L1_0$ type. Previous optical metallography and X-ray studies reveal two principal modes of ordering.[4] Below 815° C and above ~ 600° C the change in X-ray diffraction lines during ordering is described as " continuous ". The fundamental cubic lines gradually broaden into bands that are later resolved into the tetragonal lines corresponding to the ordered structure. At temperatures below 600° C the X-ray sequence is described as " discontinuous ". The tetragonal lines appear beside, although distinct from, the cubic lines and grow in intensity at the expense of the latter. Both sequences have been interpreted as resulting from the nucleation and growth of ordered particles within the disordered matrix. The line broadening above 600° C was attributed to strain arising from coherency

Manuscript received 3 July 1968. H. N. Southworth, M.A., Ph.D., and B. Ralph, M.A., Ph.D., are in the Department of Metallurgy, University of Cambridge.

maintained between the particles and matrix. Microtwinning of the ordered particles was believed to occur at a later stage, whereupon the coherency was lost and the strain was relieved. The existence of this twinning was deduced from optical micrographs showing extensive striations developing in the microstructure. At temperatures below 600° C the absence of line broadening was attributed to the early relief of coherency strain by a recrystallization reaction. The microstructure showed ordered regions growing with an irregular interface.

The present study has been primarily concerned with ordering at 500 and 660° C. At 500° C the sequence of X-ray lines is discontinuous, in agreement with the previous work. However, it is clear that the tetragonal lines do *not* appear initially in their final positions, as was previously reported.[4] This indicates that the " ordered " regions on their initial appearance are not fully ordered, i.e. do not possess their maximum possible degree of tetragonality. As the lines move to their final positions they become sharper, as do the superlattice lines. The slight initial line broadening could be due to one or more of three causes: (i) small size of the ordered particles; (ii) strain (e.g. coherency strain); (iii) a range in the degree of order within the ordered regions. Since it is obvious that in the earlier stages the ordered structure is a gradually changing transition state on the way to the maximum degree of order, there is no reason to assume that the same stage of development has been reached in every such region. Thus, the third explanation for the line broadening is very reasonable, while the other two are ruled out by the metallographic results.

A detailed theory of the image contrast from alloys in the field-ion microscope has recently been developed.[1,5,6] Particular attention is paid to PtCo and the interpretation of differently ordered microstructures, as well as of point and plane defects, is possible.

At 500° C it is found that large ordered domains are formed, in contrast to the fine-scale nucleation that might be expected from classical nucleation theory, at such a low temperature. In agreement with the X-ray results, only a partial degree of long-range order is present and this is not uniform. The interface between these domains and the matrix is irregular and somewhat diffuse, with respect to both its physical extent and the order gradient. The matrix itself exhibits a high degree of short-range order compared with the disordered state. The observation of an irregular interface is in accord with the previous optical observations. However, we believe this to be characteristic of the fundamental ordering process and not of strain-induced recrystallization. The investigation into ordering at 660° C is still proceeding. There is, however, no evidence for a two-phase mechanism of ordering, and it is suggested that the extensive X-ray line broadening is due to the rapid homogeneous ordering of the entire matrix. A complex array of differently orientated domains is formed at an early stage. The degree of long-range order increases homogeneously with time to its equilibrium value.

In a stoichiometric alloy there is no change in composition on superlattice formation, and hence no influence of concentration gradient on the mechanism. Since no long-range transport of atoms is required, local atomic interchanges alone are needed to build up the ordered structure. Thus, in principle this could occur by a homogeneous process, an increase in the degree of short-range order gradually leading to formation of long-range order. Opposing this mechanism in the $L1_0$ superlattice is the fact that the ordered structure possesses lower symmetry than the disordered, and shape and volume changes must be accommodated. This could engender a heterogeneous mode of transformation and it was previously believed that, at all temperatures, plates of the ordered phase were nucleated in coherency with the {101} planes of the disordered matrix. Calculation of area mismatch from room-temperature X-ray data showed this relationship to lead to maximum coherency.[3]

What was not realized was that the anisotropy of the ordered lattice towards thermal expansion[7] would cause the degree of this coherency to be a function of the ordering temperature. Another, although separate factor exerting a similar influence would be the degree of order within the ordered particle, i.e. its degree of tetragonality. The volume free energy of ordering will increase with decreasing temperature below the critical temperature in the normal way. However, superlattice formation is a cooperative phenomenon, and it is suggested that a most significant factor is that the ordering energy will thus be a function of the degree of order already attained in addition to its temperature-dependence.

The actual mode of ordering found at a given temperature should be determined by a balance of these order- and temperature-dependent factors. For example, a highly ordered domain would have a high driving force for growth since atoms adding on to it would release maximum volume free energy. However, it would also be furthest in structure from that of the matrix, and the surface and volume strain-energy terms opposing growth would be higher.

At 500° C the volume change is small, although the {101} coherency strain would be high. A relatively large driving force is potentially available. The mechanism is seen as one of an initial small increase in short-range order throughout the specimen. Homogeneous nucleation of (partially) long-range-ordered domains occurs on a *coarse* scale, and these domains sweep through the matrix at an irregular interface. Since the available ordering energy is large, some of it may be sacrificed in forming only partial long-range order and thereby lowering the strain-energy terms. The interface can progress rapidly, not being dependent on the limited amount of diffusion at 500° C to accomplish extensive long-range ordering. The process is subsequently completed by a homogeneous increase in the degree of order within these partially ordered domains.

A very different balance will hold for ordering just below the critical temperature (833° C), where a third mode of ordering is found. This is certainly nucleation and growth of ordered plates at the expense of the disordered matrix. However, here the crystallography is martensitic,[8] the macroscopic shape change implying a lattice correspondence and hence a coherently moving interface. It appears likely that the low driving force available here necessitates such a mode of growth, with cooperative atom movements occurring in order to maximize the free-energy change of the reaction.

At 660° C, where the rate of the reaction is close to its maximum, it appears that the matrix orders homogeneously to a far greater extent than at 500° C. The {101} interface coherency strain here is low, and many differently orientated domains lying on these planes do result. It can be shown how this process could relieve strains due to the volume change on ordering. Both these differently orientated domains *and* the matrix are partially ordered, and the final stage is once again a homogeneous increase in the degree of order up to the equilibrium value.

Thus, ordering in PtCo begins homogeneously with a general increase in the degree of short-range order. A complex balance of certain temperature- and order-dependent factors then determines the intermediate reaction path. Finally, the degree of long-range order increases homogeneously to its equilibrium value. Only near the equilibrium temperature does the reaction approximate to one of classical nucleation and growth. It is interesting to note that the observations on ordering at 500° C bear similarities to theoretical predictions made by Hillert[9] for homogeneous nucleation in an ordering system. The present authors believe that the most fruitful approach to the problem of mechanism will be analogous to that made to the phenomenon of spinodal decomposition.[10] It is not immediately evident, however, how the latter approach, essentially dealing with free energy as a function of composition, will be modified to deal with free energy as a function of degree of order at constant composition.

Finally, it can be noted that it may be possible to explain the mechanism of ordering in CuAu in a similar way to PtCo. Here, in contrast to PtCo, the lower-temperature X-ray sequence is continuous and the higher discontinuous. This could be due simply to a different balance of the factors discussed previously. What we interpret as a slight range in the degree of order in PtCo at low temperatures could be a substantial one in CuAu, leading to the continuous sequence. This may imply only that the interface region is more diffuse. At higher temperatures in CuAu the extent to which the matrix orders homogeneously before a two-phase process sets in could be quite small. The martensitic mode of ordering in CuAu would be explained in a similar way to PtCo.

References

1. H. N. Southworth, Ph.D. Thesis, Univ. Cambridge, **1968.**
2. F. N. Rhines and J. B. Newkirk, *Trans. Amer. Soc. Metals,* 1953, **45,** 1029.
3. J. B. Newkirk, R. Smoluchowski, A. H. Geisler, and D. L. Martin, *J. Appl. Physics,* 1951, **22,** 290.
4. J. B. Newkirk, A. H. Geisler, D. L. Martin, and R. Smoluchowski, *Trans. Amer. Inst. Min. Met. Eng.,* 1950, **188,** 1249.
5. H. N. Southworth and B. Ralph, *Phil. Mag.,* 1966, **14,** 383.
6. H. N. Southworth and B. Ralph, " Applications of Field-Ion Microscopy " (Conference held at Georgia Institute of Technology, **1968**), (edited by R. F. Hochman, *et al.*), in the press.
7. J. H. Phillips, Ph.D. Thesis, Univ. Nottingham, **1955.**
8. J. S. Bowles and A. S. Malin, *J. Australian Inst. Metals,* 1960, **5,** 131.
9. M. Hillert, *Acta Met.,* 1961, **9,** 525.
10. J. W. Cahn, *Trans. Met. Soc. A.I.M.E.,* 1968, **242,** 166.

Research Note

Re-Establishment of Short-Range Order during Annealing of a Cold-Worked Ag–Pd Alloy

K. Krishna Rao

Thermodynamic, thermoelectric, and galvanomagnetic studies[1–3] indicate that the Ag–Pd system exhibits short-range order (SRO) within certain composition ranges. Consistent with the theories predicted by Gibson[4] and by Asch and Hall,[5] alloys in this system that show SRO have higher electrical-resistivity values when compared with their homogeneous random structures. Cold work destroys the SRO, leading to a decrease in resistivity. The resistivity recovery spectrum and recovery kinetics of these cold-worked alloys are influenced by the re-establishment of the equilibrium SRO. These resistivity recovery effects were investigated in some Ag–Pd alloys by Chen and Nicholson[2] and by Krishna Rao.[3]

Chen and Nicholson employed isochronal and isothermal annealing to study the electrical-resistivity recovery kinetics in an Ag–41·8 wt.-% Pd alloy, cold-worked to 9% and 32% RA. They identified two stages in the isochronal recovery curve. The first stage results in an increase in resistivity beyond the annealed value, while the second shows a decrease to the annealed value. They associated the first stage with the re-establishment of SRO and the second with the annihilation of excess vacancies. They also found that the time at which the maximum in resistivity occurs and its magnitude depend on the annealing temperature, being greater at lower temperatures. In this note we present an alternative explanation for the recovery stages.

Manuscript received 3 July 1968. K. Krishna Rao, Ph.D., is in the Mechanical Engineering Department, University of Nebraska, Lincoln, Nebraska, U.S.A.

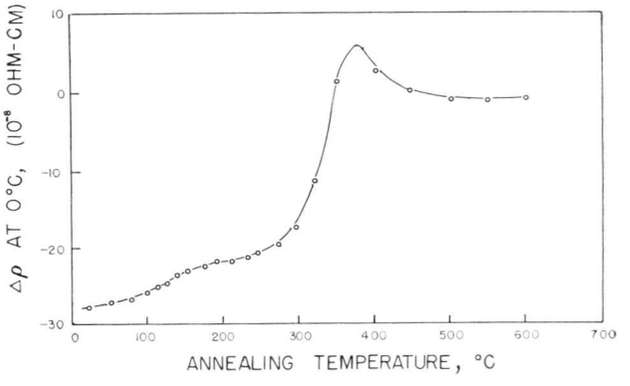

Fig. 1 *Isochronal recovery curve (from Ref.* 3) *of an Ag–41·8 wt.-% Pd alloy cold drawn* 9%. $\Delta\rho = (\rho - \rho_0)$; ρ = *measured resistivity and* ρ_0 = *resistivity for fully annealed alloy.*

We assume that in these alloys SRO represents highly ordered regions surrounded by a nearly random matrix. Deformation causes reduction in the size of the ordered regions and eventually destroys them. It is possible that not all the regions are destroyed even by heavy deformation. The recovery of the cold-worked alloy involves rearrangement of the atoms to form ordered regions, the average size increasing monotonically as a function of time. The details of the atomic processes involved in the growth of the ordered regions may be difficult to assess, but the isochronal recovery curve observed by Chen and Nicholson[2] and reproduced in Fig. 1 suggests three main stages rather than two as they

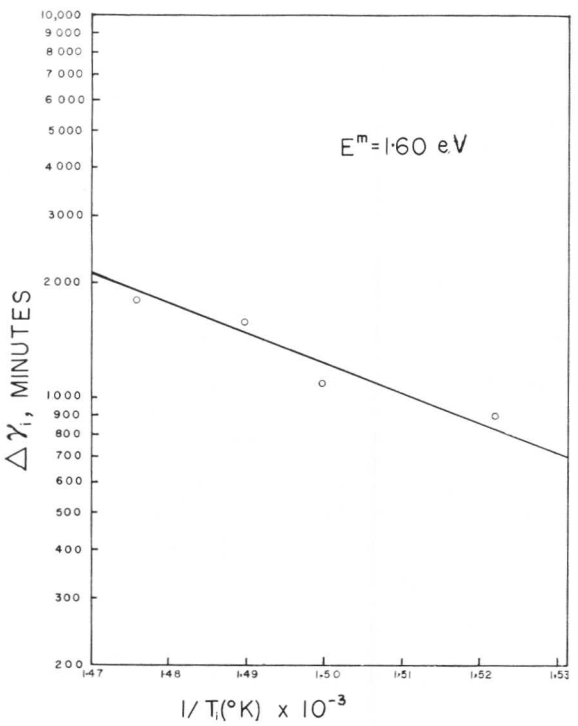

Fig. 2 Plot of ln $\Delta\gamma_i$ *vs.* 1/T *for Stage III.* T = *absolute temperature;* $\Delta\gamma_i$ = *time interval in min.*

proposed. The temperature ranges of the three stages can be identified as (I) 23–170° C, (II) 180–375° C, and (III) 375–450° C. We have calculated the activation energies for these stages from their isothermal and isochronal curves using Meechan–Brinkman[6] and cross-cut methods. The earlier stages, I and II, which may be transient in nature, were analysed on the basis of the cross-cut method. Stage III, which approximately represents a steady state, was analysed using the Meechan–Brinkman method. Fig. 2 shows a plot of ln $\Delta\gamma_i$ vs. $1/T$ for this stage. The straight-line criterion for a singly activated process is seen to hold and the activation energy is found to be 1·60 eV. Our value for this stage is only approximate because of the assumptions made in the calculations. The values for the first and second stages are 0·63 and 2·57 eV, respectively. These energies are found to be very close to those observed by Kim and Flanagan[7] in Au–30 at.-% Pd alloy. The activation energy of 0·63 eV for the first stage suggests that it involves the migration of vacancies resulting in local atomic rearrangement. It is hard to predict the atoms involved in this rearrangement but the essential result is the formation of clusters. The resistivity increase due to cluster formation overshadows the decrease in resistivity due to vacancy annihilation.

The activation energy for Stage II is 2·57 eV. Nachtrieb *et al.*[8,9] have studied the self-diffusion of Ag and Pd in Ag–Pd alloys within the concentration range 0–20 at.-% Pd and found that Pd decreases the rate of self-diffusion of Ag. The activation energy for self-diffusion of Ag was calculated to be of the order of 1·9 eV in pure Ag and was found not to vary with Pd concentration. The activation energy for self-diffusion of Pd in this system is 2·48 eV and it was also found not to depend on concentration. Our calculated activation energy of 2·57 eV for Stage II is of the order of that for self-diffusion of Pd in the Ag–Pd alloys and suggests that Stage II can be identified with migration of Pd atoms. The growth of the ordered regions at early times seems to be devoid of major solvent-atom migration.

The growth postulate for SRO suggests that the resistivity should show a maximum at a critical size of the clusters before it reaches the value for the annealed alloy. The value of the resistivity maximum should depend on the annealing temperature, being larger at lower temperatures. This may be attributed to nucleation taking place more quickly at lower temperatures, thus giving a greater number of clusters. Since diffusion is involved during growth, the time it takes to reach the maximum at lower temperatures should be greater. The isothermal recovery studies of Chen and Nicholson[2] at 305 and 350° C show resistivity maxima whose temperature- and time-dependences correspond to the predictions above. Similar resistivity maxima were also observed by Jaumot and Sawatzky[10] in their isothermal study of quenched and cold-worked Cu–Pd alloys that show order. These authors also suggested that the resistivity maximum is a result of the size of the nuclei but identified the nuclei as ordered regions. In contrast, the resistivity maximum at the end of Stage II in the alloy under discussion seems to be associated with a critical size of clusters rich in Pd atoms.

The activation energy for Stage III in Ag–41·8 wt.-% Pd alloy was calculated to be 1·6 eV. It is difficult to understand the lower activation energy of 1·6 eV in the light of the figure of 2·57 eV found in Stage II. The value is somewhat lower than the activation energy for self-diffusion of Ag and may be tentatively identified with the growth of clusters beyond the critical size, coupled with the internal rearrangement of the atoms to form ordered regions. We have not associated this decrease in resistivity with annihilation of line defects because Chen and Nicholson[2] observed no significant softening during these thermal treatments. Since no superlattice structure is observed in this alloy, long-range order cannot be a possible reason for the decrease in resistivity.

In conclusion, we identify the resistivity maximum with a critical size of clusters rich in Pd atoms. Stage I of recovery is attributed to vacancy migration resulting in local atomic rearrangement, Stage II to Pd self-diffusion, and Stage III to the growth of clusters coupled with internal rearrangement. Quantitative proof for cluster formation is lacking and more detailed kinetic data for all the stages are required. Electrical-resistivity and dilatometric studies in quenched alloys are therefore being pursued to characterize the re-ordering process.

Acknowledgements

The author expresses his sincere thanks to Professor S. S. Jaswal of the Physics Department for many helpful discussions. He is also indebted to the Research Council of the University of Nebraska for the award of the Summer Fellowship.

References

1. W. H. Aarts and A. S. Houston-Macmillan, *Acta Met.*, 1957, **5,** 525.
2. W. K. Chen and M. E. Nicholson, *ibid.*, 1964, **12,** 687.
3. K. Krishna Rao, *ibid.*, 1962, **10,** 900.
4. J. B. Gibson, *J. Physics Chem. Solids,* 1956, **1,** 27.
5. A. E. Asch and G. L. Hall, *Phys. Rev.*, 1963, **132,** 1047.
6. C. J. Meechan and J. A. Brinkman, *ibid.*, 1956, **103,** 1193.
7. M. J. Kim and W. F. Flanagan, *Acta Met.*, 1967, **15,** 753.
8. N. H. Nachtrieb, J. Petit, and J. Wehrenberg, *J. Chem. Physics,* 1957, **26,** 106.
9. R. L. Rowland and N. H. Nachtrieb, *J. Phys. Chem.*, 1963, **67,** 2817.
10. F. E. Jaumot, Jr., and A. Sawatzky, *Acta Met.*, 1956, **4,** 118.

Discussion

Professor D. WATANABE (Tohoku University, Japan): I would like to make a comment on the paper by Vere and Smallman. According to our analysis of the structure of the low-temperature modification of the TiO phase, equilibrium $TiO_{0\cdot7}$ has to be decomposed to the α phase and $TiO_{0\cdot9}$. In the equilibrium low-temperature form TiO, half the titanium sites, and half the oxygen sites on every third (110) plane are vacant.* Fig. D.V.1 shows the ordered arrangements of vacancies.

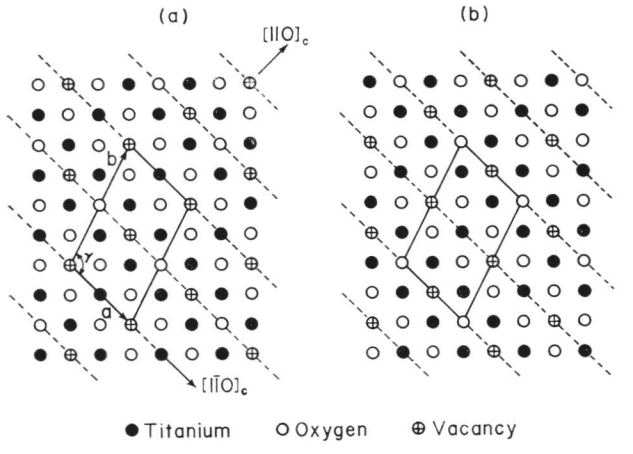

Fig. D.V.1 *Proposed arrangement of vacancies in the equilibrium low-temperature form, TiO.* (Watanabe.)

Dr. A. W. VERE (University of Birmingham): We have not observed the type of decomposition mentioned but it is conceivable that in view of the preparation technique the structure we described is in fact metastable. Nevertheless, the formation of this structure represents the first stage in the transformation and our analysis shows that this may be represented as a continuous distortion of the basic NaCl-type unit cell with increasing deviation from stoichiometry.

Mr. M. BOUCHARD (Imperial College London): I would like to draw attention to the point raised by Vere and Smallman on the order structure of the TiO system. They suggest various planes of vacancies, at every third plane of oxygen atoms, and so far as I can see this model would give a structure similar to that observed in CuAuII. Furthermore, this structure would be revealed only on a dark-field micrograph using a superlattice reflection. Has this analysis of superlattice reflections been made?

Dr. VERE: No.

Mr. BOUCHARD: I wonder if the model described would not give a cubic domain rather than a long needle as it appears on the micrographs. If the process of strain-restricted growth of a single domain repeats itself on (110) and $(1\bar{1}0)$, the APB between domains would appear square on the micrographs.

Dr. VERE: I see what you mean, but we found no evidence of this.

Professor WATANABE (*written discussion*): I do not agree with Vere and Smallman's conclusion on the distortion of the NaCl-type lattice, especially as regards the large distortion in the off-stoichiometric composition. All the diffraction patterns in Figs. 5 and 8 of their paper are interpreted to be the patterns of {110} orientation in their analyses. It is obvious, however, that some of the diffraction patterns, e.g. Figs. 5(*d*), 8(*a*), and 8(*d*), from which they have deduced the large distortion, are not {110} diffraction patterns. According to our analyses, Fig. 5(*d*) corresponds to the $(510)_c$ and Figs. 8(*a*) and (*d*) to the $(210)_c$ reciprocal lattice plane of the equiatomic TiO-type ordered lattice.* Other diffraction patterns shown in this paper are also interpreted as those of the equiatomic ordered TiO structure, and therefore it seems to us that there is no justifiable reason for considering the large distortion of the parent NaCl-type lattice in the off-stoichiometric composition.

Dr. VERE and Professor SMALLMAN (*written reply*): We regret that the captions to Figs. 5 and 8 should have been found misleading. The diffraction patterns shown in these figures exhibit clear differences in both angular relationships and relpoint spacings and it is technically true that they cannot all represent (110) cubic patterns. However, our aim was to illustrate the effect of deviation from stoichiometry upon the original (110) cubic plane and to show that the reorientation may be expressed as a continuous process. No attempt has been made to indicate the final orientation of this plane in the unit cell of the low-temperature modification.

Dr. D. J. DYSON and Dr. K. W. ANDREWS (British Steel Corporation, Rotherham) (*written discussion*): Electron-diffraction patterns similar to those shown by Vere and Smallman have been obtained from extraction replicas from steels containing vanadium and carbon.

Fig. D.V.2(*a*) shows the pattern obtained from the vanadium carbide phase oriented with [001] parallel to the beam. There are additional reflections that divide the 220 and $2\bar{2}0$ reciprocal lattice distances by 3. This effect is strictly similar to that obtained by Vere and Smallman for the titanium oxide and shown in Fig. 3(*b*) of their paper. In Fig. D.V.2(*b*) the zone axis is $[1\bar{1}0]$, and here too the 220 spacing is divided by three. In addition, both $11\bar{1}$ and 111 reciprocal lattice spacings are halved. In some cases, however, patterns from the {110} zones show either the halved spacings or the thirds, but not both. The existence of two different effects is thus probable.

Fig. D.V.2(*c*) shows a further feature which is sometimes observed. The $\bar{1}11$ spacings in this diagram—from a $[1\bar{1}2]$ zone—are divided into two as before. There are, however, rows of streaks containing several discrete maxima parallel

* D. Watanabe, J. R. Castles, A. Jostsons, and A. S. Malin, *Acta Cryst.*, 1967, **23**, 307.